

**EPOXY PHOSPHOLIPIDS: TOTAL SYNTHESIS, GENERATION AND *IN VIVO*
DETECTION OF A NEW CLASS OF OXIDATIVELY TRUNCATED LIPIDS**

By

A. CLEMENTINA MESAROS

Submitted in partial fulfillment of the requirements

For the degree of Doctor of Philosophy

Thesis Adviser: Dr. Robert G. Salomon

Department of Chemistry

CASE WESTERN RESERVE UNIVERSITY

January, 2005

CASE WESTERN RESERVE UNIVERSITY
SCHOOL OF GRADUATE STUDIES

We hereby approve the dissertation of

candidate for the Ph.D. degree *.

(signed) _____

(chair of the committee)

(date) _____

*We also certify that written approval has been obtained for any proprietary material contained therein.

TABLE OF CONTENTS

Table of Contents	iii
List of Schemes	v
List of Tables	xi
List of Figures	xii
Aknowledgements	xxviii
List of Abbreviations	xx
Abstract	xxvii
EPOXY PHOSPHOLIPIDS: TOTAL SYNTHESIS, GENERATION AND <i>IN VIVO</i>	
DETECTION OF A NEW CLASS OF OXIDATIVELY TRUNCATED LIPIDS	
Chapter 1. Introduction	1
1.1. Overview	1
1.2. First Generation Epoxides Derived from Polyunsaturated Lipids	5
1.2.1. Formation of first generation epoxides from unsaturated lipids.	5
1.2.2. Biological relevance of first generation epoxides derived from unsaturated lipids.	7
1.3. Second Generation Epoxides Derived from Polyunsaturated Lipids	8
1.3.1. Formation of epoxyalkenals.	10
1.3.2. Reactions of the epoxy-alkenals with biological nucleophiles.	12
1.4. References	16
Chapter 2. Total Synthesis and Natural Occurrence of a Phospholipid that is Analogous with the Genotoxic Aldehyde 4,5-Epoxy-2E-decenal	22

2.1. Background	23
2.2. Results and discussion	28
2.2.1. Synthesis of 1-palmitoyl-2- (13-oxo-9,10- <i>trans</i> -epoxy-octadeca-11-enoyl)- <i>sn</i> -glycero-3-phosphatidylcholine (<i>trans</i> -OETA-PC, 2.20).	28
2.2.2. Production of <i>trans</i> -OETA-PC (2.20) <i>in vitro</i> from PL-PC (2.6).	31
2.2.3. Evolution profiles of OETA-PC from oxidation of PL-PC.	37
2.2.4. Quantification of <i>trans</i> -OETA-PC (2.20) in rat retina.	40
2.2.5. Nucleotide etheno adduct formation by OETA-PC.	44
2.3. Conclusions	49
2.4. Experimental procedures.	50
2.4.1. Syntheses.	50
2.4.2. Oxidative generation of OETA-PC from PL-PC.	59
2.4.3. Detection and quantification of OETA-PC in rat retina.	63
2.4.4. Reaction of OETA-PC with dAdo, dGuo, and calf thymus DNA.	67
2.5. References	71
Chapter 3. Mechanistic Insights into the Oxidative Fragmentation of Linoleic Acid	75
3.1. Background	75
3.1.1. Hydroperoxydienes are primary oxidation products.	75
3.1.2. Oxidative fragmentation generates aldehydes.	77
3.1.3. The epoxy hydroperoxide mechanism for HNE formation.	78

3.2. Results and discussion	82
3.2.1.Synthesis of 13-oxo-9,10- <i>cis</i> -epoxyoctadeca-11-enoic acid (<i>cis</i> -OETA, 3.16).	82
3.2.2.Autoxidation of epoxy hydroperoxide 3.12.	84
3.2.3.Mechanisms for the generation of HNE.	88
3.2.4 Formation of HODA and OETA from epoxy hydroperoxide 3.12.	89
3.3. Conclusions	91
3.4. Experimental Part	92
3.5. References	106
Chapter 4. Pilot Studies	111
Part A. Ethanolamine Phospholipid Depletion by Lipid Oxidation	
4.1. Background for Part A	112
4.1.1. Membrane composition.	112
4.1.2. Phosphatidylethanolamines: an important component of biological membranes.	112
4.1.3. LDL particles.	114
4.1.4. Ethanolamine phospholipids: a target for reactive lipid oxidation products.	114
4.2. Results and discussion for Part A	117
4.2.1. PEs are not dialyzable from liposomes.	117
4.2.2. The level of dialyzable radiolabeled PE generated upon treatment with ON is <u>not</u> detectable above background.	118

4.2.3. Immunoassay indicates that dialyzable pentylpyrrole <u>is</u> generated upon treatment of PE-containing liposomes with ON.	119
4.2.4. The level of dialyzable radiolabeled PE generated upon exposure to autoxidizing AA is <u>not</u> detectable above background.	122
4.3. Conclusions for Part A	124
4.4. Experimental procedures for Part A	125
Part B. Total Synthesis of Analogues of HODA-PC and HOOA-PC	133
4.5. Background for Part B	133
4.6. Results and Discussion for Part B	135
4.7. Conclusion for Part B	139
4.8. Experimental Part for Part B	140
4.9. References	147
APPENDIX	151
BIBLIOGRAPHY	171

LIST OF SCHEMES

CHAPTER 1

Scheme 1.1	Generation of epoxy hydroxy acids 1.8 and 1.9 from the alkoxy radical 1.1 derived from 13-HPODE.	5
Scheme 1.2	Mechanism for the formation of the bis ¹⁸ O-labeled epoxy hydroxy acid 1.13 from the bis ¹⁸ O-labeled hydroperoxy acid 1.10 .	6
Scheme 1.3	Reaction of a peroxy radical with an isolated double bond.	7
Scheme 1.4	General mechanism for the formation of the epoxy alkenals.	9
Scheme 1.5	General pathways for the formation and further transformations of epoxyalkenals.	9
Scheme 1.6	A Pathway for the formation of <i>trans</i> -4,5-epoxy-(<i>E</i>)-dec-2-enal (1.19) from the linoleic acid proposed by Gardner and Selke.	10
Scheme 1.7	Formation of <i>trans</i> -4,5-epoxy-(<i>E</i>)-dec-2-enal (1.19) by peroxidation of (<i>E,E</i>)-deca-2,4-dienal (1.22) according to Gassenmeier and Schieberle.	11
Scheme 1.8	Polycondensation products from epoxyalkenals and amino compounds.	12

CHAPTER 2

- Scheme 2.1.** Formation of HODA (2.4) from the 13-HPODE (2.2) by analogy with the formation of HNE (2.5) from 9-HPODE (2.3). 23
- Scheme 2.2.** Formation of HODA (2.4) from the 13-HPODE (2.2) by analogy with the formation of HNE (2.5) from 9-HPODE (2.3). 24
- Scheme 2.3.** Formation of 4,5-EDE (2.15) from 13-HPODE (2.2). 25
- Scheme 2.4.** Formation of OETA (2.17) from the 9-HPODE (2.3). 26
- Scheme 2.5.** Formation of the etheno-adducts from 4,5-EDE (2.15). 27
- Scheme 2.6.** Retrosynthesis of *trans*-OETA-PC (2.20). 28
- Scheme 2.7.** Synthesis of hydroxy-acid intermediate 2.26. 29
- Scheme 2.8.** Synthesis of *trans*-OETA-PC (2.20). 30
- Scheme 2.9.** Possible mechanism for the formation of OETA (2.17). 37
- Scheme 2.10.** A plausible mechanism for formation of the etheno-adduct 2.19. 37

CHAPTER 3

- Scheme 3.1.** Generation of hydroxy acids from linoleic acid (LA) through hydroperoxy acid intermediates. 76
- Scheme 3.2.** Pryor and Porter's epoxy hydroperoxide mechanism. 79
- Scheme 3.3.** Synthesis of an epoxy hydroperoxide 3.12 from LA (3.1). 79
- Scheme 3.4.** Formation of HODA (3.15) and *cis*-OETA (3.16) from the epoxy hydroperoxide 3.12 by Hock rearrangement. 80

Scheme 3.5.	Formation of HODA (3.15) and <i>cis</i> -OETA (3.16) from the epoxy hydroperoxide 3.12 by a pathway involving β -scission.	81
Scheme 3.6.	Retrosynthesis of <i>cis</i> -OETA (3.16).	82
Scheme 3.7.	Synthesis of the hydroxy-acid intermediate 3.23 .	83
Scheme 3.8.	Synthesis of <i>cis</i> -OETA (3.16).	81
Scheme 3.9.	Porter's mechanisms for generating HNE from HPODEs.	88
Scheme 3.10.	Mechanism for Fe (II)-catalyzed <i>cis</i> -OETA (3.16) formation.	90
CHAPTER 4		
Scheme 4.1.	Formation of ethanolamine-derived alkylpyrroles.	114
Scheme 4.2.	IsoLGE ₂ -pyrrole and HNE-pyrrole generation from AA-PC or LA-PC.	115
Scheme 4.3.	Formation of the pentylpyrrole adduct (4.6).	118
Scheme 4.4.	Pyrrole formation from phosphatidylethanolamine 4.5 and isoLGE ₂ .	121
Scheme 4.5.	The proposed structure for HOOA-PC and HODA-PC analogues.	134
Scheme 4.6.	Total syntheses of HOOA-PC (4.21a) and HODA-PC (4.21b).	135
Scheme 4.7.	Syntheses of epoxy-HOOA-PC and epoxy-HODA-PC.	136
Scheme 4.8.	Proposed syntheses of 4.10 and 4.11 .	137

LIST OF TABLES

CHAPTER 2

Table 2.1.	Observed maximum yields of OETA-PC from PL-PC oxidized under various reactions conditions.	40
Table 2.2.	Amounts of OETA-PC (2.20) in rat retina.	43
Table 2.3.	Amounts of some phospholipids detected in rat retina.	44
Table 2.4.	Calibration equations, detection limits and extraction efficiency.	65

CHAPTER 3

Table 3.1.	Maximum yields for HODA and OETA.	85
Table 3.2.	Optimized parameters for mass spectrometer.	94
Table 3.3.	Calibration equations for HODA and OETA.	105

CHAPTER 4

Table 4.1.	ELISA data for ON in Figure 4.3.	130
Table 4.2.	ELISA data for methoxime derivative in Figure 4.3.	130
Table 4.3.	ELISA data for liposome reaction with ON in Figure 4.4.	130
Table 4.4.	ELISA data for liposome reaction with ON after adding the methoxime in Figure 4.4.	131
Table 4.5.	ELISA data for liposome reaction with ON after adding methoxylamine in Figure 4.4.	131

LIST OF FIGURES

CHAPTER 1

- Figure 1.1.** Chemical structure of some exocyclic DNA adducts. 14
- Figure 1.2.** Hypothetical scheme implicating persistent oxidative stress 15
as a major event in the development and progression of
malignant cells.

CHAPTER 2

- Figure 2.1.** Mass spectrometric fragmentation of *trans*-OETA-PC (**2.20**). 32
- Figure 2.2.** LC/ESI-MS/MS analysis of OETA-PC from oxidized PL-PC 33
liposomes.
- Figure 2.3.** LC/ESI-MS/MS analysis of OETA-PC derivatives. 34
- Figure 2.4.** Consumption of PL-PC (**2.6**) under various oxidation 38
conditions.
- Figure 2.5.** Evolution profile for production of OETA-PC (**2.20**) from aerial 39
oxidation of PL-PC liposomes promoted by Cu (II), UV or
MPO at 37 °C.
- Figure 2.6.** LC/ESI-MS/MS detection of OETA-PC (**2.20**) (718.3>184.5) 41
from rat retina.
- Figure 2.7.** LC/ESI-MS/MS detection of OETA-PC derivatives 42
(747.9>184.5 and 794.7>184.5) from rat retina.
- Figure 2.8.** LC/APCI/MS analysis of reaction between *trans*-OETA-PC 45
(**2.20**) and dGuo at 60 °C for 48 h.

Figure 2.9.	LC/APCI/MS analysis of reaction between <i>trans</i> -OETA-PC (2.20) and dAdo at 60 °C for 48 h.	45
Figure 2.10.	LC/APCI/MS analysis of reaction between <i>trans</i> -OETA-PC (2.20) and dAdo at 60 °C for 48 h.	46
Figure 2.11	Calibration curve for microphosphorus assay.	60
Figure 2.12.	Chromatogram and calibration curve for synthetic <i>trans</i> -OETA-PC (2.20).	66
Figure 2.13.	Chromatogram and calibration curve for PL-PC.	67
CHAPTER 3		
Figure 3.1.	LC/ESI-MS/MS analysis of <i>cis</i> -OETA (3.16) from oxidation mixture of 3.12.	85
Figure 3.2.	Evolution profile for HODA (3.15) produced from the epoxy hydroperoxide 3.12 during autoxidation or autoxidation in the presence of 5 mol% Fe (II) at 37 °C.	87
Figure 3.3.	Evolution profile of <i>cis</i> -OETA (3.16) produced from the epoxy hydroperoxide 3.12 during autoxidation or autoxidation in the presence of 5 mol% equivalent Fe (II) at 37 °C	87
Figure 3.4.	LC-MS chromatogram of <i>cis</i> -OETA (3.16) and the calibration curve.	104
Figure 3.5.	LC-MS chromatogram of HODA (3.15) and the calibration curve.	105

CHAPTER 4

- Figure 4.1.** **A.** A model layer formed by PCs, where ● is the hydrophobic head, and $\text{---}\overset{\text{O}}{\parallel}\text{---}$ is the hydrophilic tail. **B.** A model of arrangement of the PEs, where the same symbols are used as for panel **A.** 111
- Figure 4.2.** The radioactivity detected in the outer buffer. 117
- Figure 4.3.** Inhibition curve for binding of anti-ON-KLH to BSA-ON by BSA-6-ACA-ON (●) ON alone (■), and ON after adding 10-fold excess $\text{MeONH}_3^+\text{Cl}^-$ (▼). 119
- Figure 4.4.** Liposome reaction with ON. Inhibition curve for binding of anti-ON-KLH to BSA-ON by BSA-6-ACA-ON (the standard) (●) before adding $\text{MeONH}_3^+\text{Cl}^-$ (▼), after adding $\text{MeONH}_3^+\text{Cl}^-$ (■). 120
- Figure 4.5.** Liposome reaction with oxidation products from AA. Inhibition curve for binding of anti-ON-KLH to BSA-ON by BSA-6-ACA-ON (the standard) (●). Inhibition curve for binding of anti-ON-KLH by products from inside the bag (▼). 122
- Figure 4.6.** Schematic representation of ELISA. 129
- Figure 4.7.** Lipid oxidation products and their ability to block binding of NO_2 -LDL to CD36. 133
- Figure S 1.** The 300 MHz ^1H NMR (CDCl_3) spectrum of 2-(8-bromooctyloxy)-tetrahydropyran (**2.23**) 151
- Figure S 2.** The 75 MHz ^{13}C NMR (CDCl_3) spectrum of 2-(8-bromo- 151

	octyloxy)-tetrahydropyran (2.23).	
Figure S 3.	The 300 MHz ^1H NMR (CDCl_3) spectrum of 2-(8-hydroxy-octyloxy)-tetrahydropyran (2.21).	152
Figure S 4.	The 75 MHz ^{13}C NMR (CDCl_3) spectrum of 2-(8-bromo-octyloxy)-tetrahydropyran (2.21).	152
Figure S 5.	The 300 MHz ^1H NMR (CDCl_3) spectrum of acetic acid, 11-(tetrahydro-pyran-2-yloxy)-undec-2-enyl ester (2.24)	153
Figure S 6.	The 300 MHz ^1H NMR (CDCl_3) spectrum of acetic acid, 11-hydroxy-undec-2-enyl ester (2.25)	153
Figure S 7.	The 300 MHz ^1H NMR (CDCl_3) spectrum of 11-hydroxy-undec-9-enoic acid (2.26)	154
Figure S 8.	The 75 MHz ^{13}C NMR (CDCl_3) spectrum of 11-hydroxy-undec-9-enoic acid (2.26).	154
Figure S 9.	The 300 MHz ^1H NMR (CDCl_3) spectrum of 8-(3-hydroxymethyl-oxiranyl)octanoic acid (2.27)	155
Figure S 10.	The 75 MHz ^{13}C NMR (CDCl_3) spectrum of 8-(3-hydroxymethyl-oxiranyl)octanoic acid (2.27)	155
Figure S 11.	The 300 MHz ^1H NMR (CDCl_3) spectrum of 8-(3-formyl-oxiranyl)-octanoic acid (2.28)	156
Figure S 12.	The 75 MHz ^{13}C NMR (CDCl_3) spectrum of 8-(3-formyl-oxiranyl)-octanoic acid(2.28).	156
Figure S 13.	The 300 MHz ^1H NMR (CDCl_3) spectrum of 8-[3-(3-oxopropenyl)-oxiranyl]-octanoic acid (2.17).	157

Figure S 14.	The 75 MHz ¹³ C NMR (CDCl ₃) spectrum of 8-[3-(3-oxo-propenyl)-oxiranyl]-octanoic acid (2.17).	157
Figure S 15.	The 300 MHz ¹ H NMR (CDCl ₃) spectrum of 1-palmitoyl-2-(13-oxo-9,10- <i>trans</i> -epoxy-octadeca-11-enoyl)-sn-glycero-3-phosphatidylcholine (2.20)	158
Figure S 16.	The 75 MHz ¹³ C NMR (CDCl ₃) spectrum of 1-palmitoyl-2-(13-oxo-9,10- <i>trans</i> -epoxy-octadeca-11-enoyl)-sn-glycero-3-phosphatidylcholine (2.20).	158
Figure S 17.	The 300 MHz ¹ H NMR (CDCl ₃) spectrum of 2-(11-hydroxy-9-undecynyloxy)tetrahydropyran (3.20)	159
Figure S 18.	The 75 MHz ¹³ C NMR (CDCl ₃) spectrum of 2-(11-hydroxy-9-undecynyloxy)tetrahydropyran (3.20)	159
Figure S 19	The 300 MHz ¹ H NMR (CDCl ₃) spectrum of 2-(11-hydroxy-9(Z)-undecenyloxy)tetrahydropyran (3.17)	160
Figure S 20	The 300 MHz ¹ H NMR (CDCl ₃) spectrum of acetic acid, 11-tetrahydropyran-2-yloxy)-2(Z)-undecenyl ester (3.21)	160
Figure S 21	The 300 MHz ¹ H NMR (CDCl ₃) spectrum of acetic acid, 11-hydroxy-2(Z)-undecenyl ester (3.22).	161
Figure S 22	The 300 MHz ¹ H NMR (CDCl ₃) spectrum of 11-hydroxy-9(Z)-undecenoic acid (3.23).	161
Figure S 23	The 75 MHz ¹³ C NMR (CDCl ₃) spectrum of 11-hydroxy-9(Z)-undecenoic acid (3.23)	162
Figure S 24	The 300 MHz ¹ H NMR (CDCl ₃) spectrum of 8-(3-	162

	hydroxymethyloxiranyl)-octanoic acid (3.24).	
Figure S 25	The 75 MHz ^{13}C NMR (CDCl_3) spectrum of 8-(3-hydroxymethyloxiranyl)-octanoic acid (3.24).	163
Figure S 26	The 300 MHz ^1H NMR (CDCl_3) spectrum of 8-(3-formyloxiranyl)octanoic acid (3.25).	163
Figure S 27	The 75 MHz ^{13}C NMR (CDCl_3) spectrum of 8-(3-formyloxiranyl)octanoic acid (3.25).	164
Figure S 28	The 300 MHz ^1H NMR (CDCl_3) spectrum of 13-oxo-9,10- <i>cis</i> -epoxy-11(E)-tridecenoic acid (3.16).	164
Figure S 29	The 75 MHz ^{13}C NMR (CDCl_3) spectrum of 13-oxo-9,10- <i>cis</i> -epoxy-11(E)-tridecenoic acid (3.16).	165
Figure S 30	The 75 MHz ^{13}C NMR (CDCl_3) spectrum of 13-oxo-9,10- <i>cis</i> -epoxy-11(E)-tridecenoic acid (3.16).	165
Figure S 31	The 300 MHz ^1H NMR (CDCl_3) spectrum of 4-(3-formyloxiranyl)-4-hydroxybutyryl phosphatidylcholine (4.8).	166
Figure S 32	The 300 MHz ^1H NMR (CDCl_3) spectrum of 8-(3-formyloxiranyl)-8-hydroxy-octanoyl phosphatidylcholine (4.9).	166
Figure S 33	The 300 MHz ^1H NMR (CDCl_3) spectrum of the crude 4.22b	167

Acknowledgements

I wish to express my genuine gratitude to my research advisor Prof. Robert G. Salomon, whose care, guidance, and constant encouragement made it possible for me to present this thesis. His expert guidance, constant encouragement, support and above all, his patience and understanding enable me to achieve the results presented in this thesis. He provided me with the best education an advisor can bring to his students.

I would like to thank Dr. Seon Hwa Lee, Center for Cancer Pharmacology, University of Pennsylvania, Philadelphia for her valuable collaboration on the formation and detection of the etheno-adducts.

I would like to thank former members in Prof. Salomon's group, Dr. Yijun Deng, Dr. Xiaorong Gu, Dr. Eugenia Batyreva, Dr. Mingjiang Sun and Dr. Bogdan Gugiu for their help and their friendship. Special thanks to Bogdan and Ming whose collaboration and advice I was lucky to benefit from in all these years.

I would like to thank all my colleagues Raju, Jim, Suresh, Wujuan, Nathan, Xi, Liang, Jiayin, Laura, Wei, Bharathi and Ken for their friendship and helpful discussions.

I would also like to thank my committee members: Dr. Sayre, Dr. Dunbar, Dr. Guo and Dr. Barkley for their precious time and efforts put into my thesis, as well as helpful ideas and discussions throughout my graduate studies.

I would also like to thank Dr. Dale Ray and Dr. Jim Faulk and other staff members in the Department of Chemistry at Case Western Reserve University for their help on numerous occasions.

I would like to thank my mother for her unconditional support and encouragement through the course of my education.

Last, but not least, I would like to thank Eugen, my husband, for his constant encouragement through all these years, helpful discussions about my research and my thesis.

Clementina Mesaros

LIST OF ABBREVIATIONS AND ACRONYMS

Abbreviation	Definition
13-HODE	13-Hydroxy-9,11-octadienoic acid
13-HPODE	13-Hydroperoxy-9,11-octadecadienoic acid
9-HODE	9-Hydroxy-10,12-octadienoic acid
9-HPODE	9-Hydroperoxy-10,12-octadienoic acid
AA	Arachidonic acid
ACA	6-Aminocaproic acid
ACPI	Atmospheric pressure chemical ionization
APT	Attached proton test
BHT	Butylated hydroxytoluene
BSA	Bovine serum albumin
CD36	Platelet glycoprotein IV scavenger receptor
CEO	Chicken egg ovalbumin
CID	Collision-induced dissociation
dAdo	2'-Deoxyadenosine
DCC	Dicyclohexylcarbodiimide
dGuo	2'-Deoxyguanosine
DHA	Docosahexaenoic acid
DHA-PC	1-Palmitoyl-2-docosahexaenoyl- <i>sn</i> -glycero-3-phosphatidylcholine
DHP	Dihydropyran

DMAP	4-N,N-Dimethylaminopyridine
DMF	Dimethyl formamide
DM-PE	1,2-Myristoyl- <i>sn</i> -glycero-3-phosphatidylethanolamine
DNA	Deoxyribonucleic acid
DO-PE	1,2-Dioleoyl- <i>sn</i> -glucero-3-phosphatidylcholine
DPM	Disintegration per minute
DTPA	Diethylenetriaminepentaacetic acid
EE	Extraction efficiency
EDE	4,5-Epoxy-2 <i>E</i> -decenal
EDTA	Ethylenediaminetetraacetic acid
EI	Electron impact
ELISA	Enzyme-linked immunosorbent assay
ELS	Evaporative light scattering
EP	Ethanolamine phospholipids
ESI	Electrospray ionization
FAB	Fast atom bombardment
FITC	Fluorescein isothiocyanate
GC-MS	Gas chromatography-mass spectrometry
G-PC	1-Palmitoyl-2-(glutaroyl)- <i>sn</i> -glycero-3-phosphatidylcholine
HDdiA	4-Hydroxydodec-2-enedioic acid
HDdiA-PC	1-Palmitoyl-2-(9-hydroxy-11-carboxyundec-6-enoyl)- <i>sn</i> -glycero-3-phosphatidylcholine

HHdiA-PC	1-Palmitoyl-2-(4-hydroxy-7-carboxyhex-5-enoyl)- <i>sn</i> -glycero-3-phosphatidylcholine
HNE	4-Hydroxy-2-nonenal
HOdiA-PC	1-Palmitoyl-2-(5-hydroxy-7-carboxyhept-6-enoyl)- <i>sn</i> -glycero-3-phosphatidylcholine
HODA	9-Hydroxy-12-oxo-10 (E)-dodecenoic acid
HODA-Methoxime	9-Hydroxy-12-methoxyiminododec-10-enoic acid
HODA-PC	1-Palmitoyl-2-(9-hydroxy-12-oxododec-10-enoate)- <i>sn</i> -glycero-3-phosphatidylcholine
HOHA	4-Hydroxy-7-oxohept-5-enoic acid
HOHA-PC	1-Palmitoyl-2-(4-hydroxy-7-oxohept-4-enoyl)- <i>sn</i> -phosphatidylcholine
HOOA	5-Hydroxy-8-oxooct-6-enoic acid
HOOA-PC	2-(5-Hydroxy-8-oxooctanoyl)phosphatidylcholine
HOT	9-Hydroxy-12-oxo-10-tridecenoic acid
HPLC	High performance liquid chromatography
HRMS	High resolution mass spectrometry
Iso PGH ₂	iso[4]prostaglandin H ₂
iso[4]LGE ₂	Iso[4]levuglandin E ₂
isoLGE ₂	Isolevuglandin E ₂
J	Hyperfine coupling constant
KDdiA-PC	1-Palmitoyl-2-(9-oxo-11-carboxydodec-10-enoyl)- <i>sn</i> -glycero-3-phosphatidylcholine

KHdiA-PC	1-Palmitoyl-2-(7-carboxy-4-oxohex-5-enoyl)- <i>sn</i> -glycero-3-phosphatidylcholine
KLH	Keyhole limpet hemocyanin
KODA-PC	1-Palmitoyl-2-(9-oxo-12-oxododec-10-enoyl)- <i>sn</i> -glycero-3-phosphatidylcholine
KOdiA-PC	1-Palmitoyl-2-(7-carboxy-5-oxohept-6-enoyl)- <i>sn</i> -glycero-3-phosphatidylcholine
KOHA-PC	1-Palmitoyl-2-(4,7-dioxohept-6-enoyl)- <i>sn</i> -glycero-3-phosphatidylcholine
KOOA-PC	1-Palmitoyl-2-(5,8-dioxooct-6-enoyl)- <i>sn</i> -glycero-3-phosphatidylcholine
LA	Linoleic acid
LC	Liquid chromatography
LDL	Low density lipoprotein
LG	Levuglandins
LOOH	Lipid hydroperoxides
LPO	Alkoxy lipids
Lyso-PC	1-Palmitoyl-2-hydroxy- <i>sn</i> -glycero-3-phosphatidylcholine
MOPS	3-(N-Morpholino)propanesulfonic acid
MPO	Myeloperoxidase
MPO-NO ₂	Myeloperoxidase-hydrogen peroxide-nitrite system
MRM	Multiple reaction monitoring

MS/MS	Tandem mass spectrometry
NMO	N-Methylmorpholine N-oxide
NMR	Nuclear magnetic resonance
NO	Nitric oxide
OB-PC	1-Palmitoyl- 2-(4-oxobutyroyl)-sn-glycero-3-glycero-3-phosphatidylcholine
OETA	8-[3-(3-Oxo-propenyl)-oxiranyl]-octanoic acid
OETA-PC	1-Palmitoyl-2-(13-oxo-9,10- <i>trans</i> -epoxy-octadeca-11-enoyl)-sn-glycero-3-phosphatidylcholine
ON	4-Oxo-2-nonenal
ON-PC	1-Palmitoyl-2-(9-oxononanoeyl)- <i>sn</i> -glycero-3-phosphatidylcholine
OV-PC	1-Palmitoyl- 2-(5-oxovaleroyl)-sn-glycero-3-phosphatidylcholine
oxLDL	Oxidized low density lipoprotein
oxPC	Oxidized phosphatidylcholines
oxPE	Oxidized phosphatidylethanolamine
oxPL	Oxidized phospholipid
P-450	Cytochrome P-450
PA-PC	1-Palmitoyl-2-arachidonoyl- <i>sn</i> -glycero-3-phosphatidylcholine
PBS	Phosphate buffered saline
PC	Phosphatidylcholine

PDA	Photodiode array
PDC	Pyridinium dichromate
PE	Phosphatidylethanolamine
PLD	Phospholipase D
PL-PC	1-Palmitoyl-2-linoleoyl- <i>sn</i> -glycero-3-phosphatidylcholine
PO-PC	1-Palmitoyl-2-oleoyl- <i>sn</i> -glycero-3-phosphatidylcholine
ppm	Parts per million
PPTS	Pyridinium <i>para</i> -toluenesulfonate
PS	Phosphatidylserine
PUFA	Polyunsaturated fatty acid
Rf	Retention factor
ROS	reactive oxygen species
RP	Reverse phase
S.D.	Standard deviation
SIM	Selected ion monitoring
SO	Superoxide
SPE	Solid phase extraction
TBAF	Tetrabutylammonium fluoride
TBDMS	tert-Butyldimethylsilyl
TBDMSCl	tert-Butyldimethylsilyl chloride
THF	Tetrahydro furan
THP	Tetrahydro pyran

TIC	Total ion current
TLC	Thin layer chromatography
TPAP	Tetra-n-propyl ammonium perruthenate
UV	Ultraviolet
Vit C	Vitamin C

Epoxy Phospholipids: Total Synthesis, Generation and *in vivo* Detection of a New Class of Oxidatively Truncated Lipids

Abstract

By

Clementina Mesaros

Epoxy lipids are a relatively little studied class of oxidized phospholipids in comparison with their γ -hydroxy(oxo)- α,β -unsaturated analogs. Most of the known epoxy lipids were first studied in foods. Recent studies indicate that epoxy lipids are relevant to human diseases. Some of them readily form etheno adducts upon reaction with DNA's bases. These etheno adducts were detected in tissues from cancer patients. Thus it is important to know the chemistry of epoxy lipid formation and their reactivity with other biomolecules. Epoxy phospholipids had not been reported. However the chemistry underlying the formation of known epoxy lipids seemed likely to produce such phospholipids. To assess the natural occurrence and biological properties of these putative epoxy phospholipids, one member of this class was prepared by total synthesis. The route developed can be easily modified to allow the production of other epoxy phospholipids. The production of the new phospholipid from oxidation of linoleic acid was

demonstrated *in vitro*. The presence of this epoxy phospholipid was further detected in rat retina.

Extensive literature precedent suggests that 9-hydroperoxy-10,12 octadienoic acid and 13-hydroperoxy-9,11-octadienoic acid are the primary first generation oxidation products from linoleic acid. They can fragment to produce epoxy-truncated lipids, such as 4,5-epoxy-2(*E*)-decenal, the most studied representative of the class. Several mechanism and putative intermediates have been proposed for the formation of epoxy lipids from these lipid peroxide precursors. By examining the autoxidation of one putative intermediate, 13-hydroperoxy-9,10-cis-epoxyoctadeca-11-enoic acid, we concluded that the proposed epoxy hydroperoxide mechanism involving this intermediate is a feasible pathway for the formation of epoxy lipids.

Chapter 1

Introduction

1.1. Overview

Lipid peroxidation, the mechanisms by which this process can take place, and the numerous products that it generates have attracted considerable research efforts. This interest is due, at least in part, to the importance of lipids in biological systems and to the negative effects of the lipid peroxidation on human health.¹⁻⁵ Lipids are found in foods and they are important constituents of the human body, e.g., in membranes or low density lipoprotein (LDL). Accordingly, the literature on lipids is divided into two major categories: one is found in food journals,⁶⁻¹¹ dealing with the oxidation of the lipids and the byproducts that alter the food quality, and the other is in medical journals, dealing with the pathology induced by the products of lipid peroxidation in the body.¹²⁻¹⁴

This chapter focuses on recent research on the *epoxy phospholipids* that are produced by lipid peroxidation. They are a relatively newly studied class of lipids, but as reports are showing, they can be of very great importance to human health.^{13,15,16}

Chapter 2 will address the rationale by which the existence of a new epoxy phospholipid was postulated in our laboratories. The total synthesis of this product and its detection *in vitro* and *in vivo* will also be described.

The importance of phospholipids in human health will be discussed in Chapter 3, followed by our own contribution to the field with the synthesis of another new fragmentation product from an intermediate of lipid peroxidation, along with its detection in oxidation experiments *in vitro*.

The last chapter (Chapter 4) will have two parts. Part A will present pilot studies on phosphatidyletanolamine depletion in membranes caused by oxidation. Part B will present the synthesis of a series of analogues of 2-(9-hydroxy-12-oxododecanoyl)phosphatidylcholine (HODA-PC) and 2-(5-hydroxy-8-oxooctanoyl)phosphatidylcholine (HOOA-PC), two phospholipids previously postulated and synthesized by the Salomon group.¹⁷ In collaborative studies, these phospholipids were detected *in vivo* and some biological properties were elucidated.^{18,19}

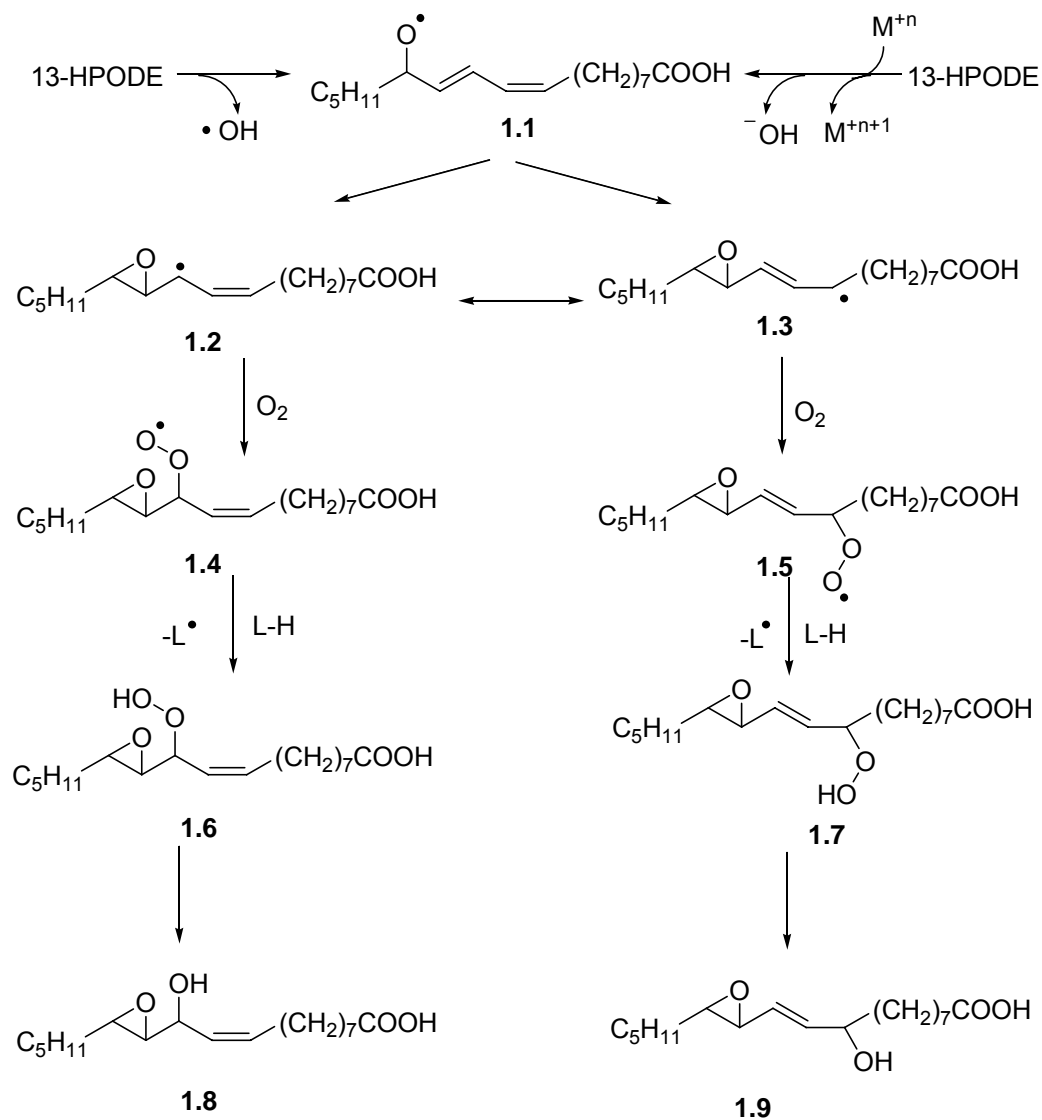
It is noteworthy that the polyunsaturated fatty acids (PUFAs) can be found in nature free or as esters, and free radicals attack them with about equal probability.¹⁵ Most PUFAs have homoconjugated double bonds, and similar or even the same oxidation products can be formed from autoxidation of various different fatty acids, e.g., 4-hydroxy-2-nonenal (HNE) can be formed from both linoleic acid (LA) and arachidonic acid (AA).¹⁵ Nevertheless, because LA was shown to be present in living organisms in quantities that exceed the quantities of AA and other PUFAs by almost an order of magnitude,²⁰ most of the literature data is focused on LA. The epoxides that are formed directly by oxidation of the double bonds in the starting acids represent the “first generation” of epoxidation products, which in turn can fragment in subsequent reactions to give rise to “second and third generations” epoxides with truncated backbones. Products of the first, second, and third generations have all been shown to have physiological relevance to human health.²¹⁻²³

1.2. First Generation Epoxides Derived from Polyunsaturated Lipids

1.2.1. Formation of first generation epoxides from unsaturated lipids.

As will be discussed in more depth in Chapter 3 of this thesis, LA forms mainly two hydroperoxides, 9-hydroperoxyoctadeca-10,12-dienoate (9-HPODE) and 13-hydroperoxyoctadeca-9,11-dienoate (13-HPODE), upon exposure to oxidants. These reactive hydroperoxides have a hydroperoxy moiety in an allylic position of a conjugated diene. They can form a large number of oxidatively truncated products. As early as 1967, there were studies on the decomposition of pure individual hydroperoxides, prepared by the selective action of the lipoxygenases.⁸ This approach of studying each HPODE individually was adopted to reduce the number of oxidation products formed in the decomposition reactions, and to facilitate the assignment of their origin.

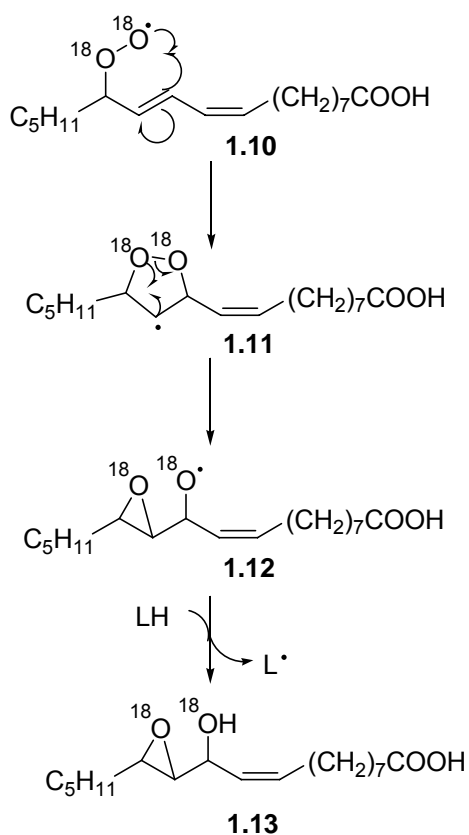
The hydroperoxides can undergo decomposition in the presence of Fe^{2+} to produce alkoxy radicals, which then can participate in three types of reactions. The largest fraction of the alkoxy radicals is converted, by hydrogen atom abstraction, to the corresponding alcohols.^{24,25} Cleavage of the alkoxy radicals to aldehydes,^{26,27} and hydrocarbon radicals that can abstract hydrogen atoms to give the corresponding hydrocarbons^{26,28} ranks second in terms of occurrence. The third type of reaction of alkoxy radicals involves initial rearrangement to mesomeric epoxy radicals like **1.2** and **1.3** in Scheme 1.1. The epoxy radicals can react with molecular oxygen to form epoxy hydroperoxy radicals **1.4** and **1.5** that then give hydroperoxides **1.6** and **1.7** (Scheme 1.1).²⁹ These can further decompose to epoxy hydroxy acids such as **1.8** and **1.9**.



Scheme 1.1 Generation of epoxy hydroxy acids **1.8** and **1.9** from the alkoxy radical **1.1** derived from 13-HPODE.

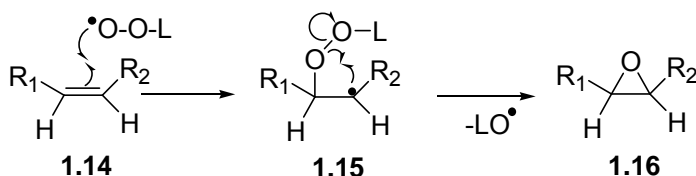
When reduced in the presence of FeCl_3 -cysteine, the epoxyhydroperoxide **1.7** was converted into the epoxy alcohol **1.9**. Thus, epoxy hydroperoxides are intermediates in the oxidative decomposition of lipids.³⁰ Epoxy hydroxy acids, such as **1.8** and **1.9**, can be easily hydrated to produce the corresponding trihydroxy acids.³¹

Experiments with ^{18}O labeled 13-HPODE elucidated a mechanism for the conversion of hydroperoxy acids into epoxy hydroxy acids.^{32,33} Because the ^{18}O was incorporated in both the epoxide ring and the hydroxyl group, the reaction is apparently intramolecular. The hydroperoxy radical **1.10**, derived from ^{18}O labeled 13-HPODE, attacks the proximal double bond at the β carbon, and an epoxy alkoxy radical **1.12** is formed by rearrangement of the intermediate **1.11** (Scheme 1.2). This is an intramolecular version of the oxygen atom transfer process outlined in Scheme 1.3 (*vide infra*). Alkoxy radical **1.12** then gives **1.13** by hydrogen atom abstraction from another lipid molecule (LH).



Scheme 1.2 Mechanism for the formation of the bis ^{18}O -labeled epoxy hydroxy acid **1.13** from the bis ^{18}O -labeled hydroperoxy acid **1.10**.^{32,33}

It is known that peroxy radicals can attack isolated double bonds (Scheme 1.3). This can result in the formation epoxy lipids by oxygen atom transfer to fatty acids other than PUFAs, such as AA and LA. Even monounsaturated fatty acids, such as palmitoleic acid (16:1) and oleic acid (18:1), can be transformed in this manner into epoxy fatty acids,^{22,34} and unsaturated steroids can be similarly epoxidized.³⁵ Epoxidation of isolated C=C bonds is common in plant lipids.³⁵



Scheme 1.3 Reaction of a peroxy radical with an isolated double bond.

1.2.2. Biological relevance of first generation epoxides derived from unsaturated lipids. Epoxy alkenyl radicals like **1.2** and **1.3** in Scheme 1.1 can abstract hydrogen from another LA molecule to form epoxides of linoleic acid. Epoxides derived from LA were detected in tissues after burn injury³⁶ or following myocardial infarct.²²

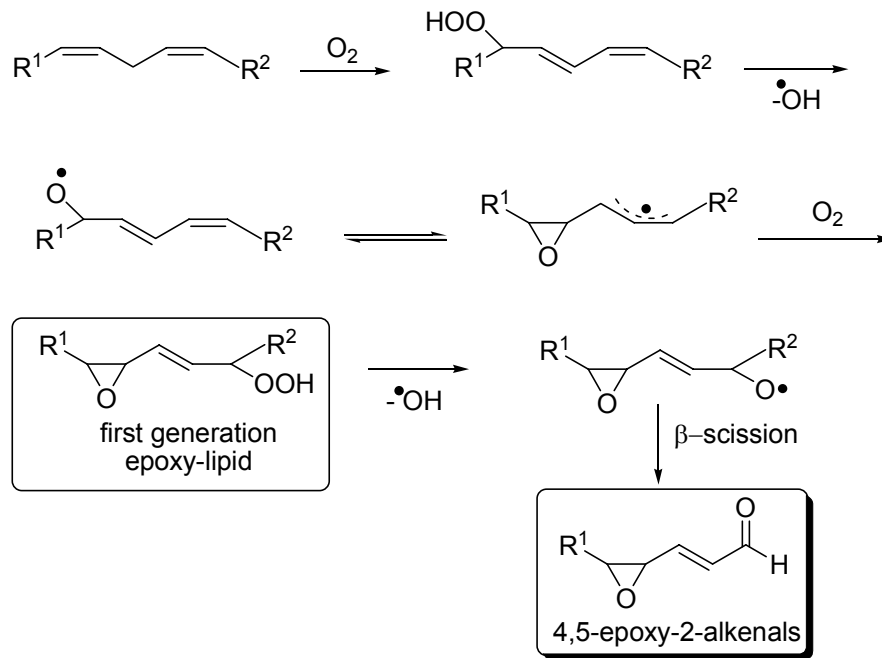
The epoxy acids resulting from peroxidation of lipids can react with nucleophilic centers¹⁵ in biomolecules with concomitant opening of the epoxide ring. Therefore, they are likely to have physiological relevance.

The first epoxy acid to be identified as an inhibitor of the respiratory activity in the heart and liver of rats was 12,13-epoxy-9-hydroperoxy-10-octadecenoate.³⁷ 9,10-Epoxy-12-octadecenoate, also named leukotoxin, was found in human burned skin and in lung lavages in patients with adult respiratory distress syndrome.^{14,38} It was shown to have a highly toxic effect on cellular

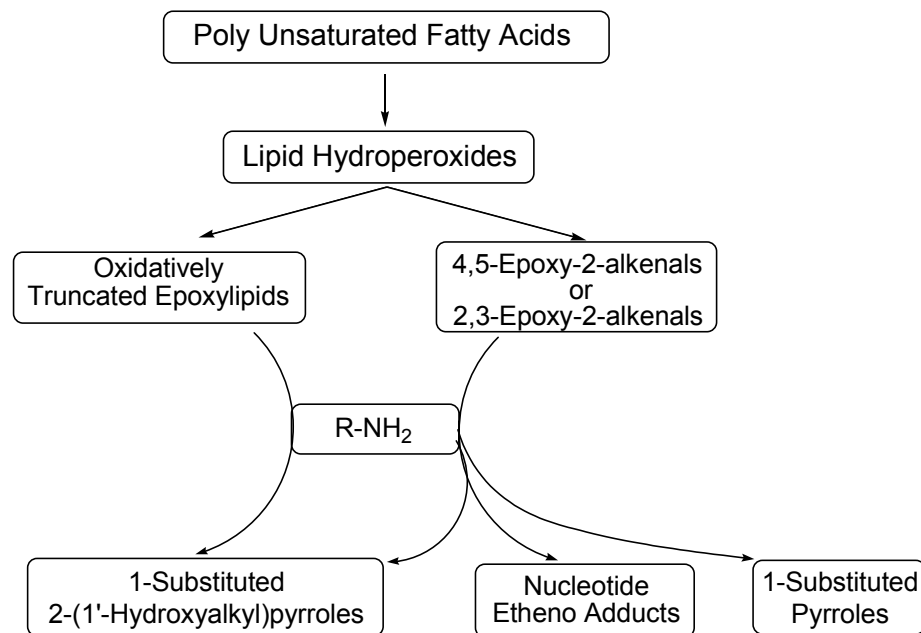
function (hence its name).³⁶ 9,10-Epoxy-12-octadecenoate exhibits anti-tumor and anti-fungal effects,²¹ but it also has a highly toxic effect on mitochondria³⁹ and depresses cardiac function.³⁶ Leukotoxin is biosynthesized in mammalian cells by a microsomal P-450-linked monooxygenase, called epoxygenase.²¹ Leukotoxin can be hydrolyzed to hydroxy acids by the cytosolic or microsomal epoxide hydrolases.³⁹

1.3. Second Generation Epoxides Derived from Polyunsaturated Lipids

The second generation of epoxy lipids, refers to epoxy lipids that result from fragmentation of the initial lipid backbone (Scheme 1.4). A large body of work describes the epoxides involved in the decomposition of foods.⁶⁻¹¹ There are mainly two types of truncated epoxy lipids: 2,3-epoxy alkanals and 4,5-epoxy-2-alkenals. The aldehydes are more stable than their putative intermediate free radical precursors and, therefore, can diffuse from the place of their formation, reach and attack both intracellular and extracellular targets. The targets can be distant from the initial free radical oxidative occurrence. Therefore, these oxidative fragmentation products might be considered a type of “second toxic messenger”.⁴⁰ As presented in Scheme 1.5, they can react with amino groups in other biomolecules. The products of such alkylation reactions may be implicated in the pathology of diseases.⁴¹⁻⁴³

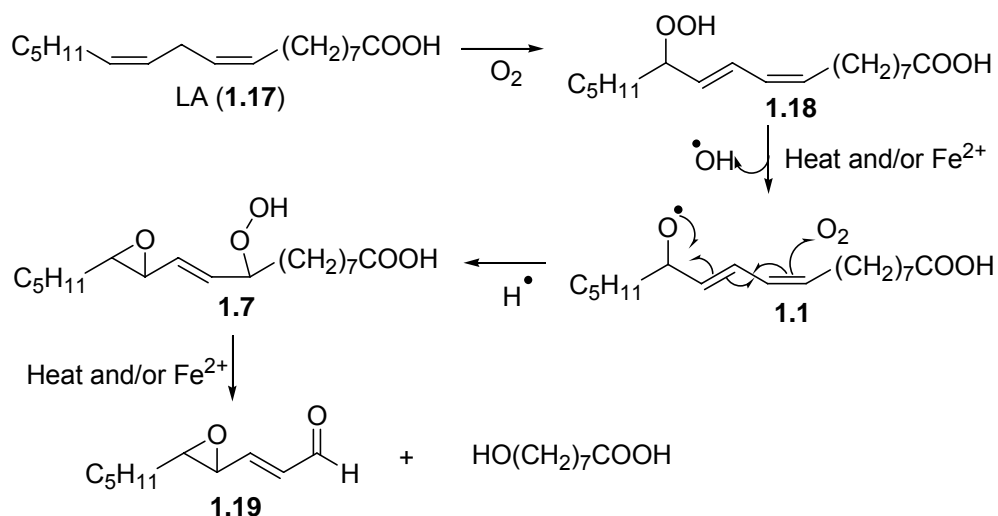


Scheme 1.4. General mechanism for the formation of the epoxy alkenals.¹⁶



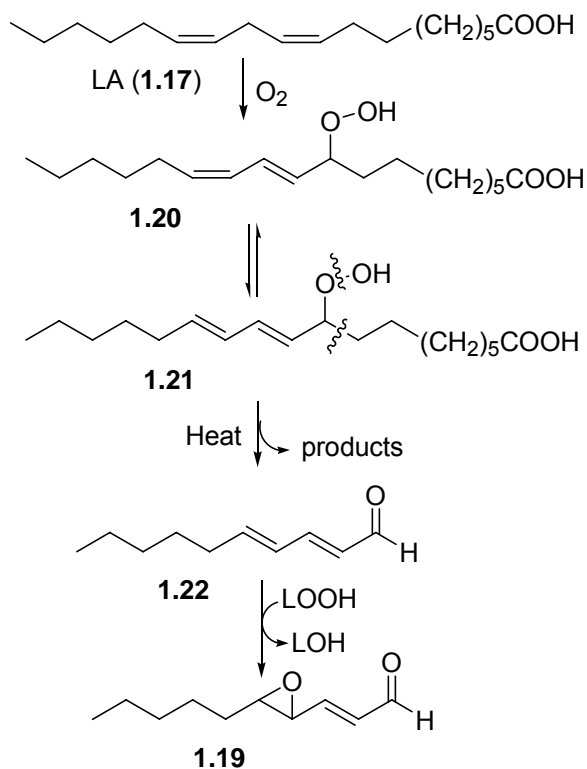
Scheme 1.5 General pathways for the formation and further transformations of epoxy alkenals.⁴⁴

1.3.1. Formation of epoxyalkenals. The epoxyalkenals were first observed in model systems^{7,10,45} and some fat containing foods.⁹ *Trans*-4,5-epoxy-(*E*)-hept-2-enal, reported in 1978,⁹ was the first example of this class of oxidatively-truncated lipid. The same chemistry that results in the formation of this epoxy alkenal should generate a family of 4,5-epoxy-2-alkenals from various different PUFAs. Two plausible routes have been proposed for the generation of 4,5-epoxy-2-alkenals. One (Scheme 1.6) envisions the decomposition of an epoxy hydroperoxide intermediate **1.7**.¹⁰ The conventional free-radical scission mechanism was further confirmed by the same authors.⁷ They heated the pure epoxy hydroperoxides synthesized by epoxidation of only one hydroperoxy acid (in this case, 13-HPODE, **1.18**) to induce molecular decomposition, and identified *trans*-4,5-epoxy-2*E*-decenal (**1.19**). This method is believed to result in a cascade of homolytic reactions that will lead in the end to the β -scission of the radicals and the carbons chain will be cleaved.⁷



Scheme 1.6 A pathway for the formation of *trans*-4,5-epoxy-2(*E*)-decenal (**1.19**) from the linoleic acid proposed by Gardner and Selke.⁷

Another route that can result in the generation of **1.19** (Scheme 1.7) involves the formation of 2,4-decadienal (**1.22**) as a key intermediate.⁶

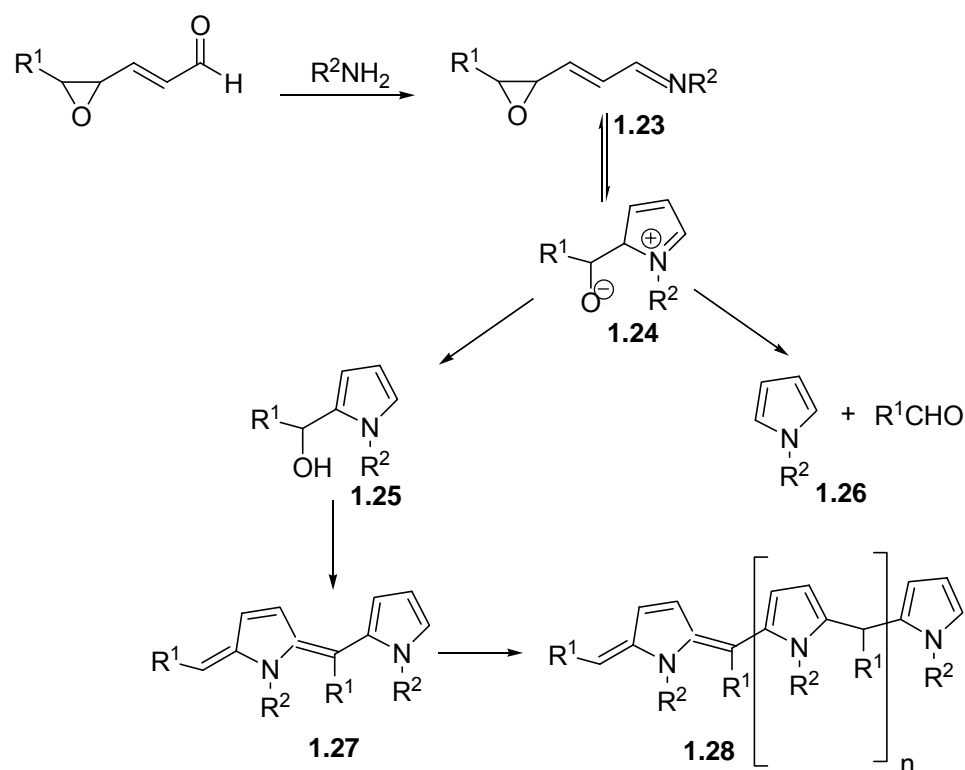


Scheme 1.7 Formation of *trans*-4,5-epoxy-2(E)-decenal (**1.19**) by peroxidation of (E,E)-deca-2,4-dienal (**1.22**) according to Gassenmeier and Schieberle.⁶

Other analogous epoxy aldehydes, found in various foods, include 4,5-epoxy-2(E)-heptenal,^{7,10,45} 4,5-epoxy-2(E)-nonenal^{46,47}, 4,5-epoxy-2(E)-decenal,^{7,10} and 2,3-epoxyoctanal.^{23,46} Although no analogous truncated epoxy alkenal phospholipids have been reported, there is no obvious reason why the mechanisms that lead to generating **1.19** would not produce such phospholipids.

1.3.2. Reactions of the epoxy-alkenals with biological nucleophiles.

The possibility that the aldehyde group of oxidatively truncated lipids could react with amino groups in biomolecules was noted above (see Scheme 1.5). It was reported that the 4,5-epoxy-2-alkenals react with the lysine amino group⁴⁸ and with histidine residues.⁴² They can also modify amino groups in DNA bases^{23,49} and in phosphatidylethanolamine.¹⁶ Two types of pyrrole derivatives are produced in the reaction with primary amines: N-substituted 2-(1-hydroxyalkyl)pyrroles **1.25** and N-substituted pyrroles **1.26** (Scheme 1.8).⁵⁰



Scheme 1.8 Polycondensation products from epoxyalkenals and amino compounds.¹⁶

The N-substituted pyrroles formed from the reaction of epoxy alkenals with phosphatidylethanolamine are relatively stable. As yet, they have been identified

only in food products.⁵¹ Pyrrole derivatives have been identified in oxidized LDL,^{52,53} and they are abundant in blood plasma from patients with renal disease or atherosclerosis and are present in atherosclerotic plaques.¹⁴ However, they were believed to be formed from the reaction of HNE with primary amines.¹⁴ The N-substituted 2-(1-hydroxyalkyl)pyrroles (**1.25**) “are unstable and polymerize spontaneously producing dimers, trimers, tetramers and in the end, lipofuscin-like pyrroles” (**1.28**).^{54,16} Lipofuscin consists of autofluorescent lysosomal storage bodies that accumulate in many tissues during senescence, also known as age-pigment.⁵⁵ More studies are needed to determine the different affinities of the epoxy aldehydes for proteins or phosphatidylethanolamine. The understanding of these processes may be of value for designing therapeutic measures to prevent the pathological modifications that lead to numerous health problems.^{48,56,57}

Studies of the reaction of epoxy alkenals with amino phospholipids *in vitro*¹⁶ indicate that these lipids can compete with proteins for adduction by the oxidatively truncated lipids. However further studies, especially *in vivo*, would be relevant to be carried out in order to achieve a conclusion about the relative rates of reaction with various amino compounds available in the organism, taking into account also the relative distribution of these biomolecules.¹⁶

The attack of bifunctional lipids such as epoxides on DNA bases produces etheno adducts (Figure 1.1).⁵⁸⁻⁶⁰ Etheno adducts have been found in DNA from healthy human tissues,⁶⁰ but the levels were increased in inflammatory conditions.⁶¹ These observations suggested that such DNA adducts could have an important role in diseases associated with inflammatory conditions. There are

also reports^{62,63,64} noting that all etheno (ϵ)-adducts are “potentially mutagenic *in vivo*.” Although there are various repair enzymes that might remove the ϵ -adducts from the genome,⁵⁸ in some cases accumulations will occur (see also Figure 1.2).

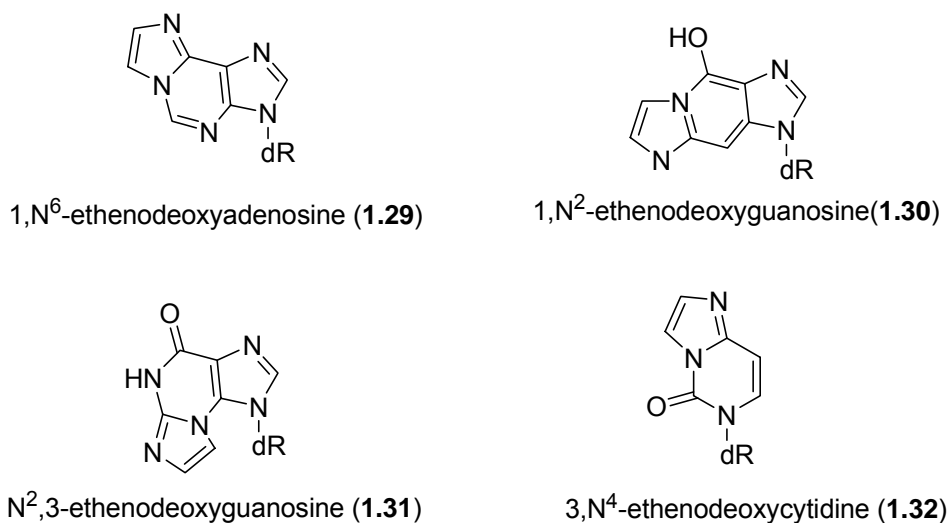


Figure 1.1 Chemical structure of some exocyclic DNA adducts.

The connection between elevated levels of reactive oxygen (and nitrogen) species (ROS) and several types of cancers is well established.⁶¹ Recently, it also was reported that the levels of etheno-DNA adducts in pancreas, breast, or cancer-prone^{65,66} patients are also significantly higher than in healthy individuals. This prompted the development of *in vivo* methods of detection, and these adducts were proposed as biomarkers for oxidative stress and lipid peroxidation, and implicitly with utility for prevention and diagnosis of cancer. The authors outlined a hypothesis for the role of *persistent* oxidative stress on lipids in promotion and progression of carcinogenesis, as illustrated in Figure 1.2.

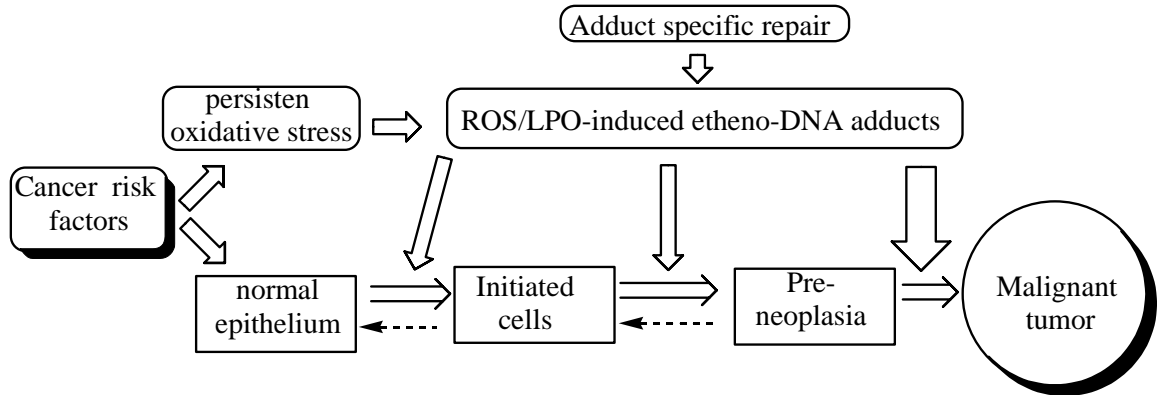


Figure 1.2. Hypothetical scheme implicating persistent oxidative stress as a major event in the development and progression of malignant cells.⁶¹

External or genetic risk factors trigger the production of ROS, which convert lipids to oxidatively truncated products such as epoxy alkenals. These species react with DNA to generate the promutagenic etheno-adducts. When the load of this oxidative damage exceeds the ability of repair enzymes to replace the mutagenic genes, the rates of mutations are increased leading eventually to malignant cells and tumors.

1.4 References

- (1) Horrocks, L. A.; Farooqui, A. A. *Prostaglandins, Leukot. Essent. Fatty Acids* **2004**, *70*, 361-372.
- (2) Trigatti, B. L.; Krieger, M.; Rigotti, A. *Arterioscler. Thromb. Vasc. Biol.* **2003**, *23*, 1732-1738.
- (3) Corwin, R. L. *Prostaglandins, Leukotrienes and Essential Fatty Acids* **2003**, *68*, 379-386.
- (4) Januszewski, A. S.; Alderson, N. L.; Metz, T. O.; Thorpe, S. R.; Baynes, J. W. *Biochem. Soc. Trans.* **2003**, *31*, 1413-1416.
- (5) Spiteller, G. *Med. Hypoth.* **2003**, *60*, 69-83.
- (6) Gassenmeier, K.; Schieberle, P. *J. Am. Oil Chem. Soc.* **1994**, *71*, 1315-1319.
- (7) Gardner, H. W.; Selke, E. *Lipids* **1984**, *19*, 375-380.
- (8) List, G. R.; Hoffman, R. L.; Moser, H. A.; Evans, C. D. *J. Am. Oil Chem. Soc.* **1967**, *44*, 485-7.
- (9) Swoboda, P. A.; Peers, K. E. *J. Sci. Food Agric.* **1978**, *29*, 803-807.
- (10) Selke, E.; Rohwedder, W. K.; Dutton, H. J. *J. Am. Oil Chem. Soc.* **1980**, *1*, 25-30.
- (11) Buettner, A. *J. Agric. Food Chem.* **2004**, *52*, 2339-2346.
- (12) Chio, K. S.; Tappel, A. L.; Imagawa, T. *Biochem.* **1969**, *8*, 2827-32.
- (13) Hartley, D. P.; Kroll, D. J.; Petersen, D. R. *Chem. Res. Toxic.* **1997**, *10*, 895-905.

- (14) Salomon, R. G.; Kaur, K.; Podrez, E.; Hoff, H. F.; Krushinsky, A. V.; Sayre, L. M. *Chem. Res. Tox* **2000**, *13*, 557-64.
- (15) Spiteller, G. *Chem. Phys. Lipids* **1998**, *95*, 105-162.
- (16) Zamora, R.; Hidalgo, F. J. *Chem. Res. Toxicol.* **2003**, *16*, 1632-1641.
- (17) Deng, Y. H.; Salomon, R. G. *J. Org. Chem.* **1998**, *63*, 7789-7794.
- (18) Podrez, E. A.; Batyreva, E.; Shen, Z.; Zhang, R.; Deng, Y.; Sun, M.; Gugiu, B. G.; Finton, P. J.; Shen, L.; Febbraio, M.; Hayn, M.; Silverstein, R. L.; Hoff, H. F.; Salomon, R. G.; Hazen, S. L. *J. Biol. Chem.* **2002**, 38517-23.
- (19) Podrez, E. A.; Poliakov, E.; Shen, Z.; Zhang, R.; Deng, Y.; Sun, M.; Finton, P. J.; Shan, L.; Febbraio, M.; Hajjar, D. P.; Silverstein, R. L.; Hoff, H. F.; Salomon, R. G.; Hazen, S. L. *J. Biol. Chem.* **2002**, *277*, 38517-23.
- (20) Esterbauer, H.; Gebicki, J.; Puhl, H.; Jurgens, G. *Free Radic. Biol. Med.* **1992**, *13*, 341-90.
- (21) Ozawa, T.; Nishikimi, M.; Sugiyama, S.; Taki, T.; Hayakawa, M.; Shionoya, H. *Biochem. Int.* **1988**, *16*(2), 369-73.
- (22) Dudda, A.; Kobelt, F.; Spitelers, G. *Chem. Phys. Lipids* **1996**, *82*, 39-45.
- (23) Lee, S. H.; Oe, T.; Blair, I. A. *Chem. Res. Toxicol.* **2002**, *15*, 300-304.
- (24) Kuhn, H. *Prog. Lipid Res.* **1996**, *35*, 203-26.
- (25) Reinaud, O.; Delaforge, M.; Boucher, J. L.; Rocchiccioli, F.; Mansuy, D. *Biochem. Biophys. Res. Commun.* **1989**, *161*, 883-91.

- (26) Garssen, G. J.; Vliegthart, J. F. G.; Boldingh, J. *Biochem. J.* **1971**, *122*, 327-332.
- (27) Hamberg, M. *Adv. Prostaglandin Thromboxane Leukotrienes Res.* **1990**, *21A*, 117-124.
- (28) Gardner, H. W.; Weisleder, D.; Plattner, R. D. *Plant Physiol.* **1991**, *97*, 1059-1072.
- (29) Gardner, H. W.; Kleiman, R. *Biochim. Biophys. Acta* **1981**, *665*, 113-24.
- (30) Gardner, H. W.; Weisleder, D.; Kleiman, R. *Lipids* **1978**, *13*, 246-52.
- (31) Gardner, H. W.; Kleiman, R.; Weisleder, D. *Lipids* **1974**, *9*, 696-706.
- (32) Garssen, G. J.; Veldink, G. A.; Vliegthart, J. F. G.; Boldingh, J. *Europ. J. Biochem.* **1976**, *62*, 33-6.
- (33) Dix, T. A.; Marnett, L. J. *J. Am. Chem.Soc.* **1983**, *105*, 7001-7002.
- (34) Walther, U.; Spitteller, G. *Fett. Wissenschaft Technologie* **1993**, *95*, 472-4.
- (35) Meyer, W.; Spitteller, G. *Liebigs Ann. Chem.* **1993**, *12*, 1253-6.
- (36) Ozawa, T.; Sugiyama, S.; Hayakawa, M.; Taki, F.; Hanaki, Y. *Biochem. Biophys. Res. Comm.* **1988**, *152*, 1310-18.
- (37) Imagawa, T.; Kasai, S.; Matsui, K.; Nakamura, T. *J. Biochem.* **1982**, *92*, 1109-1121.

- (38) Sakai, T.; Ishizaki, T.; Nakai, T.; Miyabo, S.; Matsukawa, S.; Hayakawa, M.; Ozawa, T. *Free Radic. Biol. Med.* **1996**, *20*, 607-612.
- (39) Ozawa, T.; Hayakawa, M.; Takamura, T.; Sugiyama, S.; Suzuki, K.; Iwata, M.; Taki, F.; Tomita, T. *Biochem. Biophys. Res. Com.* **1986**, *134*, 1071-1078.
- (40) Esterbauer, H.; Schaur, R. J.; Zollner, H. *Free Radic. Biol. Med.* **1991**, *11*, 81-128.
- (41) Toyokuni, S.; Uchida, K.; Okamoto, K.; Hattori-Nakakuki, Y.; Hiai, H.; Stadtman, E. R. *Proc. Natl. Acad. Sci. USA* **1994**, *91*, 2616-20.
- (42) Zamora, R.; Alaiz, M.; Hidalgo, F. J. *Chem. Res. Toxicol.* **1999**, *12*, 654-660.
- (43) Hidalgo, F. J.; Zamora, R. *Chem. Res. Toxicol.* **2000**, *13*, 501-508.
- (44) Zamora, R.; Hidalgo, F. J. *Biochim. Biophys. Acta* **1995**, *1258*, 319-327.
- (45) Frankel, E. N.; Neff, W. E.; Selke, E. *Lipids* **1981**, *16*, 279-85.
- (46) Buettner, A.; Schieberle, P. *J. Agric. Food Chem.* **2001**, *49*, 3881-3884.
- (47) Gardner, H. W.; Hamberg, M. *J. Biol. Chem.* **1993**, *268*, 6971-7.
- (48) Spickett, C. M.; Rennie, N.; Winter, H.; Zambonin, L.; Landi, L.; Jerlich, A.; Schaur, R. J.; Pitt, A. R. *Biochem. J.* **2001**, *355(Pt 2)*, 449-57.
- (49) Lee, S. H.; Oe, T.; Blair, I. A. *Science* **2001**, *292*, 2083-2085.
- (50) Zamora, R.; Hidalgo, F. J. *Lipids* **1994**, *29*, 243-249.
- (51) Zamora, R.; Alaiz, M.; Hidalgo, F. J. *J. Agric. Food Chem.* **1999**, *47*, 1942-1947.

- (52) Kaur, K.; Salomon, R. G.; O'Neil, J.; Hoff, H. F. *Chem. Res. Tox.* **1997**, *10*, 1387-96.
- (53) Podrez, E. A.; Hoppe, G.; O'Neil, J.; Sayre, L. M.; Sheibani, N.; Hoff, H. F. *J. Lipid Res.* **2000**, *41*, 1455-1463.
- (54) Hidalgo, F. J.; Zamora, R. *J. Biol. Chem.* **1993**, *268*, 16190-16197.
- (55) Katz, M. L.; Robison, W. G. *Archiv. Geront. Geriat.* **2002**, *34*, 169-184.
- (56) Berliner, J. A.; Subbanagounder, G.; Leitinger, N.; Watson, A. D.; Vora, D. *Trends. Cardiovasc. Med.* **2001**, *11*, 142-7.
- (57) Bochkov, V. N.; Kadl, A.; Huber, J.; Gruber, F.; Binder, B. R.; Leitinger, N. *Nature* **2002**, *419*, 77-81.
- (58) Gros, L.; Ishchenko, A. A.; Sapparbaev, M. *Mutation Res.* **2003**, *531*, 219-229.
- (59) el Ghissassi, F.; Barbin, A.; Nair, J.; Bartsch, H. *Chem. Res. Tox.* **1995**, *8*, 278-283.
- (60) Nair, J.; Barbin, A.; Guichard, Y.; Bartsch, H. *Carcinogenesis* **1995**, *16*, 613-7.
- (61) Bartsch, H.; Nair, J. *Toxicol.* **2000**, *153*, 105-114.
- (62) Pandya, G. A.; Moriya, M. *Biochem.* **1996**, *35*, 11487-92.
- (63) Levine, R. L.; Yang, I. Y.; Hossain, M.; Pandya, G. A.; Grollman, A. P.; Moriya, M. *Cancer res.* **2000**, *60*, 4098-104.
- (64) Cheng, K. C.; Preston, B. D.; Cahill, D. S.; Dosanjh, M. K.; Singer, B.; Loeb, L. A. *Proc. Natl.Acad.Sci. USA* **1991**, *88*, 9974-8.

- (65) Nair, J.; Barbin, A.; Velic, I.; Bartsch, H. *Mut. Res.* **1999**, *424*, 59-69.
- (66) Boothman, D. A.; Geller, A. I.; Pardee, A. B. *FEBS Lett.* **1989**, *258*, 159-62.

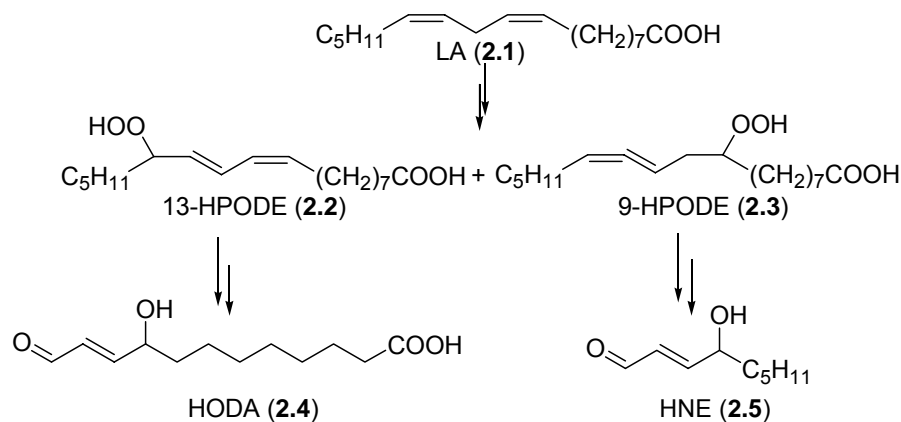
Chapter 2

Total Synthesis and Natural Occurrence of a Phospholipid that is Analogous with the Genotoxic Aldehyde 4,5-Epoxy-2E-decenal

2.1. Background

Linoleic acid is the most abundant polyunsaturated fatty acid (PUFA) in the human body.¹ Truncated phospholipids containing aldehyde functionality, and the corresponding acids, are generated by oxidative cleavage of linoleyl phospholipids. These lipid peroxidation products contribute to the pathogenesis of numerous chronic² and degenerative diseases including cardiovascular diseases, cancer, immune-system decline, brain dysfunction and cataracts.³

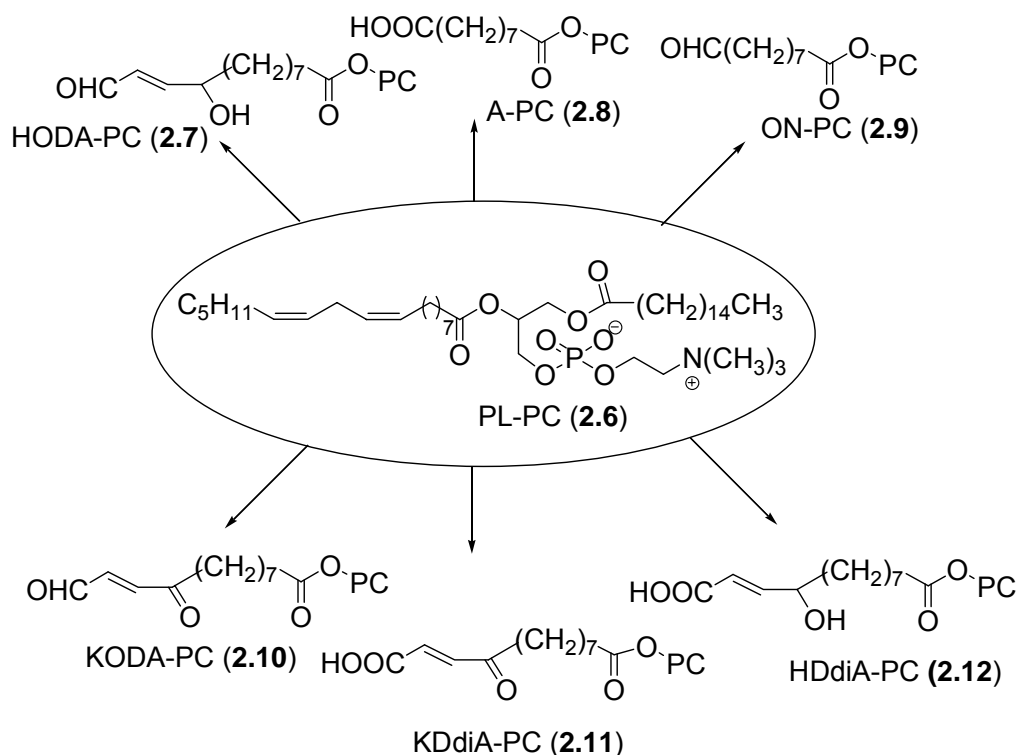
Hydroperoxides can be derived from linoleic acid (LA, **2.1**) both enzymatically and nonenzymatically. Cell injury can initiate lipid peroxidation, leading to generation of oxidation products through nonenzymatic reactions, induced by free radicals. 9(*S*)-Hydroperoxy-(*Z,E*)-9,11-octadecadienoic acid (9-HPODE, **2.3**) is produced by the action of cyclooxygenases 1 and 2.⁴ It is a precursor of 4-hydroxynon-2-enal (HNE, **2.5**) (Scheme 2.1). Various lipoxygenases enantioselectively transform linoleic acid into the hydroperoxide isomers, 9-HPODE (**2.3**) 13-HPODE (**2.2**)⁵ while free radical-induced oxidation delivers racemic hydroperoxides.



Scheme 2.1 Formation of HODA (**2.4**) from the 13-HPODE (**2.2**) by analogy with the formation of HNE (**2.5**) from 9-HPODE (**2.3**).

Previous studies in the Salomon group, based on analogy with the free radical-induced oxidative generation of HNE (**2.5**), demonstrated the formation of a phospholipid analogue of HNE, 9-hydroxy-12-oxo-10-dodecenoic acid (HODA, **2.4**) from linoleic acid (Scheme 2.1).⁶ It was further proposed that the HODA ester of 2-lysophosphatidylcholine (PC), HODA-PC (**2.7**), would undergo chemistry analogous to that of HNE and would have biological activity. The availability of abundant supplies of HODA (**2.4**) and its PC ester (**2.7**) by total synthesis was valuable for testing these hypotheses.

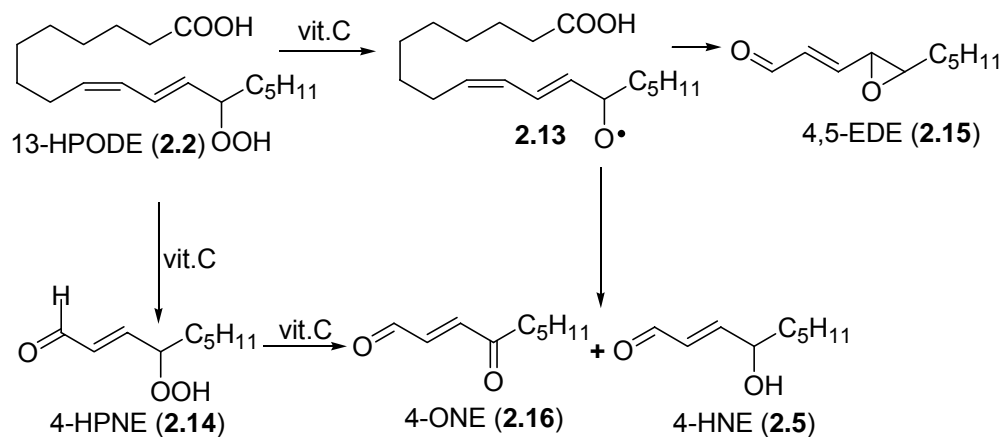
The Salomon group has synthesized many other oxidized phospholipids (Scheme 2.2) to test hypotheses about the oxidation products that might be derived from the linoleic acid ester of 2-lyso-phosphatidylcholine (PL-PC, **2.6**).



Scheme 2.2. Some oxidation products from PL-PC.

The availability of adequate amounts of all these oxidized phospholipids, prepared by unambiguous total synthesis, allowed for their biological activity to be studied. The Salomon group and collaborators demonstrated that the keto-aldehyde (KODA-PC, **2.10**), the keto acid (KDdiA-PC, **2.11**) and the hydroxy acid (HDdiA-PC, **2.12**) (Scheme 2.2) are components of the bioactive product fractions from myeloperoxidase (MPO)-mediated oxidation of PL-PC (**2.6**).⁷ These oxidized phospholipids (oxPCs) are also ligands for the scavenger receptor CD36 and may mediate the recognition of oxidized low-density lipoprotein (oxLDL) by macrophages. The keto acid (KDdiA-PC, **2.11**) is the most active. These compounds are enriched in atherosclerotic lesions in rabbits.⁸ Together, these observations suggest that the oxidized lipids may promote foam cell formation from macrophages by oxLDL endocytosis by the receptor CD36.⁸

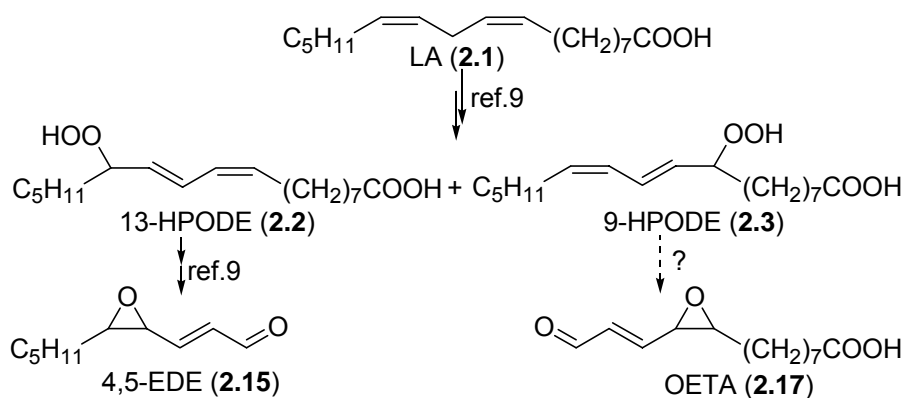
Other groups are also studying the oxidation products from linoleic acid. Blair et. al⁹ reported that vitamin C promotes the formation of 4,5-epoxy-2(*E*)-decenal (4,5-EDE, **2.15**) *in vitro* from 13-(*S*)-hydroperoxy-(*Z,E*)-9,11-octadecadienoic acid (13-HPODE, **2.2**) under oxidative conditions (Scheme 2.3). Blair's



Scheme 2.3. Formation of 4,5-EDE (**2.15**) from 13-HPODE (**2.2**).⁹

experiments⁹ showed that vitamin C levels comparable to the intracellular concentration reached with a dose of 200 mg per day - the recommended daily dose of vitamin C for healthy adults - could give rise to substantial amounts of DNA damage *in vivo* through the known reaction of 4,5-EDE with DNA¹⁰

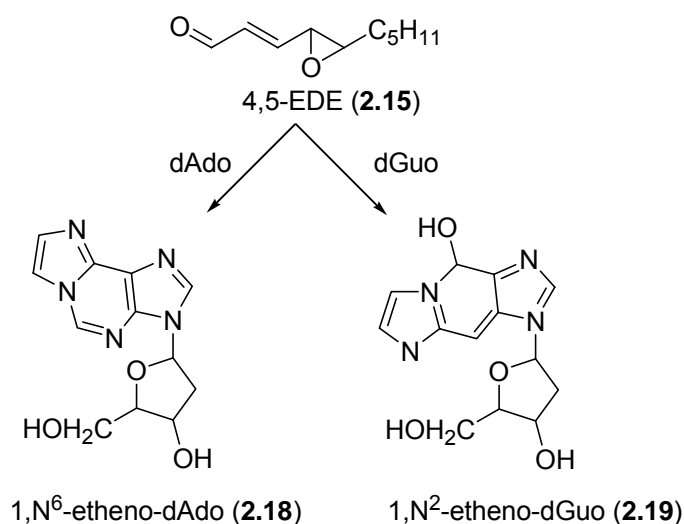
Since 4,5-EDE (**2.15**) is produced *in vitro* from the 13-HPODE (**2.2**)⁹, we reasoned that an analogous compound, i.e., 13-oxo-9,10-epoxytridecenoic acid (OETA, **2.17**) should result from 9-HPODE (**2.3**), via similar oxidative pathways (Scheme 2.4). In this case, there should also be a phospholipid analogue, because linoleic acid and compounds derived from it by oxidative stress (see also Scheme 2.2) exist as phospholipid esters *in vivo*. Therefore, we expected oxidative cleavage of 9-HPODE-PC to produce the corresponding ester of OETA (**2.17**), OETA-PC (**2.20**).



Scheme 2.4. Formation of OETA (**2.17**) from the 9-HPODE (**2.3**).

In a more recent study,¹¹ the Blair group demonstrated clearly that 4,5-EDE (**2.15**) forms etheno adducts (*vide infra*) with deoxy-adenosine (dAdo) and deoxy-guanosine (dGuo) (Scheme 2.5). These results provided a significant correlation between a product of lipid peroxidation and a mutagenic DNA lesion.

The etheno-adducts of DNA, when formed *in vivo*, are normally repaired. However, in diseased individuals, these lesions are not repaired and subsequent DNA replication leads to mutations¹² or apoptosis.¹³ Mutations in protooncogenes and tumor suppressor genes have been directly implicated in human cancer.¹² Etheno adducts are mutagenic. They have been detected in human tissue samples.¹⁴ An unsubstituted etheno-dAdo adduct **2.18** was shown to arise from the reaction of 4,5-EDE (**2.5**) with dAdo (Scheme 2.5).



Scheme 2.5. Formation of the etheno-adducts from 4,5-EDE (**2.15**).

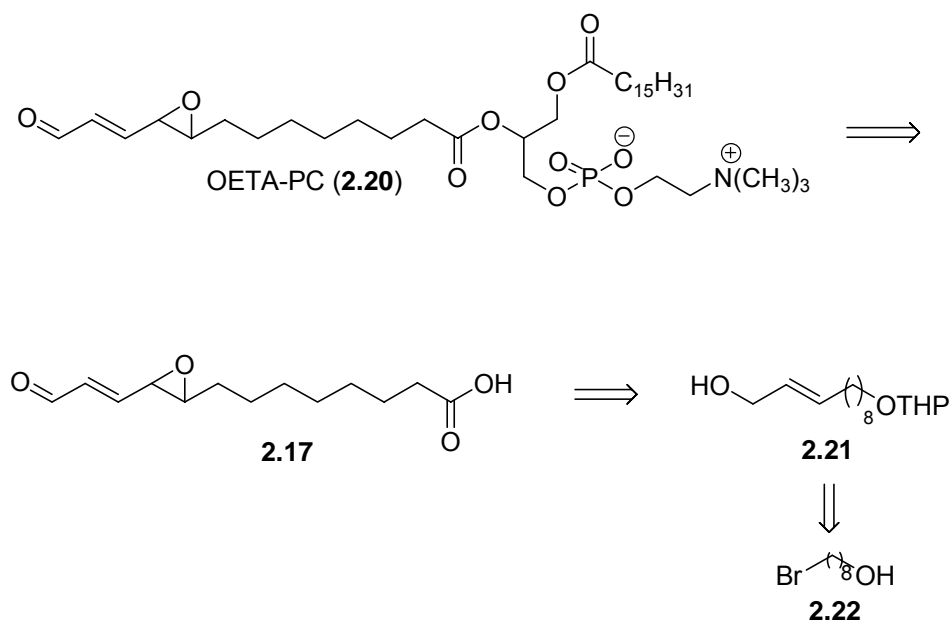
In this chapter the practical total synthesis of OETA-PC, as well as its generation from PL-PC and its detection *in vivo* will be described. In addition, *in vitro* experiments performed in our collaborator Ian Blair's group demonstrated that *trans*-OETA-PC forms DNA adducts as predicted by analogy with the chemistry of 4,5-EDE (**2.15**). These data are presented here as well.

2.2. Results and Discussion

2.2.1. Synthesis of 1-palmitoyl-2- (13-oxo-9,10-*trans*-epoxy-octadeca-11-enoyl)-*sn*-glycero-3-phosphatidylcholine (*trans*-OETA-PC, **2.20).** To facilitate studies of the generation, chemistry and biology of *trans*-OETA-PC (**2.20**) we engaged in a synthetic program targeting this product. The route established is short and utilizes straightforward steps that are easy to execute.

Trans-OETA-PC (**2.20**) was envisioned to arise from the acid **2.17** via an esterification reaction with commercially available lyso-phosphatidylcholine (lyso-PC). Intermediate **2.17** could be generated from an allylic alcohol **2.21** by epoxidation of the *E* double bond and chain homologation (Scheme 2.6). In turn, intermediate **2.21** might be assembled through alkylation of propargyl alcohol with a hydroxyl protected derivative of the commercially available bromohydrin

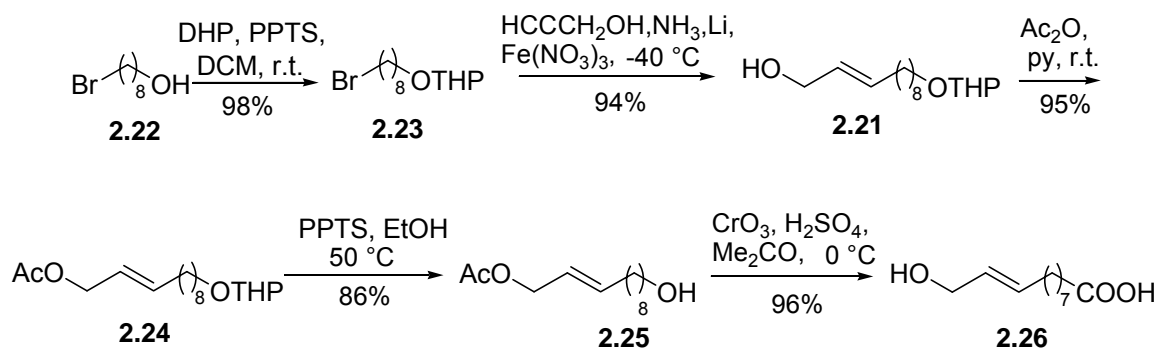
2.22.



Scheme 2.6. Retrosynthesis of *trans*-OETA-PC (**2.20**).

Previously, Goerger and Hudson¹⁵ published the synthesis of parinaric acid, starting from 9-decen-1-ol. In five rather elaborate steps, they obtained the intermediate **2.21**. Starting from the bromo-alcohol **2.22**, we arrived at the same intermediate, in only 2 steps, with a 92% overall yield. The very convenient, one pot reaction developed by Patterson¹⁶ for the conversion of terminal acetylenic alcohols into (*E*)-olefinic alkenols, succeeded when we used a 2:1 ratio of the propargyl alcohol to the electrophile **2.23**, to generate the allylic alcohol **2.21**. This protocol produced exclusively the *E* isomer of **2.21** (Scheme 2.7) as expected.

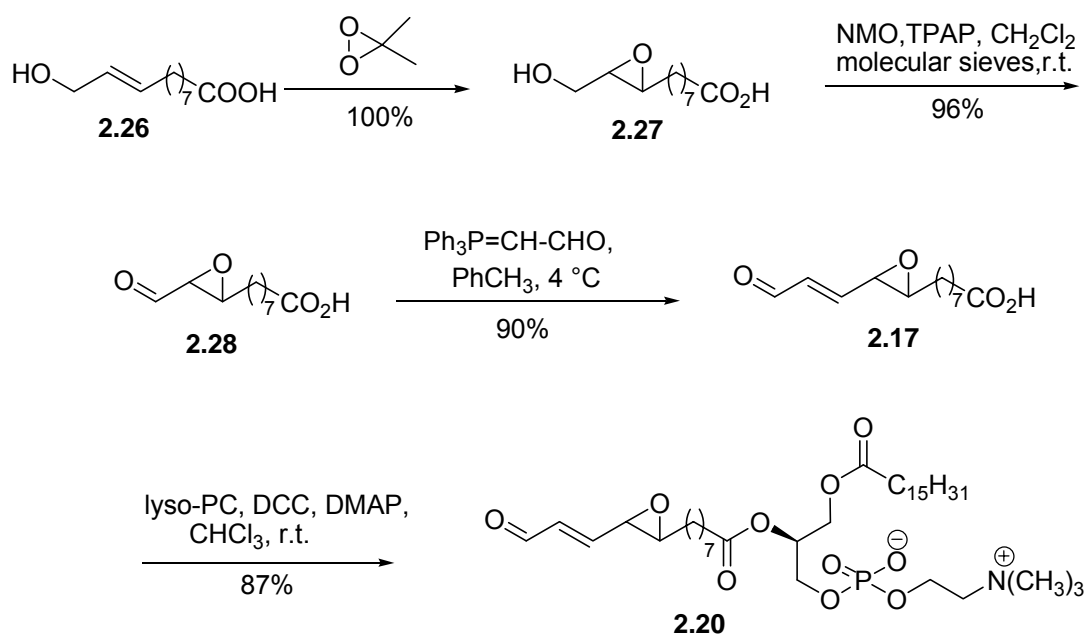
The allylic hydroxyl of **2.21** was protected as an acetate and the primary alcohol was deprotected to **2.25** via established procedures^{17,35} (Scheme 2.7). The alcohol **2.25** was then oxidized and deprotected during workup to provide the *seco*-acid **2.26** in one step, as the only product (by NMR). The conversion of the intermediate acetoxy acid to the hydroxyl acid **2.26** was the serendipitous result of acidifying the reaction mixture to pH 1 using 6M HCl. This catalyzed solvolysis of the allylic acetate group.



Scheme 2.7. Synthesis of hydroxy-acid intermediate **2.26**.

In anticipation of the Wittig homologation (see Scheme 2.8), we had envisioned a route involving protection of the acid with simultaneous hydrolysis of the allylic acetate.¹⁸ We decided, however, to carry on with the acid **2.26**, saving thus two steps. Protection of the acid functionality as an ester proved indeed to be unnecessary.¹⁹

Epoxidation of alcohol **2.26** was performed initially with a system composed from commercially available oxone, acetone and water, but the recovery of the product was difficult, and the yields were modest (52-64%). When carried out with a freshly prepared²⁰ solution of dioxirane in acetone, the reaction was completed in 30 minutes at room temperature to give pure epoxide **2.27** quantitatively, after removing the solvents and volatile byproducts under reduced pressure.



Scheme 2.8. Synthesis of *trans*-OETA-PC (**2.20**).

Oxidation of the free alcohol in **2.27** with TPAP/NMO²¹ proceeded in excellent yield to afford the aldehyde **2.28** in sufficiently high purity after a simple filtration through a short silica gel plug. The homologated aldehyde (\pm)-OETA (**2.17**) was obtained in good yield from the aldehyde-epoxy-acid **2.28** by a Wittig reaction at 4 °C when the reaction was allowed to proceed for 3 days.²² The DMAP/DCC-promoted coupling of the acid **2.17** with commercially available lyso-phosphatidilcholine (lyso-PC) gave the final product **2.20** in 87% yield, after reacting for 10 days at room temperature.

2.2.2. Production of *trans*-OETA-PC (2.20) *in vitro* from PL-PC (2.6).

To demonstrate that OETA-PC **2.20** can be produced by oxidation of unsaturated phospholipids *in vitro*, PL-PC liposomes were oxidized under various reaction conditions. In one experiment, the liposomes were irradiated with 350 nm UV light in phosphate-buffered saline (PBS) at room temperature in the air. In parallel experiments PL-PC liposomes were oxidized with copper (II) or peroxyxynitrate produced from a myeloperoxidase (MPO)-NO₂⁻-glucose/glucose oxidase system.²³ To minimize transition metal-induced oxidation, the buffer was supplemented with a metal chelator, diethylenetriaminepentaacetic acid (DTPA). The oxidation reaction mixture was sampled at various times. Catalase was added to quench the reactions by removing hydroperoxides from the samples. To prevent further autoxidation of the samples during processing and storage, butylated hydroxytoluene (BHT) was also added. Lipids were extracted using a

slightly modified Bligh and Dyer method²⁴ as described in the experimental part, dried under a nitrogen stream at room temperature, stored under argon in the dark at -80 °C until they were analyzed (usually not more than 24 h). The extracts were analyzed by LC/ESI-MS/MS. Preliminary identification of product peaks was achieved by comparing retention times with authentic samples. The authentic sample of *trans*-OETA-PC (**2.20**), synthesized as described above, was characterized by high-resolution mass spectrometry and multinuclear NMR. Positive ion ESI-MS/MS analysis of the authentic lipid yielded both parent and daughter ions that were used as the specific mass transition ion pairs in LC/ESI-MS/MS analysis. A common daughter ion m/z 184 was produced in all samples, as found for all other phosphatidylcholines detected previously in our lab. The retention time and the parent/daughter ion pair were collectively used to identify a peak in the oxidation reaction product mixture chromatographs.

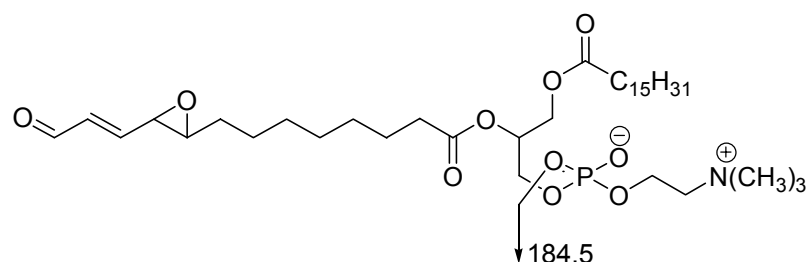


Figure 2.1. Mass spectrometric fragmentation of *trans*-OETA-PC (**2.20**).

Oxidized PL-PC liposomes from all three experiments produced the expected oxidatively truncated OETA-PC (**2.20**) (Figure 2.2) in various yields. A single peak with a retention time that is identical to the *trans*-OETA-PC (**2.20**) standard (Figure 2.2 A) is present in the multiple reaction monitoring (MRM)

chromatogram of PL-PC oxidation product mixtures (Figure 2.2 B) demonstrating the generation of *trans*-OETA-PC (**2.20**) in these oxidation experiments.

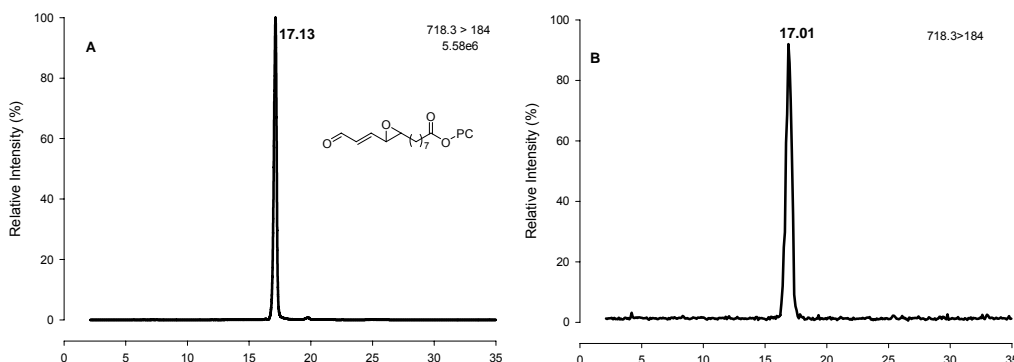


Figure 2.2. LC/ESI-MS/MS analysis of OETA-PC from oxidized PL-PC liposomes. **A.** Synthetic *trans*-OETA-PC (**2.20**) standard (parent m/z 718.3), MRM chromatogram (daughter m/z 184.5); **B.** *trans*-OETA-PC detected in oxidized PL-PC liposomes, MRM chromatogram (718.3 \rightarrow 184.5)

A solution of PL-PC (100 ng) in 50 μ L of methanol was irradiated with 350 nm UV light and then chromatographed on a Prodigy ODS C18 column (150 \times 2 mm, 5 μ m, Phenomenex, Torrance, CA) with a binary solvent gradient, starting from 100% water for the first 5 min, then a linear change to 100% methanol in 15 min, 100% methanol hold for 20 min at a flow rate of 0.2 mL/min. All the mobile phase solvents were supplied with 0.2% formic acid to enhance the MS signal. Mass transitions of interest were monitored by a Micromass Quattro Ultima triple quadrupole mass spectrometer. A collision energy of 25 V, a cone voltage of 30 V, and an electrospray capillary voltage of 30 kV were used.

To further confirm the identity of the peaks detected, the product mixtures of oxidation of PL-PC liposomes were treated with methoxylamine hydrochloride to derivatize the aldehyde functional group.

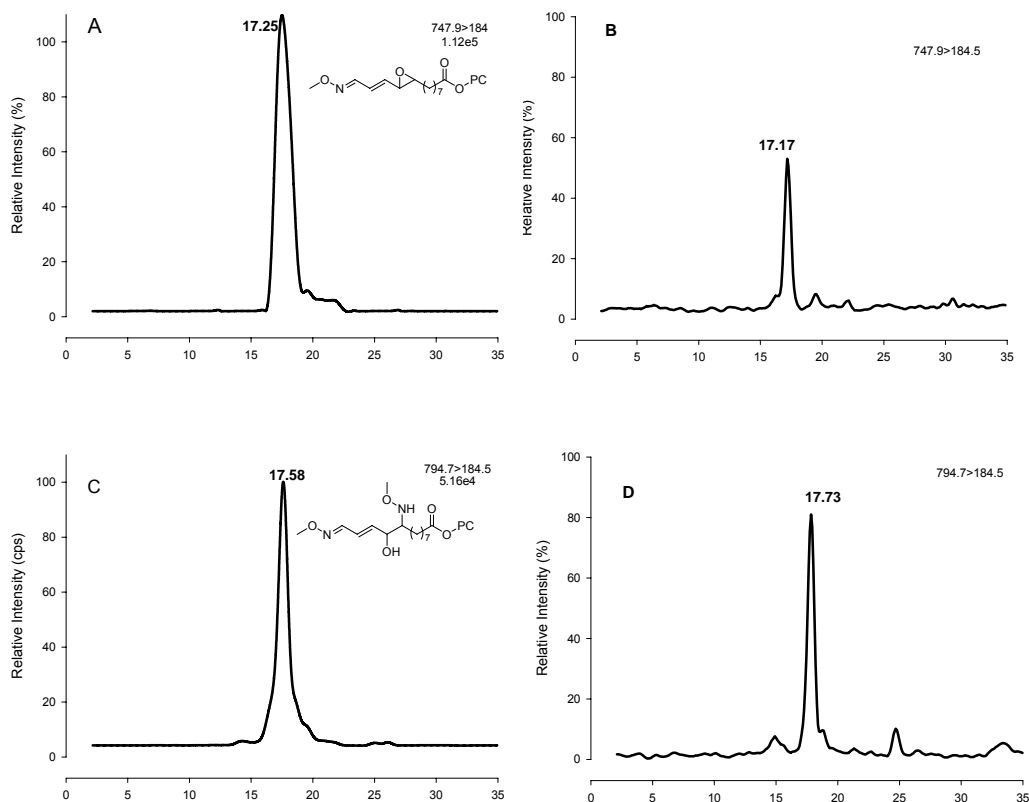


Figure 2.3. LC/ESI-MS/MS analysis of OETA-PC derivatives. **A.** The methoxime of OETA-PC standard (parent m/z 747.9), MRM chromatogram (daughter m/z 184); **B.** The methoxime of OETA-PC detected in derivatized oxidized PL-PC liposomes, MRM chromatogram (747.9 \rightarrow 184.5) **C.** The bis-methoxime of OETA-PC standard (parent m/z 794.7), MRM chromatogram (daughter m/z 184); **D.** The bis-methoxime of OETA-PC detected in derivatized oxidized PL-PC liposomes, MRM chromatogram (794.7 \rightarrow 184.5)

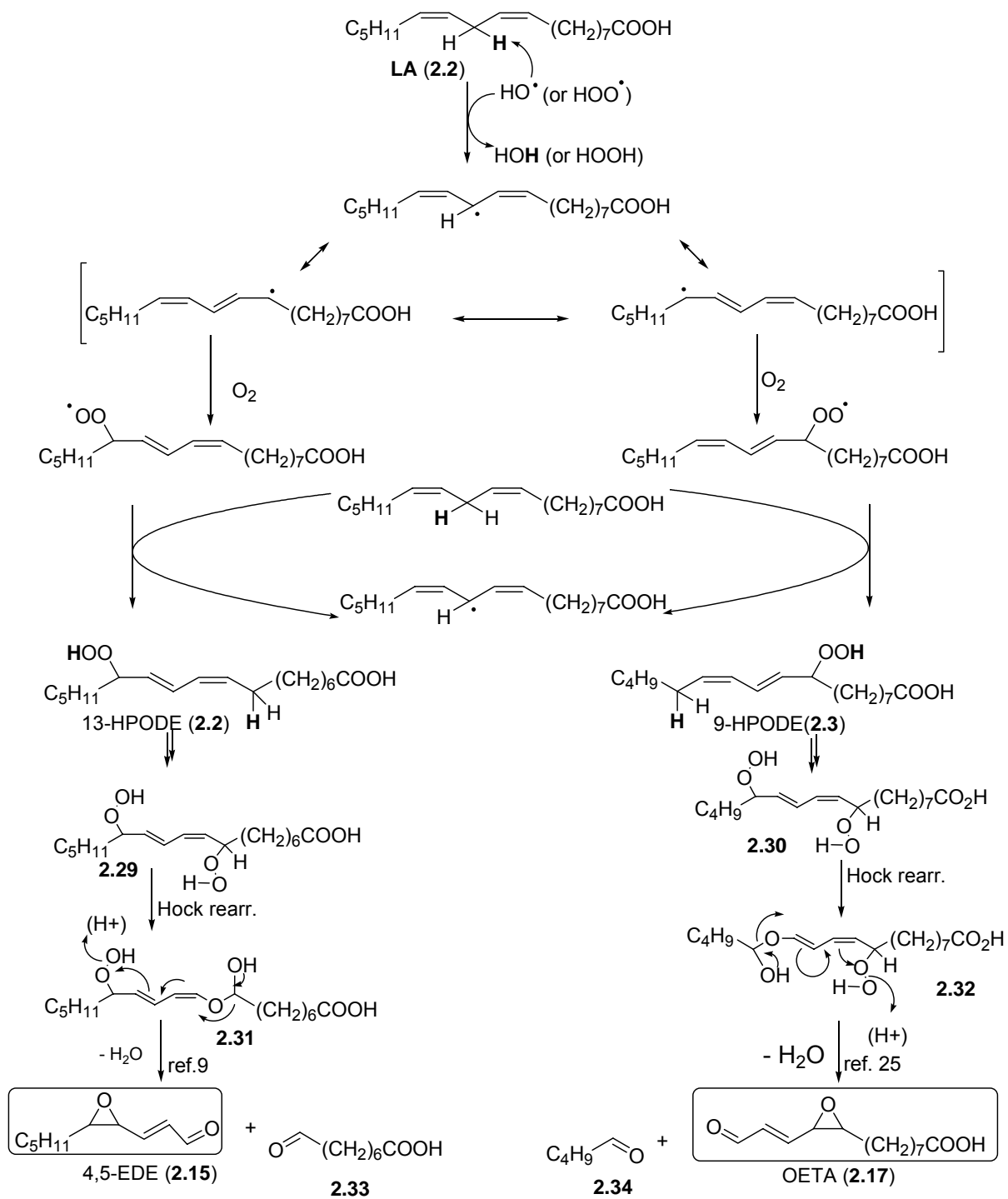
Methoxime derivatization of a single aldehyde or ketone carbonyl results in a net mass increase of 29Da. Methoxime derivatives of pure *trans*-OETA-PC (**2.20**) were prepared to provide authentic samples for analyzing product mixtures from PL-PC oxidation. Each derivative was purified using a C18 mini-column and then analyzed by LC-MS in the positive ion mode. Methoxime derivatization of the synthetic standard of *trans*-OETA-PC (**2.20**) resulted in the expected m/z 747.9, which correspond to a methoxime modification (29 Da) of the aldehyde group of *trans*-OETA-PC (m/z 718.3) (Figure 2.3.A). In addition, an unexpected bis-methoxylamine derivative (m/z 794.7) was produced, in which both the aldehyde and the epoxy group of *trans*-OETA-PC **2.20** are modified by methoxylamine (Figure 2.3 C).

Both derivatives display a common daughter ion m/z 184.5 ($C_5H_{15}NO_4P$, see Appendix). The bis-methoxime derivative of OETA-PC is presumably generated through opening of the epoxy functionality under the derivatization conditions. Typical MRM chromatograms of oxidized PL-PC liposomes after derivatization are presented in Figure 2.2. Before derivatization, no peaks corresponding to derivatized standards were observed. After derivatization, new peaks corresponding to derivatized standards appeared with a parallel loss of the peak corresponding to *trans*-OETA-PC (**2.20**).

A plausible free radical-induced mechanism to account for generation of the epoxy aldehydes 4,5-EDE (**2.15**)⁹ and OETA (**2.17**)²⁵ is presented in Scheme 2.9. Exposure of linoleic acid (**2.1**), or similarly PL-PC, to oxidants generated in the respiratory cascade *initiates* the process by a hydrogen atom abstraction

from the bis-allylic position to generate a pentadienyl radical that, upon oxidation with molecular oxygen, forms two hydroperoxy radicals (see Scheme 2.9). These highly reactive species enter a *propagation* cycle by abstracting hydrogen from a new molecule of linoleic acid (**2.1**) to give hydroperoxides 13-HPODE (**2.2**) and 9-HPODE (**2.3**). We propose that **2.2** and **2.3** can enter another oxidation cycle, similar with the one just described, to generate the bis-hydroperoxides **2.29** and **2.30**, respectively. These bis-hydroperoxides can undergo Hock rearrangements²⁶ of either one of their hydroperoxide (–OOH) groups. The intermediates shown, **2.31** and **2.32**, are those that give rise to the epoxides **2.15** and **2.17**, respectively. Decomposition of the unstable enol-hemiacetal moiety in these intermediates, in tandem with epoxide formation/water elimination would result in **2.15** and **2.17**, respectively. If the proposed mechanism is valid, the other epoxides should also be generated from **2.29** and **2.30**, respectively, via a similar Hock rearrangement/ decomposition sequence starting from the other –OOH groups (pathways not shown). Efforts to identify the bis-hydroperoxides *in vitro* are currently underway in our laboratory.

There are other possible mechanisms by which the epoxide formation can take place, especially *in vivo* where some members of the cytochrome P-450 enzyme group can catalyze the epoxidation of the fatty acids.²⁷⁻²⁹



Scheme 2.9. Possible mechanism for the formation of OETA (2.17).

2.2.3. Evolution profiles of OETA-PC from oxidation of PL-PC.

Quantification of *trans*-OETA-PC (2.20) in reaction product mixtures from

oxidation of PL-PC was achieved by LC/ESI-MS/MS in the positive ion mode using the MRM function. Appropriate $[M+H]^+$ and a common daughter ion m/z 184 were monitored. Calibration curves were produced using the synthetic authentic sample of **2.20** and the commercially available PL-PC. Accurate determination of the amounts of these phospholipids were determined by a microphosphorous assay (see experimental part). Standard curves were generated by incorporating a fixed amount of 1,2-dimyristoyll-*sn*-glycero-3-phosphatidylethanolamine (DM-PE) as internal standard and various amounts of the analyte, and plotting peak area ratio versus analyte mol ratio. Trace amounts of *trans*-OETA-PC (**2.20**) were detected in the commercial PL-PC. The amounts of *trans*-OETA-PC (**2.20**) detected in the commercial PL-PC were subtracted from the values of the oxidation product.

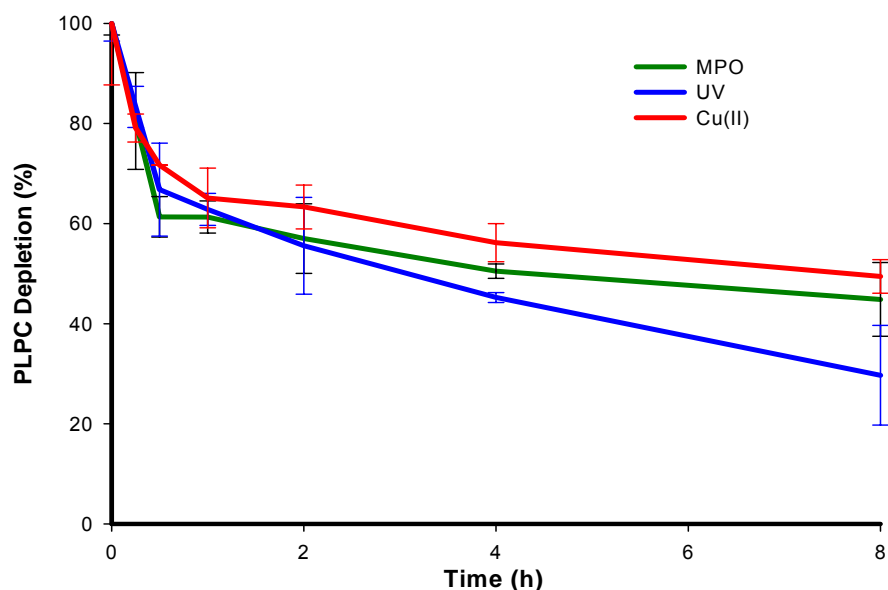


Figure 2.4. Consumption of PL-PC (**2.6**) under various oxidation conditions. Data are the average of two sets of independent experiments.

The consumption of PL-PC was greatest under UV light, but the yield of *trans*-OETA-PC (**2.20**) was higher when the vesicles were oxidized with the MPO-NO₂⁻-glucose/glucose oxidase system.

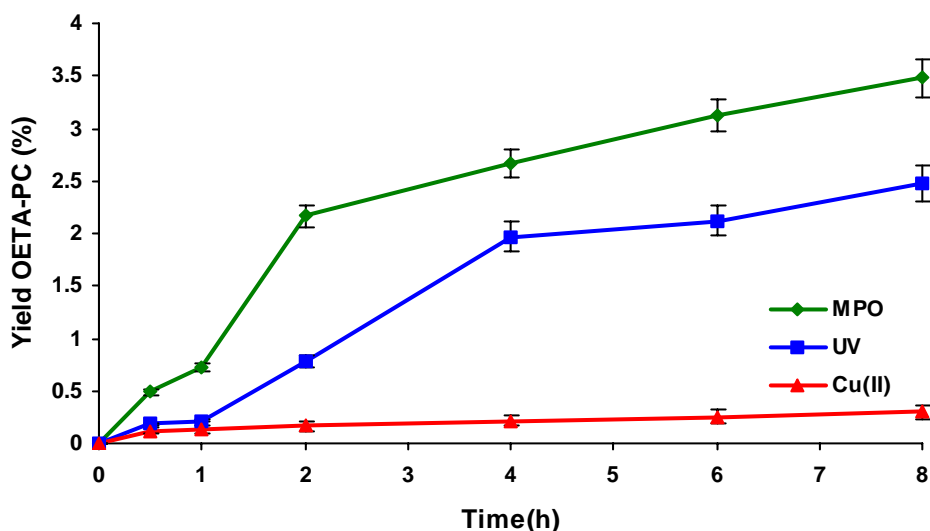


Figure 2.5. Evolution profile for production of OETA-PC (**2.20**) from aerial oxidation of PL-PC liposomes promoted by Cu(II), UV or MPO at 37 °C. Quantification was achieved with LC/ESI-MS/MS. The yields were calculated by dividing the amount of each analyte by the amount of starting PL-PC. Data are the average of two sets of independent experiments.

The product evolution profiles for oxidation promoted by the MPO-NO₂⁻-glucose/glucose oxidase system and UV are similar, rising steadily in the first two hours and more slowly afterwards. The Cu(II) oxidation resulted in a much lower yield of *trans*-OETA-PC (**2.20**). This may be because Cu(II) not only catalyzes the oxidation of PL-PC (**2.6**) but also promotes further oxidation of *trans*-OETA-PC (**2.20**) to other products, e.g., the corresponding carboxylic acid. Table 2.1

shows the maximum yields for *trans*-OETA-PC (**2.20**) produced by different oxidation methods.

Table 2.1 Observed maximum yields of OETA-PC from PL-PC oxidized under various reactions conditions.

	MPO	UV	Cu(II)
<i>Trans</i>-OETA-PC (%)	3.4	2.4	0.2

2.2.4. Quantification of *trans*-OETA-PC (2.20**) in rat retina.** Because many reports indicated that light damage induces the peroxidation of polyunsaturated fatty acids (PUFA) in retina, we expected that the peroxidation of PL-PC, the PC ester of PL, in retina would produce OETA-PC (**2.20**) as found in our *in vitro* experiments. Other oxidized phosphatidylcholines (oxPC), derived from PL-PC, were identified previously in rat retina by Dr. Sun in our laboratory.³⁰ In order to examine if OETA-PC (**2.20**) is present in intact retinas, retinas harvested by Mary Rayborn, Dr. Xiarong Gu, and Jiayin Gu from albino rats were analyzed by LC/ESI-MS/MS. The retinas from five rats were harvested. To prevent contamination by blood, or *in vitro* oxidation, the retinas were rinsed with a saline antioxidant cocktail (PBS, DTPA, and BHT). The retinas were immediately homogenized manually in a plastic vial using a stainless steel pestle coated with Teflon. Lipid extraction (see Experimental Procedures) using the procedure of Bligh and Dyer²⁴ was then performed immediately after homogenization. The extracted lipids were analyzed by LC/ESI-MS/MS in the

positive ion mode. After removing the solvents, the residue was redissolved in chloroform:methanol (1:1) and 1/5 of the sample was injected into the LC-MS. *Trans*-OETA-PC (**2.20**) and the standard DM-PE were monitored simultaneously in an experiment performed by Dr. Bogdan Gugiu.³¹ Figure 2.6 B is the MRM chromatogram showing the presence of *trans*-OETA-PC (**2.20**) in rat retina. The retention time (17.1 min), parent ion and daughter ion were collectively used to identify LC/ESI-MS/MS peak by comparison with the authentic standard (Figure 2.6.A) as described previously for the generation of *trans*-OETA-PC (**2.20**) by *in vitro* oxidation of PL- PC.

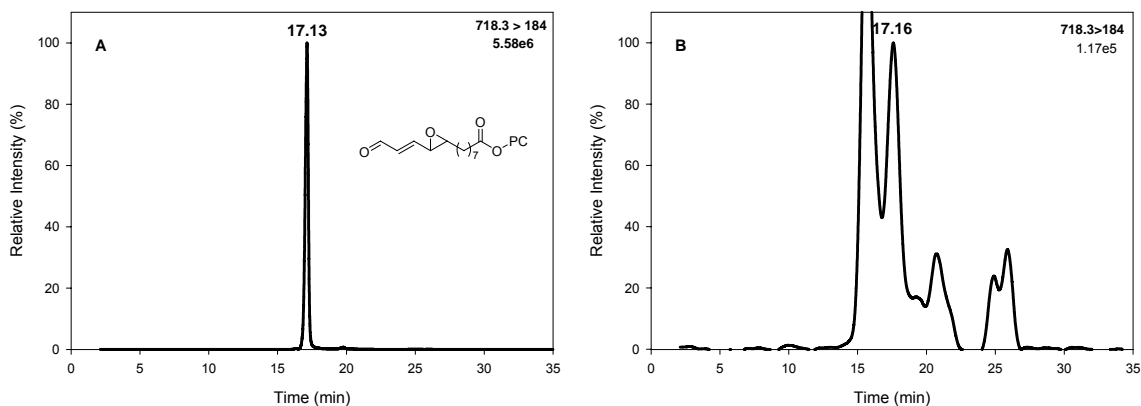


Figure 2.6. LC/ESI-MS/MS detection of OETA-PC (**2.20**) (718.3>184.5) from rat retina. (A) Synthetic standard **2.20**. (B) Rat retina extract.

Multiple peaks are present in the chromatogram of the rat retina sample. A peak at 17.16 min has the same retention time and MRM as the authentic **2.20** (Figure 2.6.B). The other peaks in Figure 2.6B are unidentified PCs – because they produce a 184.5 Da fragment – that are isomeric with OETA-PC. To further

verify the structure of the HPLC peak presumed to be **2.20**, the sample from the rat retina was derivatized with methoxylamine hydrochloride (Figure 2.7).

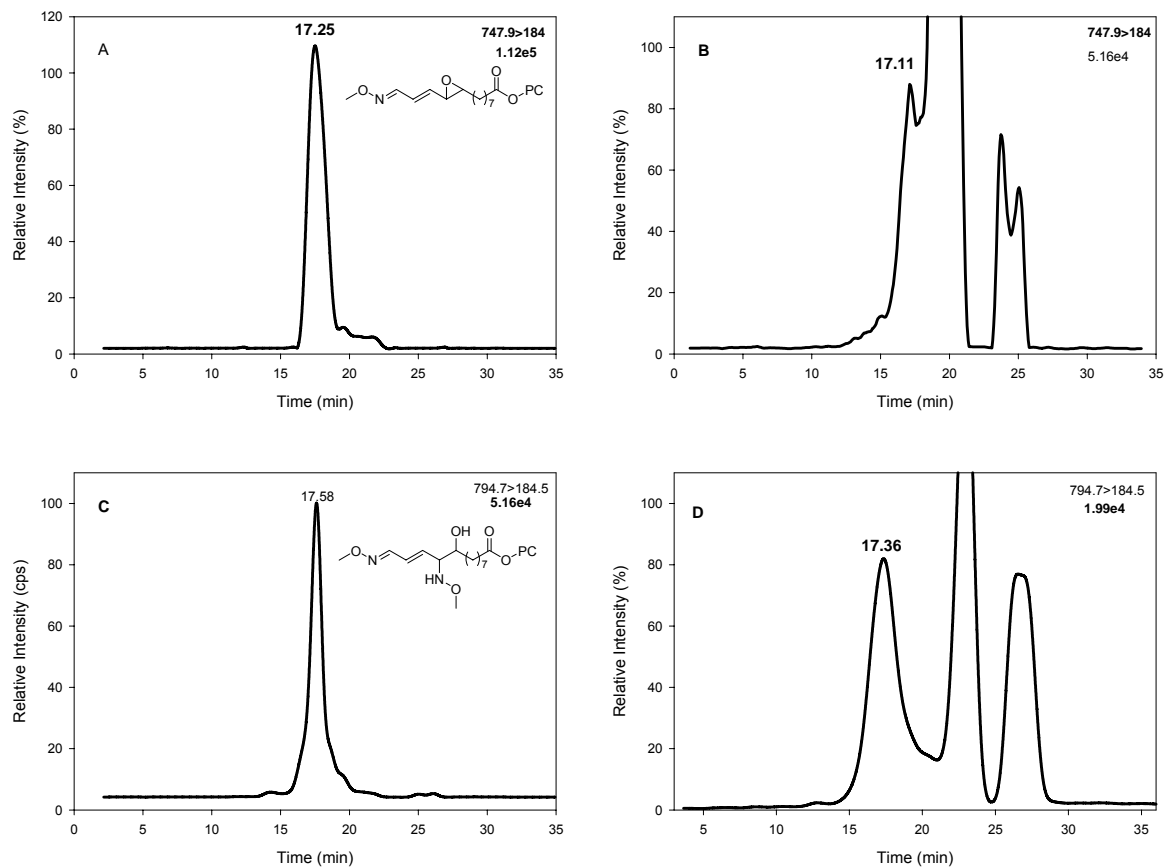


Figure 2.7. LC/ESI-MS/MS detection of OETA-PC derivatives (747.9>184.5 and 794.7>184.5) from rat retina. **A.** The methoxime of OETA-PC standard (parent m/z 747.9), MRM chromatogram (daughter m/z 184); **B.** The methoxime of OETA-PC detected in the derivatized rat retina, MRM chromatogram (747.9 \rightarrow 184.5). **C.** The bis-methoxime of OETA-PC standard (parent m/z 794.7), MRM chromatogram (daughter m/z 184); **D.** The bis-methoxime of OETA-PC detected in the derivatized rat retina, MRM chromatogram (794.7 \rightarrow 184.5).

Methoxime derivatization of a single aldehyde results in a net increase of 29 Da as already mentioned. The chromatogram of a monomethoxime derivative of pure *trans*-OETA-PC **2.20**, prepared as described in the previous paragraph, is presented in Figure 2.7A. A peak in the chromatogram of the derivatized rat retina extract exhibited the same retention time MRM as the derivatized standard (Figure 2.7.B). Before derivatization no peaks corresponding to the derivatized standard appeared. After derivatization new peaks appeared with a concomitant disappearance of the peak of the *trans*-OETA-PC **2.20**.

The absolute amounts of OETA-PC **2.20** detected in 5 rats are presented in Table 2.2. The values were calculated employing the calibration curve and extraction coefficient (determined by LC/ESI-MS/MS as described in the experimental part). For details on statistical data analysis see the Appendix.

Table 2.2 Amounts of OETA-PC (**2.20**) in rat retina.

Animal	OETA-PC (pmol) average*
1	0.27±0.01
2	0.42±0.32
3	0.47±0.30
4	0.20±0.03
5	0.30±0.08

The average amount of *trans*-OETA-PC (**2.20**) in rat retina, 0.33 pmol, is relatively low, compared to oxPCs derived from DHA-PC, e.g., HOHA-PC (2.5 pmol) or KOHAPC (1.7 pmol). In part, this is because PL-PC is present in lower amounts³⁰ than DHA-PC in the rat retina (see Table 2.3).

Table 2.3. Amounts of some phospholipids detected in rat retina ³⁰.

Phospholipid	Absolute amount (nmol)
PA-PC	2.64±0.32
PL-PC	2.06±0.32
DHA-PC	7.0±0.24
HOHA-PC	.0025±0.0023
KOHA-PC	.0017±0.0012

2.2.5. Nucleotide etheno adduct formation by OETA-PC. These experiments were performed by Dr. Seon Hwa Lee from University of Pennsylvania

Reaction with dGuo. A solution of *trans*-OETA-PC (**2.20**) was added to deoxyguanosine (dGuo) or deoxyadenosine (dAdo) in Chelex-treated phosphate buffer and the mixture was incubated for 48 h at 60 °C. LC/APCI/MS analysis of the reaction product mixture from dGuo after 48 h revealed the presence of one major adduct together with residual dGuo. The dGuo adduct eluted at retention time of 15.5 min in system 1 (Figure 2.8). Its APCI mass spectrum revealed an intense MH⁺ at *m/z* 292, together with a BH₂⁺ ion at *m/z* 176. MS² analysis MH⁺ (*m/z* 292) resulted in a BH₂⁺ product ion at *m/z* 176. These LC/MS characteristics are identical to those for authentic 1,*N*²-etheno-dGuo.¹¹

Reaction with dAdo. LC/APCI/MS analysis of the reaction mixture from dAdo after 48 h using gradient system 1 revealed the presence of one dAdo adduct (retention time: 21.0 min) together with residual dAdo at a retention time: 12.8 min (Figure 2.9). The LC/MS characteristics of this adduct were identical to authentic 1,*N*⁶-etheno-dAdo.¹¹ Its mass spectrum exhibited an intense MH⁺ at

m/z 276, together with a BH_2^+ ion at m/z 160. MS^2 analysis of MH^+ m/z 276 gave rise to exclusive formation of the BH_2^+ product ion at m/z 160.

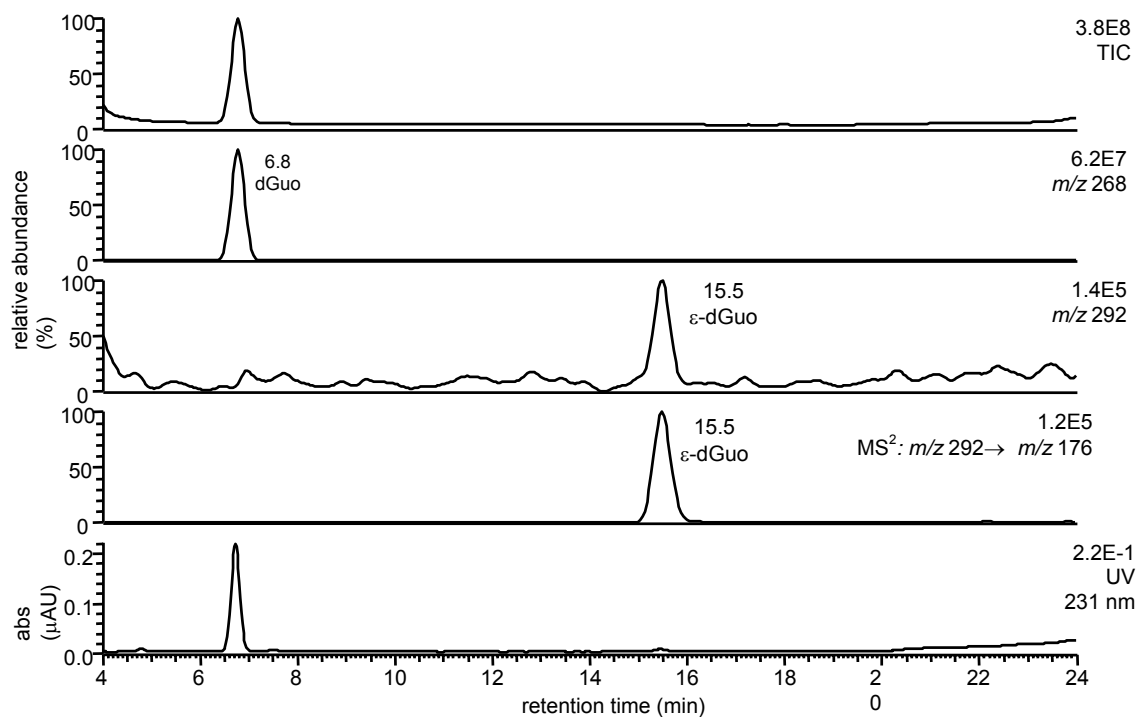


Figure 2.8. LC/APCI/MS analysis of reaction between *trans*-OETA-PC (**2.20**) and dGuo at 60 °C for 48 h.

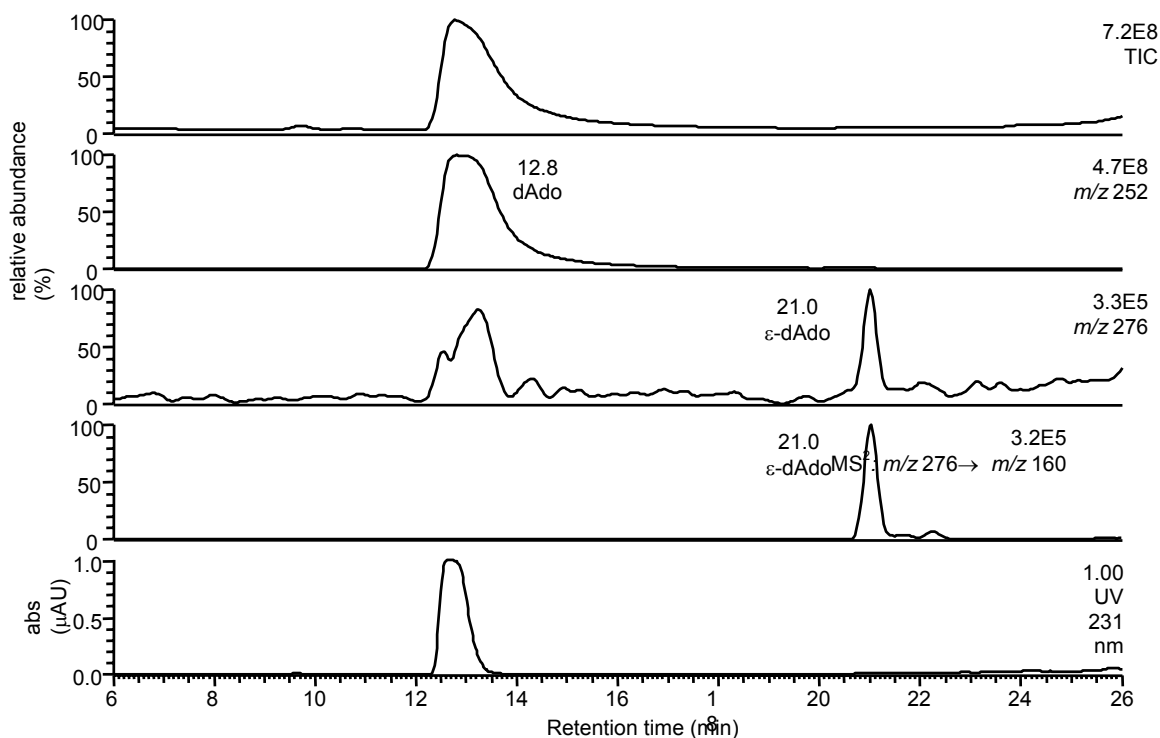


Figure 2.9. LC/APCI/MS analysis of reaction between *trans*-OETA-PC (**2.20**) and dAdo at 60 °C for 48 h.

Formation of Etheno-dGuo and Etheno-dAdo in Calf-Thymus DNA.

Calf-thymus DNA was treated with an approximately equimolar amount of *trans*-OETA-PC (**2.20**). The DNA was then hydrolyzed with a mixture of DNase I, nuclease P1 and alkaline phosphatase in MOPS buffer. These hydrolysis conditions were shown to give essentially quantitative recovery of normal DNA bases. Modified DNA-bases were separated from normal bases using the SPE procedure described in the Experimental section. Etheno-dGuo and etheno-dAdo were detected in the DNA hydrolysate (Figure 2.10). Based on a 71 % recovery through the extraction and hydrolysis procedure, the signals for etheno-dGuo and

etheno-dAdo corresponded to 3.5 and 5.5 adducts/ 10^7 normal bases, respectively.

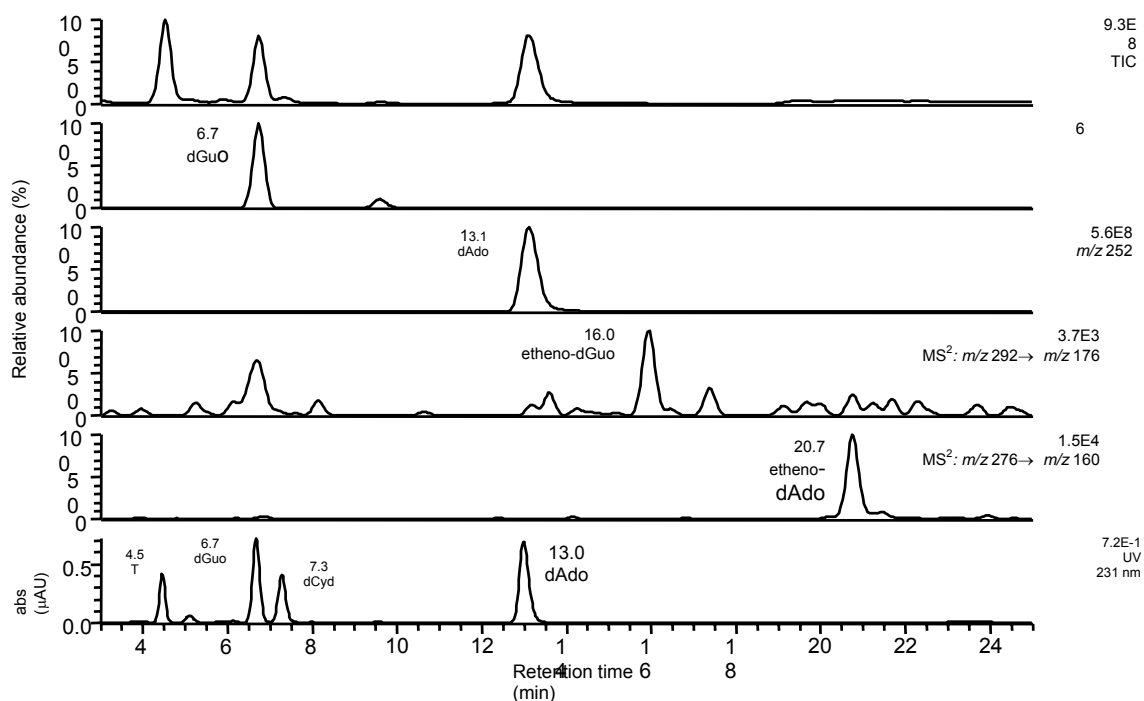
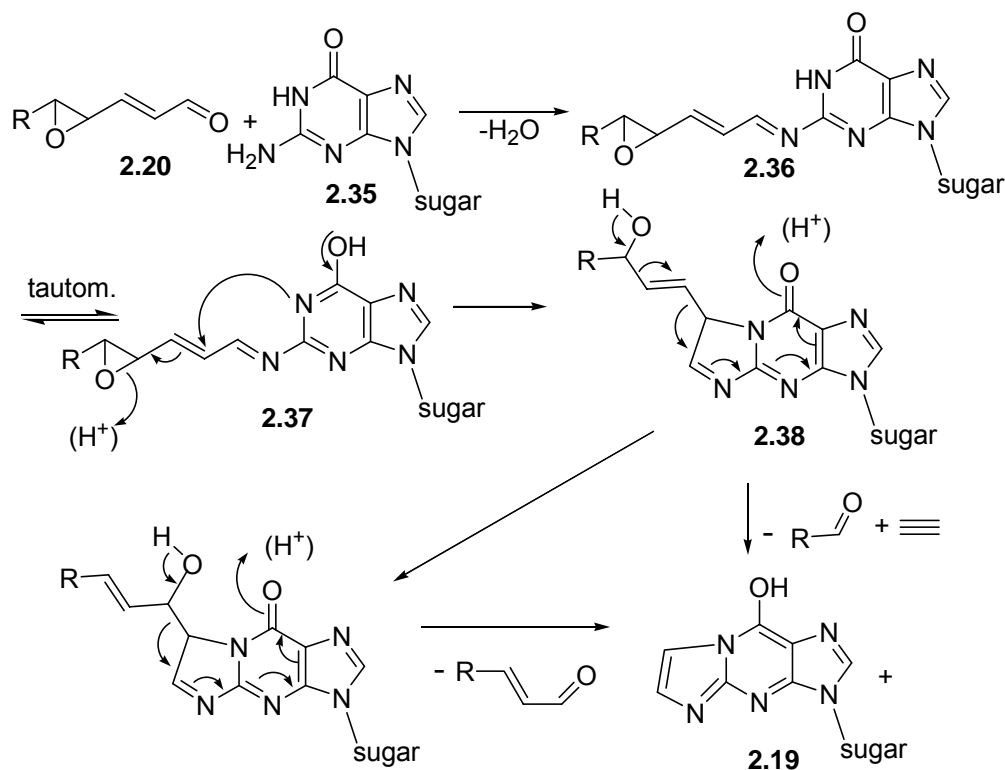


Figure 2.10. LC/APCI/MS analysis of reaction between *trans*-OETA-PC (**2.20**) and calf thymus DNA at 60 °C for 48 h.

My suggested mechanism that accounts for the reaction of OETA-PC (**2.20**) with dAdo, or dGuo to give the *unsubstituted* etheno-dAdo adduct **2.18** or etheno-dGuo adduct **2.19** (see Scheme 2.5) is presented in Scheme 2.10 for the case of dGuo (**2.35**).



Scheme 2.10. A suggested mechanism for formation of the etheno-adduct **2.19**.

First, condensation of the aldehyde group of **2.20** with the amino group of dGuo (**2.35**) generates the corresponding imine **2.36**. Then a nitrogen adjacent to the imine group of this intermediate, in the appropriate tautomeric form, opens the allylic epoxide via a S_Ni , i.e., allylic inversion, attack on the α -carbon of the imine to generate the allylic alcohol **2.38**. The breakdown of intermediate **2.38** to etheno-dGuo (**2.19**) involves a vinylogous retroaldol reaction that generates etheno-dGuo adduct **2.19**, the aldehyde **2.39**, and acetylene. The energy released owing to aromatization of the tricyclic purine-derived base in **2.19** and the favorable entropy of this fragmentation reaction, i.e., decomposition of intermediate **2.38** to three molecules, facilitate the cleavage of two C-C bonds, albeit the yield is low.¹¹ The proposed pathway is in agreement with the finding

that in a control experiment, 4,5-epoxy-2(*E*)-decenal, **2.15**, is stable to the reaction conditions *in the absence of dGuo or dAdo*.¹¹

2.3. Conclusions

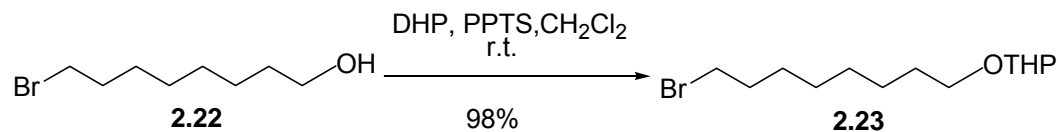
An efficient, practical total synthesis was accomplished for *trans*-OETA (**2.17**) and *trans*-OETA-PC (**2.20**) starting from a commercially available, inexpensive bromo-alcohol. This synthesis provides ready access to adequate amounts of the pure lipids needed for further biological studies. The pure *trans*-OETA-PC (**2.20**) served as a standard that enabled the identification of this epoxyaldehyde in the oxidation product mixture from the linoleic acid ester of 2-lysoPC (PA-PC) generated *via* three different methods: Cu (II), MPO and UV. *Trans*-OETA-PC was also identified *in vivo* in the lipidic extract of the rat retina and the amount of *trans*-OETA-PC in rat retina was quantified. In collaboration with Dr. Blair's group from the University of Pennsylvania, *trans*-OETA-PC (**2.20**) was shown to form mutagenic etheno-adducts with dAdo and dGuo, as well as with the DNA.

2.4. Experimental Part

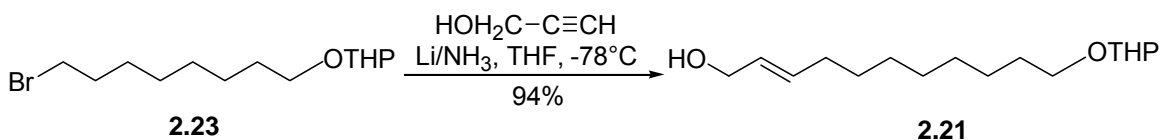
2.4.1. Syntheses

General methods: ^1H NMR spectra were recorded on Varian Gemini spectrometers operating at 200 or 300 MHz using CHCl_3 (δ 7.24 ppm) as internal standard. All chemical shifts are reported in parts per million (ppm) on the δ scale relative to the solvent used. ^1H NMR spectra are presented as follows: multiplicity is given as (s, singlet; d, doublet; dd, doublet of doublets; t, triplet; q, quartet, qAB, quartet AB, m, multiplet), coupling constants (Hz), number of protons. ^{13}C NMR spectra were recorded on Varian Gemini spectrometers operating at 50 MHz and 75 MHz using CDCl_3 (δ 77.0) as internal standard. Signal multiplicities were established by DEPT experiments. High-resolution mass spectra were recorded on a Kratos AEI MS25 RFA high-resolution mass spectrometer at 20 eV.

Thin layer chromatography (TLC) was performed on glass plates precoated with silica gel (Kieselgel 60 F₂₅₄, E. Merck, Darmstadt, Germany); R_f values are quoted for plates of thickness 0.25 mm. The plates were visualized by viewing the plates under short-wave length UV light or by exposure to iodine vapor. Phospholipid spots were visualized using a molybdenum-based detection spray.³² Flash chromatography was performed using Silica Gel 60A, 32-63 μm from Sorbent Technologies, Atlanta, GA, USA or ICN SiliTech 32-63 D 60A from ICN Biomedicals GmbH Eschwege, Germany.

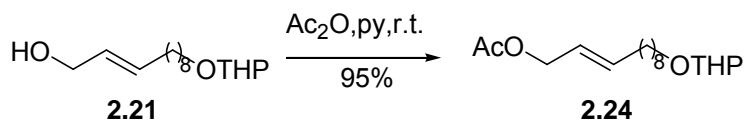
2-(8-Bromo octyloxy)tetrahydropyran (2.23)

Pyridinium *p*-toluenesulfonate (PPTS, 217 mg, 0.86 mmol) was added to a solution of the alcohol **2.22** (1942 mg, 8.67 mmol) and dihydropyran (DHP, 1.1 g, 13 mmol, freshly distilled) in dry methylene chloride (40.0 mL).¹⁷ The resulting solution was stirred overnight at room temperature, then diluted and extracted with ethyl acetate, washed with brine and dried on sodium sulphate. The solvent was removed with a rotary evaporator. The crude product was purified by flash chromatography on a silica gel column (10% ethyl acetate in hexanes) to afford **2.23** (2.5 g, 98%): TLC (8% ethyl acetate in hexanes) $R_f = 0.28$. $^1\text{H NMR}$ (CDCl_3 , 300 MHz): δ 4.55 (t, $J = 3$ Hz, 1H), 3.81-3.88 (m, 1H), 3.67-3.74 (tt, $J_1 = 6$ Hz, $J_2 = 6$ Hz, 1H), 3.51-3.32 (m, 2H), 1.30-1.87 (18H). $^{13}\text{C-NMR}$ (75 MHz, CDCl_3): 98.92 (CH), 67.65 (CH_2), 62.43 (CH_2), 34.06 (CH_2), 32.84 (CH_2), 30.83 (CH_2), 29.74 (CH_2), 29.30 (CH_2), 28.74 (CH_2), 28.15 (CH_2), 26.18 (CH_2), 25.54 (CH_2), 19.76 (CH_2).

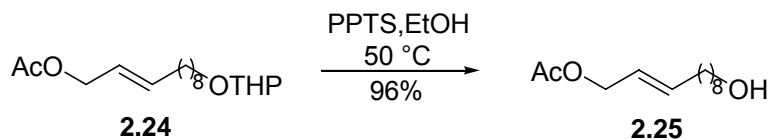
11-(Tetrahydropyran-2-yloxy)undec-2-en-1-ol (2.21)

Liquid ammonia (33 mL) and iron(III) nitrate (20 mg) were placed in a 100 mL three-necked flask equipped with a magnetic stirrer, dry ice/acetone-cooled condenser and drying tube with potassium hydroxide for protection from

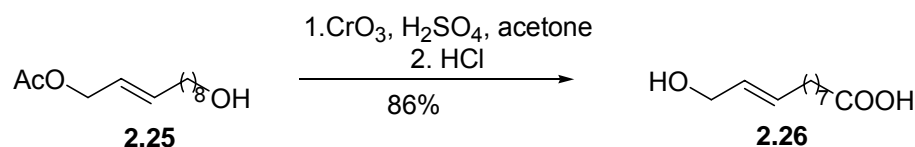
moisture. To this mixture, lithium (200 mg, 28.8 mmol) was added in portions allowing the blue color to dissipate between additions. Propargylic alcohol (1 mL, 17 mmol) in tetrahydrofuran (8 mL, freshly distilled) was added over 25 min and the reaction mixture was then allowed to reflux for 100 min. 2-(8-Bromo octyloxy) tetrahydropyran (**2.23**, 2.5 g, 8.5 mmol) in tetrahydrofuran (7 mL) was then added over 35 min and the mixture was allowed to reflux for 135 min. Lithium wire (50 mg, 7.2 mmol) was added resulting in a persistent blue color in the mixture.¹⁶ After 30 min, sufficient ammonium chloride was added to dispel the blue color. Most of the ammonia was evaporated under a stream of nitrogen and the residue was poured onto ice (50 g). The resultant mixture was extracted with diethyl ether (3 × 30 mL), and then ethyl acetate (2 × 50 mL). The combined organic extract was dried and concentrated by rotary evaporation to give a residue that was purified by flash chromatography on a silica gel column with 25% ethyl acetate in hexanes to afford compound **2.21** (2.1g, 91%): TLC (ethyl acetate/hexanes 1:4) $R_f = 0.3$; $^1\text{H NMR}$ (300MHz, CDCl_3) δ 5.55-5.72 (m, 2H), 4.55 (t, $J = 3$ Hz, 1H), 3.81-3.88 (m, 1H), 3.67-3.74 (tt, $J_1 = 6$ Hz, $J_2 = 6$ Hz, 1H), 3.51-3.32 (m, 2H), 1.98-2.04 (m, 2H), 1.30-1.87 (18H). $^{13}\text{C-NMR}$ (75 MHz, CDCl_3): 133.52 (CH), 128.9 (CH), 98.89 (CH), 67.71 (CH_2), 63.86(CH_2), 62.39 (CH_2), 32.22 (CH_2), 30.82 (CH_2), 29.77 (CH_2), 29.43 (CH_2), 29.12 (CH_2), 26.24 (CH_2), 25.54 (CH_2), 19.74 (CH_2).

Acetic acid, 11-(tetrahydropyran-2-yloxy)undec-2-enyl ester (2.24)

A solution of acetic anhydride from a newly opened bottle (~1.3 g, 12.4 mmol) in pyridine (5 mL, freshly distilled) was cooled in an ice bath. A solution of **2.21** (2.2 g, 8 mmol) in pyridine (4 mL, freshly distilled) was added in one portion and the mixture was stirred for 3 h at 0 °C, and then for 3 more hours while being warmed to room temperature.¹⁵ It was then poured onto a mixture of ice (30 g) and hexanes (20 mL), shaken, and then the layers were separated. The aqueous layer was extracted with hexanes (3 × 10 mL). The combined organic layers were washed with water and brine and then dried over Na₂SO₄. The sample was concentrated by rotary evaporation to give a residue that was purified by flash chromatography on a silica gel column with 12% ethyl acetate in hexanes to afford compound **2.24** (2.37 g, 95%): TLC (ethyl acetate/hexanes 1:9) *R_f* = 0.32; ¹H NMR (300MHz, CDCl₃) δ 5.48-5.57 (m, 1H), 5.69-5.79 (m, 1H), 4.55 (t, *J* = 3 Hz, 1H), 3.81-3.88 (m, 1H), 3.67-3.74 (tt, *J*₁ = 6 Hz, *J*₂ = 6 Hz, 1H), 3.51-3.32 (m, 2H), 2.00 (s, 3H), 1.98-2.04 (m, 2H), 1.30-1.87 (18H).

Acetic acid, 11-hydroxyundec-2-enyl ester (2.25)

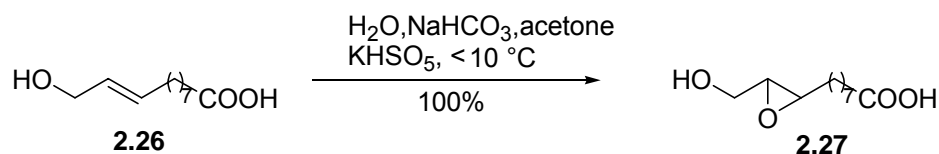
A solution of THP ether **2.24** (2.3 g, 7.5 mmol) and pyridinium *p*-toluenesulfonate (PPTS, 237 mg, 0.75 mmol) in absolute ethanol (12.5 mL, freshly distilled over CaH₂) was heated for 6 h at 50 °C. The sample was concentrated by rotary evaporation and the residue was taken up in ethyl acetate (10 mL) to give a milky suspension that was transferred to a separatory funnel.^{17,35} The reaction flask was rinsed with water (5 mL) and ethyl acetate (5 mL), and then the washes were added to the separatory funnel and shaken to give two clear phases that were separated. The organic layer was washed with water (3 mL), 1% NaHCO₃ (3 mL), and brine and then dried on Na₂SO₄. The solvent was removed with a rotary evaporator and the residue was purified by flash chromatography on a silica gel column with 30% ethyl acetate in hexanes to afford compound **2.25** (1.64 g, 96%): TLC (ethyl acetate/hexanes 3:7) *R*_f = 0.37; ¹H NMR (300MHz, CDCl₃) δ 5.48-5.58 (m, 1H), 5.69-5.79 (m, 1H), 4.48 (d, *J* = 6 Hz, 2H), 3.58-3.64 (m, 2H), 2.03 (s, 3H), 1.98-2.04 (m, 2H), 1.23-1.56 (14H).

11-Hydroxyundec-9-enoic acid (2.26)

A 250 mL round-bottom flask was charged with Jones reagent (8 mL, 2.67 M $\text{Na}_2\text{Cr}_2\text{O}_7$ in 4 M H_2SO_4) and acetone (40 mL). A solution of **2.25** (1.2 g, 5.2 mmol) in acetone (40 mL) was added dropwise at 0 °C from a funnel over 2 h. The color changed from orange to dark-brown. The mixture was stirred at room temperature for 4 additional h, and then the solution was decanted from the orange residue. The residue was dissolved in water (30 mL) and the color changed to green-blue. This was extracted with ethyl acetate (3 × 10 mL). The organic extracts were added to the decanted solution. Solvents were then removed by rotary evaporation to give a brown residue. This was dissolved in water (30 mL) and extracted with ethyl acetate (3 × 20 mL). The organic solution was washed with water (20 mL) to remove residual chromium species¹⁵ and then extracted with 10% NaOH (20 mL). The aqueous phase was acidified with 6 M HCl to pH 1 and then extracted with ethyl acetate (4 × 10 mL). The combined organic extracts were washed with water (10 mL) and brine (10 mL) and then dried on Na_2SO_4 . The yellow-green color of the organic phase gradually fades to become colorless. The solvent was removed with a rotary evaporator and the white fluffy solid residue was purified by flash chromatography on a silica gel column with 70% ethyl acetate in hexanes to afford compound **2.26** (1.04 g, 86%): TLC (ethyl acetate/hexanes 1:1) $R_f = 0.28$; $^1\text{H NMR}$ (300MHz, CDCl_3) δ

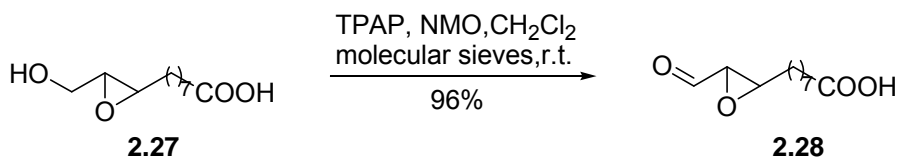
5.55-5.72 (m, 2H), 4.06 (d, $J = 3$ Hz, 2H), 2.32 (t, $J = 6$ Hz, 2H), 2.0-2.03 (m, 2H), 1.58-1.63 (m, 2H), 1.21-1.35 (8H).

8-(3-Hydroxymethyl oxiran-2-yl)octanoic acid (**2.27**)



A solution of dioxirane in acetone²⁰ (8.8 mL, 60mM), was added dropwise to a solution of **2.26** (120 mg, 0.6 mmol) in chloroform (4 mL) at room temperature. The resulting mixture was stirred for an additional 15 min at room temperature. The solvents were removed by rotary evaporation. The desired compound **2.27** was obtained in quantitative yield. ¹H-NMR (300 MHz, CDCl₃): δ 3.91-3.56 (2H), 2.96-2.89 (m, 2H), 2.32 (t, 2H, $J = 7.3$ Hz), 1.63-1.31 (12H). ¹³C-NMR (75 MHz, CDCl₃): 179.3 (C), 61.6(CH₂), 58.98(CH), 56.39(CH), 34.00 (CH₂), 31.45(CH₂), 29.11(CH₂), 29.08(CH₂), 28.90(CH₂), 25.83(CH₂), 24.63 (CH₂). HRMS (FAB): m/z calculated for C₁₁H₂₀O₄ [(M-H)⁺] 217.1440 found 217.1445.

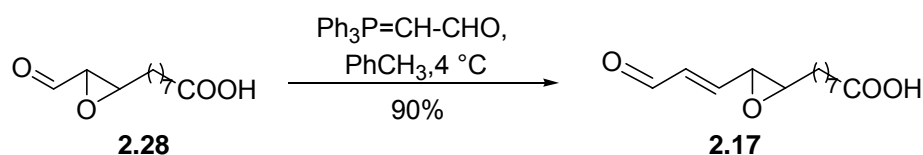
8-(3-Formyl oxiran-2-yl)octanoic acid (**2.28**)



The alcohol **2.27** (130 mg, 0.6 mmol) was dissolved in dichloromethane (60 mL, freshly distilled) containing 4-Å molecular sieves and 4-methylmorpholine N-oxide (NMO, 105 mg, 0.9 mmol). Solid tetrapropylammonium perruthenate

(TPAP, 32 mg, 0.091mmol, 0.15 equiv.) was then added under argon ²¹, and the resulting green mixture stirred at room temperature for 2 h, until TLC analysis showed the complete disappearance of the starting material and the appearance of a new spot ($R_f = 0.26$) with 40% ethyl acetate in hexanes. The molecular sieves were washed with 4 times the initial volume of the ethyl acetate to recover the entire product. The solution was filtered through a 1 cm layer of silica gel on a 60 mL separatory funnel. The solvent was removed by rotary evaporation to afford the product **2.28** (123 mg, 96% yield) in high purity. ¹H-NMR(75 MHz, CDCl₃): δ 8.99 (d, 1H, $J = 6.2$), 3.20 (dt, 1H, $J = 6.9$, $J = 1.9$), 3.11 (dd, 1H, $J = 6.3$, $J = 1.9$), 2.33 (t, 2H, $J = 7.4$), 1.63-1.31 (12H). ¹³C-NMR (300 MHz, CDCl₃): 198.56 (CH), 179.83 (C), 59.17 (CH), 56.79 (CH), 33.97 (CH₂), 31.19 (CH₂), 29.04 (CH₂), 29.01 (CH₂), 28.87 (CH₂), 25.73 (CH₂), 24.59 (CH₂). HRMS (FAB): m/z calculated for C₁₁H₁₉O₄ [(M-H)⁺] 215.1283, found 215.1292.

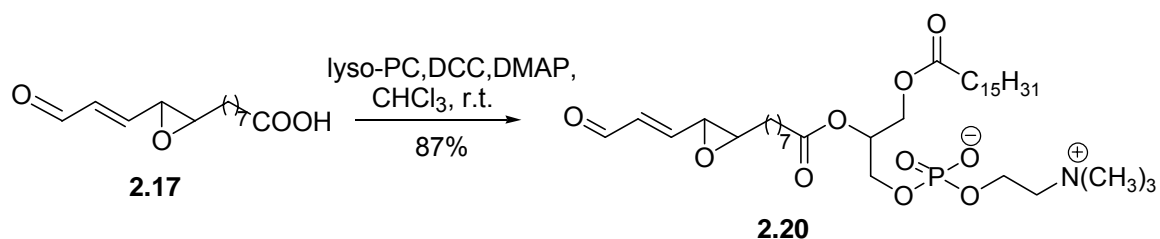
8-[3-(3-Oxo-propenyl)oxiran-2-yl]octanoic acid (**2.17**)



To a stirred suspension of formylmethylenetriphenylphosphorane (150mg, 0.495 mmol)²² in 4 mL of dry toluene at 0 °C, the aldehyde **2.28** (70 mg, 0.327 mmol) was added. The resulting mixture was stirred for 3 days at the 4 °C under argon. The solvent was removed under reduced pressure. The residue was extracted with ethyl acetate (4 × 5 mL). The aqueous phase was acidified with 2 M HCl to pH 4 and then extracted with ethyl acetate (4 × 10 mL). The combined organic extracts were washed with water (10 mL) and brine (10 mL) and then

dried on Na₂SO₄. The sample was concentrated by rotary evaporation to give a residue that was purified by flash chromatography on a silica gel column with 75% ethyl acetate in hexanes to afford compound **2.17** (70 mg, 90%): TLC (ethyl acetate/hexanes 1:1) *R_f* = 0.3. ¹H-NMR(300 MHz, CDCl₃): δ 9.53 (d, 1H, *J* = 7.6), 6.52 (dd, 1H, *J* = 15.8, *J* = 6.8) 6.35 (dd, 1H, *J* = 15.8, *J* = 7.4) 3.29 (dd, 1H, *J* = 6.9, *J* = 1.9), 2.92 (dt, 1H, *J* = 5.6, *J* = 1.9), 2.33 (t, 2H, *J* = 7.4), 1.63-1.31 (12H). ¹³C-NMR (75 MHz, CDCl₃): 192.64 (CH), 179.83 (C), 153.12 (CH), 133.57 (CH), 61.91 (CH), 56.21 (CH), 33.90 (CH₂), 31.87 (CH₂), 29.09 (CH₂), 28.90 (CH₂), 28.87 (CH₂), 25.73 (CH₂), 24.59 (CH₂). HRMS (FAB): *m/z* calculated for C₁₃H₂₁O₄ [(M-H)⁺] 241.1440, found 241.1447.

1-Palmitoyl-2-(13-oxo-9,10-*trans*-epoxyoctadeca-11-enoyl)-*sn*-glycero-3-phosphatidylcholine (*trans*-OETA-PC) (2.20)



A mixture of the acid **2.17** (9 mg, 0.037 mmol) and 2-lyso phosphatidylcholine (lyso-PC, 9.2 mg, 0.018 mmol) was dried overnight on a vacuum pump (0.1 mm Hg) equipped with a dry ice-acetone trap, at room temperature, and then was dissolved in dry CHCl₃ (1 mL, shaken with P₂O₅ for 0.5 h and distilled). Dicyclohexylcarbodiimide (DCC, 18.5 mg, 0.09 mmol) and *N,N*-dimethylaminopyridine (DMAP, 2.2 mg, 0.018 mmol) were added. The mixture was stirred for 10 days under argon. The mixture was then concentrated on a rotary evaporator and the residue was purified by flash chromatography on

a silica gel column with CHCl₃/MeOH/H₂O (16/9/1, TLC: R_f = 0.27) to produce the phospholipid, OETA-PC (**2.20**). ¹H-NMR(300 MHz, CDCl₃): δ 9.53 (d, *J* = 7.6, 1H), 6.52 (dd, *J* = 15.8, *J* = 6.8, 1H) 6.35 (dd, *J* = 15.8, *J* = 7.4, 1H), 5.17 (m, 1H), 4.29-4.40 (m, 2H), 3.80-4.12 (m, 4H), 3.35 (s, 9H), 3.29 (dd, *J* = 6.9, *J* = 1.9, 1H), 2.92 (dt, *J* = 5.6, *J* = 1.9, 1H), 2.33 (t, *J* = 7.4, 2H), 1.22-1.61 (42H), 0.85 (t, *J*=6,3H). ¹³C-NMR (300 MHz, CDCl₃): 192.64 (CH), 179.83 (C), 153.12 (CH), 133.57 (CH), 61.91 (CH), 56.21 (CH), 33.90 (CH₂), 31.87 (CH₂), 29.09 (CH₂), 28.90 (CH₂), 28.87 (CH₂), 25.73 (CH₂), 24.59 (CH₂). HRMS (FAB): *m/z* calculated for C₃₇H₆₈NO₁₀P [(M-H)⁺] 718.4660, found 718.4664.

2.4.2. Oxidative generation of OETA-PC from PL-PC

Materials. 1-Palmitoyl-2-linoleyl- *sn*-glycero-3-phosphatidylcholine (PL-PC), and 1,2-dimyristoyl-*sn*-glycero-phosphatidyl-3-ethanoamine (DM-PE) were obtained from Avanti Polar Lipids (Alabaster, AL) and MPO was supplied by Calbiochem (La Jolla, CA). Dry pyridine and chloroform were supplied by ACROS (New Jersey, USA).

Microphosphorus assay. The amount of synthetic lipid was calibrated with a standard microphosphorus assay,³³ that was modified to measure phospholipids at the level of 1 to 2 μg of phospholipids. A known amount of lipid was digested with 0.2 mL of perchloric acid (72%) in a glass 5 mL disposable cell culture tube, that is heated to boiling by a Reacti-Therm III heating module (Pierce, Rockford, IL) for 4 min. A yellow color appeared and then disappeared during the process. Water (2.1 mL), 5% aqueous ammonium molybdate (0.1 mL)

and 0.1 mL of aqueous amidol reagent containing 1% amidol (2,4-diaminophenol dihydrochloride) and sodium bisulfite (20%) were sequentially added to the tube, that was then vortexed after the addition. The tube was covered with a beaker, and heated in a boiling water bath for 7 min. Then the tube was cooled, and the absorbance of the stable blue color was measured with a UV-vis spectrometer at 830 nm in a 1 cm cuvette after 15 min. A standard calibration curve (Figure 2.11) was obtained using 0 $\mu\text{g P}$, 0.5 $\mu\text{g P}$, 1 $\mu\text{g P}$, 2 $\mu\text{g P}$, 3 $\mu\text{g P}$, 4 $\mu\text{g P}$, 5 $\mu\text{g P}$ obtained from a stock solution of KH_2PO_4 (2 $\mu\text{g P/mL}$).

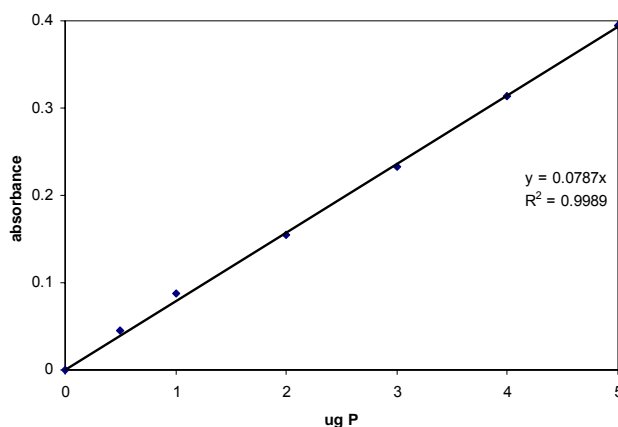


Figure 2.11. Calibration curve for microphosphorus assay.

Lipid oxidation. The dry lipids, PL-PC (1mg) were hydrated at 37 °C for 1 h in phosphate buffer (1 mL) supplemented with DTPA to minimize transition metal-induced autoxidation. Then the hydrated PL-PC was made into unilamellar vesicles by extrusion using an Avanti Mini-Extruder (Avanti Polar Lipids, Inc). For the Cu (II) oxidation, 10 μl of a solution of 500 μM CuCl_2 was added to 1.99 mL of vesicles. For the UV-induced oxidation, the vesicles (2 mL) were kept in a quartz tube placed in the center of a Rayonet photochemical reactor with three 80 watt low pressure mercury UV (350 nm) Rayonet lamps (Southern New England

Ultraviolet, Midtown, CT). The temperature was maintained at about 28 °C. The MPO oxidation was performed with the MPO-NO₂⁻-glucose/glucose oxidase system.²³ Sampling (200 µL) was performed at various times, and the reaction was stopped by adding BHT (2 µL, 40 µM), and catalase (7 µL, 300 µM).²³ For quantification purposes, the lipid extraction was performed immediately using a slightly modified Bligh and Dyer method²⁴ and the samples were dried in a stream of nitrogen at room temperature. The dried samples were stored in vials sealed under argon at -80 °C.

LC/ESI-MS/MS analysis. A standard curve was generated by incorporating a fixed amount of internal standard (1,2-myristoyl-*sn*-glycero-3-phosphatidylethanolamine, DM-PE), and varying the levels of the analyte, and plotting peak area ratio versus analyte mol ratio for each sample. LC-MS analysis of oxidized lipids was performed on a Quattro Ultima mass spectrometer (Micromass, Wythenshawe, UK) equipped with an electrospray ionization (ESI) probe interfaced with a Waters 2790 (Waters, Milford, MA) HPLC system. OETA-PC (50 µg, determined by aliquoting a solution of a known concentration, see microphosphorous assay for determining the absolute amount of lipid) was dissolved in 1 mL of chloroform/methanol (1:1). The solution (100 µL) was diluted with 400 µL of chloroform/methanol (1:1). To this solution (50 µL) the DM-PE standard (50 µL, 5-15 ng) was added and the mixture was chromatographed on a Prodigy ODS C18 column (150 × 2 mm, 5 µm, Phenomenex, Torrance, CA.) with a binary solvent gradient, starting from 50% water in methanol with a linear gradient to 100% methanol over 10 min, and then 100% methanol for 20 min at a

flow rate of 0.2 mL/min. All the mobile phase solvents contained 0.2% formic acid to enhance the MS signal. The total ion current was obtained in the mass range of m/z 200 – 1000 at 30V of cone energy in the positive ion mode. Three kV was applied to the electrospray capillary. All compounds were monitored in the positive ion mode (ES+) for the parent ion and the major daughter ion, previously determined by direct injection using ESI. The optimal collision energy determined to obtain the most intense daughters was 20 eV. In Table 2.3 are given the calibration equation for OETA-PC and PL-PC, as well as the extraction efficiencies determined as follows. Liposomes containing 10 μg of OETA-PC and the corresponding precursors (PL-PC), and 130 μg (50% of the total lipid content of liposomes) of DP-PC were prepared as described previously (*vide infra*). After Bligh and Dyer extraction, the amounts recovered were determined by LC-MS relative to DM-PE added prior to analysis and compared to a mixture composed of 10 μg from the OETA-PC and precursors and the same amount of DM-PE. Extraction efficiency for OETA-PC is $37.6 \pm 6.7\%$.

Derivatization of phospholipids. Methoxime derivatives of lipids were prepared by suspending the lipid (50 μg), dried in a stream of nitrogen, in 200 μL of freshly dried pyridine with 10% methoxylamine hydrochloride. The reaction mixture was incubated for 2 h at room temperature. Solvents and volatile by-products were removed under a nitrogen stream, and residues were resuspended in chloroform:methanol (1:1). Nonlipid components were removed by passing the solution through a C18 cartridge (Superclean LC-18 S-PE tubes, 3 mL, Supelco Inc., Bellefonte, PA), as follows. The reaction mixture dissolved in

50% methanol (1 mL) was loaded onto an S-PE cartridge, which was previously equilibrated by passing 10 mL of water. Then, the column was eluted with a gradient of water and methanol: 50% methanol (10 mL), 60% methanol (5 mL), 75% methanol (5 mL), 90% methanol (10 mL), and then pure methanol. The derivatized lipids eluted with 90% - 100% methanol. Lipids were dried again under a nitrogen stream. Derivatives of standard were characterized by ESI-MS/MS, and chromatographed on a Prodigy ODS C18 column (150 × 2 mm, 5 µm, Phenomenex, Torrance, CA) using the same HPLC conditions described above for oxidized lipids. The eluate was introduced into an LC/ESI-MS/MS operated in the positive ion mode. The analytes were detected by multiple reaction monitoring (MRM). Mass transitions, m/z 747.9 → 184.5 and m/z 794.7 → 184.5 for OETA-PC methoxime derivatives were monitored.

2.4.3. Detection and quantification of OETA-PC in rat retina

Extraction of phospholipids from retina. Rat retinas were harvested from 5 normal albino rats by Mary Rayborn and Dr. Gu. To prevent contamination by blood, or *in vitro* oxidation, the retinas were rinsed with saline antioxidant cocktail (saline PBS pH 7.4, containing 40 µM DTPA, and 4 nM BHT). The retinas were immediately homogenized manually in a plastic vial using a stainless steel pestle coated with Teflon, and lipid extraction was then performed immediately after homogenization using the method of Bligh and Dyer.²⁴ The extract was dried under a stream of nitrogen and sealed under argon and kept at -80 °C for 24 h before being analyzed by LC-MS.

Quantitative analysis of phospholipids. Lipid extracts were redissolved in HPLC grade solvents (methanol, 50%, chloroform, 50%) and used for analysis. LC/ESI-MS/MS analyses of the extracts were performed on a Quattro Ultima mass spectrometer (Micromass, Wythenshawe, UK) equipped with an electrospray ionization (ESI) probe interfaced with a Waters 2790 (Waters, Milford, MA) HPLC system. Separation of lipids was achieved on a Prodigy ODS C18 column (150 × 2 mm, 5 μm, Phenomenex, Torrance, CA) at a flow rate of 0.2 mL/min. The same solvent gradient was adopted for qualitative analysis. Mass spectrometric analysis was performed online using ESI tandem mass spectrometry in the positive multiple reaction monitoring (MRM) mode (cone energy 30 V/collision energy 20 eV). The MRM transitions used to detect the oxidized phospholipid were the mass to charge ratio (m/z) for the molecular cation $[M+H]^+$ and their respective daughter ion. Mass transitions, m/z 718.3 → 184.5 for OETA-PC, m/z 759.1 → 184 for PL-PC, were monitored simultaneously. Calibration curve for quantitative analysis of OETA-PC and PL-PC was constructed by adding a fixed amount of internal standard (DM-PE) into various amounts of authentic samples. The chromatograms and calibration curves are presented in Figures 2.12 and 2.13 (*vide infra*). Equations describing the calibration curves are presented in Table 2.3 (*vide infra*). Although we did not have the authentic standard, we also monitored theoretical ion pairs parent/daughter for the corresponding acid of OETA-PC, i.e., in which the carboxaldehyde has been oxidized to a carboxyl group: m/z 734.5 → 184. When

standard become available, these data can be used to provide identification and quantification of the acid.

Calculation of OETA-PC levels in rat retina: $n_A = y/(n_{st})(a)(EE)$; n_A = mole analyte, y = peak area ratio, a = from calibration curves ($y = ax$), n_{st} = moles of internal standard used, EE = extraction efficiency (from Table 2.3)

Table 2.4 Calibration equations, detection limits and extraction efficiency

Compound	Calibration Equation	Detection Limit (fmol)	Extraction efficiency
OETA-PC	$y=2.1835x$ ($R^2=0.9993$)	9	37.6 ± 6.7
PL-PC	$y=0.920x$ ($R^2=0.9913$)	2	58.8 ± 1.6

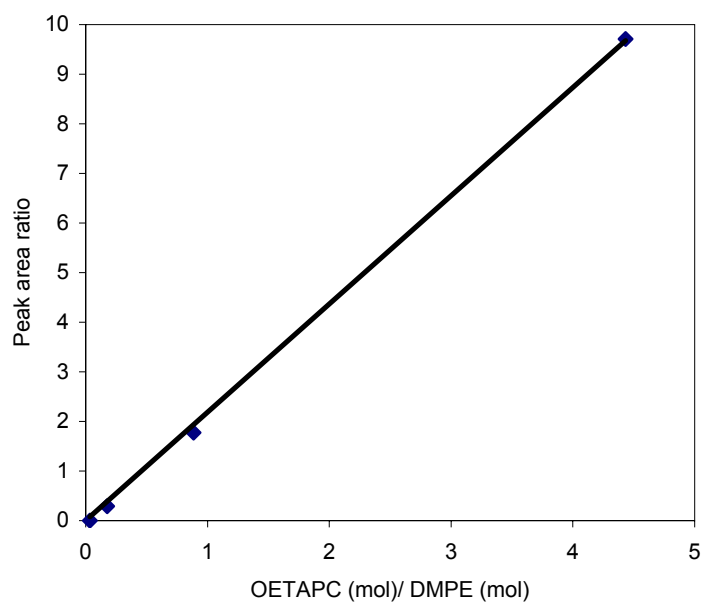
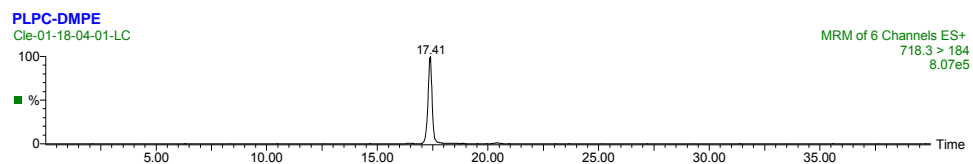


Figure 2.12. Chromatogram and calibration curve for synthetic *trans*-OETA-PC (2.20) 1,2-myristoyl-*sn*-glycero-3-phosphatidylethanolamine, (DM-PE) was used as an internal standard.

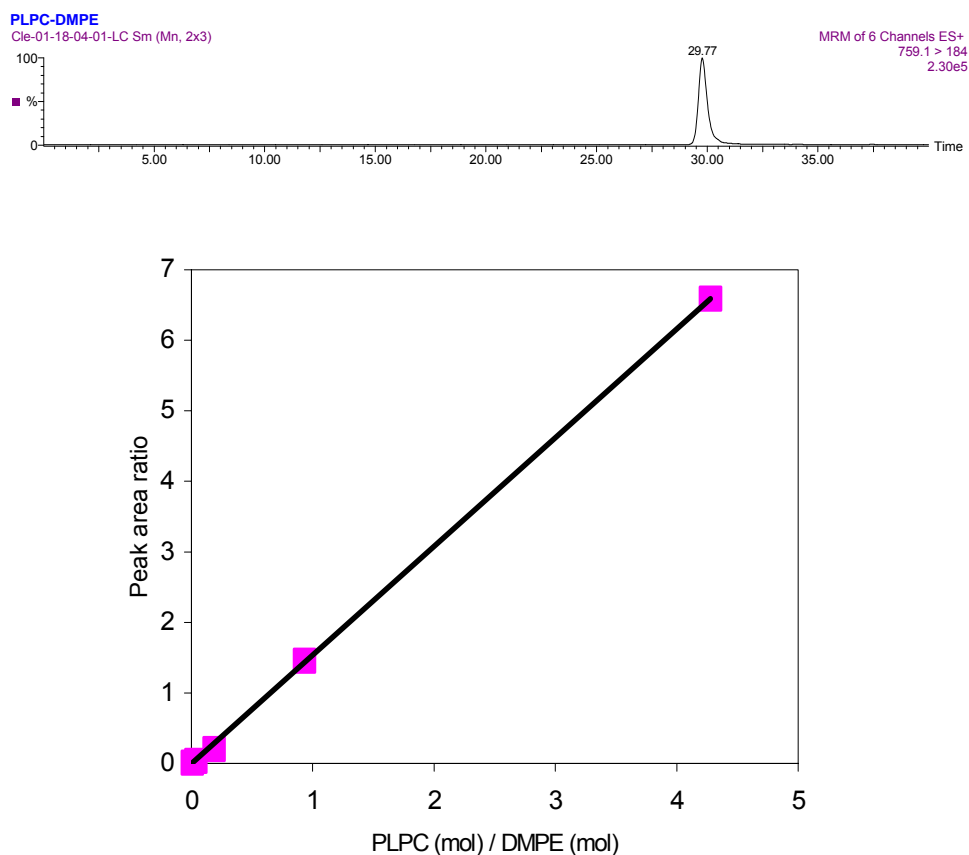


Figure 2.13. Chromatogram and calibration curve for PL-PC 1,2-myristoyl-*sn*-glycero-3-phosphatidylethanolamine, (DM-PE) was used as an internal standard.

2.4.4. Reaction of OETA-PC with dAdo, dGuo, and calf thymus DNA

Generation and detection of etheno adducts. These experiments were performed by Dr. Seon Hwa Lee from University of Pennsylvania.

Materials. Ammonium acetate, 2'-deoxyguanosine (dGuo), and 2'-deoxyadenosine (dAdo) were purchased from Sigma-Aldrich. (St. Louis, MO). Supelclean LC-18 solid-phase extraction (SPE) column was from Supelco (Bellefonte, PA). Chelex-100 chelating ion exchange resin (100-200 mesh size) was from Bio-Red Laboratories (Hercules, CA). HPLC grade water and

acetonitrile were obtained from Fisher Scientific Co. (Fair Lawn, NJ). ACS grade ethanol was obtained from Pharmco (Brookfield, CT). Gases were supplied by BOC Gases (Lebanon, NJ).

Liquid chromatography. Chromatography for LC/MS/UV experiments was performed using a Waters Alliance 2690 HPLC system (Waters Corp., Milford, MA) and a Hitachi L-4200 UV detector at 231 nm. Gradient system 1 consisted of a Synergi Polar RP column (250 x 4.6 mm i.d., 4 μ m; Phenomenex, Torrance, CA) at a flow rate of 1 mL/min. Solvent A was 5 mM ammonium acetate in water, and solvent B was 5 mM ammonium acetate in acetonitrile. The linear gradient was as follows: 6 % B at 0 min, 6 % B at 2 min, 10% B at 15 min, 80% B at 25 min, 80 % B at 35 min, 6 % B at 37 min, 6 % B at 45 min. Separations were performed at room temperature.

Mass spectrometry. Mass spectrometry was conducted using a Thermo Finnigan LCQ ion trap mass spectrometer (Thermo Finnigan, San Jose, CA) equipped with an APCI source in the positive ion mode. The LCQ operating conditions were as follows: vaporizer temperature at 450 °C, heated capillary temperature at 150 °C, with a discharge current of 5 μ A applied to the corona needle. Nitrogen was used as the sheath (80 psi) and auxiliary (5 arbitrary units) gas to assist with nebulization. Full scanning analyses were performed in the range of m/z 100 to m/z 800. Collision-induced dissociation (CID) experiments coupled with multiple tandem mass spectrometry (MS^n) employed helium as the collision gas. The relative collision energy was set at 20 % of the maximum (1 V).

Reaction of OETA-PC with DNA bases. A solution of OEPA-PC (**2.20**) (1.44 mg, 2 μ mol) in ethanol (36 μ L) was added to dGuo (2.67 mg, 10 μ mol) or dAdo (2.52 mg, 10 μ mol) in Chelex-treated 100 mM phosphate buffer (pH 7.4, 314 μ L). After sonication for 15 min, the reaction mixture was incubated at 60 °C for 48 h. The samples were filtered through a 0.2 μ m Costar cartridge prior to analysis of a portion of the sample (20 μ L) by LC/MS using gradient system 1.

Preparation of OETA-PC-modified calf thymus DNA. Calf thymus DNA (500 μ g, 1.68 μ mol) was dissolved in 100 mM phosphate buffer (pH 7.4, 314 μ L) and treated with OETA-PC (**2.20**) (1.44 mg, 2 μ mol) in ethanol (36 μ L). After sonication for 15 min, the reaction mixture was incubated at 60 °C for 48 h. Samples were placed on ice for 30 min, the DNA was precipitated by adding ice-cold ethanol (1050 μ L) followed by ice-cold 2.9 M sodium acetate (35 μ L). The samples were centrifuged at 4,000 x g for 15 min and the supernatant was removed. The DNA pellet was washed with ethanol/water (1 mL, 7:3 v/v) and residual solvent was removed by evaporation under nitrogen.

Enzymatic hydrolysis of OETA-PC-modified calf thymus DNA. The modified DNA pellet was dissolved in 1 mL of 10 mM MOPS containing 100 mM NaCl (pH 7.0) by sonication for 5 min. DNase I (556 units) dissolved in 200 μ L of 10 mM MOPS containing 120 mM MgCl₂ (pH 7.0) was added and the sample was incubated for 90 min at 37 °C. At the end of this incubation, 50 μ L of 10 mM MOPS containing 100 mM NaCl (pH 7.0) and 15.5 units of nuclease P1 was added followed by 25 mM ZnCl₂ (50 μ L). The incubation was then continued for

2 h at 37 °C. Finally, 30 units of alkaline phosphatase in 0.5 mL of 0.4 M MOPS (pH 7.8) was added and this was followed by an additional 1-h incubation.

Isolation of DNA adducts from modified calf thymus DNA. The hydrolysate was applied directly to a solid phase extraction (SPE) cartridge (1 g, 6 mL, Supelclean LC-18, Supelco, Bellefonte, PA) that had been pre-washed with acetonitrile (15 mL) followed by water (15 mL). The cartridge was washed with water (4 mL) and methanol/water (1 mL; 5:95, v/v). Etheno-dGuo and etheno-dAdo were eluted in acetonitrile/water (6 mL; 50:50, v/v). The elutes were evaporated to dryness under nitrogen and dissolved in water (100 µL). LC/MS analysis was conducted on a 20 µL aliquot of this solution using gradient system 1.

2.5. References

- (1) Spiteller, G. *Chem. Phys. Lipids* **1998**, *95*, 105-162.
- (2) Esterbauer, H.; Gebicki, J.; Puhl, H.; Jurgens, G. *Free Radic. Biol. Med.* **1992**, *13*, 341-90.
- (3) Ames, B. N.; Shigenaga, M. K.; Hangen, T. M. *Proc. Natl. Acad. Sci. USA* **1993**, *90*, 7915-7922.
- (4) Hamberg, M.; Samuelson, B. *J. Biol. Chem.* **1967**, *242*, 5366.
- (5) Kamitani, H.; Geller, M.; Eling, T. *J. Biol. Chem.* **1998**, *242*, 21569.
- (6) Deng, Y.; Salomon, R. G. *J. Org. Chem.* **1998**, *63*, 7789-7794.
- (7) Podrez, E. A.; Poliakov, E.; Shen, Z.; Zhang, R.; Deng, Y.; Sun, M.; Finton, P. J.; Shan, L.; Gugiu, B.; Fox, P. L.; Hoff, H. F.; Salomon, R. G.; Hazen, S. L. *J. Biol. Chem.* **2002**, *277*, 38503-16.
- (8) Podrez, E. A.; Poliakov, E.; Shen, Z.; Zhang, R.; Deng, Y.; Sun, M.; Finton, P. J.; Shan, L.; Febbraio, M.; Hajjar, D. P.; Silverstein, R. L.; Hoff, H. F.; Salomon, R. G.; Hazen, S. L. *J. Biol. Chem.* **2002**, *277*, 38517-23.
- (9) Lee, S. H.; Oe, T.; Blair, I. A. *Science* **2001**, *292*, 2083-2085.
- (10) Levine, M.; Conry-Cantilena, C.; Wang, Y.; Welch, R. W.; Washko, P. W.; Dhariwal, K. R.; Park, J. B.; Lazarev, A.; Graumlich, J. F.; King, J.; Cantilena, L. R. *Proc. Natl. Acad. Sci. USA* **1996**, *93*, 3704-3709.
- (11) Lee, S. H.; Oe, T.; Blair, I. A. *Chem. Res. Toxicol.* **2002**, *15*, 300-304.
- (12) Marnett, L. *Carcinogenesis* **2000**, *21*, 361-370.

- (13) Johnson, T. M.; Yu, Z.; Ferrans, V. J.; Lowenstein, R. A.; Finkel, T. *Proc. Natl. Acad. Sci. USA* **1996**, *93*, 11848-11852.
- (14) Burchman *Mutagenesis* **1998**, *13*, 287-305.
- (15) Goerger, M. M.; Hudson, B. S. *J. Org. Chem.* **1988**, *53*, 3148-3153.
- (16) Patterson, J. *Synthesis* **1984**, 337.
- (17) Miyashita, M.; Yoshikoshi, A.; Grieco, P. *J. Org. Chem.* **1977**, *42*, 3772-3774.
- (18) Sun, M.; Deng, Y.; Batyreva, E.; Sha, W.; Salomon, R. G. *J. Org. Chem.* **2002**, *67*, 3575-3584.
- (19) Nicolaou, K. C.; Roschangar, F.; Vourloumis, D. *Angew. Chem. Int. Ed.* **1998**, *37*, 2014-2045.
- (20) Adam, W.; Hadjirapoglou, L. *Topics Curr. Chem.* **1993**, *164*, 45-62.
- (21) Kobierski, M. E.; Kim, S.; Murthi, K. K.; Iyer, R. S.; Salomon, R. G. *J. Org. Chem.* **1994**, *59*, 6044-6050.
- (22) Katsuki, T.; Lee, A. W. M.; Ma, P.; Martin, V. S.; Masamune, S.; Sharpless, K. B.; Tuddenham, D.; Walker, F. J. *J. Org. Chem.* **1982**, *47*, 1373-1378.
- (23) Gu, X.; Sun, M.; Gugiu, B.; Hazen, S.; Crabb, J. W.; Salomon, R. G. *J. Org. Chem.* **2003**, *68*, 3749-3761.
- (24) Bligh, E.; Dyer, W. *Can J Biochem. Physiol.* **1959**, *37*, 911-917.
- (25) Mesaros, C.; Salomon, R. G. *Org. Lett.* **2004**, *to be submitted*.

- (26) Hiatt, R. In *Organic Peroxides*; D., S., Ed.; Willey-Interscience: 1971; Vol. 2, p 65-70.
- (27) Chacos, N.; Falck, J. R.; Wixtrom, C.; Capdevila, J. *Biochem. Biophys. Res. Commun.* **1982**, *104*, 916-922.
- (28) Oliw, E. H. *Biochem. Biophys. Res. Commun.* **1983**, *111*, 644-651.
- (29) Jin, S.; Makris, T. M.; Bryson, T. A.; Sligar, S.; Dawson, J. *J. Am. Chem. Soc.* **2003**, *125*, 3406-3407.
- (30) Sun, M. Ph. D Thesis, CASE, 2003.
- (31) Gugiu, B. Ph. D Thesis, CASE, 2004.
- (32) Dittmer, J. C.; Lester, R. L. *J. Lipids Res.* **1964**, *5*, 126-127.
- (33) Kates, M. *Techniques of lipidology : isolation, analysis, and identification of lipids*; 2nd rev. ed.; Elsevier: Amsterdam ; New York, 1986.

Chapter 3

**Mechanistic Insights into the Oxidative
Fragmentation of Linoleic Acid**

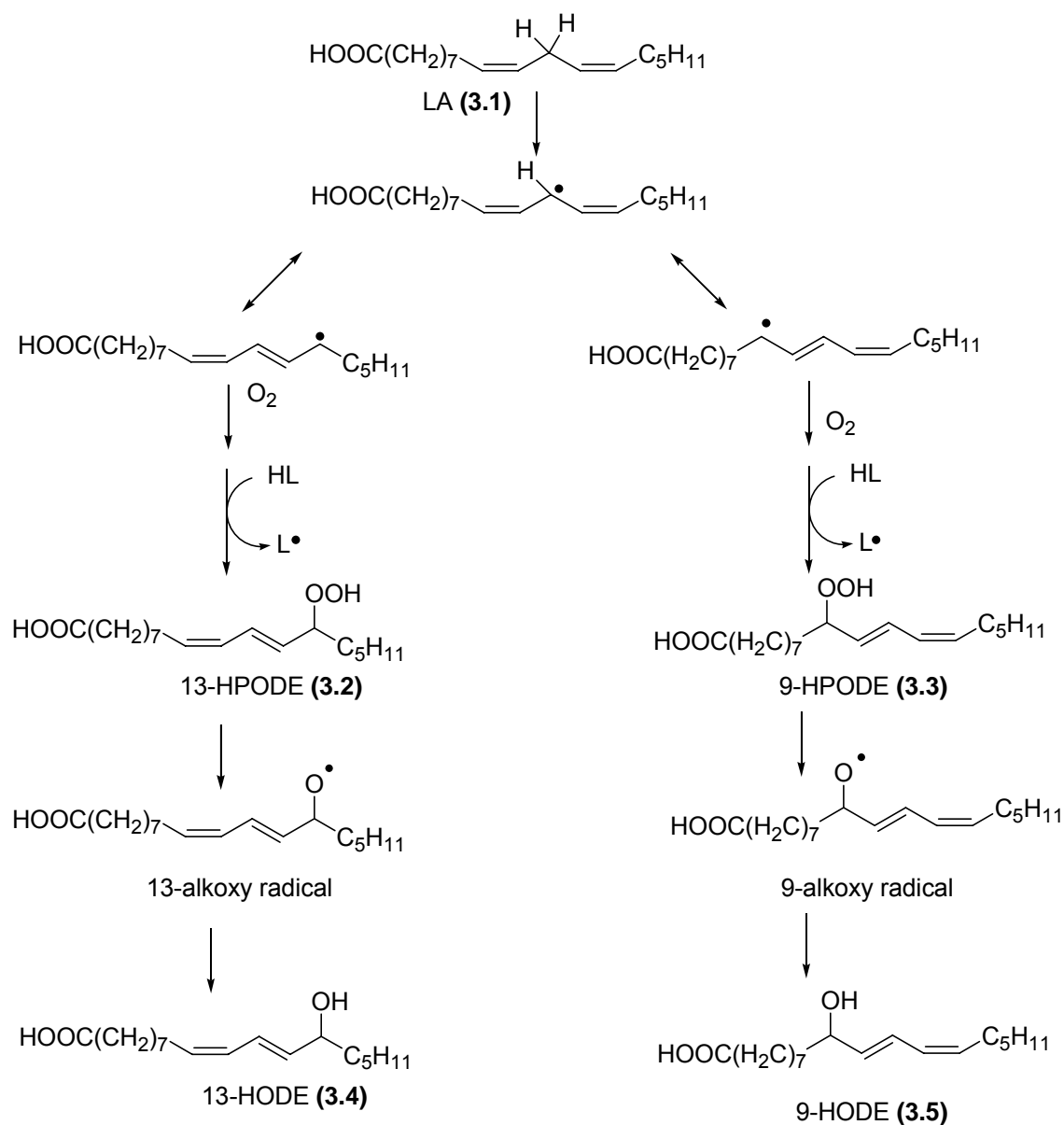
3.1. Background

Lipid oxidation is important to normal physiological processes, such as the enzyme-promoted biosynthesis of prostaglandins, thromboxanes, and prostacyclins. It may be recruited in the immune response (oxidative burst) or programmed cell death (apoptosis), and contributes to changes associated with aging.^{1,2} It is also involved in pathological processes such as the ischemia-reperfusion injury associated with heart attacks and stroke,^{3,4} atherosclerosis,^{5,6} Alzheimer's disease,^{7,8} and may contribute to Parkinson's disease,⁹ diabetes,¹⁰ as well as amyotrophic lateral sclerosis.¹¹ Involvement of oxidized phospholipids is suspected in the pathogenesis of several chronic inflammatory diseases such as antiphospholipid antibody syndrome,¹² rheumatoid arthritis,^{13,14} inflammatory bowel disease,¹⁵ and multiple sclerosis.^{15,16}

Lipid peroxidation is a complex process in which molecular oxygen and lipids react by a free radical chain process.¹⁷⁻¹⁸ Oxygen free radical species are known to be generated by a variety of enzymatic as well as nonenzymatic reactions. The nonspecific autoxidation of polyunsaturated fatty acids (PUFAs) leads to formation of a large number of reactive products.

3.1.1. Hydroperoxydienes are primary oxidation products. Linoleic acid (LA, **3.1**) is the most abundant PUFA in mammals. It is also the simplest and most widely studied PUFA. Therefore, LA (**3.1**) is commonly used to study and demonstrate the mechanisms of lipid peroxidation. Two linoleic acid hydroperoxides (LOOHs), 9-hydroperoxy-10,12-octadienoic acid (9-HPODE, **3.3**)

and 13-hydroperoxy-9,11-octadecadienoic acid (13-HPODE, **3.2**) generally are believed to be the primary lipid peroxidation products from LA (Scheme 3.1).¹⁹



Scheme 3.1. Generation of hydroxy acids from linoleic acid (LA) through hydroperoxy acid intermediates.

Two types of important free radicals, alkoxy radicals (LO•) and peroxy radicals (LOO•) are generated by cleavage of LOOH. These reactive free

radicals initiate the degradation of LOOH via a free radical pathway to generate various lipid oxidation products.

Besides autoxidation, hydroperoxides can also be generated by the action of lipoxygenases. Hydroperoxyacids are reduced to hydroxyacids *in vivo* by selenium-containing enzymes, such as glutathione peroxidase.^{20,21} 9-HPODE (**3.2**) or 13-HPODE (**3.3**) can produce alkoxy radicals, especially in the presence of redox active metal ions, e.g., Fe^{2+} , and most of these radicals are converted quickly to corresponding alcohols by hydrogen atom abstraction (Scheme 3.1). Hydroperoxy acids **3.4** and **3.5** are thought to be the precursors for γ -hydroxyalkenals. The hydroxy acids were considered to be stable end products, which may serve as markers in clinical research.²² However, recent studies by the Salomon group revealed that, in the presence of initiators of free radical oxidation, the hydroxy acids **3.4** and **3.5** undergo oxidative fragmentation to γ -hydroxyalkenals²³ as readily as the hydroperoxy acids **3.2** and **3.3**.

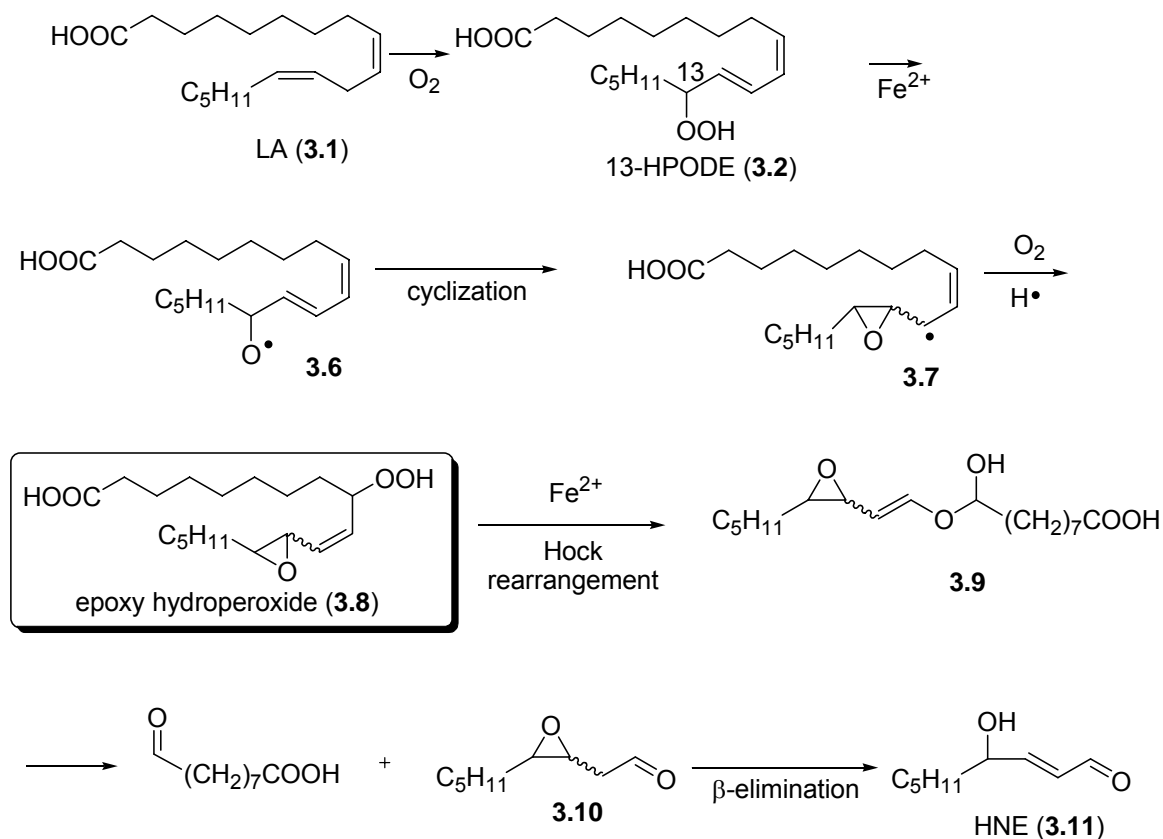
3.1.2. Oxidative fragmentation generates aldehydes. Lipid peroxidation in biological systems generates aldehydic compounds, e.g., the formation of 9-oxononanoic acid (ONA) from LA.²⁴ Among the aldehydic compounds found, α,β -unsaturated aldehydes are a significant class from lipid peroxidation. e.g., the formation of 9-hydroxy-12-oxododec-10-enoic acid (HODA) and 4-hydroxy-2-nonenal (HNE) from LA. These α,β -unsaturated aldehydes are often cytotoxic, genotoxic and mutagenic.

Considerably increased levels of HNE and several other α,β -unsaturated aldehydes are found in plasma and various organs under conditions of oxidative

stress.²⁴ Since these compounds are chemically reactive and capable, without prior metabolism, of covalently binding to cellular nucleophilic groups, such as proteins and DNA^{25,26}, the potential for being toxic and capable of modifying cellular processes is inherently present in every member of this class.^{27,28} For example, HNE has been intensively studied for decades from the perspective of lipid peroxidation mechanisms and with respect to its biological importance. Substantial evidence suggests that modification of proteins by HNE is involved in the pathogenesis of atherosclerosis and many other chronic diseases.^{27,29-30}

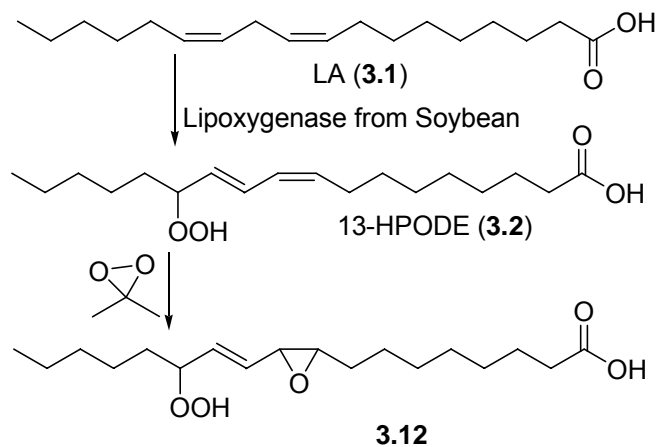
3.1.3. The epoxy hydroperoxide mechanism for HNE formation.

Several mechanisms by which HNE is formed from the LA have been proposed but their validity has rarely been tested. For the formation of HNE from fatty acids generally and linoleic acid particularly, Esterbauer's group was the first to show that the reaction can be catalyzed by iron.³¹ Later, it was proposed that HNE (**3.11**) can be produced from 13-HPODE (**3.2**) via an epoxy hydroperoxide (**3.8**) intermediate³² (Scheme 3.2). According to this mechanistic hypothesis, the hydroperoxide (**3.2**) reacts with Fe(II) to produce an alkoxy free radical (**3.6**). This free radical (**3.6**) rearranges and reacts with molecular oxygen to produce the epoxy hydroperoxide (**3.8**), which can fragment²² to produce HNE (**3.11**). Even though the compound (**3.8**) has been isolated³³ from reaction product mixtures from the oxidation of 13-HPODE (**3.2**), access to epoxy hydroperoxide **3.8** is limited.



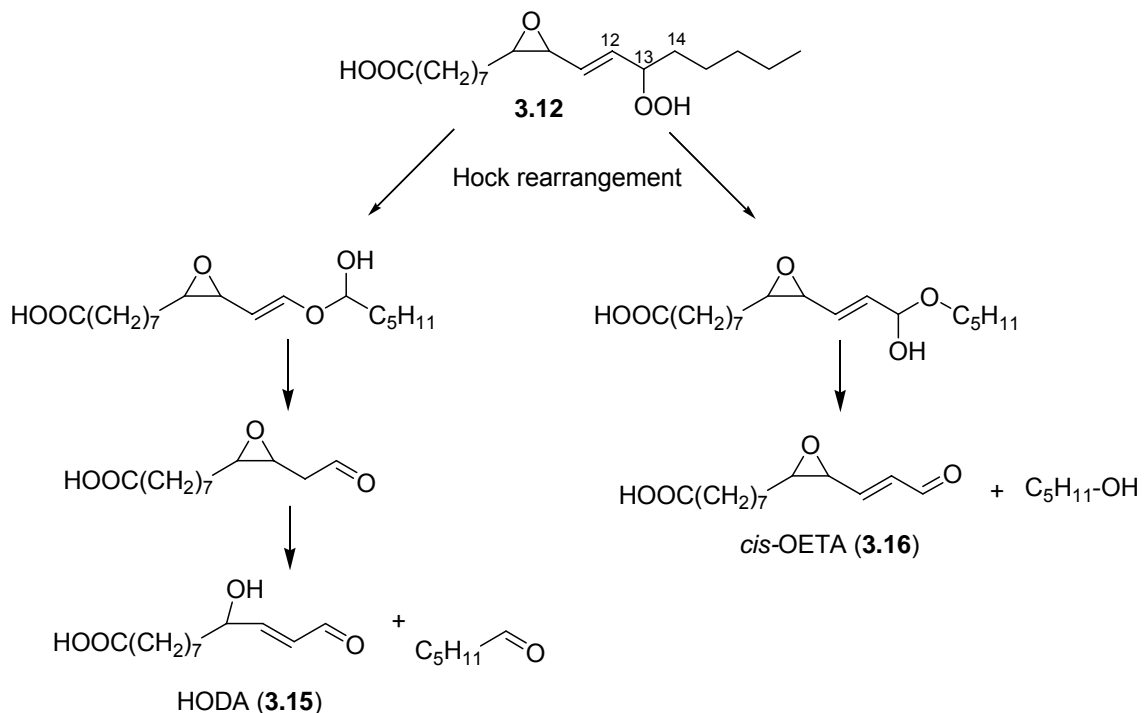
Scheme 3.2. Pryor and Porter's epoxy hydroperoxide mechanism.

To explore such fragmentation reactions, Mingjiang Sun synthesized an epoxy hydroperoxide isomer **3.12** of **3.8** by selective epoxidation³⁴ of 13-HPODE (**3.2**) with dimethyl dioxirane (Scheme 3.3).



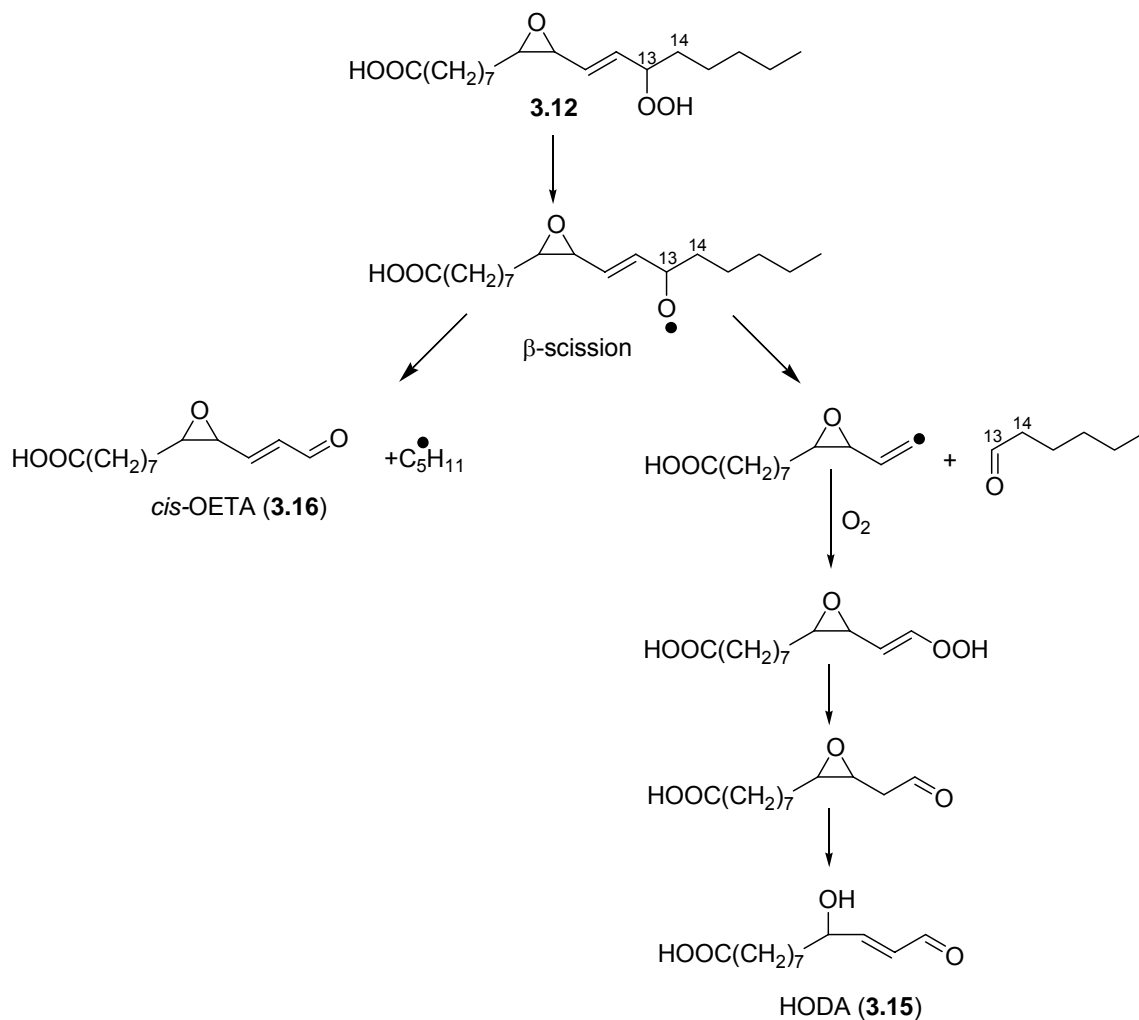
Scheme 3.3 Synthesis of an epoxy hydroperoxide **3.12** from LA (**3.1**)

The epoxy hydroperoxide (**3.12**) was oxidized under various conditions.³² In analogy with the mechanistic hypothesis of Scheme 3.2 for transformation of **3.8** to HNE (**3.11**), C12-C13 fragmentation of **3.12** would produce HODA (**3.15**) (Scheme 3.4). However, in the previous studies by Mingjiang Sun, only small amounts (< 1%) of HODA (**3.15**) were produced upon decomposition of **3.12**.³⁴



Scheme 3.4. Formation of HODA (**3.15**) and *cis*-OETA (**3.16**) from the epoxy hydroperoxide **3.12** by Hock rearrangement.

It occurred to us that an alternative fragmentation of **3.12**, involving C13-C14 cleavage, could produce an epoxy alkenal, *cis*-OETA (**3.16**) through a Hock rearrangement (Scheme 3.4). The formation of **3.15** and **3.16** from **3.12** might also occur through an entirely different mechanism, β -scission of an alkoxy radical derived from **3.12** (Scheme 3.5).



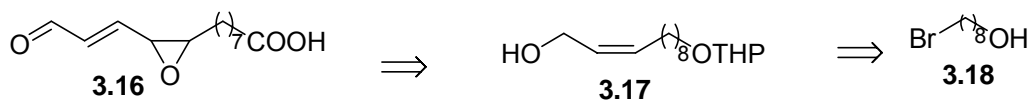
Scheme 3.5. Formation of HODA (**3.15**) and *cis*-OETA (**3.16**) from the epoxy hydroperoxide **3.12** by a pathway involving β -scission.

In this chapter the total synthesis of the C13-C14 cleavage product, *cis*-OETA (**3.16**), and its production from decomposition of the epoxy hydroperoxide **3.12** are described.

3.2. Results and Discussion

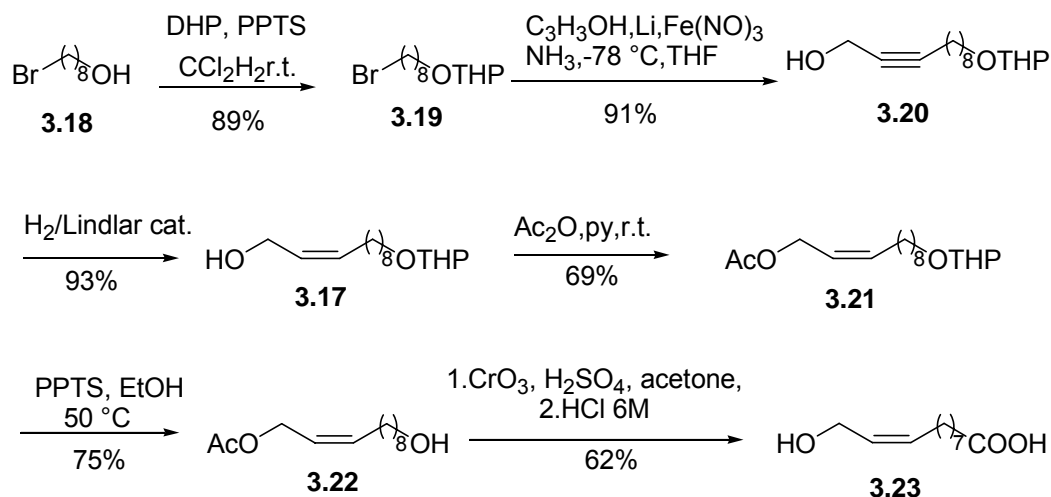
3.2.1. Synthesis of 13-oxo-9,10-*cis*-epoxyoctadeca-11-enoic acid (*cis*-OETA, **3.16).** We needed an authentic sample of pure *cis*-OETA (**3.16**) to establish the formation of this product from the fragmentation of the epoxy hydroperoxide **3.12**. To prepare *cis*-OETA (**3.16**), we envisioned a route starting from the *Z*-allylic alcohol **3.17** using the same protocol as for the synthesis of the natural product *trans*-OETA-PC (see Chapter 2, Schemes 2.7 and 2.8).

In this case, the acid **3.16** (*cis*-OETA) was expected to be available by epoxidation of the *Z* double bond of the allylic alcohol **3.17** (Scheme 3.6). In turn, intermediate **3.17** should be available from the bromohydrin **3.18**.



Scheme 3.6. Retrosynthesis of *cis*-OETA.

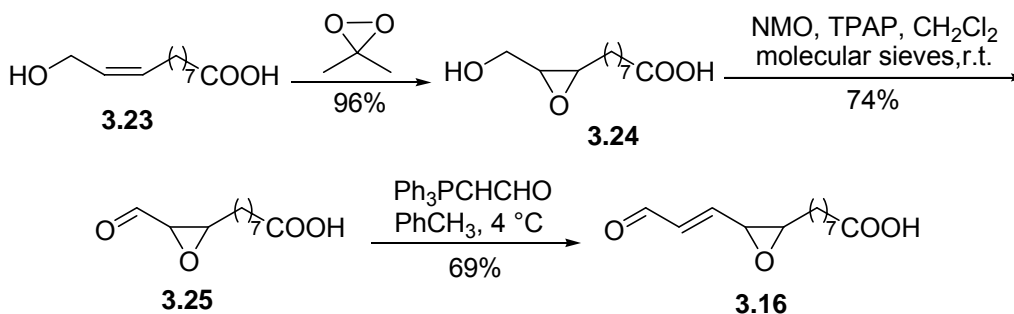
Starting from the commercially available bromo alcohol **3.18**, as for the *trans*-OETA (see Chapter 2), the alcohol group was first protected as a THP ether. The one pot process developed by Patterson³⁴ for the conversion of terminal acetylenic alcohols into (*E*)-olefinic alkenols, was stopped before the reduction of the triple bond, and the reduction was performed in a separate step (Scheme 3.7). When we used a 2:1 ratio of the propargyl alcohol to the electrophile **3.19** to generate the alcohol **3.20**, the yield was 91%. Reduction of the triple bond was performed with molecular hydrogen and Lindlar catalyst. The hydrogenation protocol produced exclusively the *Z* isomer **3.17** in 93% yield.



Scheme 3.7. Synthesis of the hydroxy-acid intermediate **3.23**.

The allylic hydroxyl of **3.17** was protected as an acetate and the primary alcohol was deprotected to deliver **3.22** via established procedures^{35,35} (Scheme 3.7). This alcohol was then oxidized with the Jones reagent. As expected, workup of the oxidation reaction product mixture with 6M HCl converted the allylic acetate into an allylic alcohol. The yields were much lower than in the case of the *E* isomer – 62% compared to 96% for the *trans* isomer – due to competing *Z-E* isomerization of the double bond. Apparently, the solvolytic reaction proceeds by a $\text{S}_{\text{N}}1$ mechanism. However, gradient flash chromatography allowed separation of the isomers. The epoxidation of alcohol **3.23** was carried out with a freshly prepared³³ solution of dioxirane in acetone. The reaction was completed in 15 min at room temperature to give pure epoxide **3.24** almost quantitatively. In the oxidation reaction of the free alcohol in **3.24** to an aldehyde in **3.25** with TPAP/NMO³⁶ at room temperature, the starting material was completely consumed in 3 h, but the yield was modest. The yield was increased, by allowing

the reaction to go for only 2 h and by adding the TPAP/NMO at 0 °C. The epoxy alkenal, *cis*-OETA (**3.16**), was obtained from the epoxy aldehydic acid **3.25** by a Wittig reaction at 4 °C for 2 days³⁷



Scheme 3.8. Synthesis of *cis*-OETA (**3.16**).

3.2.2. Autoxidation of epoxy hydroperoxide 3.12. In analogy with Pryor and Porter's postulated mechanism for the generation of HNE³², we expected that the synthetic epoxy hydroperoxide **3.12** would produce HODA (**3.15**) upon fragmentation at the C12-C13 bond (Schemes 3.4 and 3.5). In addition, however, as indicated earlier in this chapter, C13-C14 cleavage is expected to produce 13-oxo-9,10-epoxy-11(*Z*)-tridecenoic acid (*cis*-OETA, **3.16**). To test this hypothesis, **3.12** was induced to undergo autoxidation and iron-catalyzed decomposition at 37 °C. Epoxy hydroperoxide **3.12** was freshly prepared to avoid pre-oxidation and assure accuracy in the quantification of the oxidation products. The maximum yields for the detection of HODA (**3.15**) and *cis*-OETA (**3.16**) or the corresponding PC esters are presented in Table 3.1. The detection of these two products from **3.12** is the main focus of this chapter. The additional data in Table 3.1 are for comparison.

Table 3.1. Maximum yields for HODA and OETA.

substrate	catalyst	HODA %	HODA-PC %	OETA %	OETA-PC %
LA-PC (3.1)	UV		1.1±0.3		2.2±0.3 ^b
	MPO		1.6±0.2		3±0.2
	Cu(II)		0.1±0.07		0.3±0.02 ^b
13-HPODE (3.4)	none	5 ^a		0.3±0.09 ^b	
	Fe(II)	-		2.2±0.7 ^b	
3.12	none	0.5±0.09		0.3±0.03 ^c	
	Fe(II)	0.3±0.02		4.5±0.04 ^c	

^a Experiment done by M. Sun. ^b Trans isomer. ^c Cis isomer.

The production of HODA (**3.15**) and *cis*-OETA (**3.16**) from **3.12** was monitored by LC/ESI-MS/MS. By comparison with an authentic sample of *cis*-OETA (**3.16**), we identified **3.16** in the autoxidation product mixture from **3.12** (Figure 3.1).

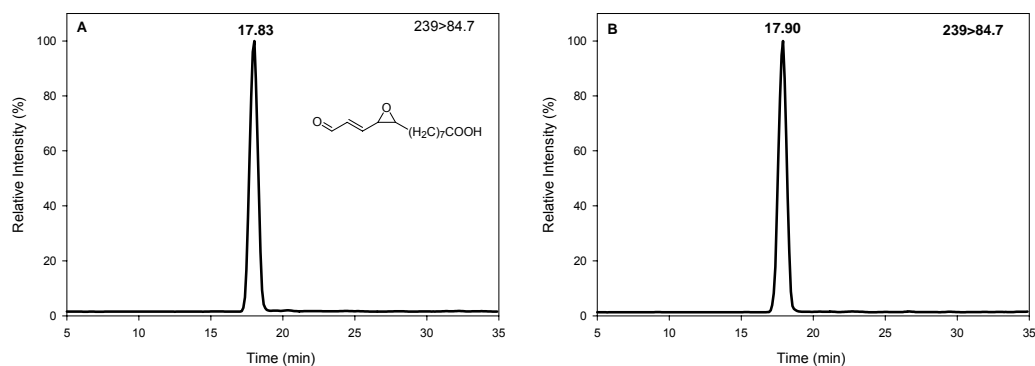


Figure 3.1. LC/ESI-MS/MS analysis of *cis*-OETA (**3.16**) from the oxidation mixture of **3.12**. **A.** Synthetic *cis*-OETA (**3.16**) standard (parent *m/z* 239), MRM chromatogram (daughter *m/z* 84.7). **B.** *cis*-OETA detected in the oxidation mixture of **3.12**, MRM chromatogram (239→ 84.7).

The experiments were done in plastic vials to avoid the unintended involvement of transition metals present in glass. *Cis*-OETA (**3.16**) detected in the reaction product mixture from **3.12** exhibited the same retention time as that

of authentic **3.16** and the same MRM. HODA (**3.15**) had been identified previously in the reaction mixture from **3.12**.³⁴ However, to make an accurate comparison between the yields of the HODA (**3.15**) and *cis*-OETA (**3.16**), the production of HODA (**3.15**) was also quantified in the same experiment.

Yields of HODA (**3.15**) and *cis*-OETA (**3.16**) were determined quantitatively by LC/ESI-MS/MS. The yields of HODA (**3.15**) from the epoxy hydroperoxide **3.12** were low, 0.3% - 0.5%, under both conditions examined (Figure 3.2), and were an order of magnitude lower than that (about 5%) obtained from 13-HPODE (**3.3**)³⁴ under the same conditions (graph not shown). This suggests that the epoxy hydroperoxide **3.12** is not a major precursor contributing to the production of HODA (**3.15**) from 13-HPODE (**3.2**). Since Fe (II) treatment resulted in a lower yield of HODA, Fe (II) either suppresses the formation of HODA (**3.15**) or catalyzes its decomposition, or both. The time course for production of HODA from **3.12** (Figure 3.2) clearly shows that HODA is not stable in the presence of Fe (II). In striking contrast, the yield of *cis*-OETA (**3.16**) from the epoxy hydroperoxide **3.12**, 4.5% in the presence of Fe(II) (Figure 3.3), was more than an order of magnitude higher than the yield of HODA (0.3%) under the same conditions.

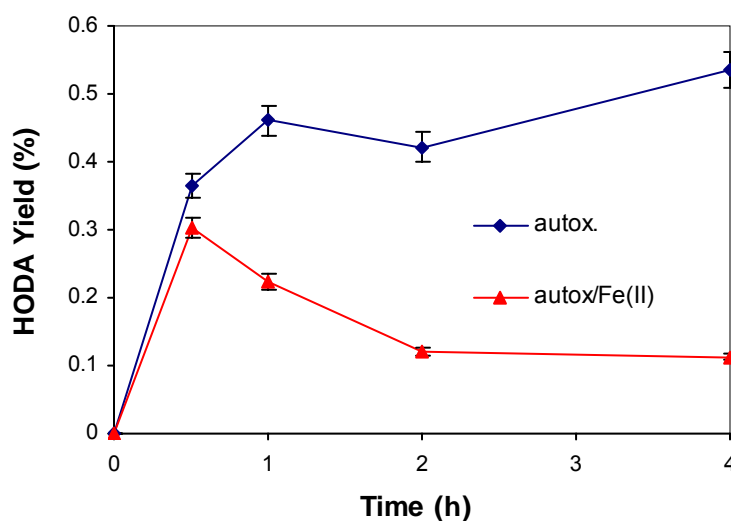


Figure 3.2. Evolution profile for HODA (**3.15**) produced from the epoxy hydroperoxide **3.12** during autoxidation or autoxidation in the presence of 5 mol% Fe(II) at 37 °C. Quantification was achieved by LC/ESI-MS/MS. The yields were calculated by dividing the amount of each analyte by the amount of starting **3.12**. Data are the average of three sets of independent experiments.

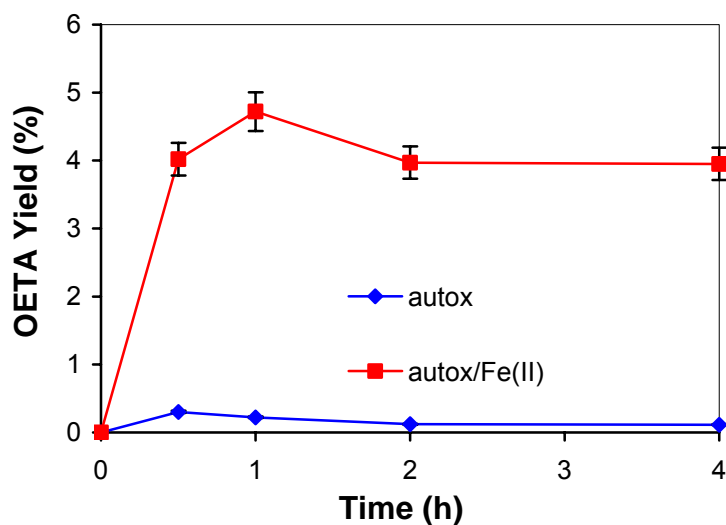
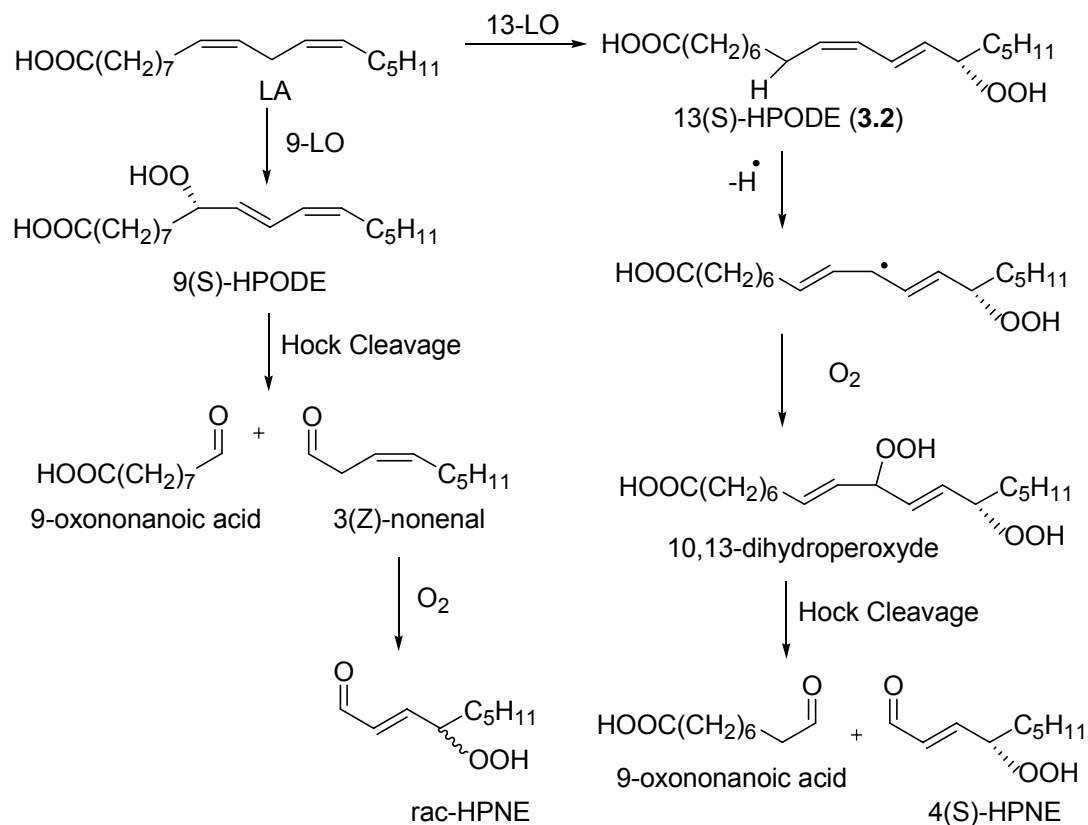


Figure 3.3. Evolution profile of *cis*-OETA (**3.16**) produced from the epoxy hydroperoxide **3.12** during autoxidation or autoxidation in the presence of 5 mol% equivalent Fe(II) at 37 °C. Quantification was achieved with LC/ESI-MS/MS. The yields were calculated by dividing the amount of each analyte by the amount of starting **3.12**. Data are the average of three sets of independent experiments.

3.2.3. Mechanisms for the generation of HNE. Porter³⁸ recently concluded that the generation of the γ -hydroxyalkenal HNE (**3.11**) from HPODEs involves the production of 4-HPNE through two alternative pathways (see Scheme 3.9 below) involving Hock rearrangements of LA-derived mono and dihydroperoxides. In these recent experiments, 4(S)-HPNE is obtained with nearly complete retention of configuration from optically pure 13(S)-HPODE (Scheme 3.9). However, some loss of optical purity ($\sim 10\%$) was observed implying that *minor* pathways, e.g., involving Hock rearrangement of the epoxy hydroperoxide **3.8** (Scheme 3.2), could occur in parallel with the pathways in Scheme 3.9. This view agrees with our conclusion that the epoxy hydroperoxide **3.12** is only a minor precursor for the γ -hydroxyalkenal HODA.



Scheme 3.9. Porter's mechanisms for generating HNE from HPODEs.³⁸

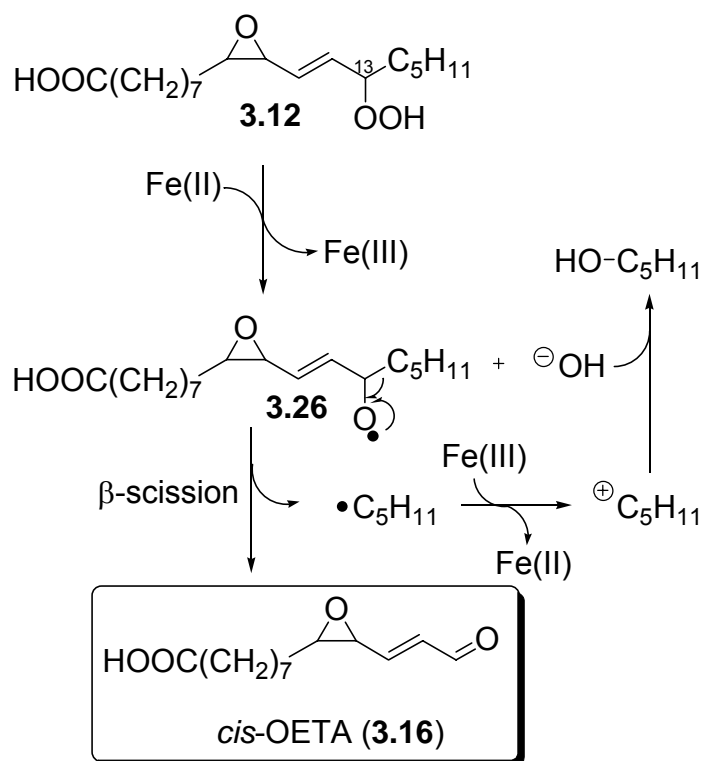
3.2.4. Formation of HODA and OETA from epoxy hydroperoxide 3.12.

The hydroperoxide **3.12** can fragment either by C13-C14 cleavage to produce *cis*-OETA (**3.16**) or C12-C13 cleavage to produce HODA (**3.15**). Hock rearrangement favors the migration of a vinyl group over an alkyl group.³⁷ In contrast, β scission favors the production of an alkyl radical over a vinyl radical.^{39,40} Thus, C12-C13 cleavage more likely proceeds by a heterolytic mechanism involving Hock rearrangement (Scheme 3.4) to produce HODA (**3.15**), while C13-C14 cleavage to produce OETA (**3.16**) may involve a free radical β scission mechanism (Scheme 3.5).

In analogy with the mechanistic hypothesis of Scheme 3.2 for transformation of the epoxy hydroperoxide **3.8** into HNE (**3.11**), C12-C13 fragmentation of the epoxy hydroperoxide **3.12** could produce HODA (**3.15**) (Scheme 3.4). Although this fragmentation does occur, it only can account for a minor fraction of γ -hydroxy alkenals produced during lipid peroxidation. This suggests that the mechanistic possibility proposed by Pryor and Porter in 1990,³² through the epoxy hydroperoxide (**3.8**) (Scheme 3.2), is indeed only a minor pathway that could account for the slight loss of optical purity found in recent studies of the formation of HNE from 13(S)-HPODE (see Scheme 3.9).³⁸

Fe(II) promotes fragmentation of epoxy hydroperoxide 3.12 to give *cis*-OETA. An alternative fragmentation of **3.12**, involving C13-C14 bond cleavage, can produce *cis*-OETA (**3.16**). In the presence of Fe(II), the yield of *cis*-OETA (**3.16**) from **3.12** is an order of magnitude higher than that of HODA (**3.15**).

For the generation of *cis*-OETA, (**3.16**) from epoxy hydroperoxide **3.12**, the iron-catalyzed free radical β -scission process detailed in Scheme 3.10 seems likely. Fenton type Fe(II) induced homolysis of the hydroperoxy group in **3.12** generates hydroxide, Fe(III), and the alkoxy radical **3.26**. A homolytic β -scission (C13-C14 bond) of this intermediate generates *cis*-OETA (**3.16**), and an *n*-pentyl radical. Oxidation of the *n*-pentanyl radical produces an *n*-pentyl cation and regenerates Fe(II). Capture of the pentyl cation by hydroxide generates pentanol.



Scheme 3.10. Mechanism for Fe(II)-catalyzed *cis*-OETA (**3.16**) formation.

3.3. Conclusions

An unambiguous total synthesis of *cis*-13-oxo-9,10-epoxy-11(*Z*)-tridecenoic acid (*cis*-OETA, **3.16**) was accomplished. Fragmentation of an epoxy hydroperoxide **3.12** to HODA (**3.15**) does occur in analogy with Pryor and Porter's hypothetical route to HNE (Scheme 3.2), but this reaction can only account for a minor fraction of γ -hydroxy alkenals produced during lipid peroxidation. This agrees with Porter's recent conclusions on the pathways to HNE from HPODEs.³⁸ The C12-C13 cleavage more likely proceeds by a heterolytic mechanism involving Hock rearrangement to produce HODA (**3.15**). *Cis*-OETA (**3.16**) is a major product from decomposition of the epoxy hydroperoxide **3.12**, especially in the presence of Fe(II). The C13-C14 cleavage to produce *cis*-OETA (**3.16**) most likely involves β scission of an intermediate alkoxy radical. Generation of the alkoxy radical can be catalyzed by Fe(II) through Fenton chemistry.

3.4 Experimental Part

General methods. Proton magnetic resonance (^1H NMR) spectra were recorded on a Varian Gemini spectrometer operating at 300 MHz. Proton chemical shifts are reported in parts per million (ppm) on the δ scale relative to CDCl_3 (δ 7.24). ^1H NMR spectral data are tabulated in terms of multiplicity of proton absorption (s, singlet; d, doublet; t, triplet; m, multiplet; br, broad), coupling constants (Hz), number of protons. Carbon magnetic resonance (^{13}C NMR) spectra were recorded on a Varian Gemini spectrometer operating at 75 MHz and chemical shifts are reported relative to solvents. All high resolution mass spectra were recorded on a Kratos AEI MS25 RFA high resolution mass spectrometer at 20 eV. All solvents were distilled under a nitrogen atmosphere prior to use. Methylene chloride was freshly distilled over calcium hydride. Chloroform was dried over phosphorus pentoxide. Tetrahydrofuran (THF) was freshly distilled over potassium and benzophenone. All reaction flasks were flame dried under argon before use. All materials were obtained from Aldrich or Acros unless otherwise specified.

Chromatography was performed with ACS grade solvent (ethyl acetate and hexanes). Thin layer chromatography (TLC) was performed on glass plates precoated with silica gel (Kieselgel 60 F₂₅₄, E. Merck, Darmstadt, West Germany). R_f values are quoted for plates of thickness 0.25 mm. The plates were visualized with iodine or phosphomolybdic acid reagent. For the visualization of the peroxides a ferrous thiocyanate reagent which was prepared just before use by dissolving ferrous ammonium thiocyanate (5 g) and concentrated sulphuric

acid (1mL) in water (100mL). The hydroperoxide spot appears reddish in color if peroxide is present. Flash column chromatography was performed on 230 - 400 mesh silica gel supplied by E. Merck. All other chemicals were obtained from Aldrich or Acros. For all reactions performed in an inert atmosphere, argon was used unless specified. High performance liquid chromatography (HPLC) purification was performed with HPLC grade solvents using a Waters M600A solvent delivery system and a Waters U6K injector or a Waters 717 auto sampler. The eluants were monitored using an ISCO V⁴ UV-VIS detector, or a Waters 2996 photodiode array detector as well as a SEDEX 55 ELS detector.

Mass spectrometry. LC/ESI-MS/MS analysis of the column eluant was performed on a Quattro Ultima (Micromass, Wythenshawe, UK). The mass spectrometer was connected with Waters 2790 as a solvent delivery system and an auto-injector. The source temperature was maintained at 100 °C, and the desolvation temperature at 200 °C. The drying gas (N₂) was maintained at ca. 450 L/h, and the cone flow gas at ca. 50 L/h. The multiplier was set at an absolute value of 500. Optimized parameters can be found in Table 3.2. MS scan at *m/z* 20-400 were obtained for standard compounds. Argon was used as collision gas at a pressure of 5 psi for MS/MS analysis. For MS/MS analysis, the collision energy was optimized for each compound. For multiple reaction monitoring (MRM) experiments, the optimum collision energy (giving the strongest signal) was determined for each product-daughter *m/z* ion pair. For all compounds, the mass spectrometer was operated in the negative ion mode.

Table 3.2. Optimized parameters for mass spectrometer.

	Acidic Compounds
Ion Mode	negative
Capillary (KV)	3
Cone (V)	30
Hex 1 (V)	0
Aperture (V)	0
Hex 2 (V)	0.5
LM 1 Resolution	10
HM 1 Resolution	10
Ion Energy 1	1
LM 2 Resolution	15
HM 2 Resolution	15
Ion Energy 2	2

Chromatography. The online chromatographic separation was obtained using a 150 × 2.0 mm i.d. Prodigy ODS-2.5 μ column (Phenomenex, UK), with a binary solvent (water and methanol) gradient. The solvents were supplemented with 0.2% formic acid, whenever the mass spectrometer was operated in positive mode. The gradient started with 100% water and rose to 100% methanol linearly in 15 min, and elution was continued for 5 min with 100% methanol. Then the

gradient was reversed to 100% water in 0.5 min, and then held for 9.5 min at 100% water. The solvents were delivered at 200 $\mu\text{L}/\text{min}$.

13-Hydroperoxyoctadeca-9,11-dienoic acid (3.2), 13-HPODE was prepared following reported procedures.⁴¹ ^1H NMR (300 MHz, CDCl_3) δ 6.52 (dd, $J_1 = 15$ Hz, $J_2 = 12$ Hz, 1H), 5.97 (t, $J_1 = 12$ Hz, 1H), 5.4 - 5.6 (2H), 4.2 - 4.4 (dd, $J_1 = 12$ Hz, $J_2 = 6$ Hz, 1H), 3.42 (dd, $J_1 = 7.1$ Hz, $J_2 = 4.6$ Hz, 1H), 3.0 - 3.2 (m, 1H), 2.32 (t, $J = 7.3$ Hz, 2 H), 1.1-1.8 (20H), 0.85 (t, $J = 6.6$ Hz, 3H).

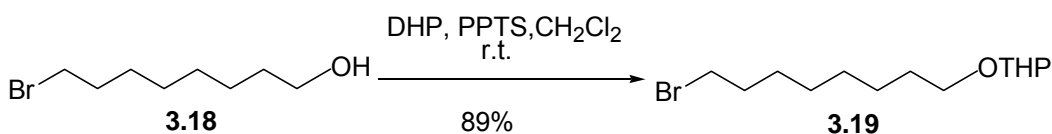
13-Hydroperoxy-*cis*-9,10-epoxyoctadeca-11-enoic acid (3.12). For the oxidation experiments, this compound was always prepared freshly, according to the procedure reported previously³⁴ with the only modification being that the reaction was allowed to proceed for more than 5 min. Sometimes as long as half an hour was needed for the reaction to go to completion. Briefly, dioxirane (500 μL , 7.8 mM) was added dropwise to the solution of 13-HPODE (**3.2**) (10 mg, 0.032 mmol) in chloroform. The resulting mixture was stirred for 15 min. The solvents were then removed by rotary evaporation. The desired compound was cleanly obtained in quantitative yield. ^1H NMR (300 MHz, CDCl_3) δ 5.84 (dd, $J_1 = 15.7$ Hz, $J_2 = 7.5$ Hz, 1H), 5.61 (dd, $J_1 = 15.7$ Hz, $J_2 = 7.5$ Hz, 1H), 4.2 - 4.4 (m, 1H), 3.42 (dd, $J_1 = 7.1$ Hz, $J_2 = 4.6$ Hz, 1H), 3.0-3.2 (m, 1H), 2.32 (t, $J = 7.3$ Hz, 2 H), 1.1-1.8 (20H), 0.85 (t, $J = 6.6$ Hz, 3H).

9-(2-Oxanyloxy)-11-(3,3-dimethyl-2,4-dioxolanyl)undec-10-enoic acid (preHODA) was used as internal standard and was prepared as described previously.⁴² ^1H NMR (300 MHz, CDCl_3) δ 5.5-5.9 (2H) 4.62 (m, 1H), 4.49 (m,

1H), 4.04 (3H), 3.83 (m, 1H), 3.54 (m, 1H), 3.44 (m, 1H), 2.53 (t, $J = 7.4$ Hz, 2H), 1.80 (2H), 1.4-1.75 (8H), 1.39 (s, 3H), 1.36 (s, 3H), 1.2-1.4 (8H).

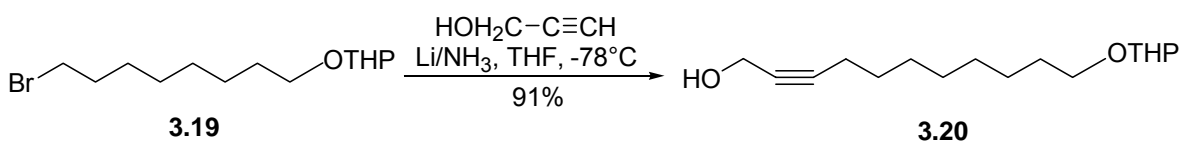
9-Hydroxy-12-oxo-10-dodecenoic acid (HODA, 3.15) was synthesized according to the published protocol⁴² ^1H NMR (CDCl_3 , 300 MHz) δ 9.57 (d, $J = 7.8$ Hz, 1H), 6.80 (dd, $J_1 = 15.6$ Hz, $J_2 = 3.8$ Hz, 1H), 6.28 (dd, $J_1 = 15.6$ Hz, $J_2 = 7.8$ Hz, 1H), 6.80 (dd, $J_1 = 15.6$ Hz, $J_2 = 3.8$ Hz, 1H), 6.28 (dd, $J_1 = 15.6$, $J_2 = 7.8$ Hz, 1H), 4.40 (m, 1H), 2.43 (t, $J = 7.3$ Hz, 2 H), 1.5-1.7 (4H), 1.2-1.4 (8H).

2-(8-Bromooctyloxy)tetrahydropyran (3.19)



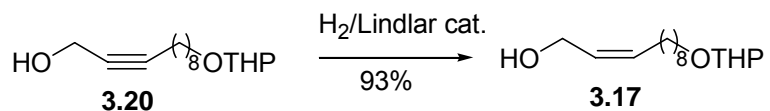
3.19 was prepared as described in Chapter 2. ^1H NMR (CDCl_3 , 300 MHz): δ 4.55 (t, $J = 3$ Hz, 1H), 3.81-3.88 (m, 1H), 3.67-3.74 (tt, $J_1 = 6$ Hz, $J_2 = 6$ Hz, 1H), 3.51-3.32 (m, 2H), 1.30-1.87 (18H). ^{13}C -NMR (75 MHz, CDCl_3): 98.92 (CH), 67.65 (CH_2), 62.43 (CH_2), 34.06 (CH_2), 32.84 (CH_2), 30.83 (CH_2), 29.74 (CH_2), 29.30 (CH_2), 28.74 (CH_2), 28.15 (CH_2), 26.18 (CH_2), 25.54 (CH_2), 19.76 (CH_2).

2-(11-Hydroxy-9-undecynyloxy)tetrahydropyran (3.20)

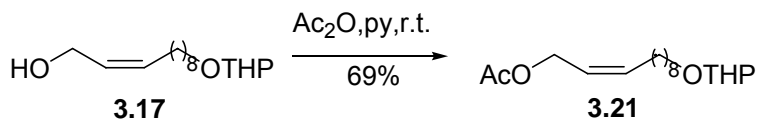


Liquid ammonia (20 mL) and iron(III) nitrate (2 mg) were placed in a 100 mL three-necked flask equipped with a mechanical stirrer, dry ice-cooled condenser and a drying tube with potassium hydroxide for protection from

moisture. To this mixture, lithium (20 mg, 2.8 mmol) was added in portions allowing the blue color to dissipate between additions. Propargyl alcohol (0.5 mL, 9 mmol) in tetrahydrofuran (1 mL, freshly distilled) was added over 25 min and the reaction mixture was then allowed to reflux 100 min. 2-(8-Bromooctyloxy) tetrahydropyran (**3.19**, 250 mg, 0.85 mmol) in tetrahydrofuran (1 mL) was then added over 35 min and the mixture was allowed to reflux for 135 min.⁴³ After 30 min, sufficient ammonium chloride was added to dissipate the blue color; most of the ammonia was evaporated under a stream of nitrogen and the residue was poured onto ice (5 mg). The resultant mixture was extracted with diethyl ether (3 × 3 mL), and then ethyl acetate (2 × 5 mL). The combined organic phases were dried and concentrated by rotary evaporation to give a residue that was purified by flash chromatography on a silica gel column with 25% ethyl acetate in hexanes to afford compound **3.20** (211 mg, 91%): TLC (ethyl acetate/hexanes 1:4) R_f = 0.3; ^1H NMR (300MHz, CDCl_3) δ 4.55 (t, J = 3 Hz, 1H), 4.11 (d, J =3, 1H), 3.81-3.88 (m, 1H), 3.67-3.74 (tt, J_1 = 6 Hz, J_2 =6 Hz, 1H), 3.51-3.32 (m, 2H), 1.98-2.04 (m, 2H), 1.30-1.87 (18H). ^{13}C -NMR (75 MHz, CDCl_3): 98.89 (CH), 74.07(CH), 70.31(CH), 67.71 (CH₂), 62.86(CH₂), 58.04 (CH₂), 30.82 (CH₂), 30.82 (CH₂), 29.77 (CH₂), 29.43 (CH₂), 29.12 (CH₂), 26.24 (CH₂), 25.54 (CH₂), 19.74 (CH₂).

2-(11-Hydroxy-9(Z)-undecenyl)tetrahydropyran (3.17)

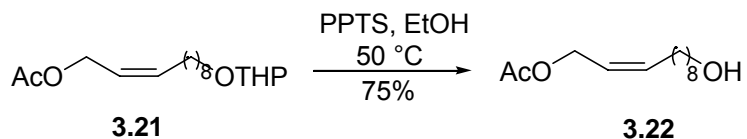
3.17 (211 mg, 0.787 mmol), in absolute ethanol (1 mL) was dissolved in a 5 mL round-bottomed flask. Lindlar catalyst (5 mg, Pd on BaSO₄) and a few (3) drops of quinoline were added and the mixture was stirred magnetically under hydrogen supplied from a balloon.⁴⁴ The reaction was monitored by TLC. The olefinic product **3.17** moves a little faster than the starting material. After completion (2 h) of the reaction, the mixture was filtered to remove the catalyst. The ethanol was removed on a rotary evaporator. Dichloromethane (2 mL) was added to the residue and it was washed with 5% aq. HCl, brine, then dried on Na₂SO₄ and solvent rotary evaporated. The resulting product was purified by flash chromatography on a silica gel column with 25% ethyl acetate in hexanes to afford compound **3.17** (197 mg, 93%): TLC (ethyl acetate/hexanes 1:4) *R_f* = 0.3; ¹H NMR (300MHz, CDCl₃) δ 5.46-5.61(m, 2H), 4.55 (t, *J* = 3 Hz, 1H), 3.81-3.88 (m, 1H), 3.67-3.74 (tt, *J*₁ = 6 Hz, *J*₂ = 6 Hz, 1H), 3.51-3.32 (m, 2H), 1.98-2.04 (m, 2H), 1.30-1.87 (18H).

Acetic acid, 11-(tetrahydropyran-2-yloxy)-2(Z)-undecenyl ester (3.21)

A solution of acetic anhydride from a newly opened bottle (64 mg, 0.62 mmol) in pyridine (1 mL, freshly distilled) was cooled in an ice bath. A solution of **3.17** (55 mg, 0.2 mmol) in pyridine (1 mL, freshly distilled) was added in one

portion and the mixture was stirred 3 h at 0 °C, and then for 3 h more while being warmed to room temperature.⁴⁵ It was then poured onto a mixture of ice (5 g) and hexanes (3 mL), shaken, and then separated. The aqueous layer was extracted with hexanes (3 × 1 mL), and then the combined organic layers were washed with water and brine and then dried over Na₂SO₄. The sample was concentrated by rotary evaporation to give a residue that was purified by flash chromatography on a silica gel column with 10% ethyl acetate in hexanes to afford compound **3.21** (44 mg, 69%): TLC (ethyl acetate/hexanes 1:9) *R_f* = 0.32; ¹H NMR (300MHz, CDCl₃) δ 5.57-5.66 (m, 1H), 5.45-5.53 (m, 1H), 4.58 (t, *J* = 3 Hz, 1H), 3.81-3.88 (m, 1H), 3.67-3.74 (tt, *J*₁ = 6 Hz, *J*₂ = 6 Hz, 1H), 3.51-3.32 (m, 2H), 2.00 (s, 3H), 1.98-2.04 (m, 2H), 1.30-1.87 (18H).

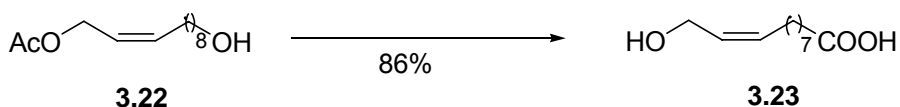
Acetic acid, 11-hydroxy-2(Z)-undecenyl ester (3.22)



A solution of **3.21** (44mg, 0.14 mmol) and pyridinium *p*-toluenesulfonate (PPTS, 5 mg, 0.015 mmol) in absolute ethanol (2 mL, freshly distilled over CaH₂) was heated 3 h at 40 °C. The sample was concentrated by rotary evaporation and the residue was taken up in ethyl acetate (3 mL) to give a milky solution which was transferred to a separatory funnel.⁴⁵ The reaction flask was rinsed with water (2 mL) and ethyl acetate (3 mL), and then the washes were added to the separatory funnel and shaken to give two clear phases, that were separated. The organic layer was washed with water (1 mL), 1% NaHCO₃ (1 mL), and brine, and then dried on Na₂SO₄. The solvent was removed by rotary evaporation and the

residue was purified by flash chromatography on a silica gel column with 20% ethyl acetate in hexanes to afford compound **3.22** (24 mg, 75%): TLC (ethyl acetate/hexanes 3:7) $R_f = 0.35$; $^1\text{H NMR}$ (300MHz, CDCl_3) δ 5.48-5.58 (m, 1H), 5.69-5.79 (m, 1H), 4.48 (d, $J = 6$ Hz, 2H), 3.58-3.64 (m, 2H), 2.03 (s, 3H), 1.98-2.04 (m, 2H), 1.23-1.56 (14H).

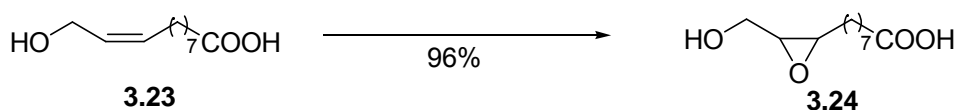
11-Hydroxy-9(*Z*)-undecenoic acid (**3.23**)



A 50 mL round-bottomed flask was charged with Jones reagent (1.5 mL, 2.67 M $\text{Na}_2\text{Cr}_2\text{O}_7$ in 4 M H_2SO_4) and acetone (8 mL). A solution of **3.22** (23 mg, 0.1 mmol) in acetone (8 mL) was added dropwise at 0°C from a funnel over 2 h. The color changed to dark-brown. The mixture was stirred at room temperature for 4 additional h, and then the solution was decanted from the orange residue. The residue was dissolved in water (5 mL) whereupon the color changed to greenish-blue. This was extracted with ethyl acetate (3×3 mL). The organic extracts were added to the decanted solution. The solvents were removed by rotary evaporation to give a brown residue, that was dissolved in water (10 mL), and extracted with ethyl acetate (3×10 mL). The solution was washed with water (10 mL), to remove residual chromium species⁴⁵ and then extracted with 10% NaOH (10 mL). The aqueous phase was acidified with 6 M HCl to pH 1 and then extracted with ethyl acetate (4×3 mL). The combined organic extracts were washed with water (3 mL) and brine (3 mL) and then dried on Na_2SO_4 . The organic phase lost its yellow-green color gradually to become pale yellow. The

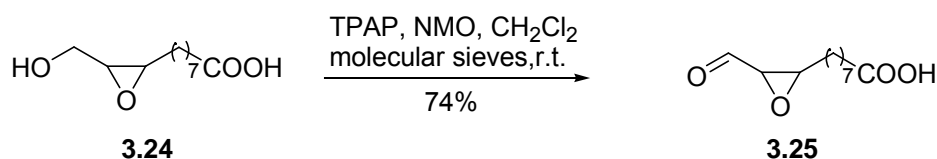
solvent was removed by rotary evaporation and the white fluffy solid residue was purified by flash chromatography on a silica gel column with 70% ethyl acetate in hexanes for the first 10 fractions and then with 75% ethyl acetate in hexanes, to afford compound **3.23** (12.5 mg, 62%): TLC (ethyl acetate/hexanes 1:1) $R_f = 0.28$; $^1\text{H NMR}$ (300MHz, CDCl_3) δ 5.46-5.61 (m, 2H), 4.12 (d, $J = 3$ Hz, 2H), 2.32 (t, $J = 6$ Hz, 2H), 2.0-2.03 (m, 2H), 1.58-1.63 (m, 2H), 1.21-1.35 (8H).

8-(3-Hydroxymethyl-*cis*-oxiran-2-yl)octanoic acid (**3.24**)



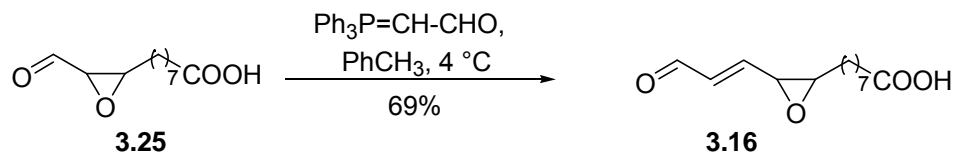
A solution of dioxirane in acetone (8 mL, 64mM)⁴⁶, was added dropwise to a solution of **3.23** (12.5 mg, 0.625 mmol) in chloroform (3 mL) at room temperature. The resulting mixture was stirred for an additional 15 min at room temperature. The solvents were then removed by rotary evaporation. The desired compound **3.24** was obtained in almost quantitative yield (13mg, 96%) without further purification. $^1\text{H-NMR}$ (300 MHz, CDCl_3): δ 3.82 (dd, $J = 12$, $J = 3$, 1H), 3.62 (dd, $J = 12$, $J = 3$, 1H), 3.06 (m, 2H), 2.32 (t, 2H, $J = 7.3$ Hz), 1.63-1.31 (12H). $^{13}\text{C-NMR}$ (75 MHz, CDCl_3): 179.3 (C), 60.85 (CH_2), 57.01(CH), 56.39(CH), 34.00 (CH_2), 31.45(CH_2), 29.11(CH_2), 29.08(CH_2), 28.90(CH_2), 25.83(CH_2), 24.63 (CH_2). HRMS (FAB): m/z calculated for $\text{C}_{11}\text{H}_{20}\text{O}_4$ [(M-H)⁺] 217.1440 found 217.1430.

8-(3-Formyl-*cis*-oxiran-2-yl)octanoic acid (**3.25**)



The alcohol **3.24** (13 mg, 0.06 mmol) was dissolved in dichloromethane (6 mL, freshly distilled) containing 4-Å molecular sieves and 4-methylmorpholine N-oxide (NMO, 10 mg, 0.09 mmol). Solid tetrapropylammonium perruthenate (TPAP, 3 mg, 0.009 mmol, 0.1 equiv.) was then added under argon⁴⁷ at 0 °C, and the resulting green mixture stirred at room temperature for 2 h, when TLC analysis showed complete disappearance of the starting material and the appearance of a new spot ($R_f = 0.2$) with 35% ethyl acetate in hexanes. The molecular sieves had to be washed with 4 times the initial volume of the ethyl acetate to recover the entire product. The solution was filtered through a small bed of silica gel (1 cm) in a separatory funnel. The solvent was removed by rotary evaporation to afford pure **3.25** (9.4 mg, 74% yield). ¹H-NMR(75 MHz, CDCl₃): δ 9.47 (d, 1H, $J = 6.$), 3.35 (dt, 1H, $J = 6.9$, $J = 1.9$), 3.23-3.29 (m, 1H), 2.36 (t, 2H, $J = 7.4$), 1.71-1.25 (12H). ¹³C-NMR (300 MHz, CDCl₃): 199.23 (CH), 180.02 (C), 59.17 (CH), 57.94 (CH), 34.02 (CH₂), 29.03 (CH₂), 29.01 (CH₂), 28.98 (CH₂), 28.87 (CH₂), 25.73 (CH₂), 24.59 (CH₂). HRMS (FAB): m/z calculated for C₁₁H₁₉O₄ [(M-H)⁺] 215.1283, found 215.1270.

13-Oxo-9,10-*cis*-epoxy-11(E)-tridecenoic acid (3.16)



To a stirred suspension of formylmethylenetriphenylphosphorane (5.7mg, 0.019 mmol)⁴⁸ in 1 mL of dry toluene at 0 °C, the aldehyde **3.25** (2.6 mg, 0.012 mmol) was added. The resulting mixture was stirred for 2 days at the 4 °C under argon. The solvent was the removed by rotary evaporation. The residue was

extracted with ethyl acetate (4 × 1 mL). The aqueous phase was acidified with 2 M HCl to pH 4 and then extracted with ethyl acetate (4 × 1 mL). The combined organic extracts were washed with water (1 mL) and brine (1 mL) and then dried on Na₂SO₄. The sample was concentrated by rotary evaporation to give a residue that was purified by flash chromatography on a silica gel column with 55% ethyl acetate in hexanes to afford compound **3.16** (2 mg, 69%): TLC (ethyl acetate/hexanes 1:1) *R_f* = 0.3. ¹H-NMR(300 MHz, CDCl₃): δ 9.59 (d, 1H, *J* = 8.9), 6.68 (dd, 1H, *J* = 15, *J* = 6) 6.4 (dd, 1H, *J* = 15, *J* = 6) 3.63 (dd, 1H, *J* = 6, *J* = 6.1), 3.26 (m, 1H), 2.35 (t, 2H, *J* = 9), 1.65-1.33 (12H). ¹³C-NMR (75 MHz, CDCl₃): 192.48 (CH), 178.81(C), 150.52(CH), 135.30 (CH), 60.22(CH), 55.20 (CH), 33.81 (CH₂), 29.12 (CH₂), 29.09 (CH₂), 28.90 (CH₂), 28.87 (CH₂), 25.73 (CH₂), 24.63 (CH₂).

Autoxidation of 13-hydroperoxy-9,10-*cis*-epoxy-11(E)-octadecaenoic acid (3.12) Five 1 mL plastic vials containing aliquots of 13-hydroperoxy-9,10-*cis*-epoxy-11(Z)-octadecaenoic acid (**3.12**, 10 μg) as a neat film were incubated at 37 °C in a moist chamber. At 0, 0.5, 1, 2, 4 h, a vial was removed from the incubator, and the samples were stored at -80 °C under argon. Before analysis the samples were dissolved with methanol (100 μL) containing 20 ng of internal standard (preHODA). The samples (50 μL) were injected into an LC/ESI-MS/MS, and the amount of HODA (**3.15**) and *cis*-OETA (**3.16**) in the autoxidation reaction mixture were monitored simultaneously.

To examine the effect of iron on the fragmentation product distribution, water (10 μL) containing 5% FeSO₄ was added to each of the 5 vials and the

vials were vortexed for 20 sec. to distribute the FeSO_4 , and then the mixtures were incubated under the same conditions as above. After incubation, from each vial the water was evaporated with a stream of nitrogen, and the samples were stored under argon at $-80\text{ }^\circ\text{C}$ and analyzed as described above.

Quantification of compounds: HODA (**3.15**), and *cis*-OETA (**3.16**) were quantified by LC-ESI-MS/MS with MRM function. For HODA (**3.15**), the mass transition m/z 227.3 to 84 was monitored (Figure 3.4). For *cis*-OETA (**3.16**), the mass transition m/z 239 to 84.7 was monitored (Figure 3.5). For internal standard (preHODA) the mass transition m/z 382.9 to 100.6 was monitored. Calibration curves were built by injecting various amounts of HODA (**3.15**) and *cis*-OETA (**3.16**) and 10 ng internal standard (preHODA) into the LC/ESI-MS/MS (Figure 3.4 and 3.5). The calibration equations are presented in Table 3.3.

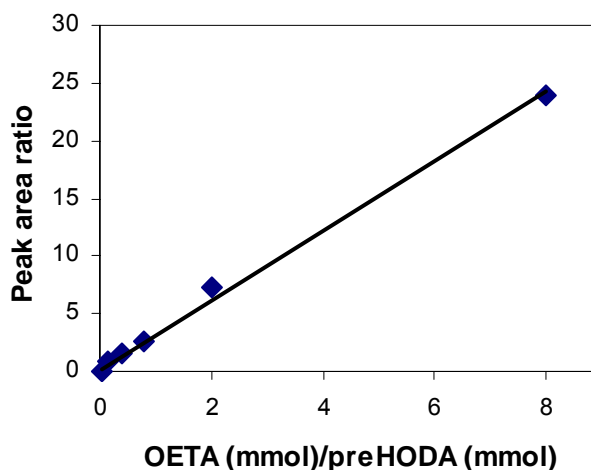
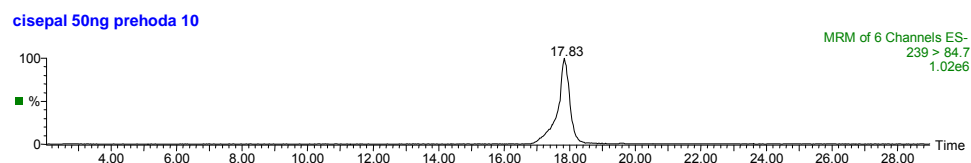


Figure 3.4. LC-MS chromatogram of *cis*-OETA (**3.16**) and the calibration curve; 9-(2-oxanyloxy)-11-(3,3-dimethyl-2,4-dioxolanyl)undec-10-enoic acid (10 ng) (preHODA) was used as internal standard.

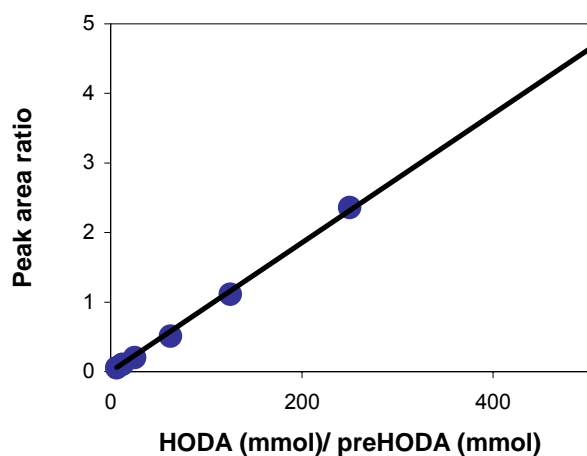
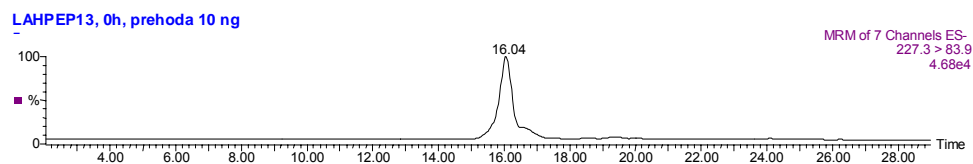


Figure 3.5. LC-MS chromatogram of HODA (**3.15**) and the calibration curve; 9-(2-Oxanyloxy)-11-(3,3-dimethyl-2,4-dioxolanyl)undec-10-enoic acid (10 ng) (preHODA) was used as internal standard.

Table 3.3 Calibration equations

Compound	Calibration Equation
<i>Cis</i> -OETA (3.16)	$y=2.1835x$ ($R^2=0.9993$)
HODA (3.15)	$y=0.920x$ ($R^2=0.9913$)

3.5. References

- (1) Sawada, M.; Carlson, J. C. *J. Gerontol.* **1987**, *38*, 419-428.
- (2) Sawada, M.; Carlson, J. C. *Mech. Ageing Dev.* **1987**, *41*, 125-137.
- (3) van Kooten, F.; Ciabattini, G.; Patrono, C.; Dippel, D. W.; Koudstaal, P. J. *Stroke* **1997**, *28*, 1557-63.
- (4) Re, G.; Azzimondi, G.; Lanzarini, C.; Bassein, L.; Vaona, I.; Guarnieri, C. *Eur. J. Emerg. Med.* **1997**, *4*, 5-9.
- (5) Esterbauer, H.; Schmidt, R.; Hayn, M. *Adv. Pharmacol.* **1997**, *38*, 425-456.
- (6) Berliner, J. A.; Heinecke, J. W. *Free Radic. Biol. Med.* **1996**, *20*, 707-727.
- (7) Deibel, M. A.; Ehmann, W. D.; Markesbery, W. R. *J. Neurol. Sci.* **1996**, *143*, 137-42.
- (8) Bermejo, P.; Gomez-Serranillos, P.; Santos, J.; Pastor, E.; Gil, P.; Martin-Aragon, S. *Gerontology* **1997**, *43*, 218-222.
- (9) Olanow, C. W. *Ann. Neurol.* **1992**, *32*, S2-9.
- (10) Salahudeen, A. K.; Kanji, V.; Reckelhoff, J. F.; Schmidt, A. M. *Nephrol. Dial. Transplant.* **1997**, *12*, 664-668.
- (11) Davies, K. J. A. *Biochem. Soc. Symp.* **1995**, *61*, 1-31.
- (12) Horkko, S.; Miller, E.; Dudl, E.; Reaven, P.; Curtiss, L. K.; Zvaifler, N. J.; Terkeltaub, R.; Pierangeli, S. S.; Branch, D. W.; Palinski, W.; Witztum, J. L. *J. Clin. Invest.* **1996**, *98*, 815-825.

- (13) Winyard, P. G.; Tatzber, F.; Esterbauer, H.; Kus, M. L.; Blake, D. R.; Morris, C. J. *Ann. Rheum. Dis.* **1993**, *52*, 677-680.
- (14) Mapp, P. I.; Grootveld, M. C.; Blake, D. R. *Med. Bull.* **1995**, *51*, 419-436.
- (15) Toshniwal, P. K.; Zarling, E. *J. Neurochem Res.* **1992**, *17*, 205-207.
- (16) Newcombe, J.; Li, H.; Cuzner, M. L. *Neuropathol. Appl. Neurobiol.* **1994**, *20*, 152-162.
- (17) Dix, T. A.; Aikens, J. *Chem. Res. Toxicol.* **1993**, *6*, 2-18.
- (18) Gardner, H. W. *Free Radic. Biol. Med.* **1989**, *7*, 65-86.
- (19) Tallman, K. A.; Roschek, B.; Porter, N. A. *J. Am. Chem. Soc.* **2004**, *asap*.
- (20) Kuhn, H. *Prog. Lipid Res.* **1996**, *35*, 203-26.
- (21) Reinaud, O.; Delaforge, M.; Boucher, J. L.; Rocchiccioli, F.; Mansuy, D. *Biochem. Biophys. Res. Commun.* **1989**, *161*, 883-91.
- (22) Chabert, P.; Ousset, J. B.; Mioskowski, C. *Tet. Lett.* **1989**, *30*, 179-182.
- (23) Sun, M.; Salomon, R. G. *J. Am. Chem. Soc.* **2004**, *126*, 5699-5708.
- (24) Carmen Vigo-Pelfrey, E. **1990**, *Vol. I*.
- (25) Lee, S. H.; Oe, T.; Blair, I. A. *Science* **2001**, *292*, 2083-2085.
- (26) Lee, S. H.; Oe, T.; Blair, I. A. *Chem. Res. Toxicol.* **2002**, *15*, 300-304.
- (27) Esterbauer, H.; Schaur, R. J.; Zollner, H. *Free Radic. Biol. Med.* **1991**, *11*, 81-128.

- (28) Witz, G. *Free Radic. Biol. Med.* **1989**, 7, 333-349.
- (29) Hoff, H. F.; O'Neil, J.; Chisolm, G. M. d.; Cole, T. B.; Quehenberger, O.; Esterbauer, H.; Jurgens, G. *Arteriosclerosis* **1989**, 9, 538-549.
- (30) Palinski, W.; Yla-Herttuala, S.; Rosenfeld, M. E.; Butler, S. W.; Socher, S. A.; Parthasarathy, S.; Curtiss, L. K.; Witztum, J. L. *Arteriosclerosis* **1990**, 10, 325-335.
- (31) Esterbauer, H. *Aldehydic products of lipid peroxidation*; Academic Press: London, 1982.
- (32) Pryor, W. A.; Porter, N. A. *Free Radic. Biol. Med.* **1990**, 8, 541-3.
- (33) Gardner, H. W.; Weisleder, D.; Kleiman, R. *Lipids* **1978**, 13, 246-252.
- (34) Sun, M. Ph. D., CASE, 2003.
- (35) Requena, J. R.; Fu, M. X.; Ahmed, M. U.; Jenkins, A. J.; Lyons, T. J.; Baynes, J. W.; Thorpe, S. R. *Biochem. J.* **1997**, 322, 317-25.
- (36) Hamberg, M. *Lipids* **1975**, 10, 87-92.
- (37) Hiatt, R. In *Organic Peroxides*; D., S., Ed.; Willey-Interscience: 1971; Vol. 2, p 65-70.
- (38) Schneider, C.; Tallman, K. A.; Porter, N. A.; Brash, A. R. *J. Bio. Chem* **2001**, 276, 20831-20838.
- (39) Gardner, H. W.; Plattner, R. D. *Lipids* **1984**, 19, 294-299.
- (40) O'Neal, H. E.; Benson, S. W. *Free Radicals*; Wiley & Sons: New York, 1973.
- (41) Matthew, J. A.; Chan, H. W.; Galliard, T. *Lipids* **1977**, 12, 324-6.

- (42) Deng, Y. H.; Salomon, R. G. *J. Org. Chem.* **1998**, *63*, 7789-7794.
- (43) Patterson, J. *Synthesis* **1984**, 337.
- (44) Yadov, J. S. *Tetrahedron: Asymmetry* **2001**, *12*, 2129-2135.
- (45) Goerger, M. M.; Hudson, B. S. *J. Org. Chem.* **1988**, *53*, 3148-3153.
- (46) Adam, W.; Hadjirapoglou, L. *Topics Curr. Chem.* **1993**, *164*, 45-62.
- (47) Kobierski, M. E.; Kim, S.; Murthi, K. K.; Iyer, R. S.; Salomon, R. G. *J. Org. Chem.* **1994**, *59*, 6044-6050.
- (48) Katsuki, T.; Lee, A. W. M.; Ma, P.; Martin, V. S.; Masamune, S.; Sharpless, K. B.; Tuddenham, D.; Walker, F. J. *J. Org. Chem.* **1982**, *47*, 1373-1378.

Chapter 4

Pilot Studies

Part A. Ethanolamine Phospholipid Depletion by Lipid Oxidation

4.1. Background for Part A

4.1.1. Membrane composition. All biological membranes are composed of a lipid bilayer matrix associated with proteins. Since these lipids contain a substantial amount of polyunsaturated fatty acids (PUFAs) that are prone to oxidation, and due to our aerobic environment, it is understandable that lipid oxidation plays a key role in human health.

The bilayer of lipids is formed mostly from phosphatidylcholines (PCs). PCs are known to be a “bilayer-forming” type of lipid. The hydrophilic “head” and the hydrophobic “tail” have comparable dimensions so it is thermodynamically favorable to form a layer (Figure 4.1.A).¹

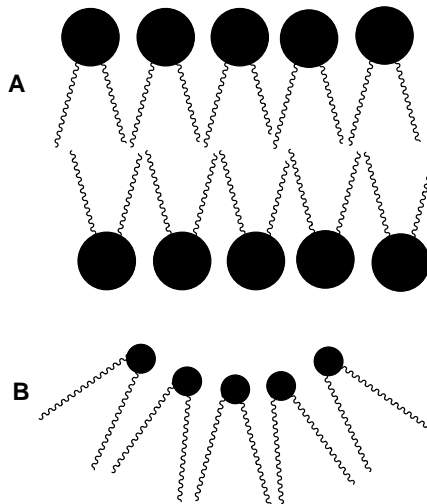



Figure 4.1. A. A model layer formed by PCs, where ● is the hydrophobic head, and  is the hydrophilic tail. **B.** A model of arrangement of the PEs, where the same symbols are used as for panel A.

4.1.2. Phosphatidylethanolamines: an important component of biological membranes. Other components of biological membranes, besides

PCs, include phosphatidylethanolamines (PEs) (Figure 4.1.B). PEs are “non-bilayer” type lipids, i.e., they do not form bilayers by themselves (Figure 4.1.B). “Non-bilayer” lipids are necessary for functional reconstitution of membrane proteins¹ and are required for efficient protein transport across the plasma membrane.² The “non-bilayer” lipids, due to their small head group, can change the lateral pressure across the membrane, and this can facilitate the insertion of proteins. They incorporate more space between the lipid head groups, and have a higher packing density in the acyl chain region. Changing the lateral pressure can also influence the function of proteins and their interactions within the membrane. Another role of the PEs is to promote the formation of curved structures during processes like membrane fusion (see Figure 4.1.B).³

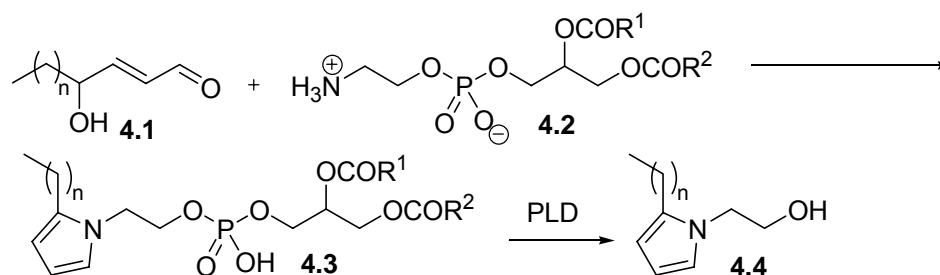
Even though it is known that PE prefers to organize itself in non-bilayer structures, it is noteworthy that biomembranes contain a substantial amount of this non-bilayer lipid. The fact that levels of non-bilayer lipids are precisely regulated implies “that they are of considerable functional importance”.¹ Therefore, modification of ethanolamine phospholipids (EPs) by reactions of their primary amino residues with lipid oxidation products could compromise membrane function, e.g., by causing depletion of EPs or otherwise impairing their ability to stabilize membrane proteins. Apparently, the loss of biological activity associated with their depletion is restored upon replacing the EPs.¹

It is noteworthy that in mitochondrial membrane the percent of EPs is relatively high. Mitochondrial membrane is especially vulnerable to oxidative damage because various free radical species are generated during mitochondrial

respiration. Modification of PE by lipid oxidation products such as HNE was proposed to account for the formation of fluorescent chromolipids upon oxidation of rat liver mitochondria.^{4,5} The EPs are abundant in the photoreceptor disk membranes of the retina as well.⁶ Thus, in spite of the fact that PEs cannot form membranes by themselves, PEs have a very important role in stabilizing the functional integrity of membranes.^{7,8}

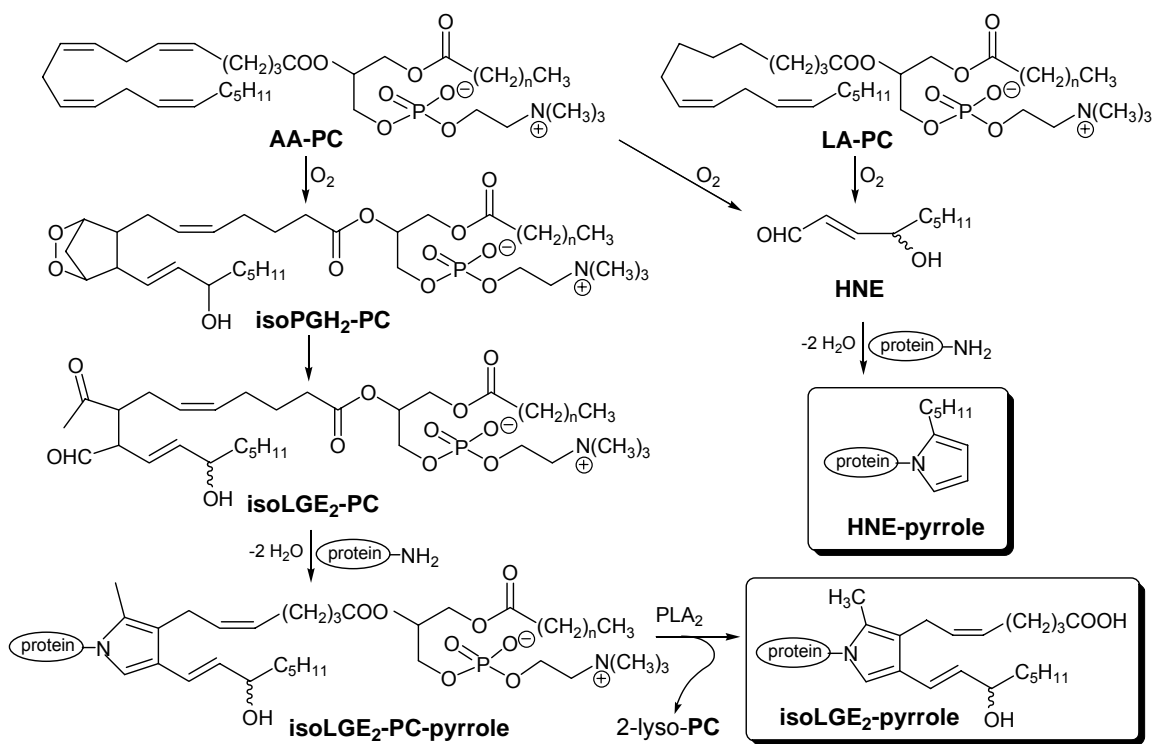
4.1.3. LDL particles. The chemistry of membrane lipid oxidation is similar to the oxidative chemistry that occurs in low-density lipoprotein (LDL). LDL is a spherical particle of 180-250 Å diameter. It has a core composed of cholesteryl esters and triglycerides, and an outer shell of phospholipids and unesterified cholesterol, and only a single 550-kD molecule of apolipoprotein B-100 (apoB-100). ApoB-100 has approximately 350 lysyl residues. Ethanolamine phospholipids (EPs) constitute only a few percent of total LDL phospholipids. In the human LDL, the EPs are 40% PE and 60% plasmenylethanolamine.⁹ Upon oxidation of LDL, modification of PEs is likely to occur.

4.1.4. Ethanolamine phospholipids: a target for reactive lipid oxidation products. The ethanolamine phospholipids can react with products from lipid peroxidation like the hydroxy aldehyde **4.1**, or other similar bifunctional electrophiles, to form pyrrole adducts **4.3**. Cleavage of the pyrrole adducts by phospholipase D (PLD) would produce the corresponding ethanolamine-derived alkylpyrroles **4.4**.



Scheme 4.1 Formation of ethanolamine-derived alkylpyrroles.

The PUFAs from LDL are highly susceptible towards oxidation, and in the human body free radical species are readily generated. The free radical-induced oxidative degradation of PUFAs can lead to various classes of compounds, among which the isolevuglandins (isoLGs) and some γ -hydroxy- α,β -unsaturated aldehydes, e.g., 4-hydroxynonenal (HNE), were previously studied by our group.^{10,11} These reactive oxidation products can modify proteins and DNA and alter the functionality of membranes, proteins, and cells. They can bind covalently to the lysyl ϵ -amino groups of apoB-100, or as some of our recent experimental data suggest, to some other amino groups available in the LDL.¹² Previously, it was found by the Salomon group that, during oxidation of LDL, arachidonyl phosphatidylcholine (AA-PC) is converted into isoLGE₂-PC by a nonenzymatic, free radical pathway (Scheme 4.2). Thus, phospholipid endoperoxides, e.g. the 2-lysophosphatidylcholine (PC) ester of isoPGH₂-PC, are generated and these rearrange to isoLGs. Free radical-induced oxidative fragmentation of AA-PC or LA-PC produces 4-hydroxy-2(E)-nonenal (HNE). Both HNE and isoLGs react with protein lysyl ϵ -amino groups to form pyrroles.



Scheme 4.2 IsoLGE₂-pyrrole and HNE-pyrrole generation from AA-PC or LA-PC.

Both isoLG- and HNE-derived pyrroles can be detected with polyclonal antibodies. Native LDL was oxidized at 37 °C with a free radical generating system and the particle-bound products were separated from non particle-bound products by membrane ultrafiltration or dialysis, and analyzed separately. It was found¹² that the ultrafiltrate (non particle-bound) showed ~60% of the total immunoreactivity for both isoLGE₂-pyrrole and HNE-pyrrole epitopes.

In another experiment, a mixture of LDL was incubated with radiolabeled HNE, and the unbound HNE was removed by dialysis against phosphate buffered saline (PBS). The resulting LDL-HNE adducts, that contained no dialyzable “free HNE”, were subjected to lipid extraction. 64% of the total LDL-HNE adduct radioactivity was found¹³ in the lipid extract. Moreover, the lipid

extract was separated on a reverse phase SepPak™ cartridge. More than 35% of its radioactivity eluted in the same fraction as authentic radiolabeled phosphatidylethanolamine (PE), suggesting that HNE-PE adduct(s) were formed. Possible explanations for the non protein-bound immunoreactivity found in oxidized LDL include HNE-derived pentylpyrrole and LGE₂-pyrrole derivatives of peptides (from oxidatively fragmented apoB-100) or pyrrole derivatives of ethanolamine phospholipids (EPs) that include phosphatidylethanolamine (PE) and plasmenylethanolamine in about equal amounts.⁴ Covalent adduction of HNE with PE is known^{4,5} and the SepPak™ elution experiment strongly supports this later explanation.

4.2. Results and Discussion for Part A

4.2.1. PEs are not dialyzable from liposomes. A model study using liposomes was conducted to test the hypothesis that modification of ethanolamine phospholipids by pyrrole-forming reactions with lipid oxidation products converts cationic ammonium groups into neutral pyrrole derivatives resulting in ejection from the outer shell of low density lipoproteins (LDLs). Unilamellar vesicles made from 1-palmitoyl-2-oleoylphosphatidylcholine (PO-PC, 1.3μM) and radiolabeled 1,2-dioleoyl-L-3-phosphatidyl[2-¹⁴C]ethanolamine (DO-PE) (45nM) were dialyzed for 3 days at 37 °C in air against pH 7.4 PBS buffer (0.1M). Aliquots were removed at various times from the outer buffer and analyzed by liquid scintillation counting. The radioactivity detected outside was around the background level, and if plotted on the scale of the total reactivity from inside the bag, no radioactivity was detected in the outer buffer, indicating

that the radioactive phosphatidylethanolamine is “traped” within the vesicles (Figure.4.2)

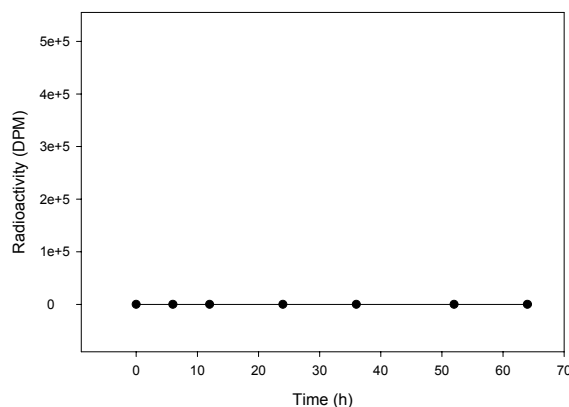
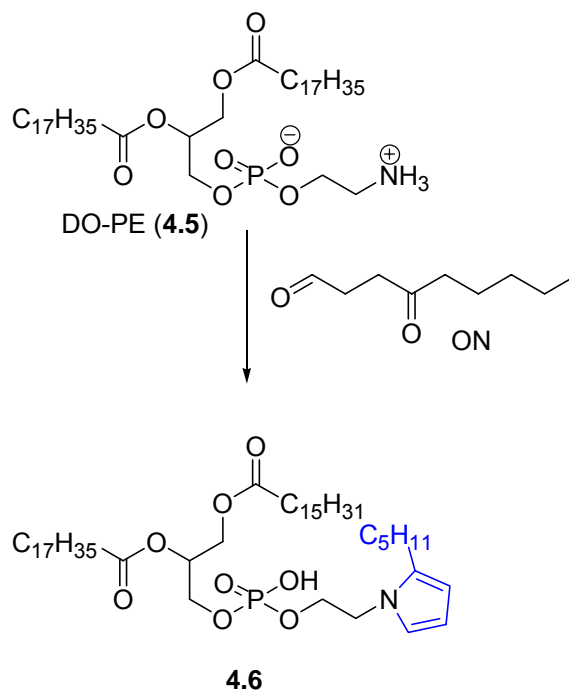


Figure 4.2. The radioactivity detected in the outer buffer.

4.2.2. The level of dialyzable radiolabeled PE generated upon treatment with ON is not detectable above background. The primary amino group in DO-PE (4.5) is expected to react with HNE to generate pentylpyrrole derivatives analogous to the reaction with proteins (see Scheme 4.2). We choose to generate pentylpyrrole derivatives of the amino group of DO-PE by treatment with 4-oxononanal (ON) (Scheme 4.3) because ON is known to react rapidly with the primary amines to give the same pentylpyrroles in high yields. The nitrogen in the *aromatic* pyrrole ring has a reduced basicity and remains, therefore, unprotonated and uncharged at physiological pH. We postulated that the unprotonated pentylpyrrole might leave the membrane and therefore radioactivity would be detected in the solution outside of a dialysis bag.

The solution outside the dialysis bag was replaced with buffer that contained 4-oxononanal (ON, 2 μ M). The vesicles inside the dialysis bag were

dialyzed again for three days and aliquots were removed at various times and analyzed by liquid scintillation counting. The result was a straight line with the points around the background levels, similar with the one in Figure 4.2, i.e., amount of radioactivity, if any, that dialyzed into the outer solution was too little to be detected above background.



Scheme 4.3. Formation of the pentylpyrrole adduct (4.6).

4.2.3. Immunoassay indicates that dialyzable pentylpyrrole is generated upon treatment of PE-containing liposomes with ON. The possibility that the pentylpyrrole was formed but did not leave the liposomes was investigated. Pyrrole formation was detected by enzyme-linked immunosorbent assay (ELISA) using 4-oxononanal-keyhole limpet hemocyanin adduct (ON-KLH) antibody, bovine serum albumin 6-aminocaproic acid (BSA-6-ACA)-ON as standard, and BSA-ON as coating agent. First the immunological response to

ON only was tested. Chicken egg ovalbumin (CEO) is present during the ELISA assay and ON can react with CEO to generate pyrrole-derivatives. Indeed, ON alone, gives an immunologic pentylpyrrole response (Figure 4.3.).

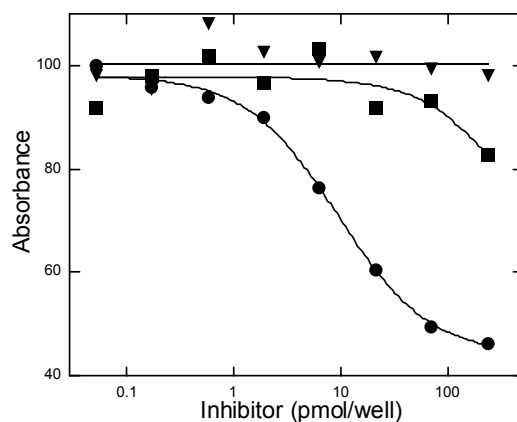


Figure 4.3. Inhibition curve for binding of anti-ON-KLH to BSA-ON by BSA-6-ACA-ON (●) ON alone (■), and ON after adding 10-fold excess $\text{MeONH}_3^+\text{Cl}^-$ (▼)

To remove the immunological response due to free ON (Figure 4.3), the ON solution was treated with a 10-fold excess methoxylamine hydrochloride (20μ). An ELISA assay was performed on the ON solution after “neutralization” of the free 4-oxononanal with $\text{MeONH}_3^+\text{Cl}^-$ (Figure 4.3). There was no longer any immune response to the reaction mixture solution, i.e., the concentration of pentylpyrrole epitopes was negligible. An ELISA assay was then performed on the liposome-ON reaction product mixture that had been dialyzed for 3 days. In Figure 4.4 the immunological response of the dialysate before (Figure 4.4) and after “neutralization” (Figure 4.4) of the unreacted 4-oxononanal with 10-fold excess of methoxylamine hydrochloride is shown. Clearly some of the

immunoreactivity exhibited by the dialysate (Figure 4.4) cannot be attributed to the free ON. Rather, the formation of a dialyzable DO-PE-based pentylpyrrole that was ejected from the liposome is indicated. The concentration of the pentylpyrrole epitope in the sample was 0.37 nmol/mL, which corresponds to a 10% conversion of the initial DO-PE. If a corresponding 10% of the radiolabeled PE dialyzed into the outer solution, the level of radioactivity in that solution is calculated to be 37 DPM for a 10 μ L aliquot. This is not distinguishable from the background level of 35-40 DPM.

To examine whether some pentylpyrrole was formed but not released from the vesicles, i.e., nondialysable, an ELISA was done on the solution inside the bag.

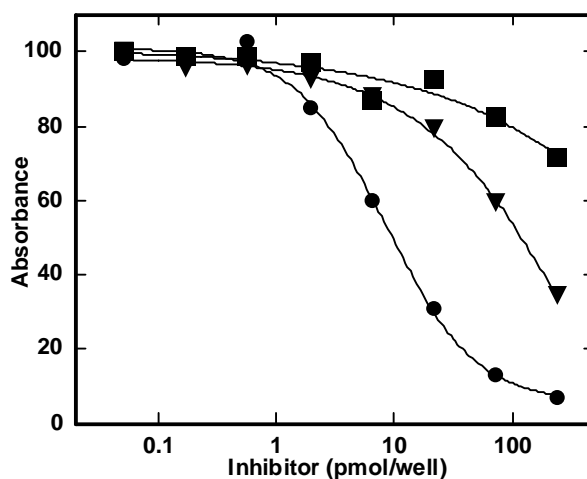
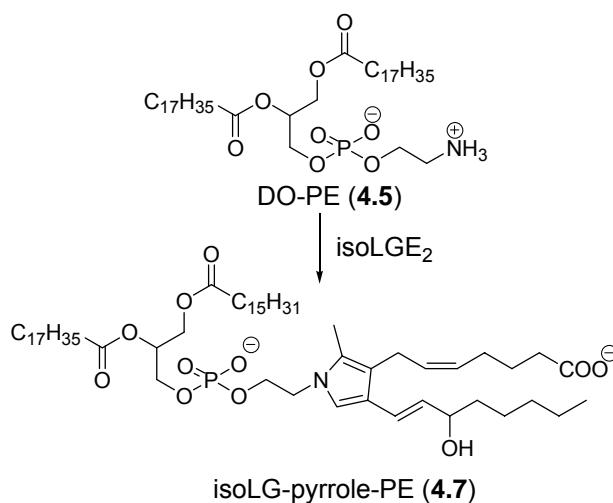


Figure 4.4. Liposome reaction with ON. Inhibition curve for binding of anti-ON-KLH to BSA-ON by BSA-6-ACA-ON (the standard) (●) before adding $\text{MeONH}_3^+\text{Cl}^-$ (▼), after adding $\text{MeONH}_3^+\text{Cl}^-$ (■)

The concentration of pentylpyrrole was found to be about the same, 0.34 nmol/mL, as in the outer solution. This result suggests that equilibrium was

obtained between the pyrrole inside and outside the bag. Due to the large volume of the outer solution (about 15 mL) most of the pyrrole generated in the reaction is found dialyzed into the outer solution.

4.2.4. The level of dialyzable radiolabeled PE generated upon exposure to autoxidizing AA is not detectable above background. In another experiment, vesicles containing radiolabeled PE were dialyzed at 37 °C in air against a solution of 8 μ M arachidonic acid (AA), 20mM sodium ascorbate and 0.8 mM $\text{FeSO}_4 \cdot 7\text{H}_2\text{O}$ in PBS buffer (10mM). We expected this system to generate HNE and isolevuglandins *in situ*. The latter would form pyrroles (Scheme 4.4) that would be more hydrophilic than the pentylpyrroles (from HNE or ON) and would even more effectively cause expulsion of radioactive products into the outer media. Again aliquots of the outer buffer were analyzed at different times, but no radioactivity above the background level was detected outside the dialysis bag.



Scheme 4.4. Pyrrole formation from phosphatidylethanolamine **4.5** and isoLGE₂.

The oxidation of AA will produce many reactive species including HNE. To remove any dialyzable oxidation products, the outer solution was replaced with a new PBS buffer (0.1M) and the vesicles were dialyzed for 3 days, changing the buffer every 12 hours, and analyzing the outside solution for radioactivity. At none of the times did the outside solution show any radioactivity.

The concentration of pentylpyrrole inside the bag was determined by ELISA (Figure 4.5). The aliquot used for the ELISA was from inside the bag after three days of removing all the dialysable oxidation products. The pentylpyrrole concentration was found to be 3 nmol/mL, about 10 times greater than in the model reaction with ON. This corresponds to a yield of undialysable pentylpyrrole of about 10% (based on PE) in the solution inside the dialysis bag. The molecular identity of this undialysable pentylpyrrole is unknown.

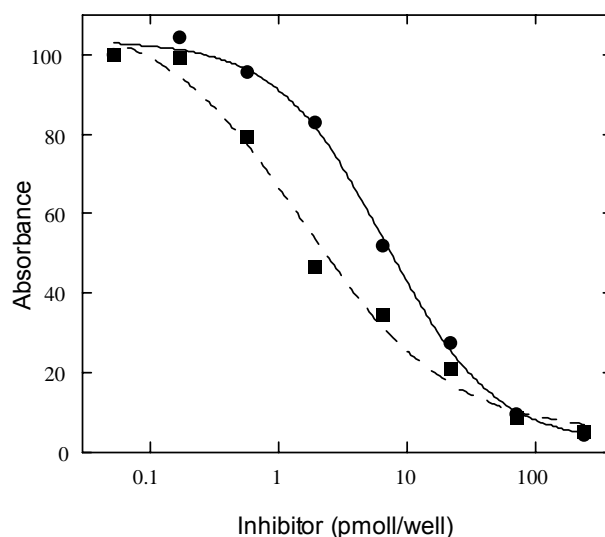


Figure 4.5. Liposome reaction with oxidation products from AA. Inhibition curve for binding of anti-ON-KLH to BSA-ON by BSA-6-ACA-ON (the standard) (●). Inhibition curve for binding of anti-ON-KLH by products from inside the bag (■).

4.3. Conclusions for Part A

Model studies were conducted for testing the “phosphatidylethanolamine depletion hypothesis”, i.e., that the reaction of PEs with lipid peroxidation products would generate derivatives that would be ejected from the vesicle membrane. Pentylpyrroles were generated by the reaction of PE with ON. A method for removing the confounding immunological ELISA response of unreacted ON (treatment with methoxylamine) was developed, and the fact that PEs contained in mixed liposomes with PCs are trapped in the particle, i.e., are not dialyzable, was confirmed. Immunological evidence indicated that PE-derived pentylpyrroles are ejected from the particle. Thus, they are dialyzable, but the levels of these dialyzable products were too low (about 10% conversion) to be confirmed by monitoring dialyzable radioactivity associated with the PE. Similar experiments involving exposure of radiolabeled PE to autoxidizing arachidonic acid also failed to generate sufficient levels of dialyzable PE-derived products to be detected above background.

4.4. Experimental procedures for Part A

General methods. See Chapter 2 for NMR and chromatography.

Absorbance values for enzyme-linked immunoassays (ELISA) were measured on a Bio Rad microplate reader using dual wavelength, 405 nm to read the plate and 650 nm as a reference. The reader was operated through a computer using the MPM 4 program from BioRad. All the assays results were refined using SigmaPlot 2001. Liquid scintillation counting was done on a Beckman LS 5801 counter with Quench curves made from a Beckman ^{14}C standard set.

Materials. Spectrapor membrane tubing (Mr cutoff 14,000 No.2) for standard dialysis was obtained from Fisher Scientific co (Pittsburgh, PA). The following commercially available materials were used as received: chicken egg ovalbumin (CEO), grade V, 99%), bovine serum albumin (BSA, fraction V, 96-99%), human serum albumin (HSA, fraction V), disodium p-nitrophenyl phosphate, arachidonic acid (Sigma, St. Louis, MO); keyhole limpet hemocyanin (KLH, ICN Biochemicals, Irvine, CA); goat anti-rabbit IgG-alkaline phosphatase (Boehringer-Manheim, Indianapolis, Indiana). Phosphate buffered saline (PBS) was prepared from a pH 7.4 stock solution containing 0.2 M $\text{NaH}_2\text{PO}_4/\text{Na}_2\text{HPO}_4$, 3.0 M NaCl, and 0.02% NaN_3 (w/w). This solution was diluted 20 fold as needed. 4-Oxohexanal was prepared according to Ballini et al.¹⁴ For ELISA, unless otherwise noted, duplicates of each sample were run on the same plate. Concentrations of binding inhibitor are expressed in units of pmol/well. Since 50 μL of sample or standard solutions were loaded into each well on the ELISA plates, this corresponds to pmol/50 μL .

Vesicle preparation. Commercially available phosphatidylcholine PO-PC (1 mg, 1.3 μ M) in 1 mL chloroform was vortexed in a large glass test tube (16 mL) with 100 μ L (45 nmol) 1,2-dioleoyl-L-3-phosphatidyl[2- 14 C] ethanolamine in toluene/ethanol solution (550,000 DPM, specific activity 55mCi/mmol). The phospholipid mixture was dried under a gentle stream of argon. The tube was set at an angle so that the phospholipids form a thin film on the side of the tube. The gas stream was sufficiently slow not to blow any of the solution out of the tube. To the tube of dried phospholipids, 1mL of freshly prepared 50mM pH 7.4 PBS solution was added at room temperature. The solution was vortexed vigorously to completely solvate the dried phospholipids in buffer. Then the sample in the test tube was incubated for 30 min at 37 °C. After the sample was fully hydrated (cloudy homogenate), it was loaded into a gas-tight syringe and carefully attached to one end of a mini-extruder. An empty gas-tight syringe was attached to the other end of the mini-extruder. If the empty syringe's plunger is set to zero, the syringe will fill automatically as the lipid is extruded through the membrane. The plunger of the filled syringe was gently pushed until the lipid solution was completely transferred to the initially empty syringe. Then the plunger of the latter syringe was gently pushed to transfer the solution back to the original syringe. The last two steps were repeated usually 5 times (total of 10 passes through membrane). The filled syringe was removed from the extruder and the lipid solution was transferred into a pre-hydrated dialysis bag.

Clean up. The contaminated glassware was cleaned with acetone and water. The washing acetone was placed in the proper radioactive liquid (organic)

waste container, the washing water may be disposed of as sewer waste in a designated sink if the combined amount of the sewer waste does not exceed the 20 μCi per day limit. A log of all sewer disposals was kept. All other wastes generated in the procedure, including rubber gloves, pipette tips and glassware were disposed of in a dry solid radioactive waste container and held for pick-up by the DOES. A “wipe-test” was performed to survey the working area to make sure it was “clean”, if not, any contaminated area was cleaned immediately after the experiment.

Reaction of liposomes with ON. The liposomes were dialyzed for 3 days at 37 °C against 0.1M pH 7.4 PBS (6 x 20 mL). The buffer was changed every 12 h. Aliquots (1mL) from the outer buffer were removed before changing the buffer, mixed with the standard amount of scintillation fluid and analyzed by liquid scintillation counting. The radioactivity detected outside was not distinguishable from the background level (35-40 DPM). Then oxononanal (6.2 mg, 38 μmol) in 0.5 mL of absolute ethanol was added to a freshly prepared PBS buffer (0.1M). Aliquots (1mL) from the outer buffer were removed at 6, 12, 24, 48 and 72 h mixed with the standard amount of scintillation fluid and analyzed by liquid scintillation counting. After 72 hours, an aliquot from the outer buffer was subjected to ELISA analysis to detect the pentylpyrrole epitope. Another aliquot was treated with $\text{MeONH}_3^+\text{Cl}^-$ (20 μM), at room temperature for 3 hours, and then subjected to ELISA analysis to detect the pentylpyrrole epitope.

Exposure of liposomes to autoxidizing AA. Radiolabeled liposomes were dialyzed for 3 days at 37 °C against pH 7.4 PBS (6 x 20 mL)(0.1M). The

buffer was changed every 12 h. Aliquots (1mL) from the outer buffer were removed before changing the buffer, mixed with the standard amount of scintillation fluid and analyzed by liquid scintillation counting. The radioactivity detected outside was around the background level (35-40 DPM). Then the buffer was changed with one containing 8 μ M AA, 20mM Na ascorbate and 0.8 mM $\text{FeSO}_4 \cdot 7\text{H}_2\text{O}$ in PBS buffer (10mM). Aliquots (1mL) from the outer buffer were removed at 6, 12, 24, 48 and 72 h mixed with the standard amount of scintillation fluid and analyzed by liquid scintillation counting. The radioactivity detected outside was around the background level (35-40 DPM). After 72 hours the outside solution was replaced with a new PBS buffer (0.1M), and the vesicles were dialyzed for 3 days at 37 °C against 0.1M pH 7.4 PBS (3 x 20 mL). After 72 hours, an aliquot from the solution inside the dialysis bag was subjected to ELISA analysis to detect the pyrrole epitope.

Enzyme-linked immunosorbent assay (ELISA). Each well of a 96-well microplate was coated with 4-ON-BSA (100 μ L). This coating agent was prepared by diluting a PBS stock solution containing 0.11 mM 4-ON-BSA (2200 pmol/well) to an appropriate concentration with PBS (283.75 pmol/well). For standard and each inhibitor, up to eight serial dilutions, a blank and a positive control containing no inhibitor were run. The plate was covered with a plastic lid and placed in an incubator at 37 °C for 1 h, and then allowed to cool to room temperature. After discarding the supernatant, each well was washed with pH 7.4 PBS (3 x 300 μ L) and then blocked by incubating 1 h at 37 °C with 300 μ L of 1% chicken egg ovalbumin (CEO) in pH 7.4 PBS. After cooling to room temperature,

the supernatant was discarded and the wells were rinsed with 0.1% CEO in pH 7.4 PBS (300 μ L). For each sample and the ACA-ON-BSA standard, the undiluted sample solution and aliquots (150 μ L) of up to eight 1:0.3 serial dilutions with pH 7.4 PBS or the standard were incubated in test tubes at 37 °C for 1 h with the ON-KLH antibody solutions (150 μ L). The antibody solution was prepared by adding 0.2% CEO in pH 7.4 PBS (1:100 dilution for anti ON-KLH). Blank wells were filled with 0.2% CEO in pH 7.4 PBS (100 μ L). Positive control wells were filled with the antibody solution (50 μ L) and 0.2% CEO solution (50 μ L). To the rest of the sample wells, aliquots (100 μ L, containing 50 μ L of sample solution and 50 μ L of the antibody solution) of the serial dilutions of antibody-antigen complex were added. The plate was then incubated at room temperature on a shaker for 1 h. After discarding the supernatant, the wells were washed with 0.1% CEO (3 x 300 μ L), and then goat anti-rabbit IgG-alkaline phosphatase solution (100 μ L) was added to each well. This enzyme-linked second antibody solution was prepared by diluting commercially available antibody solution (10 μ L) with 1% CEO (10 mL). The plate was then incubated at room temperature for 1 h while gently swirling on a shaker. After discarding the supernatant, the wells were washed with 0.1% CEO (3 x 300 μ L). To each well was then added a solution (100 μ L) of disodium *p*-nitrophenyl phosphate (10 mg) in water (11 mL, pH adjusted to 9.6 using NaOH) containing glycine (50 mM) and MgCl₂ (1 mM). The plate was then incubated at room temperature for about 1 h until the absorbance levels reached an appropriate level (0.6-0.7). A diagram of the ELISA chromophore generation is shown in Figure 4.3. The developing process

was terminated by adding 3 N NaOH (50 μ L) to each well before measuring the final absorbance values. The absorbance in each well was measured with a Bio Rad 450 microplate reader using dual wavelength with detection at 405 nm relative to 655 nm.

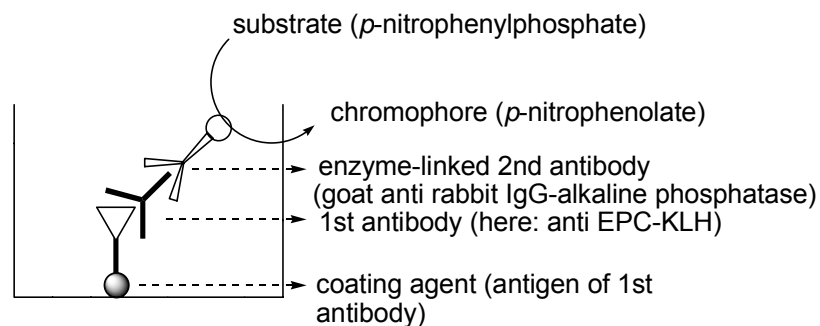


Figure 4.6. Schematic representation of ELISA.

Absorbance values for duplicate assays were averaged and then scaled such that the maximum curve fit value is close to 100 percent. The averaged and scaled percent absorbance values were plotted against the log of concentration. Theoretical curves shown for each plot were fit to the absorbance data with a four parameter logistic function, $f(x) = (a-d)/[1+(x/c)^b]+d$ using SigmaPlot[®] 2001 from Jandel Scientific Software, San Rafael, CA. Parameter a = the asymptotic maximum absorbance, b = slope at the inflection point, c = the inhibitor concentration at the 50% absorbance value (IC_{50} , reported in Tables 4.1-4.5, *vide infra*), and d = the asymptotic minimum absorbance. If necessary, constraints were placed on the parameters, usually the values for "a" and/or "d". A Cartesian graph was then created that shows plots of the experimental data (points) and calculated curves.

Table 4.1 ELISA data for ON in Figure 4.3 (page 120).

pmol/well	Absorbance	% Absorbance	Parameters	Curve fit
238.75	5.0000e-3	0.61	96.60	0.23
71.625	0.0140	1.71	1.65	1.75
21.488	0.0600	7.32	45.46	10.58
6.44	0.3920	47.81	9.9056e-9	45.53
1.93	0.6730	82.07		83.66
0.58	0.7530	91.83		94.58
0.17	0.7600	92.68		96.32
0.05	0.8490	103.54		96.56

Table 4.2 ELISA data for methoxime derivative in Figure 4.3 (page 120).

pmol/well	Absorbance	% Absorbance	Parameters	Curve fit
238.75	0.6960	92.80	99.77	92.30
71.625	0.7120	94.93	1.24	98.73
21.488	0.8080	107.73	11994.85	100.31
6.44	0.7730	103.07	1.00	100.67
1.93	0.7520	100.27		100.75
0.58	0.7470	99.60		100.77
0.17	0.7550	100.67		100.77
0.05	0.7200	96.00		100.77

Table 4.3 ELISA data for liposome reaction with ON in Figure 4.4 (page 121).

pmol/well	Absorbance	% Absorbance	Parameters	Curve fit
238.75	0.2300	30.91	100.70	31.34
71.625	0.4600	61.83	1.00	60.49
21.488	0.6252	84.03	786.81	84.04
6.44	0.6830	91.80	0.19	95.17
1.93	0.7050	94.76		99.11
0.58	0.7780	104.57		100.35
0.17	0.7750	104.17		100.73
0.05	0.7440	100.00		100.85

Table 4.4 ELISA data for liposome reaction with ON after adding the methoxime in Figure 4.4 (page 121).

pmol/well	Absorbance	% Absorbance	Parameters	Curve fit
238.75	8.9000e-3	1.66	99.77	2.71
71.625	0.0780	14.58	1.46	10.16
21.488	0.1900	35.51	112.77	37.89
6.44	0.4210	78.69	1.00	78.13
1.93	0.5210	97.38		95.97
0.58	0.5640	105.42		99.90
0.17	0.5060	94.58		100.62
0.05	0.5350	100.00		100.74

Table 4.5 ELISA data for liposome reaction with ON after adding methoxylamine in Figure 4.4 (page 123).

pmol/well	Absorbance	% Absorbance	Parameters	Curve fit
238.75	0.0030	0.61	98.60	0.28
71.625	0.0180	1.71	7.65	2.75
21.488	0.05900	7.32	44.46	11.58
6.44	0.4250	48.81	0.002	42.53
1.93	0.6830	82.07		88.68
0.58	0.8730	91.83		93.58
0.17	0.7800	92.68		95.382
0.05	0.9740	103.54		97.56

Part B. Total synthesis of analogues of HODA-PC and HOOA-PC

4.5. Background for Part B

In the Salomon lab a variety of oxidized phospholipids were prepared^{15, 16}, inspired by the conviction that such compounds should be produced *in vivo* in analogy with the free radical-induced oxidative generation of HNE. In collaborative studies, these phospholipids were detected *in vivo* and some biological properties were elucidated.^{17,18}

Recent studies implicated the scavenger receptor CD36 in a number of physiological and pathophysiological processes *in vivo* that involve cell types expressing CD36 and CD36 ligands. CD36 belongs to the family of proteins that has a role in cell adhesion and serve as lipid receptors.^{19,20} CD36 ligands include: long chain fatty acids,²¹ anionic phospholipids,^{22,23,24} LDL oxidized by copper (Cu²⁺-oxLDL),^{21,25} or by myeloperoxidase-generated reactive nitrogen species (NO₂-LDL),²⁶ apoptotic cells,²⁷ collagen,²⁸ thrombospondin,^{29,30} and shed photoreceptor outer segments.³¹ NO₂-LDL is avidly taken up and degraded by macrophages, leading to massive cholesterol deposition and foam cell formation, an essential step in lesion development. Furthermore, the scavenger receptor CD36 mediates recognition of NO₂-LDL.

A number of studies demonstrated that CD36 participates in lipid accumulation and macrophage foam cell formation *in vitro* and *in vivo*.^{32,33,34} suggesting that CD36 promotes atherosclerosis. A recent study in CD36 knockout mice confirmed a critical role for CD36 in atherogenesis.³⁵ Even though

interaction of oxidized LDL with CD36 is well documented, the exact molecular structure(s) of the CD36 ligand(s) in oxidized LDL remain ill defined.

In collaborative studies, the Salomon group identified four major structurally related oxidized phospholipids¹⁸ with CD36 binding activity (Figure 4.7).

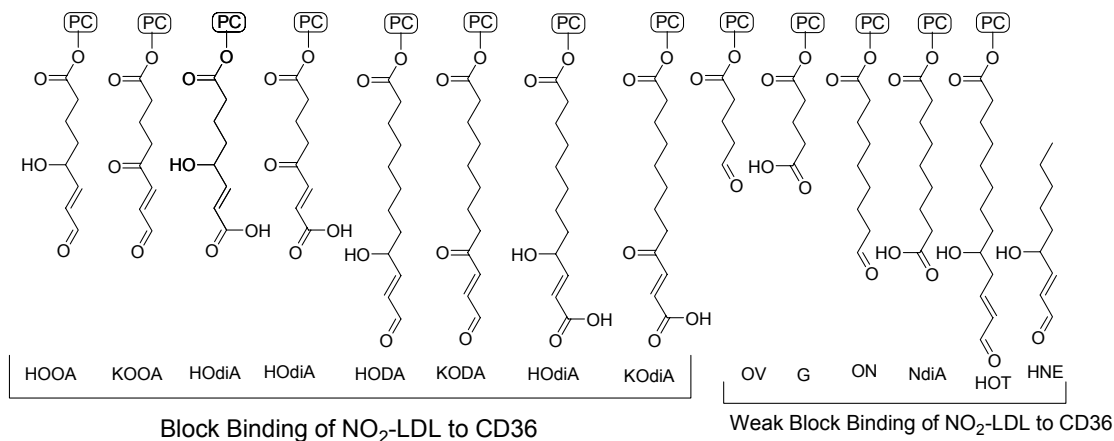
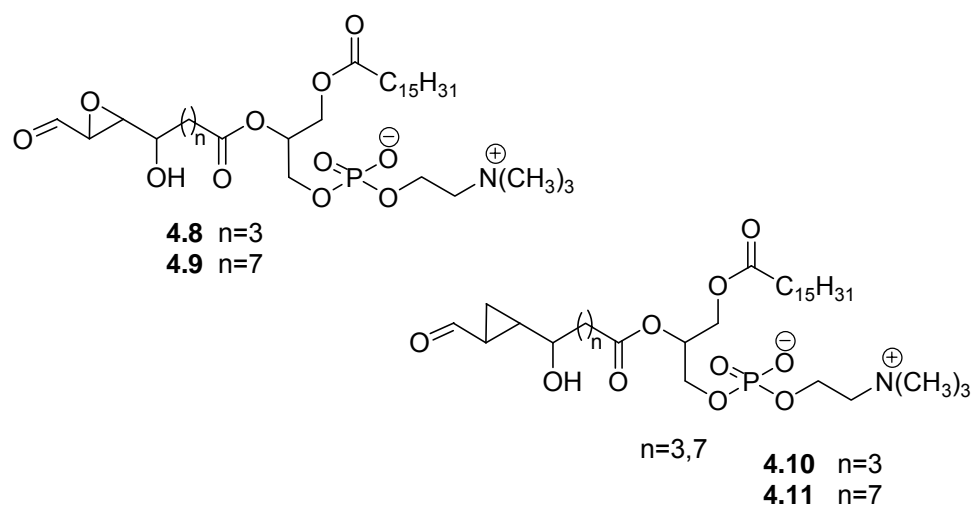


Figure 4.7. Lipid oxidation products and their ability to block binding of NO₂-LDL to CD36.

Comparison with a variety of structurally diverse analogues that showed no binding activity (Figure 4.7) revealed that the active compounds all have a sn-2 acyl group that incorporates a terminal γ -hydroxy(or oxo) α,β -unsaturated carbonyl. The eight active compounds all showed half-maximal inhibitory concentrations below 1 μ M. However, the mechanism by which these oxidized phospholipids bind to the CD36 is not well understood. In order to elucidate the role of different parts of the oxidized chain in the binding to CD36, syntheses of four analogues of the active HODA-PC and HOOA-PC were developed. In this chapter the syntheses of these analogues will be described.

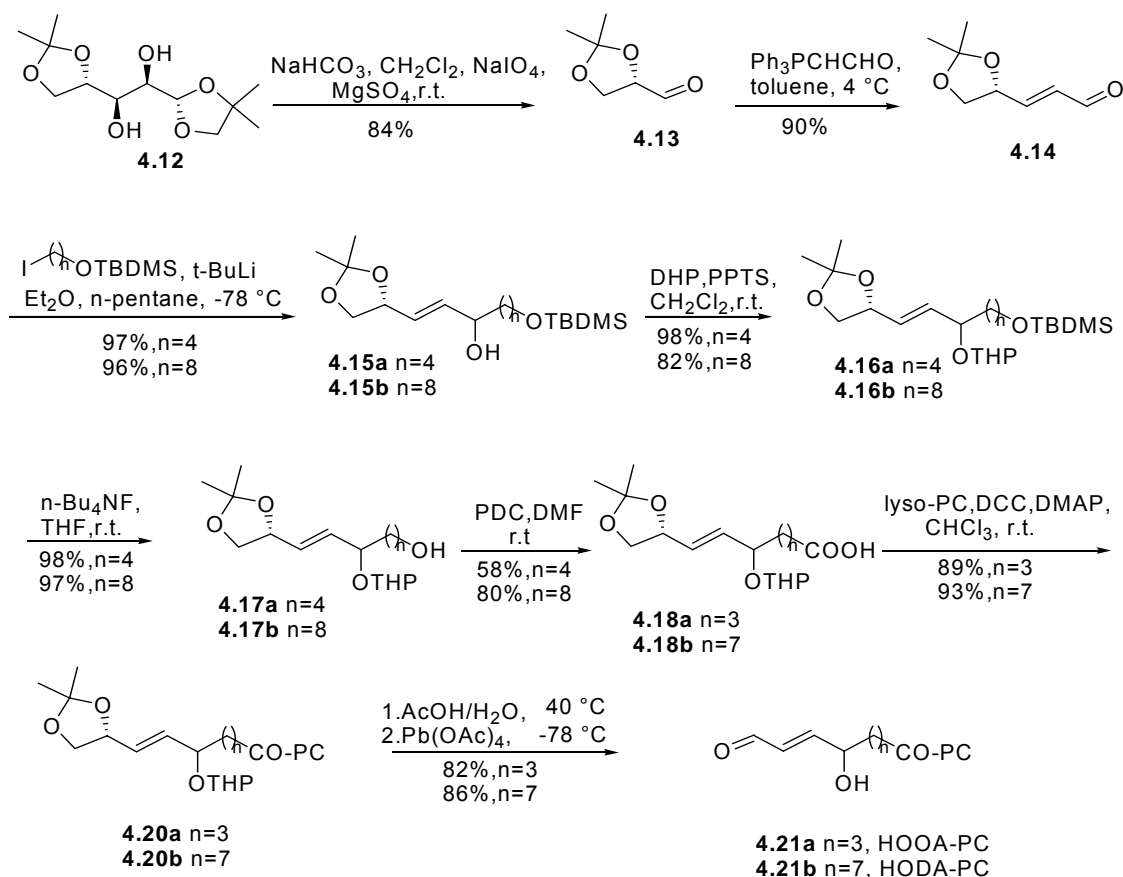
4.6. Results and Discussion

The strategy was to exploit the routes already developed in our lab for the syntheses of 2-(5-hydroxy-8-oxooctanoyl)phosphatidylcholine (HOOA-PC) and 2-(9-hydroxy-12-oxododecanoyl)phosphatidylcholine (HODA-PC)¹⁵ and to modify these routes for making analogues of these phospholipids which would be tested for their ability to block binding of NO₂-LDL at CD36. Four analogues **4.8-4.11** (Scheme 4.5) of the γ -hydroxy(or oxo) α,β -unsaturated aldehydes HOOA-PC and HODA-PC were envisioned to be readily accessible by minor modifications of the routes previously developed for the synthesis of the parent aldehydes.¹⁵



Scheme 4.5. The proposed structure for HOOA-PC and HODA-PC analogues.

Because no precursors for HOOA-PC (**4.21a**) or HODA-PC (**4.21b**) were available, I first carried out a gram-scale synthesis to provide adequate amounts of the various precursors required. Dr. Deng, a former student in our group, developed the syntheses outlined in Scheme 4.6.

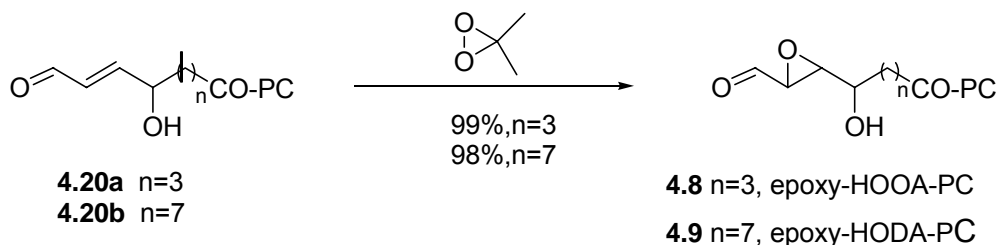


Scheme 4.6. Total syntheses of HOOA-PC (**4.21a**) and HODA-PC (**4.21b**).

My only modification of Deng's method was in the steps for coupling the aldehyde **4.14** with two different iodides ($n = 4$ and $n = 8$). Instead of the Grignard reaction used in the original design, a lithium-halogen exchange reaction was used. The yield of 1,2-addition product **4.15a** was the same as in the original design (97%), but the yield for the **4.12b** was improved from 82% to 88%. Commercially available solutions of t-BuLi are relatively easy to handle and the one-pot two-step procedure of lithium-halogen exchange and subsequent 1,2-addition to aldehyde **4.14** is faster and cleaner than the corresponding sequence that employs a highly exothermic Grignard reaction. Compounds **4.18a** and

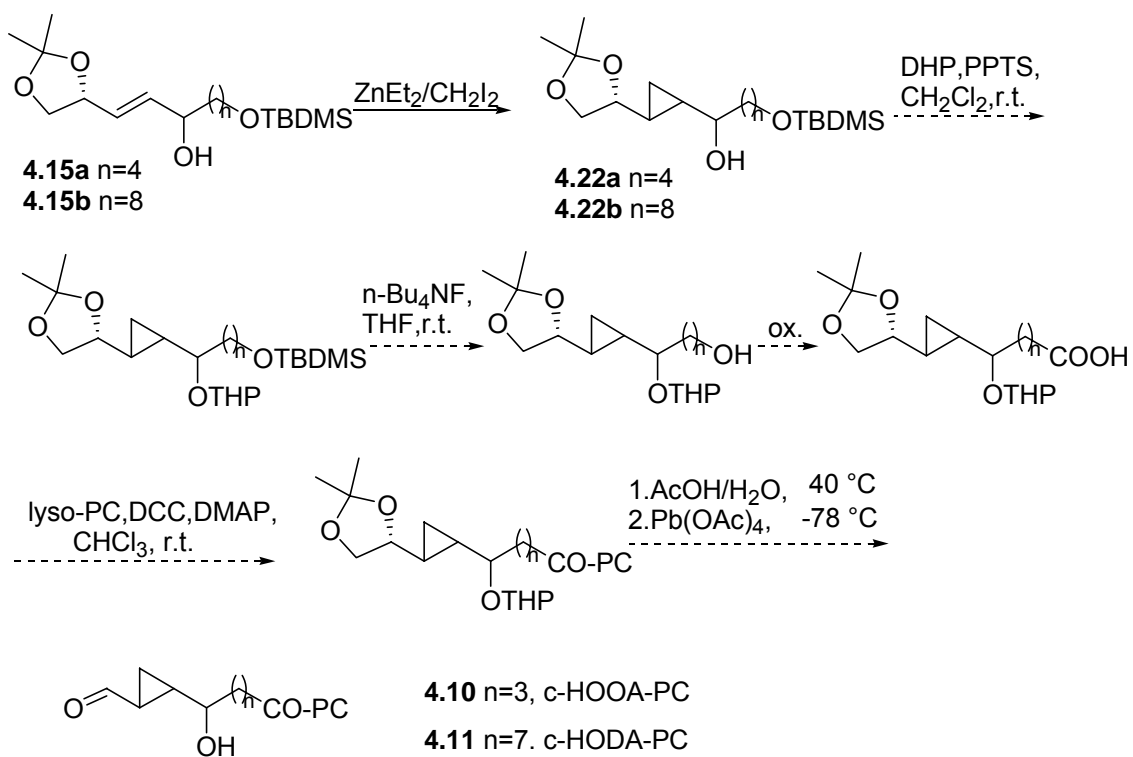
4.18b are stable intermediates and can be stored under argon at $-80\text{ }^\circ\text{C}$. They also served as precursors for the phosphatidylethanol amine analogues of **4.21a** and **4.21b**. Dr Gugiu carried out syntheses of phosphoethanolamines in our lab, and Dr. Podrez at Cleveland Clinic tested their ability to block binding of NO_2 -LDL at CD36. The results are already reported.³⁶

Having secured adequate amounts of the precursors **4.18a** and **4.18b**, the synthesis of the analogues **4.8** and **4.9** was accomplished by only one extra step from HOOA-PC and HODA-PC. The epoxidation of the double bond was done in the last step, because the deprotection of the aldehyde and alcohol with lead tetraacetate and acetic acid would have been too harsh for the epoxy ring, which is usually stable to pH 3, but not below. The reaction was run for 30 min at room temperature with a freshly prepared solution of dimethyl dioxirane in acetone (Scheme 4.7). Even though typically all the transformations on the backbone of the modified fatty acids are done *before* the coupling of the corresponding acid with the commercially available lyso-PC owing to the difficulty of purifying the resulting phospholipids, in this case the reactions were practically quantitative, and rotary evaporation of the volatile byproducts afforded the pure compounds, **4.8** and **4.9**.



Scheme 4.7. Syntheses of epoxy-HOOA-PC and epoxy-HODA-PC.

The route depicted in Scheme 4.8 was envisioned to generate the analogues **4.10** and **4.11**. Sufficient amounts of the precursors **4.15a** and **4.15b** were prepared to allow the investigation of the best route to the cyclopropanes **4.22a** and **4.22b**. The cyclopropanation reaction with diethyl zinc and diiodomethane was performed on a small scale and the NMR spectrum of the crude product showed the disappearance of the double bond and the appearance of peaks in the region where the signals from cyclopropane protons should be (below 1ppm). The proposed route (Scheme 4.8) entails reactions similar to the syntheses of HOOA-PC or HODA-PC, and the conversion of the double bond to a cyclopropane ring is not expected to add any difficulties to the synthesis. My colleague Bharathi Govindarajan will complete these syntheses.



Scheme 4.8. Proposed syntheses of **4.10** and **4.11**.

4.7. Conclusion for Part B

Four analogues of HODA-PC and HOOA-PC were designed. Two of them, epoxides **4.8** and **4.9**, were expeditiously synthesized, and viable synthetic routes to the remaining ones, cyclopropanes **4.10** and **4.11**, were designed and initiated. Completion of the latter synthesis is being pursued by another student. Future biological evaluation of these analogues is planned through collaborative efforts.

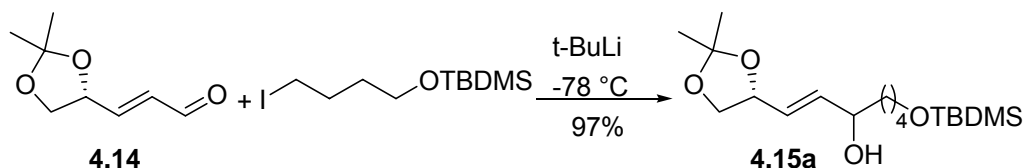
4.8. Experimental Part for Part B

General methods: see Chapter 2 for NMR and chromatography. All solvents were distilled under a nitrogen atmosphere prior to use. Methylene chloride was freshly distilled over calcium hydride. Chloroform was dried over phosphorus pentoxide. Tetrahydrofuran (THF) was freshly distilled over potassium and benzophenone. All reaction flasks were flame dried under argon before use. All materials were obtained from Aldrich or Acros unless otherwise specified.

Chromatography was performed with ACS grade solvent (ethyl acetate and hexanes). Thin layer chromatography (TLC) was performed on glass plates precoated with silica gel (Kieselgel 60 F₂₅₄, E. Merk, Darmstadt, West Germany). R_f values are quoted for plates of thickness 0.25 mm. The plates were visualized with iodine or phosphomolybdic acid reagent.

2-(3-(3,3)-Dimethyl-2,4-dioxolanyl)prop-2-enal (4.14) was synthesized according to the published protocol¹⁵ A 9.5 g supply of the aldehyde **4.14** was made ¹H NMR (300 MHz, CDCl₃) δ 9.57 (d, *J* = 7.8 Hz, 1 H), 6.74 (dd, *J* = 15.7, 5.4 Hz, 1 H), 6.33 (ddd, *J* = 15.7, 7.8, 1.2 Hz, 1 H), 4.77 (m, 1 H), 4.23 (dd, *J* = 15.6, 6.7 Hz, 1 H), 3.71 (dd, *J* = 6.7, 8.2 Hz, 1 H), 1.44 (s, 3 H), 1.40 (s, 3 H).

1-(3,3-Dimethyl-2,4-dioxolanyl)-7-(1,1,2,2-tetramethyl-1-silapropoxy)hept-1-en-3-ol (4.15a).



The iodide (1.4 g, 4.45 mmol), dried by evacuation through a Dry Ice-acetone trap on a vacuum pump overnight, was dissolved in 12 mL of freshly distilled ether and cooled at $-78\text{ }^\circ\text{C}$. A solution of $t\text{-BuLi}$ (5.5 mL, 9.8 mmol) was added dropwise over 5 min. The cooling bath was removed for 1 h. Then the mixture was cooled again to $-78\text{ }^\circ\text{C}$ and the aldehyde **4.14** (0.68 mg, 4.38 mmol) in 3 mL of dry ether was added dropwise. After removing the bath again and stirring for another 30 min, the reaction was quenched by addition of saturated aqueous NH_4Cl , then extracted with ethyl acetate, and dried with sodium sulfate. The solvent was removed with a rotary evaporator. The residue was purified by flash chromatography on a silica gel column (25 % ethyl acetate in hexanes, TLC: $R_f = 0.21$) to give **4.15a** (2.25 g, 97%); $^1\text{H NMR}$ (300 MHz, CDCl_3) δ 5.81 (ddd, $J = 15.4, 5.8, 2.7$ Hz, 1 H), 5.65, 5.64 (ddd, $J = 15.4, 6.9, 3.3$ Hz, 1 H), 4.49 (td, $J = 7.5, 6.8$ Hz, 1 H), 4.12 (m, 1 H), 4.075, 4.082 (dd, $J = 8.1, 6.2$ Hz, 1 H), 3.50-3.65 (3 H), 1.4-1.6 (12 H), 1.39 (s, 3 H), 1.35 (s, 3 H), 0.89 (s, 9 H), 0.02 (s, 6 H).

1-(5-(2-Oxanyloxy)-7-(3,3-dimethyl-2,4-dioxolanyl)hept-6-enyloxy)-1,1,2,2-tetramethyl-1-silapropane (4.16a) was synthesized according to the published protocol.¹⁵ A 2.5 g supply of **4.16a** was stocked after all the

experiments were done. ^1H NMR (300 MHz, CDCl_3) δ 5.50-5.86 (2 H), 4.55-4.68 (m, 1 H), 4.45-4.55 (m, 1 H), 4.0-4.12 (2 H), 3.82 (m, 1 H), 3.48-3.65 (3 H), 3.45 (m, 1 H), 1.3-1.9 (12 H), 1.40 (s, 3 H), 1.37 (s, 3 H), 0.86 (s, 9 H), 0.02 (s, 6 H).

5-(2-Oxanyloxy)-7-(3,3-dimethyl-2,4-dioxolanyl)hept-6-en-1-ol (4.17a)

was synthesized according to the published protocol.¹⁵ A 1.8 g supply of **4.17a** was prepared. ^1H NMR (300 MHz, CDCl_3) δ 5.50-5.85 (2 H), 4.42-4.66 (2 H), 3.88-4.14 (2 H), 3.80 (m, 1 H), 3.48-3.64 (3 H), 3.42 (m, 1 H), 1.3-1.9 (12 H), 1.39 (s, 3 H), 1.35 (s, 3 H).

5-(2-Oxanyloxy)-7-(3,3-dimethyl-2,4-dioxolanyl)hept-6-enoic acid

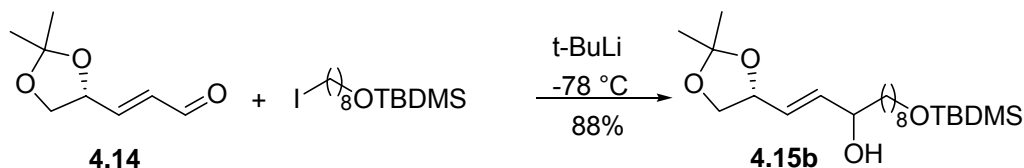
(4.18a) was synthesized according to the published protocol.¹⁵ A 0.8 g supply of **4.18a** was prepared. ^1H NMR (300 MHz, CDCl_3) δ 5.50-5.86 (2 H), 4.55-4.68 (m, 1 H), 3.88-4.18 (2 H), 3.82 (m, 1 H), 3.55 (m, 1 H), 3.45 (m, 1 H), 2.35 (2t, $J = 6.6, 7.5$ Hz, 2 H), 1.4-1.8 (10 H), 1.40 (s, 3 H), 1.36 (s, 3 H).

Precursor 4.20a of 2-(9-hydroxy-12-oxododecanoyl)phosphatidylcholine was synthesized according to the published protocol.¹⁵ ^1H NMR (300 MHz, CDCl_3) δ 5.5-5.85 (2 H), 5.18 (m, 1 H), 4.5-4.65 (m, 1 H), 4.48 (td, $J = 6.8, 6.4$ Hz, 1 H), 4.15-4.42 (3 H), 4.0-4.1 (3 H), 3.92 (m, 2 H), 3.65-3.85 (3 H), 3.55 (m, 1 H), 3.43 (m, 1 H), 3.35 (s, 9 H), 2.24 (t, $J = 7.6$ Hz, 2 H), 2.27 (m, 2 H), 1.4-1.9 (12 H), 1.39 (s, 3 H), 1.35 (s, 3 H), 1.22 (24 H), 0.85 (t, $J = 6.8$ Hz, 3 H).

2-(9-Hydroxy-12-oxododecanoyl)phosphatidylcholine (HODA-PC, 4.21a) was synthesized according to the published protocol.¹⁵ ^1H NMR (300 MHz, CDCl_3) δ 9.53 (d, $J = 7.7$ Hz, 1 H), 6.85 (dd, $J = 15.3, 3.7$ Hz, 1 H), 6.28 (dd, $J = 15.3, 8.2$ Hz, 1 H), 5.22 (m, 1 H), 4.37 (m, 1 H), 4.1-4.35 (4 H), 3.99 (m,

1 H), 3.91 (m, 1 H), 3.75 (m, 2 H), 3.30 (s, 9 H), 2.36 (m, 2 H), 2.26 (t, $J = 6.2$ Hz), 1.5-1.9 (6 H), 1.22 (24 H), 0.85 (t, $J = 6.4$ Hz).

1-(3,3-Dimethyl-2,4-dioxolanyl)-11-(1,1,2,2-tetramethyl-1-silapropoxy)-undec-1-en-3-ol (4.15b).



The iodide (2.4 g, 6.48mmoles) in a flame dried flask, was further dried by evacuation through a Dry Ice-acetone trap on a vacuum pump overnight, and then dissolved in 20 mL freshly distilled ether and the solution was cooled to -78 °C. A solution of t-BuLi (7.9 mL, 13.3 mmoles) was added dropwise over 5 min. The cooling bath was removed for 1 h. The mixture was then cooled again to -78 °C and the aldehyde **4.14** (1g, 6.4 mmoles) in 5 mL of dry ether was added dropwise. After removing the bath again and stirring for another 30 min, the reaction was quenched by addition of saturated aqueous NH_4Cl , then extracted with ethyl acetate, and the extract dried with sodium sulfate. The solvent was removed with a rotary evaporator. The residue was purified by flash chromatography on a silica gel column (30% ethyl acetate in hexanes, TLC: $R_f = 0.24$) to give **4.15b** (2.2 g, 88%). A 0.4 g supply of **4.15b** remained after all my experiments were completed (*vide infra*). ^1H NMR (300 MHz, CDCl_3) δ 5.81 (dd, $J = 15.3, 5.9$ Hz, 1 H), 5.64 (m, 1 H), 4.49 (dd, $J = 13.8, 7.4$ Hz, 1 H), 4.00-4.15 (2 H), 3.57 (t, $J = 6.5$ Hz, 2 H), 3.57 (dd, $J = 6.5, 6.7$ Hz, 1 H), 1.40-1.60 (6 H), 1.40 (s, 3 H), 1.35 (s, 3 H), 1.18-1.30 (8 H), 0.89 (s, 9 H), 0.02 (s, 6 H).

1-(9-(2-Oxanyloxy)-11-(3,3-dimethyl-2,4-dioxolanyl)undec-10-enyloxy)-1,1,2,2-tetramethyl-1-silapropane (4.16b) was synthesized according to the published protocol.¹⁵ A 1.1 g supply of **4.16b** remained after all my experiments were completed (*vide infra*). ¹H NMR (300 MHz, CDCl₃) δ 5.55-5.88 (2 H), 4.56-4.68 (m, 1 H), 4.50 (m, 1 H), 4.00-4.12 (2 H), 3.84 (m, 1 H), 3.57 (t, *J* = 6.6 Hz, 2 H), 3.55 (m, 1 H), 3.45 (m, 1 H), 1.4-1.9 (12 H), 1.40 (s, 3 H), 1.37 (s, 3 H), 1.15-1.35 (8 H), 1.40 (s, 3 H), 1.37 (s, 3 H), 0.87 (s, 9 H), 0.02 (s, 6 H).

9-(2-Oxanyloxy)-11-(3,3-dimethyl-2,4-dioxolanyl)undec-10-en-1-ol (4.17b) was synthesized according to the published protocol.¹⁵ After all my experiments were completed, a 0.3 g supply of **4.17b** remained. ¹H NMR (300 MHz, CDCl₃) δ 5.50-5.85 (2 H), 4.64 (m, 1 H), 4.50 (m, 1 H), 4.06 (dd, *J* = 8.1, 6.3 Hz, 1 H), 4.06 (m, 1 H), 3.84 (m, 1 H), 3.61 (t, *J* = 6.6 Hz, 2 H), 3.55 (m, 1 H), 3.45 (m, 1 H), 1.80 (m, 2 H), 1.65 (m, 2 H), 1.4-1.9 (8 H), 1.40 (s, 3 H), 1.37 (s, 3 H), 1.15-1.35 (8 H).

9-(2-Oxanyloxy)-11-(3,3-dimethyl-2,4-dioxolanyl)undec-10-enoic acid (4.18b) was synthesized according to the published protocol.¹⁵ After all my experiments were completed, a 0.8 g supply of **4.18b** remained. ¹H NMR (300 MHz, CDCl₃) δ 5.50-5.88 (2 H), 4.62 (m, 1 H), 4.49 (m, 1H), 4.04 (m, 3 H), 3.83 (m, 1 H), 3.54 (m, 1 H), 3.44 (m, 1 H), 2.35 (t, *J* = 7.4 Hz, 2H), 1.80 (m, 2 H), 1.4-1.75 (8 H), 1.39 (s, 3 H), 1.36 (s, 3 H), 1.2-1.4 (8 H).

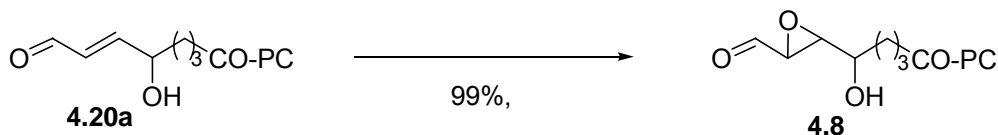
Precursor of 2-(5-hydroxy-8-oxooctanoyl)phosphatidylcholine (HODA-PC, 4.20b) was synthesized according to the published protocol.¹⁵ ¹H NMR (300 MHz, CDCl₃) δ 5.5-5.85 (2 H), 5.17 (m, 1 H), 4.54-4.67 (m, 1 H), 4.48

(m, 1 H), 4.18-4.42 (3 H), 3.96-4.14 (3 H), 3.92 (3 H), 3.72-3.98 (m, 3 H), 3.53 (m, 1 H), 3.43 (m, 1 H), 3.35 (s, 9 H), 2.25 (m, 4 H), 1.4-1.9 (13 H), 1.39 (s, 3 H), 1.37 (s, 3H), 1.22 (33 H), 0.85 (t, $J = 6.4$ Hz, 3 H).

2-(5-Hydroxy-8-oxooctanoyl)phosphatidylcholine (HODA-PC, 4.21b)

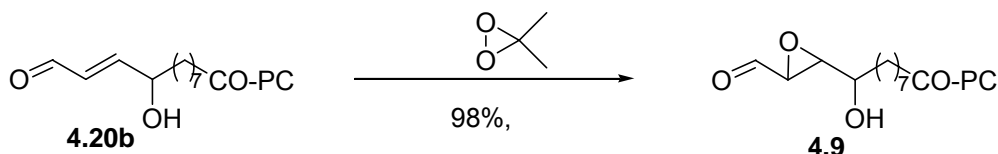
was synthesized according to the published protocol.¹⁵ ^1H NMR (300 MHz, CDCl_3) δ 9.53 (d, $J = 8.0$ Hz, 1 H), 6.86 (dd, $J = 15.5, 4.1$ Hz, 1 H), 6.28 (ddd, $J = 15.5, 8.1, 1.3$ Hz, 1 H), 5.19 (m, 1 H), 4.37 (m, 1 H), 4.32 (dd, $J = 12.1, 3.2$ Hz, 1 H), 4.1-4.35 (2 H), 4.11 (dd, $J = 12.0, 7.3$ Hz, 1 H), 3.92 (dd, $J = 6.1, 6.0$ Hz, 2 H), 3.76 (m, 2 H), 3.32 (s, 9 H), 2.28 (m, 2 H), 2.25 (t, $J = 7.5$ Hz, 2 H), 1.45-1.70 (7 H), 1.3-1.5 (12 H), 1.22 (19 H), 0.85 (t, $J = 6.5$ Hz, 3 H).

4-(3-Formyloxiranyl)-4-hydroxybutyryl phosphatidylcholine (epoxy-HOOA-PC, 4.8)



A solution of dioxirane in acetone (2 mL, 58 mM)³⁷, was added dropwise to a solution of **4.20a** (6.3 mg, 0.01 mmol) in chloroform (1 mL) at room temperature. The resulting mixture was stirred for an additional 30 min at room temperature. The solvents were removed by rotary evaporation. The desired compound **4.8** was obtained in almost quantitative yield (6.3 mg, 99%) without further purification. ^1H -NMR (300 MHz, CDCl_3): δ 9.53 (d, $J = 7.7$ Hz, 1 H), 5.22 (m, 1 H), 4.37 (m, 1 H), 4.1-4.35 (4 H), 3.99 (m, 1 H), 3.91 (m, 1 H), 3.75 (m, 2 H), 3.63 (dd, 1H, $J = 6, J = 6.1$), 3.30 (s, 9 H), 3.26 (m, 1H), 2.36 (m, 2 H), 2.26 (t, $J = 6.2$ Hz), 1.5-1.9 (6 H), 1.22 (24 H), 0.85 (t, $J = 6.4$ Hz).

8-(3-formyl-oxiranyl)-8-hydroxy-octanoyl phosphatidylcholine (epoxy-HODA-PC, 4.9)



A solution of dioxirane in acetone (1.5 mL, 62 mM)³⁷ was added dropwise to the solution of **4.20b** (6.2 mg, 0.009 mmol) in chloroform (1 mL) at room temperature. The resulting mixture was stirred for an additional 30 min at room temperature. The solvents were removed by rotary evaporation. The desired compound **4.9** was obtained in almost quantitative yield (6 mg, 98%) without further purification. ¹H-NMR (300 MHz, CDCl₃): ¹H NMR (300 MHz, CDCl₃) δ 9.53 (d, *J* = 8.0 Hz, 1 H), 5.19 (m, 1 H), 4.37 (m, 1 H), 4.32 (dd, *J* = 12.1, 3.2 Hz, 1 H), 4.1-4.35 (2 H), 4.11 (dd, *J* = 12.0, 7.3 Hz, 1 H), 3.92 (dd, *J* = 6.1, 6.0 Hz, 2 H), 3.76 (m, 2 H), 3.63 (dd, 1H, *J* = 6, *J* = 6.1), 3.32 (s, 9 H), 3.26 (m, 1H), 2.28 (m, 2 H), 2.25 (t, *J* = 7.5 Hz, 2 H), 1.45-1.70 (7 H), 1.3-1.5 (12 H), 1.22 (19 H), 0.85 (t, *J* = 6.5 Hz, 3 H).

4.9. References

- (1) Kruijff, B. *Nature* **1997**, 386, 129-130.
- (2) Rietveld, A. G.; Koorengel, M. C.; Kruijff, B. *EMBO J.* **1995**, 14, 5506-13.
- (3) Killian, J. A.; van Meer, G. *EMBO reports* **2001**, 2, 91-95.
- (4) Engelmann, B.; Brautigam, C.; Thiery, J. *Biochem. Biophys. Res. Commun.* **1994**, 204, 1235-42.
- (5) Chen, J. J.; Yu, B. P. *Free Radic. Biol. Med.* **1994**, 17, 411-418.
- (6) Miljanich, G. P.; Nemes, P. P.; White, D. L.; Dratz, E. A. *Membr. Biol.* **1981**, 60, 249-55.
- (7) Landau, E. M.; Rosenbusch, J. P. *Proc. Natl. Acad. Sci. USA* **1996**, 93, 14532-14535.
- (8) Casals, C.; Galan, A. M.; Escolar, G.; Montserrat, G.; Estelrich, J. *Chem. Phys. Lipids* **2003**, 125, 139-146.
- (9) Edelstein, C. In *Biochemistry of plasma lipoproteins*; Dekker, M., Ed. New York, 1990, p 497.
- (10) Salomon, R. G.; Kaur, K.; Podrez, E. A.; Hoff, H. F.; Krushinsky, A. V.; Sayre, L. M. *Chem. Res. Tox.* **2000**, 13, 557-64.
- (11) Sayre, L. M.; Arora, P. K.; Iyer, R. S.; Salomon, R. G. *Chem. Res. Tox.* **1993**, 6, 19-22.
- (12) Deng, Y.; Salomon, R. G. "Unpublished results" 2000.
- (13) Deng, Y. Ph. D Thesis, CASE, 2000.
- (14) Ballini, R.; Petrini, M. *Synthesis* **1986**, 12, 1024-1026.

- (15) Deng, Y. H.; Salomon, R. G. *J. Org. Chem.* **1998**, *63*, 7789-7794.
- (16) Sun, M.; Deng, Y.; Batyreva, E.; Sha, W.; Salomon, R. G. *J. Org. Chem.* **2002**, *67*, 3575-84.
- (17) Podrez, E. A.; Poliakov, E.; Shen, Z.; Zhang, R.; Deng, Y.; Sun, M.; Finton, P. J.; Shan, L.; Febbraio, M.; Hajjar, D. P.; Silverstein, R. L.; Hoff, H. F.; Salomon, R. G.; Hazen, S. L. *J. Biol. Chem.* **2002**, *277*, 38517-23.
- (18) Podrez, E. A.; Batyreva, E.; Shen, Z.; Zhang, R.; Deng, Y.; Sun, M.; Gugiu, B. G.; Finton, P. J.; Shen, L.; Febbraio, M.; Hayn, M.; Silverstein, R. L.; Hoff, H. F.; Salomon, R. G.; Hazen, S. L. *J. Biol. Chem.* **2002**.
- (19) Daviet, L.; McGregor, J. L. *Thromb. Haemost.* **1997**, *78*, 65-9.
- (20) Silverstein, R. L.; Febbraio, M. *Curr. Opin. Lipidol.* **2000**, *11*, 483-91.
- (21) Nicholson, A. C.; Frieda, S.; Pearce, A.; Silverstein, R. L. *Arterioscler. Thromb. Vasc. Biol.* **1995**, *15*, 269-75.
- (22) Ryeom, S. W.; Silverstein, R. L.; Scotto, A.; Sparrow, J. R. *J. Biol. Chem.* **1996**, *271*, 20536-9.
- (23) Tait, J. F.; Smith, C. *J. Biol. Chem.* **1999**, *274*, 3048-54.
- (24) Rigotti, A.; Acton, A. L.; Krieger, M. *J. Biol. Chem.* **1995**, *270*, 16221-16224.
- (25) Endemann, G.; Stanton, L. W.; Madden, K. S.; Bryant, C. M.; White, R. T.; Protter, A. A. *J. Biol. Chem.* **1993**, *268*, 11811-6.
- (26) Podrez, E. A.; Schmitt, D.; Hoff, H. F.; Hazen, S. L. *J. Clin. Invest.* **1999**, *103*, 1547-60.

- (27) Ren, Y.; Silverstein, R. L.; Allen, J.; Savill, J. J. *Exp. Med.* **1995**, *181*, 1857-62.
- (28) Tandon, N. N.; Kralisz, U.; Jamieson, G. A. *J. Biol. Chem.* **1995**, *264*, 7576-83.
- (29) Silverstein, R. L.; Asch, A. S.; Nachman, R. L. *J. Clin. Invest.* **1989**, *84*, 546-52.
- (30) Dawson, D. W.; Pearce, S. F.; Zhong, R.; Silverstein, R. L.; Frazier, W. A.; Bouck, N. P. *J. Biol. Chem.* **1997**, 707-17.
- (31) Ryeom, S. W.; Sparrow, J. R.; Silverstein, R. L. *J. Cell. Sci.* **1996**, *109*, 387-95.
- (32) Nozaki, S.; Kashiwagi, H.; Yamashita, S.; Nakagawa, T.; Kostner, B.; Tomiyama, Y.; Nakata, A.; Ishigami, M.; Miyagawa, J.; Kameda-Takemura, K. *J. Clin. Invest.* **1995**, *96*, 1859-65.
- (33) Nakata, A.; Nakagawa, Y.; Nishida, M.; Nozaki, S.; Miyagawa, J.; Nakagawa, T.; Tamura, R.; Matsumoto, K.; Kameda-Takemura, K.; Yamashita, S.; Matsuzawa, Y. *Arterioscler. Thromb. Vasc. Biol.* **1999**, *19*, 1333-9.
- (34) Huh, H. Y.; Pearce, S. F.; Yesner, L. M.; Schindler, J. L.; Silverstein, R. L. *Blood* . **1996**, *87*, 2020-8.
- (35) Febbraio, M.; Podrez, E. A.; Smith, J. D.; Hajjar, D. P.; Hazen, S. L.; Hoff, H. F.; Sharma, K.; Silverstein, R. L. *J. Clin. Invest.* **2000**, *105*, 1049-1056.
- (36) Gugiu, B. Ph. D Thesis, CASE, 2004.

- (37) Adam, W.; Hadjirapoglou, L. *Topics Curr. Chem.* **1993**, *164*, 45-62.

APPENDIX

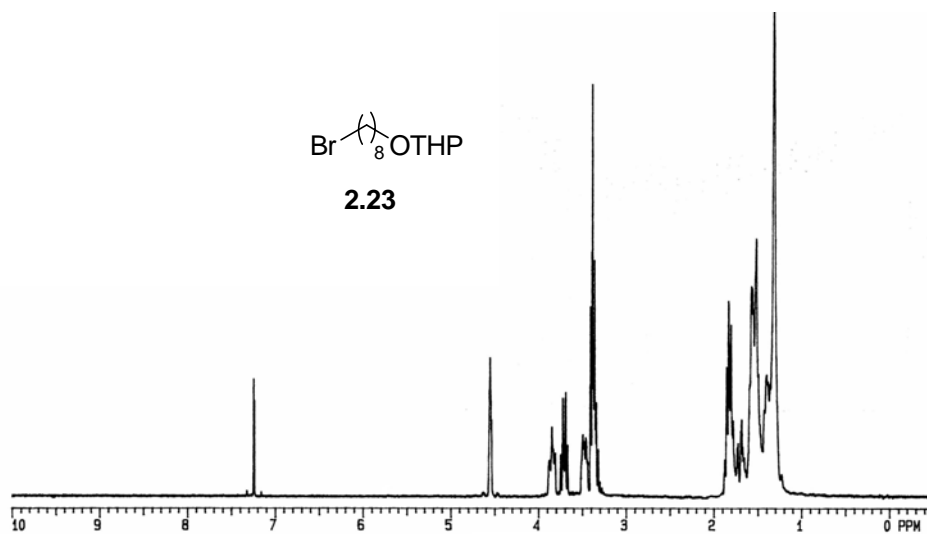


Figure S 1. The 300 MHz ¹H NMR (CDCl₃) spectrum of 2-(8-bromo-octyloxy)-tetrahydropyran (**2.23**).

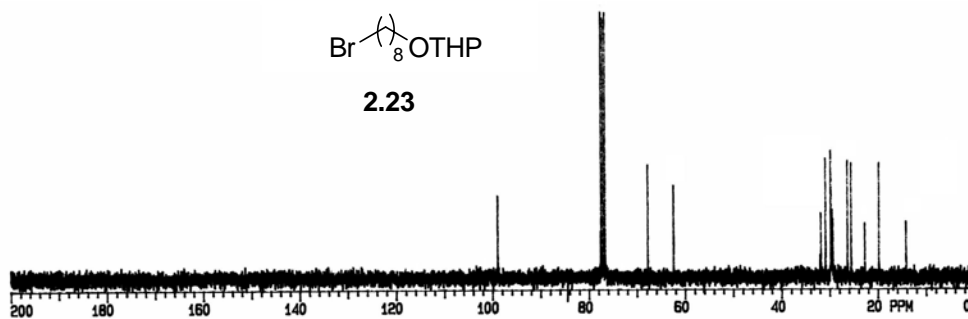


Figure S 2. The 75 MHz ¹³C NMR (CDCl₃) spectrum of 2-(8-bromo-octyloxy)-tetrahydropyran (**2.23**).

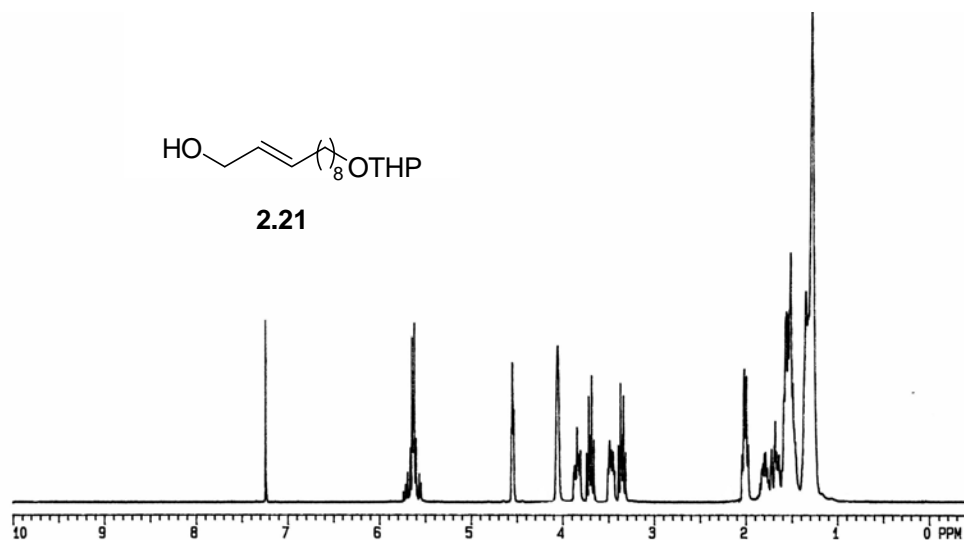


Figure S 3. The 300 MHz ¹H NMR (CDCl₃) spectrum of 2-(8-hydroxy-octyloxy)-tetrahydropyran (**2.21**).

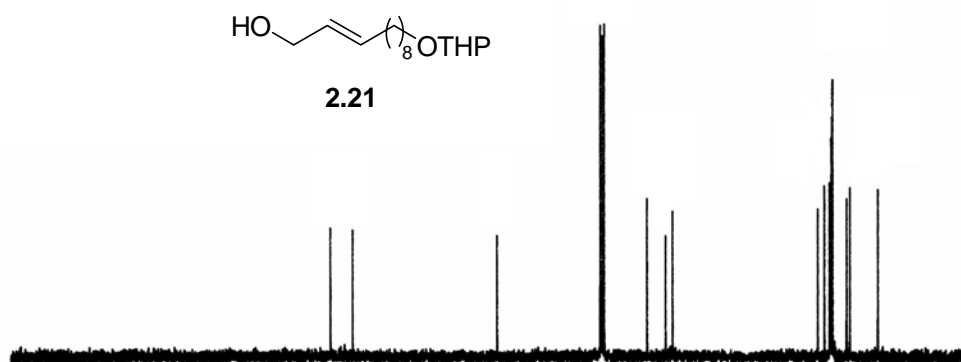


Figure S 4. The 75 MHz ¹³C NMR (CDCl₃) spectrum of 2-(8-bromo-octyloxy)-tetrahydropyran (**2.21**).

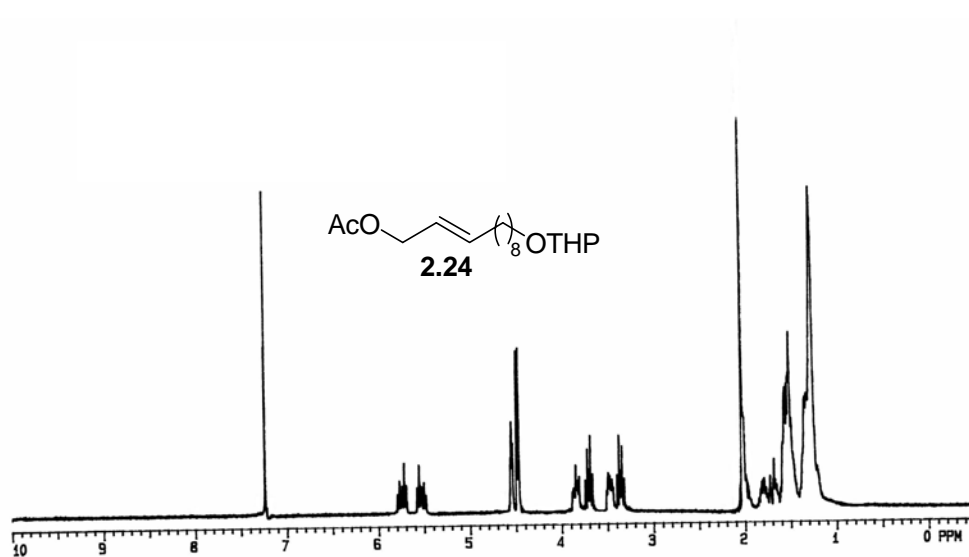


Figure S 5. The 300 MHz ¹H NMR (CDCl₃) spectrum of acetic acid, 11-(tetrahydro-pyran-2-yloxy)-undec-2-enyl ester (**2.24**)

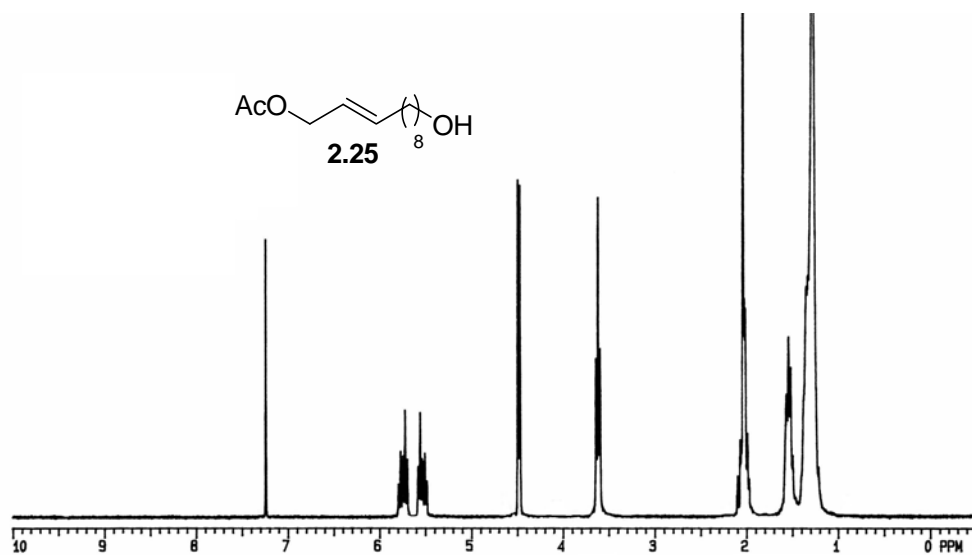


Figure S 6. The 300 MHz ¹H NMR (CDCl₃) spectrum of acetic acid, 11-hydroxy-undec-2-enyl ester (**2.25**)

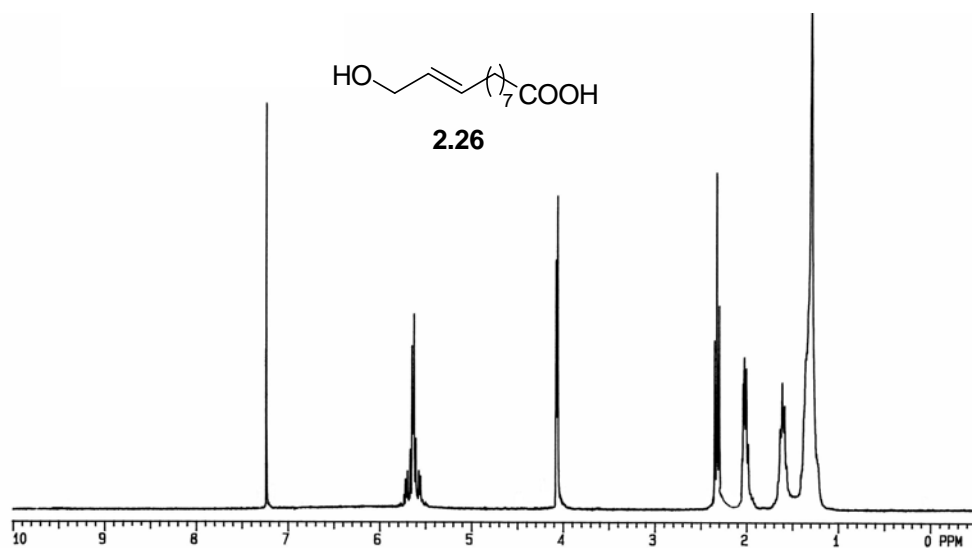


Figure S 7. The 300 MHz ^1H NMR (CDCl_3) spectrum of 11-hydroxy-undec-9-enoic acid (**2.26**)

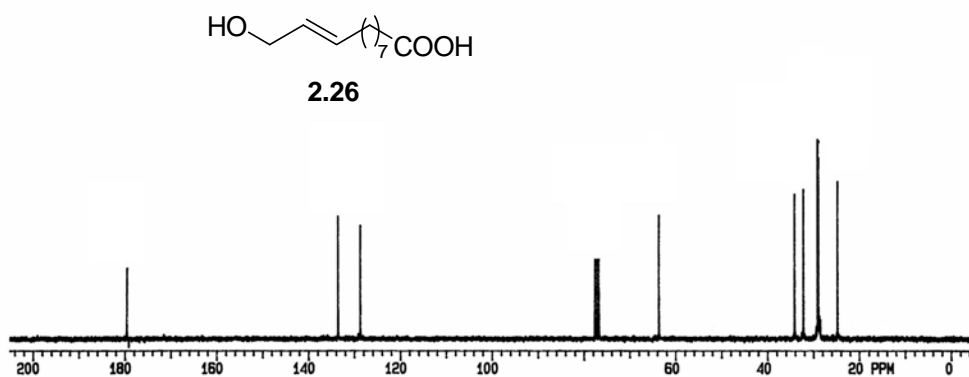


Figure S 8. The 75 MHz ^{13}C NMR (CDCl_3) spectrum of 11-hydroxy-undec-9-enoic acid (**2.26**).

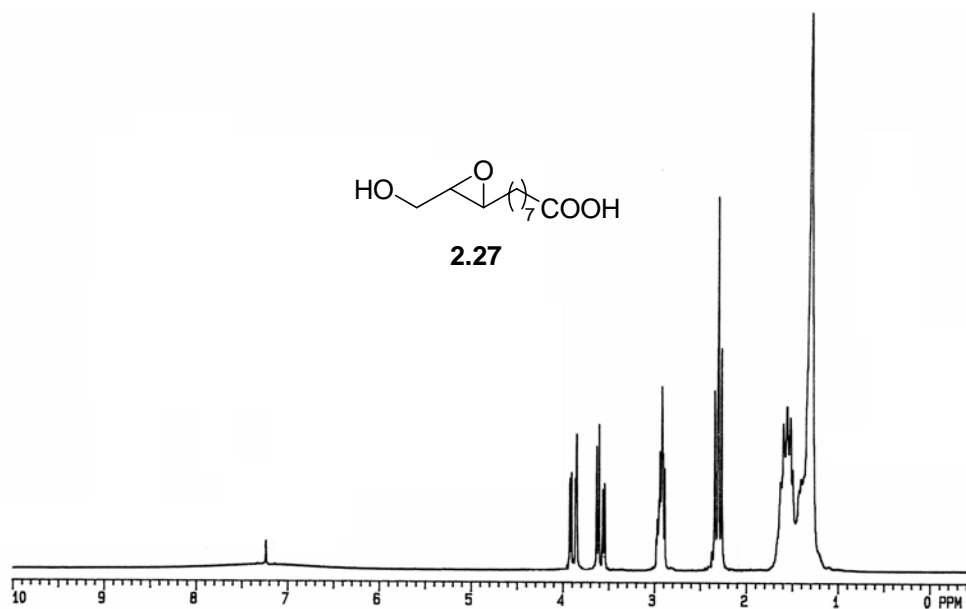


Figure S 9. The 300 MHz ^1H NMR (CDCl_3) spectrum of 8-(3-hydroxymethyl-oxiranyl)octanoic acid (**2.27**).

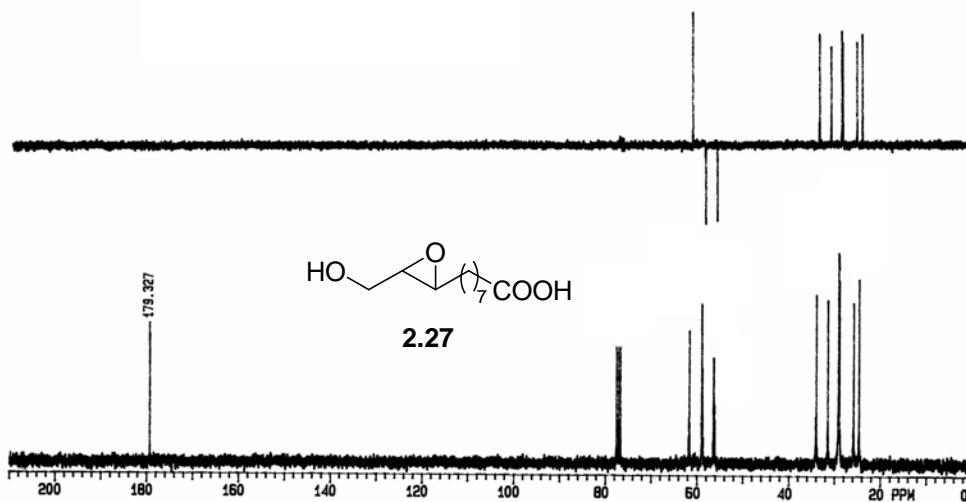


Figure S 10. The 75 MHz ^{13}C NMR (CDCl_3) spectrum of 8-(3-hydroxymethyl-oxiranyl)octanoic acid (**2.27**).

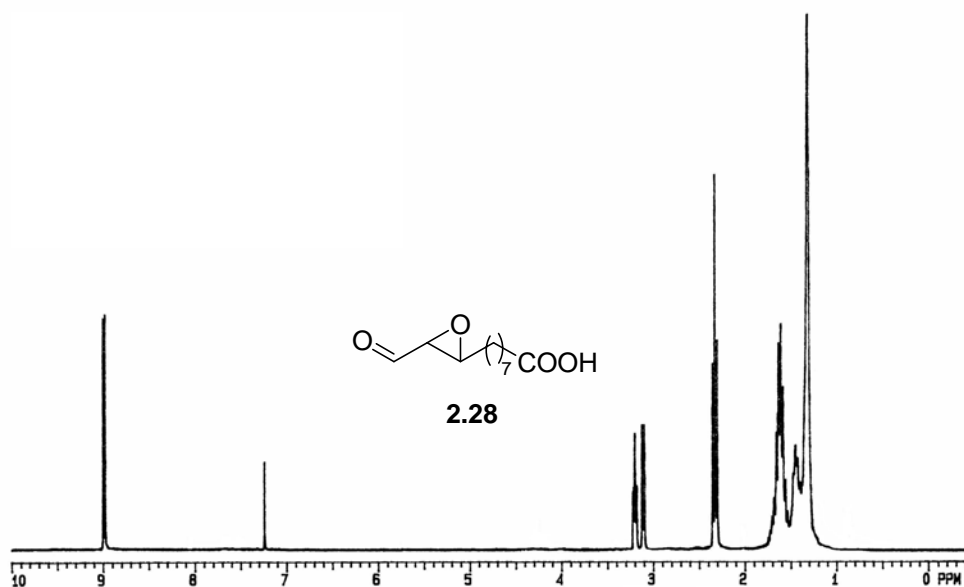


Figure S 11. The 300 MHz ¹H NMR (CDCl₃) spectrum of 8-(3-formyl-oxiranyl)-octanoic acid (2.28)

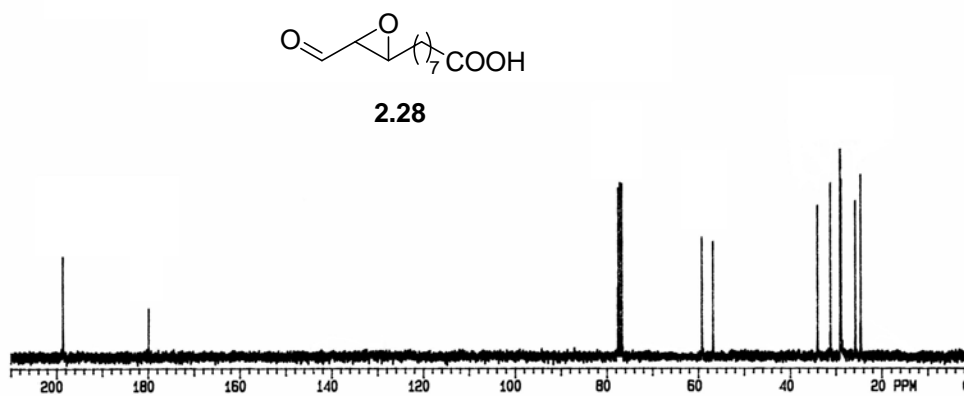


Figure S 12. The 75 MHz ¹³C NMR (CDCl₃) spectrum of 8-(3-formyl-oxiranyl)-octanoic acid(2.28).

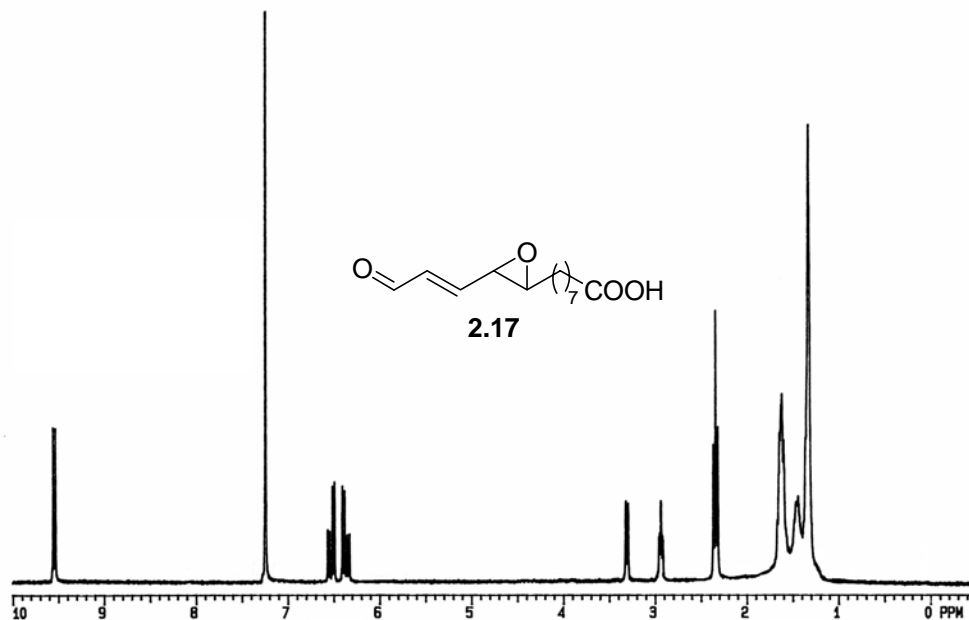


Figure S 13. The 300 MHz ^1H NMR (CDCl_3) spectrum of 8-[3-(3-oxo-propenyl)-oxiranyl]-octanoic acid (2.17).

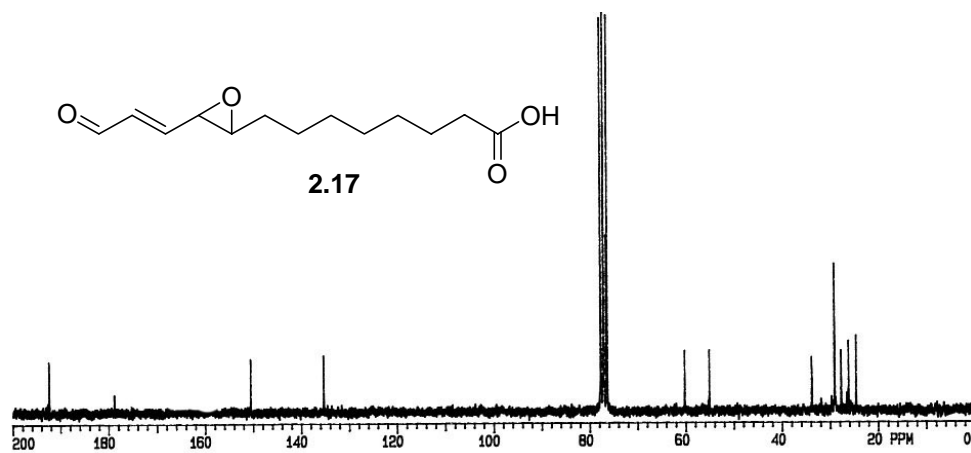


Figure S 14. The 75 MHz ^{13}C NMR (CDCl_3) spectrum of 8-[3-(3-oxo-propenyl)-oxiranyl]-octanoic acid (2.17).

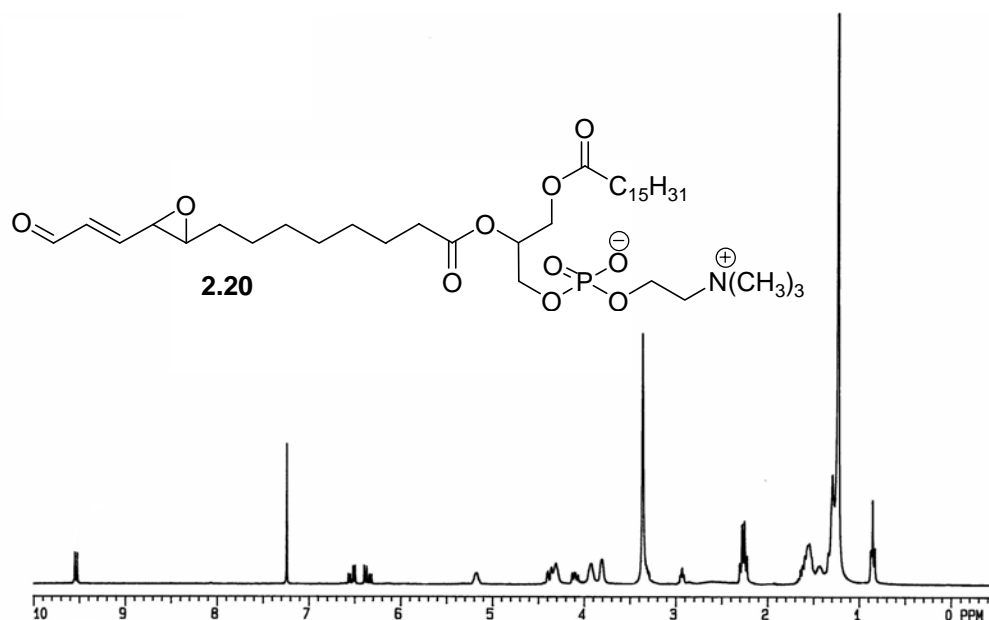


Figure S 15. The 300 MHz ¹H NMR (CDCl₃) spectrum of 1-palmitoyl-2-(13-oxo-9,10-*trans*-epoxy-octadeca-11-enoyl)-sn-glycero-3-phosphatidylcholine (**2.20**).

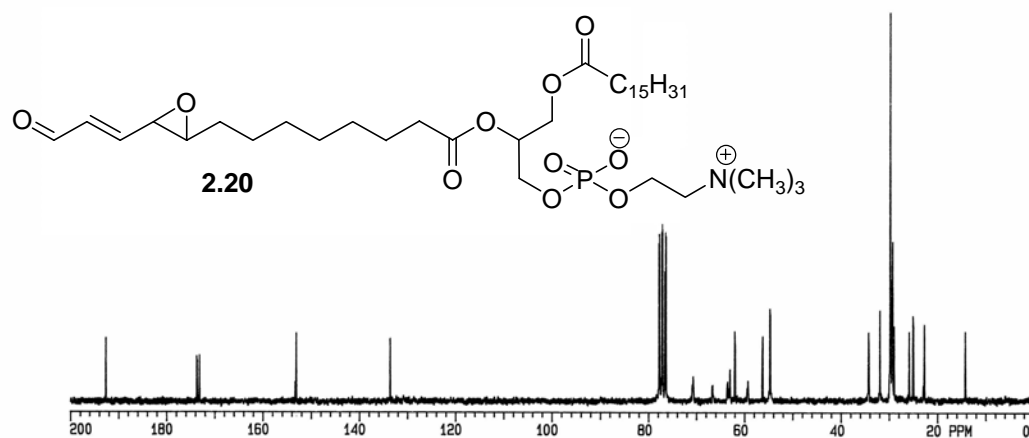


Figure S 16. The 75 MHz ¹³C NMR (CDCl₃) spectrum of 1-palmitoyl-2-(13-oxo-9,10-*trans*-epoxy-octadeca-11-enoyl)-sn-glycero-3-phosphatidylcholine (**2.20**).

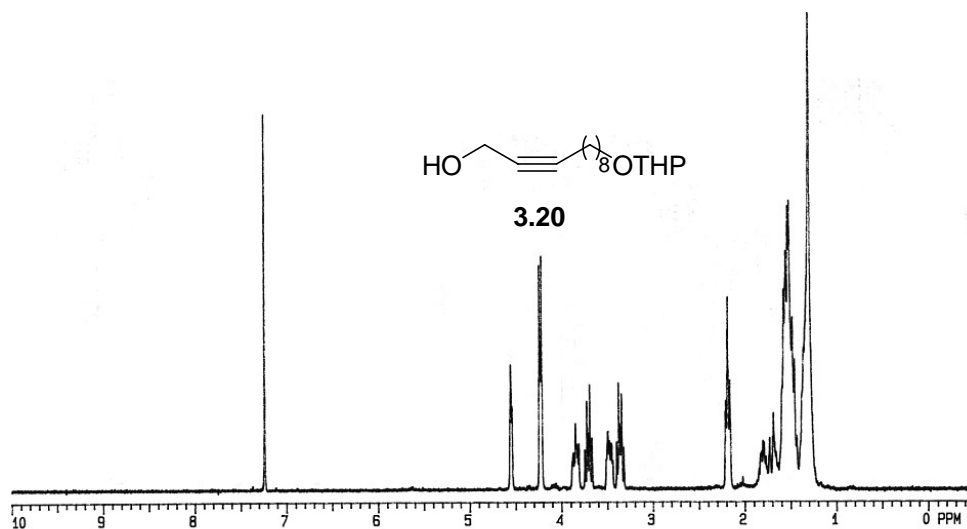


Figure S 17. The 300 MHz ¹H NMR (CDCl₃) spectrum of 2-(11-hydroxy-9-undecynoxy)tetrahydropyran (**3.20**).

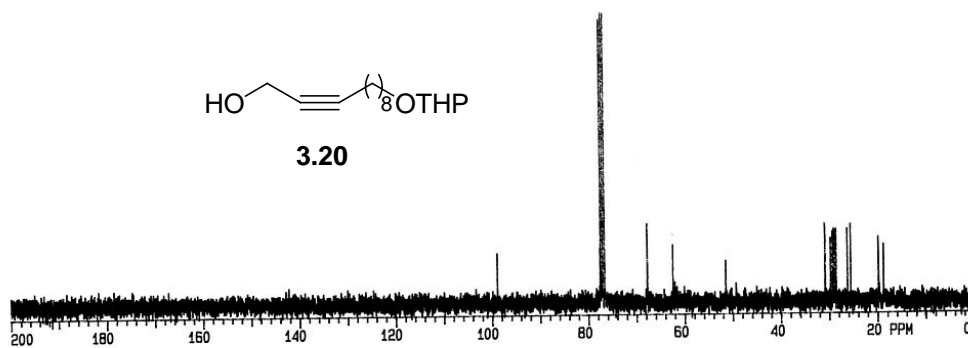


Figure S 18. The 75 MHz ¹³C NMR (CDCl₃) spectrum of 2-(11-hydroxy-9-undecynoxy)tetrahydropyran (**3.20**).

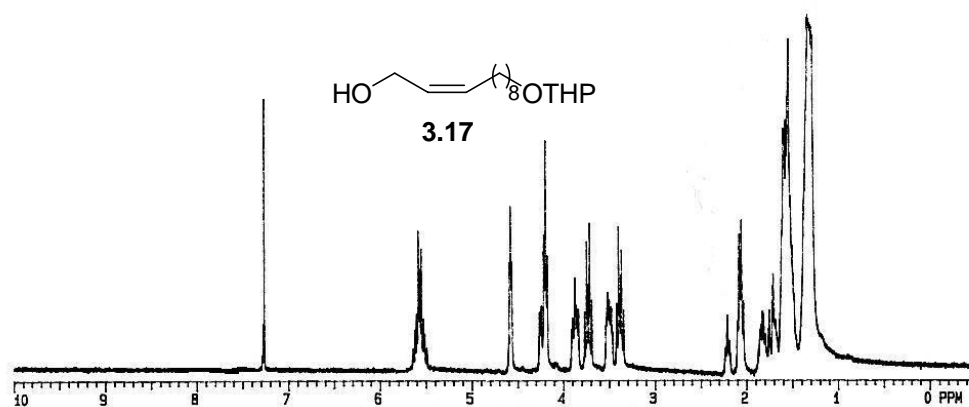


Figure S 19. The 300 MHz ¹H NMR (CDCl₃) spectrum of 2-(11-hydroxy-9(Z)-undecenyl)tetrahydropyran (**3.17**).

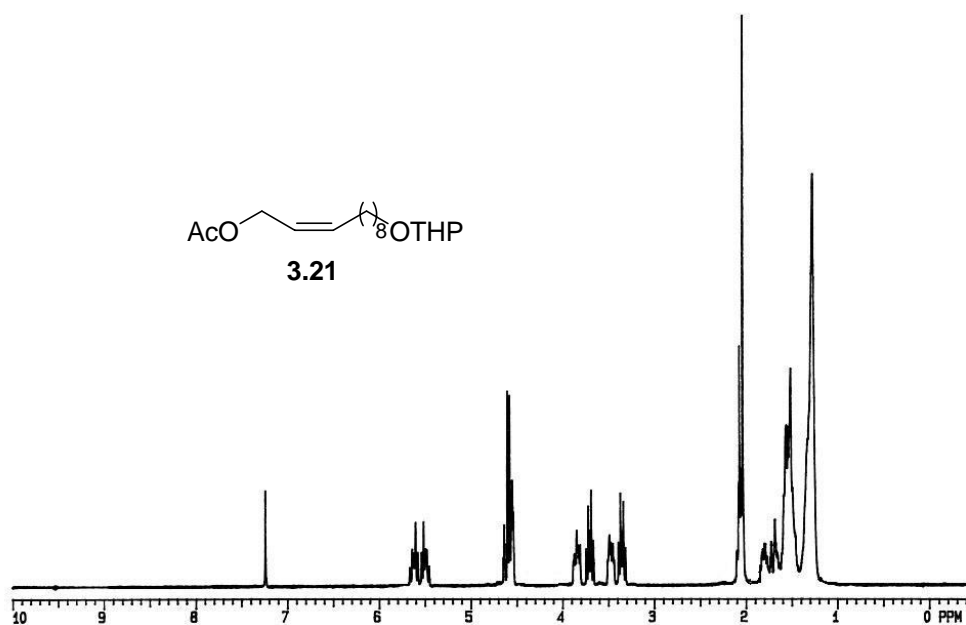


Figure S 20. The 300 MHz ¹H NMR (CDCl₃) spectrum of acetic acid, 11-tetrahydropyran-2-yl-oxy-2(Z)-undecenyl ester (**3.21**).

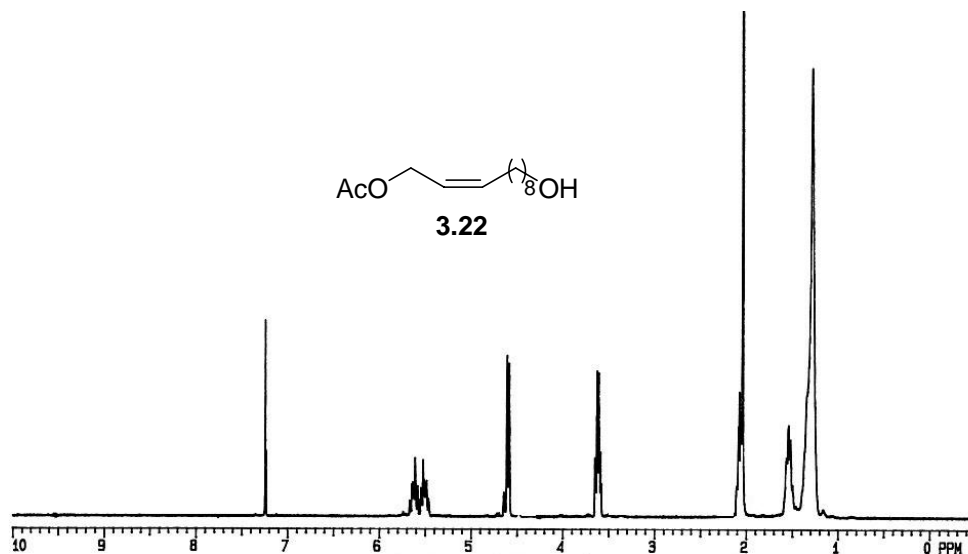


Figure S 21. The 300 MHz ¹H NMR (CDCl₃) spectrum of acetic acid, 11-hydroxy-2(Z)-undecenyl ester (**3.22**).

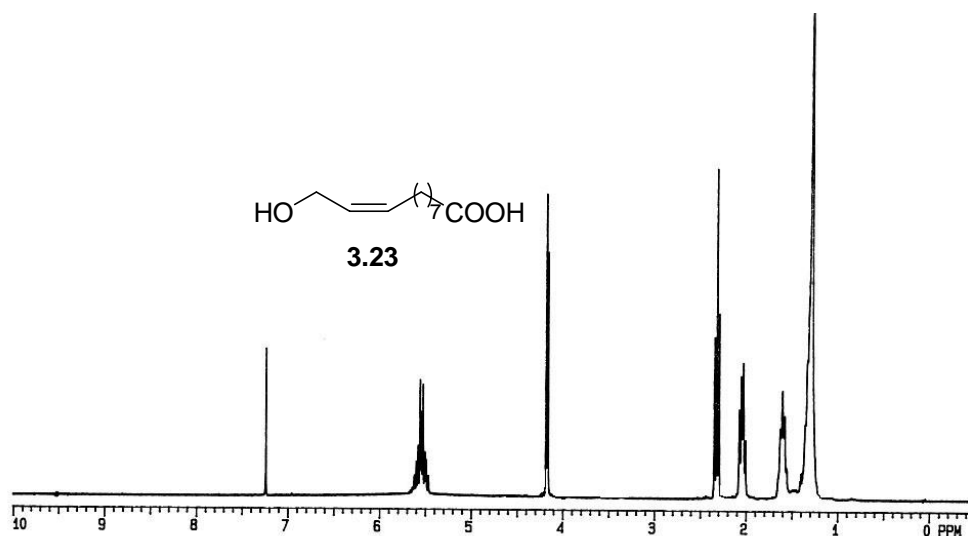


Figure S 22. The 300 MHz ¹H NMR (CDCl₃) spectrum of 11-hydroxy-9(Z)-undecenoic acid (**3.23**).

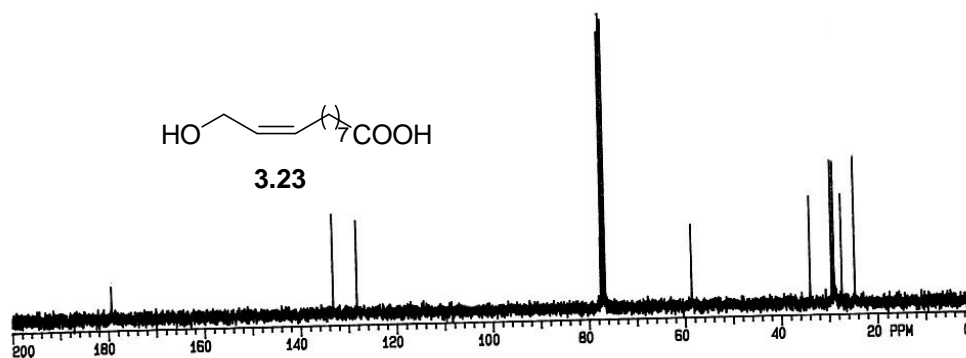


Figure S 23. The 75 MHz ¹³C NMR (CDCl₃) spectrum of 11-hydroxy-9(Z)-undecenoic acid (**3.23**).

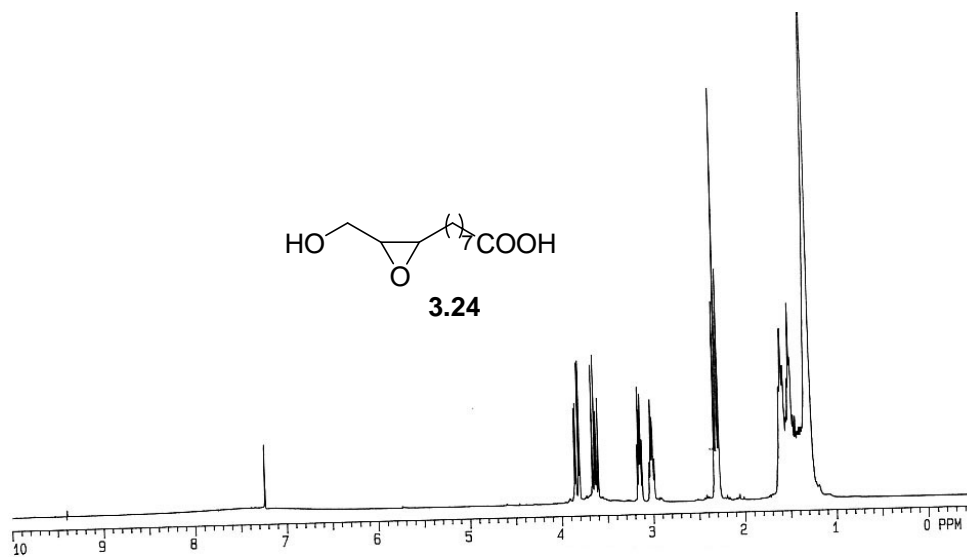


Figure S 24. The 300 MHz ¹H NMR (CDCl₃) spectrum of 8-(3-hydroxymethyloxiranyl)-octanoic acid (**3.24**).

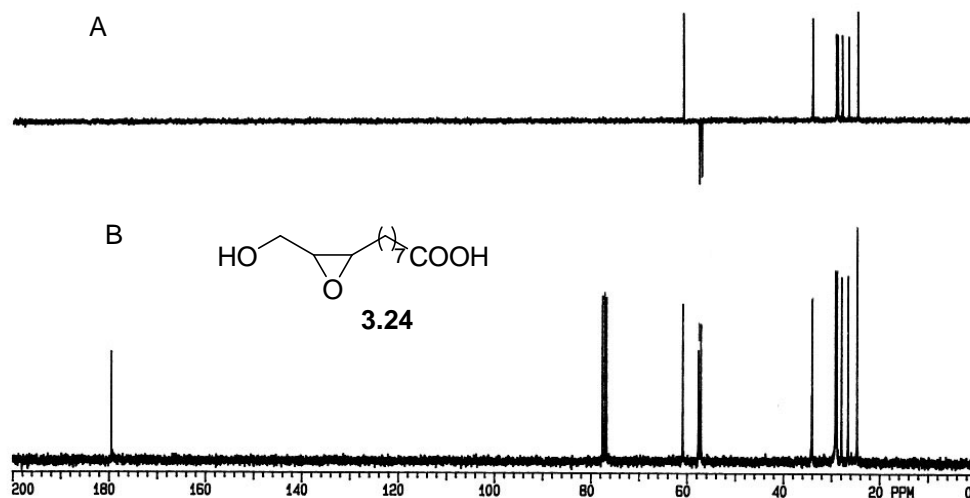


Figure S 25. The 75 MHz ^{13}C NMR (CDCl_3) spectrum of 8-(3-hydroxymethyloxiranyl)octanoic acid (**3.24**).

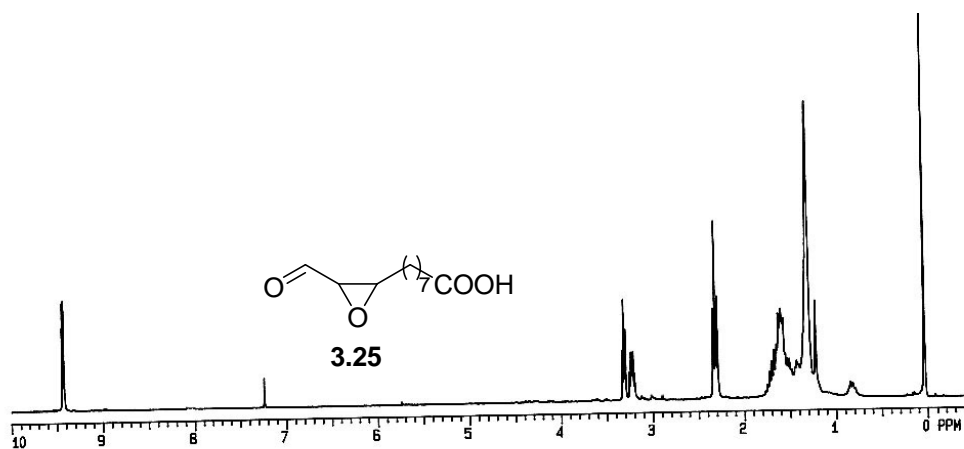


Figure S 26. The 300 MHz ^1H NMR (CDCl_3) spectrum of 8-(3-formyloxiranyl)octanoic acid (**3.25**).

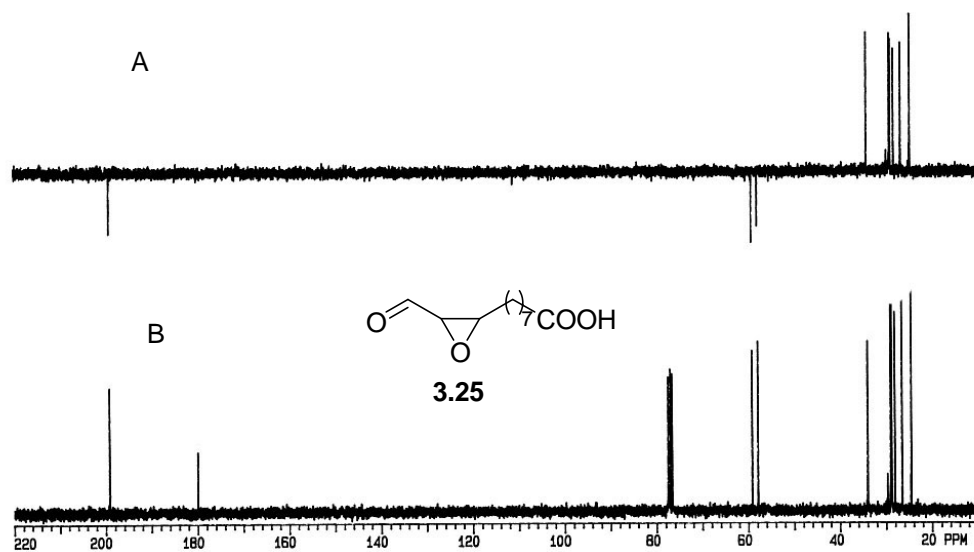


Figure S 27. The 75 MHz ^{13}C NMR (CDCl_3) spectrum of 8-(3-formyloxiranyl)octanoic acid (**3.25**).

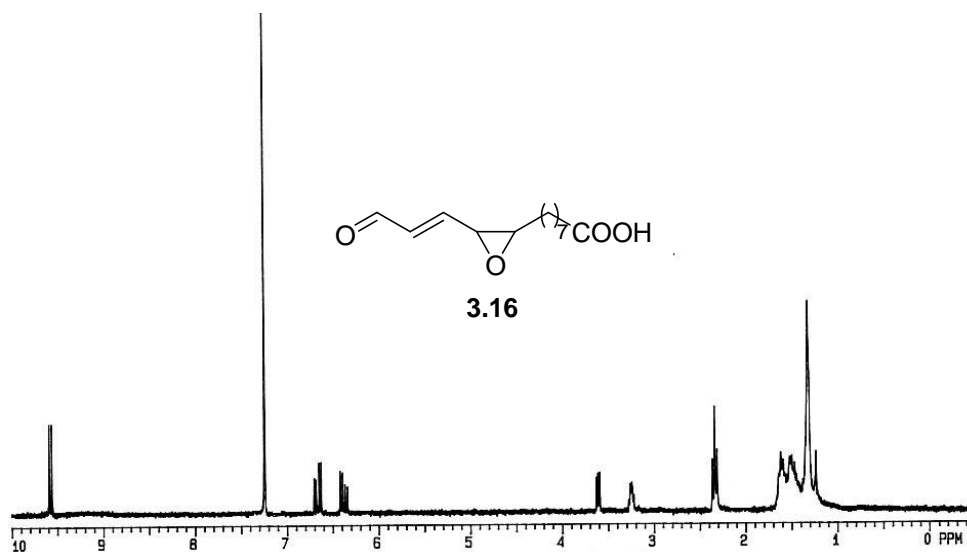


Figure S 28. The 300 MHz ^1H NMR (CDCl_3) spectrum of 13-oxo-9,10-*cis*-epoxy-11(*E*)-tridecenoic acid (**3.16**).

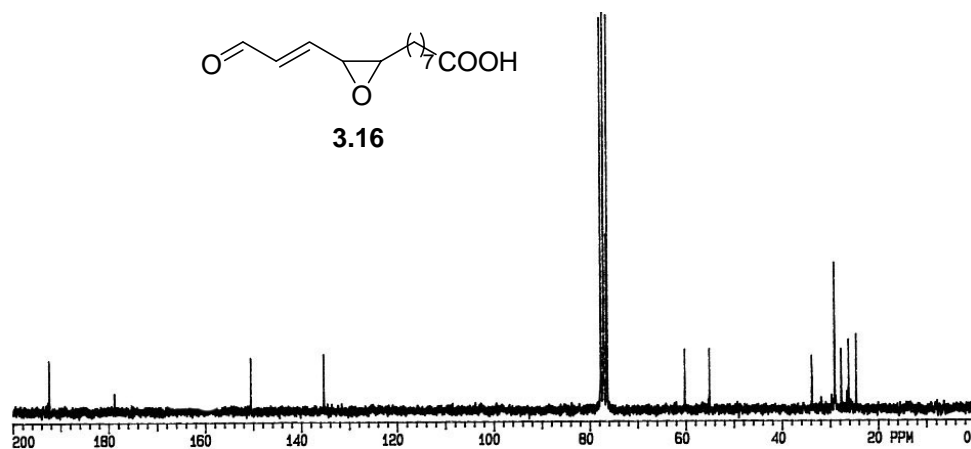


Figure S 29. The 75 MHz ^{13}C NMR (CDCl_3) spectrum of 13-oxo-9,10-*cis*-epoxy-11(*E*)-tridecanoic acid (**3.16**).

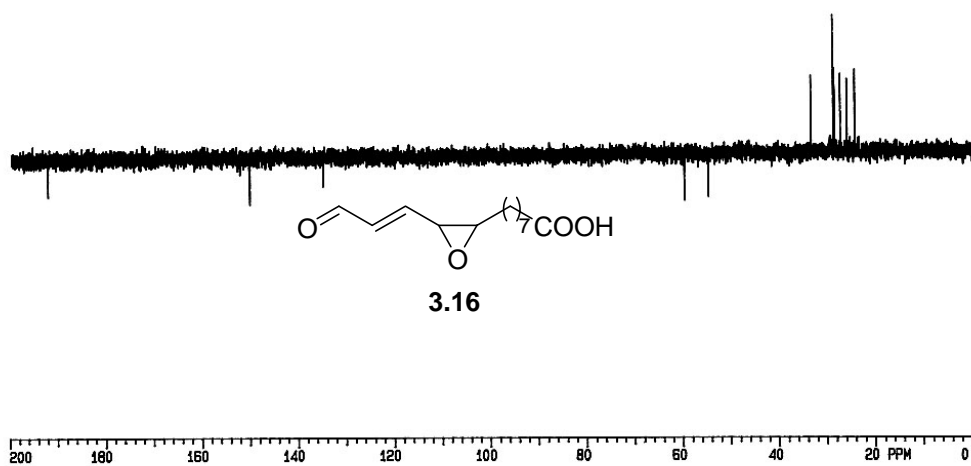


Figure S 30. The 75 MHz ^{13}C NMR (CDCl_3) spectrum of 13-oxo-9,10-*cis*-epoxy-11(*E*)-tridecanoic acid (**3.16**).

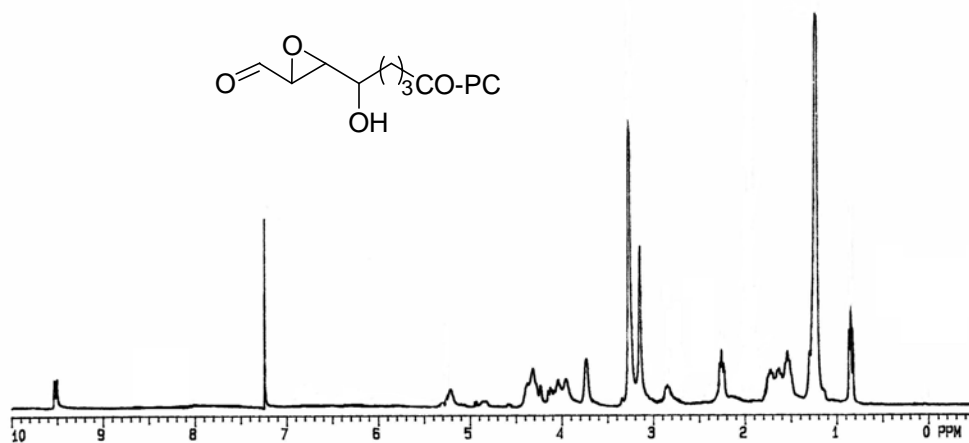


Figure S 31. The 300 MHz ¹H NMR (CDCl₃) spectrum of 4-(3-formyloxiranyl)-4-hydroxybutyryl phosphatidylcholine (**4.8**).

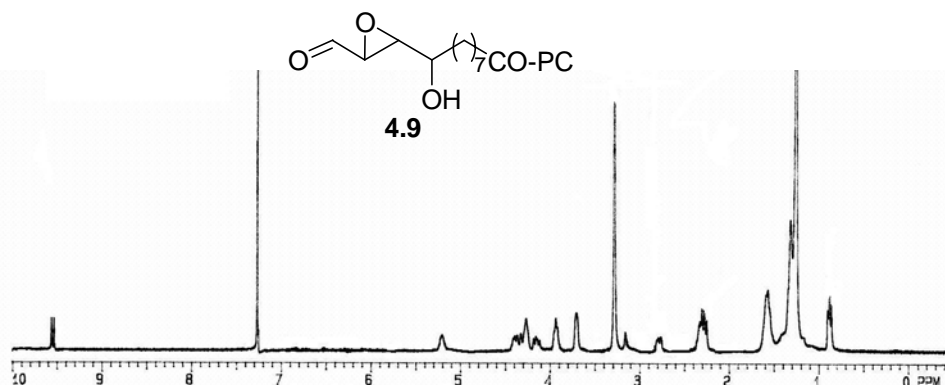


Figure S 32. The 300 MHz ¹H NMR (CDCl₃) spectrum of 8-(3-formyl-oxiranyl)-8-hydroxy-octanoyl phosphatidylcholine (**4.9**).

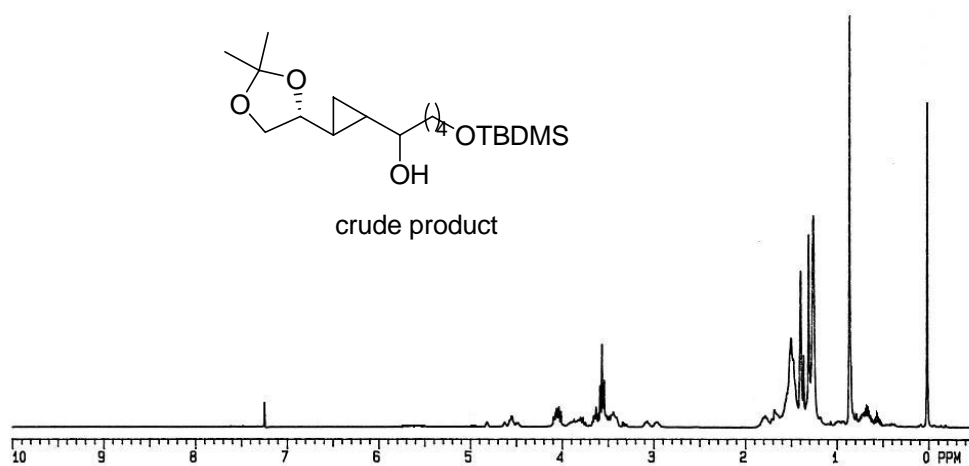


Figure S 33. The 300 MHz ¹H NMR (CDCl₃) spectrum of the crude **4.22b**.

Statistical data analysis for rat retina MS analyses

Each sample from a rat retina was analyzed by LCMS in duplicates. For each rat were analyzed 4 samples (2 for each retina). The amount of each analyte quantified in rat retina samples was calculated as follows

$$n_A = y/(n_{st})(a)(EE)$$

n_A = mole analyte, y = peak area ratio (analyte/internal standard), a = from calibration curves ($y = ax$), n_{st} = moles of internal standard used, EE = extraction efficiency.

The data generated using the above formula, employing the calibration curve equations and extraction efficiencies was treated statistically as follows.

Mean and standard deviation per animal

An average (mean) was calculated for each animal with the formula:

$$\text{AVERAGE} = \frac{\sum A}{n},$$

A = the amount of analyte in each sample (ng or nmol) analyzed in quadruplicates (AVERAGE = mean amount per animal), and n = sample, 1-4.

For each animal was calculated a standard deviation with the formula:

$$\text{STDEV} = \sqrt{\frac{n \sum A^2 - \left(\sum A\right)^2}{n(n-1)}},$$

A = amount of analyte per sample, and n = 1-4 (the total number of samples analyzed per animal).

Mean and standard deviation per group of animals analyzed (5 rats)

An average per group of animals was calculated with the formula:

$$\text{AVERAGE} = \frac{\sum A}{n},$$

A = the amount of analyte in each sample and n = 1 – 20 (the total number of samples analyzed).

A standard deviation for these data was calculated with the formula:

$$\text{STDEV} = \sqrt{\frac{n \sum A^2 - \left(\sum A\right)^2}{n(n-1)}},$$

A = amount of analyte per sample, and n = 1-20 (the total number of samples analyzed).

All data was analyzed using Microsoft Excel 2000.

BIBLIOGRAPHY

1. Adam, W. and Hadjiarapoglou L. (1993) Dioxiranes: oxidation chemistry made easy. *Topics Curr. Chem.*, **164**, 45-62.
2. Ames, B.N., Shigenaga M.K. and Hangen T.M. (1993) Oxidants, antioxidants, and the degenerative diseases of aging. *Proc. Natl. Acad. Sci. USA*, **90**, 7915-7922.
3. Ballini, R. and Petrini M. (1986) Facile and inexpensive synthesis of 4-oxoalkanoic acids from primary nitroalkanes and acrolein. *Synthesis*, **12**, 1024-1026.
4. Bartsch, H. and Nair J. (2000) Ultrasensitive and specific detection methods for exocyclic DNA adducts: Markers for lipid peroxidation and oxidative stress. *Toxicol.*, **153**, 105-114.
5. Berliner, J.A. and Heinecke J.W. (1996) The role of oxidized lipoproteins in atherogenesis. *Free Radic. Biol. Med.*, **20**, 707-727.
6. Berliner, J.A., Subbanagounder G., Leitinger N., Watson A.D. and Vora D. (2001) Evidence for a role of phospholipid oxidation products in atherogenesis. *Trends. Cardiovasc. Med.*, **11**, 142-7.
7. Bermejo, P., Gomez-Serranillos P., Santos J., Pastor E., Gil P. and Martin-Aragon S. (1997) Determination of malonaldehyde in Alzheimer's disease. A comparative study of high-performance liquid chromatography and thiobarbituric acid test. *Gerontology*, **43**, 218-222.
8. Blair, I.A. (2001) Lipid hydroperoxide-mediated DNA damage. *Experim. Geront.*, **36**, 1473-1481.

9. Bligh, E. and Dyer W. (1959) Lipids extraction. *Can. J. Biochem. Physiol.*, **37**, 911-917.
10. Bochkov, V.N., Kadl A., Huber J., Gruber F., Binder B.R. and Leitinger N. (2002) Protective role of phospholipid oxidation products in endotoxin-induced tissue damage. *Nature*, **419**, 77-81.
11. Boothman, D.A., Geller A.I. and Pardee A.B. (1989) Expression of the E. coli Lac Z gene from a defective HSV-1 vector in various human normal, cancer-prone and tumor cells. *FEBS Lett.*, **258**, 159-62.
12. Buettner, A. and Schieberle P. (2001) Aroma Properties of a homologous series of 2,3-epoxyalkenals and trans-4,5-epoxy-2-alkenals. *J. Agric. Food Chem.*, **49**, 3881-3884.
13. Buettner, A. (2004) Investigation of potent odorants and afterodor development in two Chardonnay wines using the buccal odor screening system. *J. Agric. Food Chem.*, **52**, 2339-2346.
14. Burchman (1998) Genotoxic lipid peroxidation products: their DNA damaging properties and role in formation of endogenous DNA adducts. *Mutagenesis*, **13**, 287-305.
15. Carmen Vigo-Pelfrey, E. (1990) Membrane lipid oxidation., **Vol. I.**
16. Casals, C., Galan A.M., Escolar G., Montserrat G. and Estelrich J. (2003) Physical stability of liposomes bearing hemostatic activity. *Chem. Phys. Lipids*, **125**, 139-146.

17. Chabert, P., Ousset J.B. and Mioskowski C. (1989) (3,3-Diisopropoxypropyl)triphenylarsonium ylide: a new synthetic equivalent of beta-formal vinyl anion. *Tet. Lett.*, **30**, 179-182.
18. Chacos, N., Falck J.R., Wixtrom C. and Capdevila J. (1982) *Biochem. Biophys. Res. Commun.*, **104**, 916-922.
19. Chen, J.J. and Yu B.P. (1994) Alterations in mitochondrial membrane fluidity by lipid peroxidation products. *Free Radic. Biol. Med.*, **17**, 411-418.
20. Cheng, K.C., Preston B.D., Cahill D.S., Dosanjh M.K., Singer B. and Loeb L.A. (1991) The vinyl chloride DNA derivative N2,3-ethenoguanine produces G---A transitions in *Escherichia coli*. *Proc. Natl.Acad.Sci. USA*, **88**, 9974-8.
21. Chio, K.S., Tappel A.L. and Imagawa T. (1969) Activation of ribonuclease and other enzymes by peroxidizing lipids and by malonaldehyde. *Biochem.*, **8**, 2827-32.
22. Cooper, J.L. (2003) Dietary lipids in the aetiology of Alzheimer's disease: implications for therapy. *Drugs Aging*, **20**, 399-418.
23. Corwin, R.L. (2003) Effects of dietary fats on bone health in advanced age. *Prostaglandins, Leukotrienes and Essential Fatty Acids*, **68**, 379-386.
24. Davies, K.J.A. (1995) Oxidative stress: the paradox of aerobic life. *Biochem. Soc. Symp.*, **61**, 1-31.
25. Daviet, L. and McGregor J.L. (1997) Vascular biology of CD36: roles of this new adhesion molecule family in different disease states. *Thromb. Haemost.*, **78**, 65-9.

26. Dawson, D.W., Pearce S.F., Zhong R., Silverstein R.L., Frazier W.A. and Bouck N.P. (1997) CD36 mediates the In vitro inhibitory effects of thrombospondin-1 on endothelial cells. *J. Biol. Chem.*, 707-17.
27. Deibel, M.A., Ehmann W.D. and Markesbery W.R. (1996) Copper, iron, and zinc imbalances in severely degenerated brain regions in Alzheimer's disease: possible relation to oxidative stress. *J. Neurol. Sci.*, **143**, 137-42.
28. Deng, Y. and Salomon R.G. (1998) Total synthesis of gamma-hydroxy-alpha,beta-unsaturated aldehydic esters of cholesterol and 2-lysophosphatidylcholine. *J. Org. Chem.*, **63**, 7789-7794.
29. Deng, Y. (2000). CASE, Cleveland.
30. Deng, Y. and Salomon R.G. (2000) Unpublished results.
31. Deng, Y. and Salomon R.G. (2000) Total synthesis of oxidized phospholipids. 3. The (11E)-9-hydroxy-13-oxotridec-11-enoate ester of 2-lysophosphatidylcholine. *J. Org. Chem.*, **65**, 6660-6665.
32. Dittmer, J.C. and Lester R.L. (1964) A simple, specific spray for the detection of phospholipids on thin-layer chromatograms. *J. Lipids Res.*, **5**, 126-127.
33. Dix, T.A. and Marnett L.J. (1983) Hematin-catalyzed rearrangement of hydroperoxylinoleic acid to epoxy alcohols via an oxygen rebound. *J. Am. Chem.Soc.*, **105**, 7001-7002.
34. Dix, T.A. and Aikens J. (1993) Mechanisms and biological relevance of lipid peroxidation initiation. *Chem. Res. Toxicol.*, **6**, 2-18.

35. Dudda, A., Kobelt F. and Spitelner G. (1996) Lipid oxidation products in ischemic porcine heart tissue. *Chem. Phys. Lipids*, **82**, 39-45.
36. Edelstein, C. (1990) General properties of plasma lipoproteins and apolipoproteins. In Dekker, M. (ed.), *Biochemistry of plasma lipoproteins*, New York, pp. 497.
37. el Ghissassi, F., Barbin A., Nair J. and Bartsch H. (1995) Formation of 1,N6-ethenoadenine and 3,N4-ethenocytosine by lipid peroxidation products and nucleic acid bases. *Chem. Res. Tox.*, **8**, 278-283.
38. Endemann, G., Stanton L.W., Madden K.S., Bryant C.M., White R.T. and Protter A.A. (1993) CD36 is a receptor for oxidized low density lipoprotein. *J. Biol. Chem.*, **268**, 11811-6.
39. Engelmann, B., Brautigam C. and Thiery J. (1994) Plasmalogen phospholipids as potential protectors against lipid peroxidation of low density lipoproteins. *Biochem. Biophys. Res. Commun.*, **204**, 1235-42.
40. Esterbauer, H. (1982) *Aldehydic products of lipid peroxidation*. Academic Press, London.
41. Esterbauer, H., Zollner H. and Schaur R.J. (1990) Aldehydes formed by lipid peroxidation: mechanisms of formation, occurrence, and determination, *Membrane lipid oxidation*. Vol. 1. CRC Press, Boca Raton, pp. 250.
42. Esterbauer, H., Schaur R.J. and Zollner H. (1991) Chemistry and biochemistry of 4-hydroxynonenal, malonaldehyde and related aldehydes. *Free Radic. Biol. Med.*, **11**, 81-128.

43. Esterbauer, H., Gebicki J., Puhl H. and Jurgens G. (1992) The role of lipid peroxidation and antioxidants in oxidative modification of LDL. *Free Radic. Biol. Med.*, **13**, 341-90.
44. Esterbauer, H., Schmidt R. and Hayn M. (1997) Relationships among oxidation of low-density lipoprotein, antioxidant protection, and atherosclerosis. *Adv. Pharmacol.*, **38**, 425-456.
45. Febbraio, M., Podrez E.A., Smith J.D., Hajjar D.P., Hazen S.L., Hoff H.F., Sharma K. and Silverstein R.L. (2000) Targeted disruption of the class B scavenger receptor CD36 protects against atherosclerotic lesion development in mice. *J. Clin. Invest.*, **105**, 1049-1056.
46. Frankel, E.N., Neff W.E. and Selke E. (1981) Analysis of autoxidized fats by gas chromatography-mass spectrometry: VII. Volatile thermal decomposition products of pure hydroperoxides from autoxidized and photosensitized oxidized methyl oleate, linoleate and linolenate. *Lipids*, **16**, 279-85.
47. Frankel, E.N., Neff W.E., Selke E. and Brooks D.D. (1987) Thermal and metal-catalyzed decomposition of methyl linolenate hydroperoxides. *Lipids*, **22**, 322-327.
48. Gagan, A.P. and Masaaki M. (1996) 1,N6-Ethenodeoxyadenosine, a DNA adduct highly mutagenic in mammalian cells. *Biochem. Biophys. Res. Com.*, **35**, 11487 -11492.
49. Gardner, H.W., Kleiman R. and Weisleder D. (1974) Homolytic decomposition of linoleic acid hydroperoxide. Identification of fatty acid products. *Lipids*, **9**, 696-706.

50. Gardner, H.W., Weisleder D. and Kleiman R. (1978) Formation of trans-12,13-epoxy-9-hydroperoxy-trans-10-octadecenoic acid from 13-L-hydroperoxy-cis-9, trans-11-octadecadienoic acid catalyzed by either a soybean extract or cystein-FeCl₃. *Lipids*, **13**, 246-252.
51. Gardner, H.W. and Kleiman R. (1981) Degradation of linoleic acid hydroperoxides by a cysteine . FeCl₃ catalyst as a model for similar biochemical reactions. II. Specificity in formation of fatty acid epoxides. *Biochim. Biophys. Acta*, **665**, 113-24.
52. Gardner, H.W. and Selke E. (1984) Volatiles from thermal decomposition of isomeric methyl (12S,13S)-E-12,13-epoxy-9-hydroperoxy-10-octadecadecenoates. *Lipids*, **19**, 375-380.
53. Gardner, H.W. and Plattner R.D. (1984) Linoleate hydroperoxides are cleaved heterolytically into aldehyde by a Lewis acid in aprotic solvents. *Lipids*, **19**, 294-299.
54. Gardner, H.W. (1989) Oxygen radical chemistry of polyunsaturated fatty acids. *Free Radic. Biol. Med.*, **7**, 65-86.
55. Gardner, H.W., Weisleder D. and Plattner R.D. (1991) Hydroperoxide lyase and other hydroperoxide-metabolizing activity in tissues of soybean. *Plant Physiol.*, **97**, 1059-1072.
56. Gardner, H.W. and Hamberg M. (1993) Oxygenation of (3Z)-nonenal to (2E)-4-hydroxy-2-nonenal in the broad bean (*Vicia faba* L.). *J. Biol. Chem.*, **268**, 6971-7.

57. Garssen, G.J., Vliegthart J.F.G. and Boldingh J. (1971) Anaerobic reaction between lipoxygenases, linoleic acid and its hydroperoxides. *Biochem. J.*, **122**, 327-332.
58. Garssen, G.J., Veldink G.A., Vliegthart J.F.G. and Boldingh J. (1976) The formation of threo-11-hydroxy-trans-12: 13-epoxy-9-cis-octadecenoic acid by enzymic isomerisation of 13-L-hydroperoxy-9-cis, 11-transoctadecadienoic acid by soybean lipoxygenase-1. *Europ. J. Biochem.*, **62**, 33-6.
59. Gassenmeier, K. and Schieberle P. (1994) Formation of the intense flavor compound trans-4,5-epoxy-(E)-decenal in thermally treated fats. *J. Am. Oil Chem. Soc.*, **71**, 1315-1319.
60. Goerger, M.M. and Hudson B.S. (1988) Synthesis of all trans-parinaric acid-d8 specifically deuterated in the vinyl positions. *J. Org. Chem.*, **53**, 3148-3153.
61. Grisham, M.B. (1994) Oxidants and free radicals in inflammatory bowel disease. *Lancet.*, **344**, 859-861.
62. Gros, L., Ishchenko A.A. and Sapparbaev M. (2003) Enzymology of repair of etheno-adducts. *Mutation Res.*, **531**, 219-229.
63. Gu, X., Sun M., Gugiu B., Hazen S., Crabb J.W. and Salomon R.G. (2003) Oxidatively truncated docosahexaenoate phospholipids: total synthesis, generation, and peptide adduction chemistry. *J. Org. Chem.*, **68**, 3749-3761.
64. Gugiu, B. (2004)., *Chemistry*. CASE, Cleveland.

65. Hamberg, M. and Samuelson B. (1967) Oxygenation of unsaturated fatty acids by the vesicular gland of sheep. *J. Biol. Chem.*, **242**, 5366.
66. Hamberg, M. (1975) Decomposition of unsaturated fatty acid hydroperoxides by hemoglobin: Structures of major products of 13L-hydroperoxy-9,11-octadecadienoic acid. *Lipids*, **10**, 87-92.
67. Hamberg, M. (1990) Transformations of alpha-linolenic acid in leaves of corn. *Adv. Prostaglandin Thromb. Leukot. Res.*, **21A**, 117-124.
68. Hartley, D.P., Kroll D.J. and Petersen D.R. (1997) Prooxidant-initiated lipid peroxidation in isolated rat hepatocytes: detection of 4-hydroxynonenal- and malondialdehyde-protein adducts. *Chem. Res. Toxicol.*, **10**, 895-905.
69. Hiatt, R. (1971) Hydroperoxides. In D., S. (ed.), *Organic Peroxides*. Vol. 2. Willey-Interscience, pp. 65-70.
70. Hidalgo, F.J. and Zamora R. (1993) Fluorescent pyrroles products from carbonyl-amine reactions. *J. Biol. Chem.*, **268**, 16190-16197.
71. Hidalgo, F.J. and Zamora R. (2000) Modification of bovine serum albumin structure following reaction with 4,5(E)-epoxy-2(E)-heptenal. *Chem. Res. Toxicol.*, **13**, 501-508.
72. Hoff, H.F., O'Neil J., Chisolm G.M.d., Cole T.B., Quehenberger O., Esterbauer H. and Jurgens G. (1989) Phospholipid Hydroxyalkenals Biological and Chemical Properties. *Arteriosclerosis*, **9**, 538-549.
73. Horkko, S., Miller E., Dudl E., Reaven P., Curtiss L.K., Zvaifler N.J., Terkeltaub R., Pierangeli S.S., Branch D.W., Palinski W. and Witztum J.L. (1996) Antiphospholipid antibodies are directed against epitopes of oxidized

phospholipids. Recognition of cardiolipin by monoclonal antibodies to epitopes of oxidized low density lipoprotein. *J. Clin. Invest.*, **98**, 815-825.

74. Horrocks, L.A. and Farooqui A.A. (2004) Docosahexaenoic acid in the diet: its importance in maintenance and restoration of neural membrane function. *Prostaglandins Leukot. Essent. Fatty Acids*, **70**, 361-372.

75. Huh, H.Y., Pearce S.F., Yesner L.M., Schindler J.L. and Silverstein R.L. (1996) Regulated expression of CD36 during monocyte-to-macrophage differentiation: potential role of CD36 in foam cell formation. *Blood*., **87**, 2020-8.

76. Imagawa, T., Kasai S., Matsui K. and Nakamura T. (1982) Methyl hydroperoxy-epoxy-octadecenoate as an autoxidation product of methyl linoleate: a new inhibitor-uncoupler of mitochondrial respiration. *J. Biochem.*, **92**, 1109-1121.

77. Januszewski, A.S., Alderson N.L., Metz T.O., Thorpe S.R. and Baynes J.W. (2003) Role of lipids in chemical modification of proteins and development of complications in diabetes. *Biochem. Soc. Trans.*, **31**, 1413-1416.

78. Jin, S., Makris T.M., Bryson T.A., Sligar S. and Dawson J. (2003) Epoxidation of olefins by hydroperoxo-ferric cytochrome P450. *J. Am. Chem. Soc.*, **125**, 3406-3407.

79. Johnson, T.M., Yu Z., Ferrans V.J., Lowenstein R.A. and Finkel T. (1996) Reactive oxygen species are downstream mediators of p53-dependent apoptosis. *Proc. Natl. Acad. Sci. USA*, **93**, 11848-11852.

80. Kamitani, H., Geller M. and Eling T. (1998) Expression of 15-lipoxygenase by human colorectal carcinoma Caco-2 cells during apoptosis and cell differentiation.. *J. Biol. Chem.*, **242**, 21569.
81. Kates, M. (1986) *Techniques of lipidology : isolation, analysis, and identification of lipids* (2nd rev. edn). Elsevier, Amsterdam ; New York.
82. Katsuki, T., Lee A.W.M., Ma P., Martin V.S., Masamune S., Sharpless K.B., Tuddenham D. and Walker F.J. (1982) Synthesis of saccharides and related polyhydroxylated natural products. 1. Simple alditols. *J. Org. Chem.*, **47**, 1373-1378.
83. Katz, M.L. and Robison W.G. (2002) What is lipofuscin? Defining characteristics and differentiation from other autofluorescent lysosomal storage bodies. *Archiv. Geront. Geriat.*, **34**, 169-184.
84. Kaur, K., Salomon R.G., O'Neil J. and Hoff H.F. (1997) (Carboxyalkyl)pyrroles in human plasma and oxidized low-density lipoproteins. *Chem. Res. Tox.*, **10**, 1387-96.
85. Killian, J.A. and van Meer G. (2001) The 'double lives' of membrane lipids. *EMBO reports*, **2**, 91-95.
86. Kobierski, M.E., Kim S., Murthi K.K., Iyer R.S. and Salomon R.G. (1994) Synthesis of a pyrazole isostere of pyrroles formed by the reaction of the amino groups of protein lysyl residues with levuglandin E2. *J. Org. Chem.*, **59**, 6044-6050.
87. Kruijff, B. (1997) Lipids beyond the bilayer. *Nature*, **386**, 129-130.

88. Kuhn, H. (1996) Biosynthesis, metabolization and biological importance of the primary 15-lipoxygenase metabolites 15-hydro(pero)XY-5Z,8Z,11Z,13E-eicosatetraenoic acid and 13-hydro(pero)XY-9Z,11E-octadecadienoic acid. *Prog. Lipid Res.*, **35**, 203-26.
89. Lambert, J.B., Shurvell H.F., Lightner D.A. and Cooks R.G. (1998) *Organic Structural Spectroscopy*. Prentice-Hall, Inc.
90. Landau, E.M. and Rosenbusch J.P. (1996) *Proc. Natl. Acad. Sci. USA*, **93**, 14532-14535.
91. Lee, S.H. and Blair I.A. (2000) Characterization of 4-oxo-2-nonenal as a novel product of lipid peroxidation. *Chem. Res. Tox.*, **13**, 698-702.
92. Lee, S.H., Oe T. and Blair I.A. (2001) Vitamin C-induced decomposition of lipid hydroperoxides to endogenous genotoxins. *Science*, **292**, 2083-2085.
93. Lee, S.H., Oe T. and Blair I.A. (2002) 4,5-Epoxy-2(E)-decenal-induced formation of 1,N6-etheno-2'-deoxyadenosine and 1,N2-etheno-2'-deoxyguanosine adducts. *Chem. Res. Toxicol.*, **15**, 300-304.
94. Levine, M., Conry-Cantilena C., Wang Y., Welch R.W., Washko P.W., Dhariwal K.R., Park J.B., Lazarev A., Graumlich J.F., King J. and Cantilena L.R. (1996) Vitamin C pharmacokinetics in healthy volunteers: Evidence for a recommended dietary allowance. *Proc. Natl. Acad. Sci. USA*, **93**, 3704-3709.
95. Levine, R.L., Yang I.Y., Hossain M., Pandya G.A., Grollman A.P. and Moriya M. (2000) Mutagenesis induced by a single 1,N6-ethenodeoxyadenosine adduct in human cells. *Cancer Res.*, **60**, 4098-104.

96. List, G.R., Hoffman R.L., Moser H.A. and Evans C.D. (1967) Odor evaluation of fatty methyl esters purified as urea adducts. *J. Am. Oil Chem. Soc.*, **44**, 485-7.
97. Mapp, P.I., Grootveld M.C. and Blake D.R. (1995) Hypoxia, oxidative stress and rheumatoid arthritis. *Med. Bull.*, **51**, 419-436.
98. Marnett, L. (2000) Oxyradicals and DNA damage. *Carcinogenesis*, **21**, 361-370.
99. Matthew, J.A., Chan H.W. and Galliard T. (1977) A simple method for the preparation of pure 9-D-hydroperoxide of linoleic acid and methyl linoleate based on the positional specificity of lipoxygenase in tomato fruit. *Lipids*, **12**, 324-6.
100. Mesaros, C. and Salomon R.G. (2004) Total synthesis and natural occurrence of a phospholipid analog of the genotoxic aldehyde 4,5-EDE. *Org. Lett.*, to be submitted.
101. Meyer, W. and Spiteller G. (1993) Epoxidation of carbon-carbon double bonds in terpenes by linoleic acid hydroperoxides. *Liebigs Ann. Chem.*, **12**, 1253-6.
102. Miljanich, G.P., Nemes P.P., White D.L. and Dratz E.A. (1981) The asymmetric transmembrane distribution of phosphatidylethanolamine, phosphatidylserine, and fatty acids of the bovine retinal rod outer segment disk membrane. *Membr. Biol.*, **60**, 249-55.
103. Mimms, L.T., Zampighi G., Nozaki Y., Tanford C. and Reynolds J.A. (1981) Phospholipid vesicle formation and transmembrane protein incorporation using octyl glucoside. *Biochem. Biophys. Res. Commun.*, **20**, 833-840.

104. Miyashita, M., Yoshikoshi A. and Grieco P. (1977) Pyridinium p-toluenesulfonate. A mild and efficient catalyst for the tetrahydropyranylation of alcohols. *J. Org. Chem.*, **42**, 3772-3774.
105. Nair, J., Barbin A., Guichard Y. and Bartsch H. (1995) 1,N6-ethenodeoxyadenosine and 3,N4-ethenodeoxycytine in liver DNA from humans and untreated rodents detected by immunoaffinity/³²P-postlabeling. *Carcinogenesis*, **16**, 613-7.
106. Nair, J., Barbin A., Velic I. and Bartsch H. (1999) Etheno DNA-base adducts from endogenous reactive species. *Mut. Res.*, **424**, 59-69.
107. Nakata, A., Nakagawa Y., Nishida M., Nozaki S., Miyagawa J., Nakagawa T., Tamura R., Matsumoto K., Kameda-Takemura K., Yamashita S. and Matsuzawa Y. (1999) CD36, a novel receptor for oxidized low-density lipoproteins, is highly expressed on lipid-laden macrophages in human atherosclerotic aorta. *Arterioscler. Thromb. Vasc. Biol.*, **19**, 1333-9.
108. Neuenschwander, P.F., Fiore M.M. and Morrissey J.H. (1993) Factor VII autoactivation proceeds via interaction of distinct protease-cofactor and zymogen-cofactor complexes: Implications of a two-dimensional enzyme kinetic mechanism. *J. Biol. Chem.*, **268.**, 21489-21492.
109. Newcombe, J., Li H. and Cuzner M.L. (1994) Low density lipoprotein uptake by macrophages in multiple sclerosis plaques: implications for pathogenesis. *Neuropathol. Appl. Neurobiol.*, **20**, 152-162.
110. Nicholson, A.C., Frieda S., Pearce A. and Silverstein R.L. (1995) Oxidized LDL binds to CD36 on human monocyte-derived macrophages and transfected

cell lines. Evidence implicating the lipid moiety of the lipoprotein as the binding site. *Arterioscler. Thromb. Vasc. Biol.*, **15**, 269-75.

111. Nicolaou, K.C., Roschangar F. and Vourloumis D. (1998) Chemical biology of epothilones. *Angew. Chem. Int. Ed.*, **37**, 2014-2045.

112. Nozaki, S., Kashiwagi H., Yamashita S., Nakagawa T., Kostner B., Tomiyama Y., Nakata A., Ishigami M., Miyagawa J. and Kameda-Takemura K. (1995) Reduced uptake of oxidized low density lipoproteins in monocyte-derived macrophages from CD36-deficient subjects. *J. Clin. Invest.*, **96**, 1859-65.

113. O'Neal, H.E. and Benson S.W. (1973) *Free Radicals*. Wiley & Sons, New York.

114. Olanow, C.W. (1992) An introduction to the free radical hypothesis in Parkinson's disease. *Ann. Neurol.*, **32**, S2-9.

115. Oliw, E.H. (1983) *Biochem. Biophys. Res. Commun.*, **111**, 644-651.

116. Ozawa, T., Hayakawa M., Takamura T., Sugiyama S., Suzuki K., Iwata M., Taki F. and Tomita T. (1986) Biosynthesis of leukotoxin, 9,10-epoxy-12-octadecenoate, by leukocytes in lung lavages of rat after exposure to hyperoxia. *Biochem. Biophys. Res. Com.*, **134**, 1071-1078.

117. Ozawa, T., Nishikimi M., Sugiyama S., Taki T., Hayakawa M. and Shionoya H. (1988) Cytotoxic activity of leukotoxin, a neutrophil-derived fatty acid epoxide, on cultured human cells. *Biochem. Int.*, **16(2)**, 369-73.

118. Ozawa, T., Sugiyama S., Hayakawa M., Taki F. and Hanaki Y. (1988) Neutrophil microsomes biosynthesize linoleate epoxide (9,10-epoxy-12-

octadecenoate), a biological active substance. *Biochem. Biophys. Res. Comm.*, **152**, 1310-18.

119. Palinski, W., Yla-Herttuala S., Rosenfeld M.E., Butler S.W., Socher S.A., Parthasarathy S., Curtiss L.K. and Witztum J.L. (1990) Antisera and monoclonal antibodies specific for epitopes generated during oxidative modification of low density lipoprotein. *Arteriosclerosis*, **10**, 325-335.

120. Pandya, G.A. and Moriya M. (1996) 1,N⁶-ethenodeoxyadenosine, a DNA adduct highly mutagenic in mammalian cells. *Biochem.*, **35**, 11487-92.

121. Patterson, J. (1984) A convenient one-pot procedure for the conversion of terminal acetylenic alcohols (and O-derivatives) into (E)-olefinic alcohols (or derivatives). *Synthesis*, 337.

122. Podrez, E.A., Schmitt D., Hoff H.F. and Hazen S.L. (1999) Myeloperoxidase-generated reactive nitrogen species convert LDL into an atherogenic foam *in vitro*. *J. Clin. Invest.*, **103**, 1547-60.

123. Podrez, E.A., Hoppe G., O'Neil J., Sayre L.M., Sheibani N. and Hoff H.F. (2000) Macrophage receptors responsible for distinct recognition of low density lipoprotein containing pyrrole or pyridinium adducts: models of oxidized low density lipoprotein.. *J. Lipid Res.*, **41**, 1455-1463.

124. Podrez, E.A., Poliakov E., Shen Z., Zhang R., Deng Y., Sun M., Finton P.J., Shan L., Febbraio M., Hajjar D.P., Silverstein R.L., Hoff H.F., Salomon R.G. and Hazen S.L. (2002) A novel family of atherogenic oxidized phospholipids promotes macrophage foam cell formation via the scavenger receptor CD36 and is enriched in atherosclerotic lesions. *J. Biol. Chem.*, **277**, 38517-23.

125. Podrez, E.A., Poliakov E., Shen Z., Zhang R., Deng Y., Sun M., Finton P.J., Shan L., Gugiu B., Fox P.L., Hoff H.F., Salomon R.G. and Hazen S.L. (2002) Identification of a novel family of oxidized phospholipids that serve as ligands for the macrophage scavenger receptor CD36. *J. Biol. Chem.*, **277**, 38503-16.
126. Pryor, W.A. and Porter N.A. (1990) Suggested mechanisms for the production of 4-hydroxy-2-nonenal from the autoxidation of polyunsaturated fatty acids. *Free Radic. Biol. Med.*, **8**, 541-3.
127. Re, G., Azzimondi G., Lanzarini C., Bassein L., Vaona I. and Guarnieri C. (1997) Latent acute promyelocytic leukaemia in a case of ischaemic stroke underlines the importance of prompt diagnostic confirmation prior to acute care. *Eur. J. Emerg. Med.* **1**, **4**, 5-9.
128. Reinaud, O., Delaforge M., Boucher J.L., Rocchiccioli F. and Mansuy D. (1989) Oxidative metabolism of linoleic acid by human leukocytes. *Biochem. Biophys. Res. Commun.*, **161**, 883-91.
129. Ren, Y., Silverstein R.L., Allen J. and Savill J. (1995) CD36 gene transfer confers capacity for phagocytosis of cells undergoing apoptosis. *J. Exp. Med.*, **181**, 1857-62.
130. Requena, J.R., Fu M.X., Ahmed M.U., Jenkins A.J., Lyons T.J., Baynes J.W. and Thorpe S.R. (1997) Quantification of malondialdehyde and 4-hydroxynonenal adducts to lysine residues in native and oxidized human low-density lipoprotein. *Biochem. J.*, **322**, 317-25.

131. Rietveld, A.G., Koorengevel M.C. and Kruijff B. (1995) Non-bilayer lipids are required. *EMBO J.*, **14**, 5506-13.
132. Rigotti, A., Acton A.L. and Krieger M. (1995) The class B scavenger receptors SR-BI and CD36 are receptors for anionic phospholipids. *J. Biol. Chem.*, **270**, 16221-16224.
133. Ryeom, S.W., Silverstein R.L., Scotto A. and Sparrow J.R. (1996) Binding of anionic phospholipids to retinal pigment epithelium may be mediated by the scavenger receptor CD36. *J. Biol. Chem.*, **271**, 20536-9.
134. Ryeom, S.W., Sparrow J.R. and Silverstein R.L. (1996) CD36 participates in the phagocytosis of rod outer segments by retinal pigment epithelium. *J. Cell. Sci.*, **109**, 387-95.
135. Sakai, T., Ishizaki T., Nakai T., Miyabo S., Matsukawa S., Hayakawa M. and Ozawa T. (1996) Role of nitric oxide and superoxide anion in leukotoxin 9,10-epoxy-12-octadecenoate-induced mitochondrial dysfunction. *Free Radic. Biol. Med.*, **20**, 607-612.
136. Salahudeen, A.K., Kanji V., Reckelhoff J.F. and Schmidt A.M. (1997) Pathogenesis of diabetic nephropathy: a radical approach. *Nephrol. Dial. Transplant.*, **12**, 664-668.
137. Salomon, R.G., Kaur K., Podrez E., Hoff H.F., Krushinsky A.V. and Sayre L.M. (2000) HNE-derived 2-pentylpyrroles are generated during oxidation of LDL, are more prevalent in blood plasma from patients with renal disease or atherosclerosis, and are present in atherosclerotic plaques. *Chem. Res. Tox*, **13**, 557-64.

138. Sawada, M. and Carlson J.C. (1987) Association between lipid peroxidation and life-modifying factors in rotifers. *J. Gerontol.*, **38**, 419-428.
139. Sawada, M. and Carlson J.C. (1987) Changes in superoxide radical and lipid peroxide formation in the brain, heart and liver during the lifetime of the rat. *Mech. Ageing Dev.*, **41**, 125-137.
140. Sayre, L.M., Arora P.K., Iyer R.S. and Salomon R.G. (1993) Pyrrole formation from 4-hydroxynonenal and primary amines. *Chem. Res. Tox.*, **6**, 19-22.
141. Schneider, C., Tallman K.A., Porter N.A. and Brash A.R. (2001) Two distinct pathways of formation of 4-hydroxynonenal. Mechanisms of nonenzymatic transformation of the 9- and 13-hydroperoxides of linoleic acid to 4-hydroxyalkenals. *J. Bio. Chem*, **276**, 20831-20838.
142. Schneider, C., Porter N.A. and Brash A.R. (2004) Autoxidative transformation of chiral w6 hydroxy linoleic and arachidonic acids to chiral 4-hydroxy-2E-nonenal. *Chem. Res. Toxicol.*, **17**, 937-941.
143. Selke, E., Rohwedder W.K. and Dutton H.J. (1980) Volatile components from trilinolein heated in air. *J. Am. Oil Chem. Soc.*, **1**, 25-30.
144. Sevanian, A. and Hochstein P. (1985) Mechanisms and consequences of lipid peroxidation in biological systems. *Annu. Rev. Nutr.*, **5**, 365-390.
145. Silverstein, R.L., Asch A.S. and Nachman R.L. (1989) Glycoprotein IV mediates thrombospondin-dependent platelet-monocyte and platelet-U937 cell adhesion. *J. Clin. Invest.*, **84**, 546-52.

146. Silverstein, R.L. and Febbraio M. (2000) CD36 and atherosclerosis. *Curr. Opin. Lipidol.*, **11**, 483-91.
147. Smith, M.B. and March J. (2001) *March's Advanced Organic Chemistry* (5th edn). John Willey & Sons, Inc., New York.
148. Spickett, C.M., Rennie N., Winter H., Zambonin L., Landi L., Jerlich A., Schaur R.J. and Pitt A.R. (2001) Detection of phospholipid oxidation in oxidatively stressed cells by reversed-phase HPLC coupled with positive-ionization electrospray [correction of electroscopy] MS. *Biochem. J.*, **355(Pt 2)**, 449-57.
149. Spiteller, G. (1998) Linoleic acid peroxidation- the dominant lipid peroxidation process in low density lipoprotein and its relationship to chronic diseases. *Chem. Phys. Lipids*, **95**, 105-162.
150. Spiteller, G. (2003) Are lipid peroxidation processes induced by changes in the cell wall structure and how are these processes connected with diseases? *Med. Hypotheses*, **60**, 69-83.
151. Sun, M., Deng Y., Batyreva E., Sha W. and Salomon R.G. (2002) Novel bioactive phospholipids: practical total syntheses of products from the oxidation of arachidonic and linoleic esters of 2-lysophosphatidylcholine. *J. Org. Chem.*, **67**, 3575-84.
152. Sun, M. (2003) Synthetic and mechanistic studies of lipid peroxidation in vitro and in vivo, *Chemistry*. CASE, Cleveland.

153. Sun, M. and Salomon R.G. (2004) Oxidative fragmentation of hydroxy octadecadienoates generates biologically active gamma-hydroxyalkenals. *J. Am. Chem. Soc.*, **126**, 5699-5708.
154. Swoboda, P.A. and Peers K.E. (1978) Trans-4,5-epoxyhept-trans-2-enal. The major volatile compound formed by the copper and tacopherol induced oxidation of butterfat. *J. Sci. Food Agric.*, **29**, 803-807.
155. Tait, J. F. and Smith C. (1999) Phosphatidylserine receptors: role of CD36 in binding of anionic phospholipid vesicles to monocytic cells. *J. Biol. Chem.*, **274**, 3048-54.
156. Tallman, K.A., Roschek B. and Porter N.A. (2004) Factors influencing the autoxidation of fatty acids: effect of olefin geometry of the nonconjugated diene. *J. Am. Chem. Soc.*, asap.
157. Tandon, N.N., Kralisz U. and Jamieson G.A. (1995) Identification of glycoprotein IV (CD36) as a primary receptor for platelet-collagen adhesion.. *J. Biol. Chem.*, **264**, 7576-83.
158. Toshniwal, P.K. and Zarling E. (1992) Evidence for increased lipid peroxidation in multiple sclerosis. *J. Neurochem Res.*, **17**, 205-207.
159. Toyokuni, S., Uchida K., Okamoto K., Hattori-Nakakuki Y., Hiai H. and Stadtman E.R. (1994) Formation of 4-hydroxy-2-nonenal-modified proteins in the renal proximal tubules of rats treated with a renal carcinogen, ferric nitrilotriacetate. *Proc. Natl. Acad.Sci. USA*, **91**, 2616-20.

160. Trigatti, B.L., Krieger M. and Rigotti A. (2003) Influence of the HDL receptor SR-BI on lipoprotein metabolism and atherosclerosis. *Arterioscler. Thromb. Vasc. Biol.*, **23**, 1732-1738.
161. van Kooten, F., Ciabattoni G., Patrono C., Dippel D.W. and Koudstaal P.J. (1997) Platelet activation and lipid peroxidation in patients with acute ischemic stroke. *Stroke*, **28**, 1557-63.
162. Walther, U. and Spiteller G. (1993) Formation of oleic acid epoxide during the storage of technical quality oleic acid. *Fett. Wissenschaft Technologie*, **95**, 472-4.
163. White, D.A. (1973) The phospholipid composition of mammalian tissues, *The phospholipid composition of mammalian tissues*. Elsevier, Amsterdam, pp. 441-482.
164. Winyard, P.G., Tatzber F., Esterbauer H., Kus M.L., Blake D.R. and Morris C.J. (1993) Presence of foam cells containing oxidised low density lipoprotein in the synovial membrane from patients with rheumatoid arthritis. *Ann. Rheum. Dis.*, **52**, 677-680.
165. Witz, G. (1989) Biological interactions of alpha,beta-unsaturated aldehydes. *Free Radic. Biol. Med.*, **7**, 333-349.
166. Yadov, J.S. (2001) *Tetrahedron: Asymmetry*, **12**, 2129-2135.
167. Zamora, R. and Hidalgo F.J. (1994) Modification of lysine amino groups by the lipid peroxidation product 4,5(E)-epoxy-2(E) heptenal. *Lipids*, **29**, 243-249.

168. Zamora, R. and Hidalgo F.J. (1995) Linoleic acid oxidation in the presence of amino compounds produces pyrroles by carbonyl amine reactions. *Biochim. Biophys. Acta*, **1258**, 319-327.
169. Zamora, R., Alaiz M. and Hidalgo F.J. (1999) Determination of the N-pyrrolnorleucine in fresh food products. *J. Agric. Food Chem.*, **47**, 1942-1947.
170. Zamora, R., Alaiz M. and Hidalgo F.J. (1999) Modification of histidine residues by 4,5epoxy-2-alkenals. *Chem. Res. Toxicol.*, **12**, 654-660.
171. Zamora, R. and Hidalgo F.J. (2003) Phosphatidylethanolamine modification by oxidative stress product 4,5(E)-epoxy-2(E)-heptenal. *Chem. Res. Toxicol.*, **16**, 1632-1644.